ISSN 0021-9673

Period.

VOL. 626 NO. 1 DECEMBER 16, 1992

2nd Int. Symp. on Hyphenated Techniques in Chromatography Antwerp, February 18–21, 1992

JOURNAL OF CHROMATOGRAPHY

INCLUDING ELECTROPHORESIS AND OTHER SEPARATION METHODS

SYMPOSIUM VOLUMES

EDITORS
E. Heftmann (Orinda, CA)
Z. Deyl (Prague)

EDITORIAL BOARD
E. Bayer (Tübingen)
S. R. Binder (Hercules, CA)
S. C. Churms (Rondebosch)
J. C. Fetzer (Richmond, CA)
E. Gelpí (Barcelona)
K. M. Gooding (Lafayette, IN)
S. Hara (Tokyo)
P. Helboe (Brønshøj)
W. Lindner (Graz)
T. M. Phillips (Washington, DC)
S. Terabe (Hyogo)
H. F. Walton (Boulder, CO)
M. Wilchek (Rehovot)

ELSEVIER

JOURNAL OF CHROMATOGRAPHY

INCLUDING ELECTROPHORESIS AND OTHER SEPARATION METHODS

Scope. The *Journal of Chromatography* publishes papers on all aspects of **chromatography, electrophoresis** and related methods. Contributions consist mainly of research papers dealing with chromatographic theory, instrumental developments and their applications. The section *Biomedical Applications*, which is under separate editorship, deals with the following aspects: developments in and applications of chromatographic and electrophoretic techniques related to clinical diagnosis or alterations during medical treatment; screening and profiling of body fluids or tissues related to the analysis of active substances and to metabolic disorders; drug level monitoring and pharmacokinetic studies; clinical toxicology; forensic medicine; veterinary medicine; occupational medicine; results from basic medical research with direct consequences in clinical practice. In *Symposium volumes*, which are under separate editorship, proceedings of symposia on chromatography, electrophoresis and related methods are published.

Submission of Papers. The preferred medium of submission is on disk with accompanying manuscript (see *Electronic manuscripts* in the Instructions to Authors, which can be obtained from the publisher, Elsevier Science Publishers B.V., P.O. Box 330, 1000 AH Amsterdam, Netherlands). Manuscripts (in English; *four* copies are required) should be submitted to: Editorial Office of *Journal of Chromatography*, P.O. Box 681, 1000 AR Amsterdam, Netherlands, Telefax (+31-20) 5862 304, or to: The Editor of *Journal of Chromatography, Biomedical Applications*, P.O. Box 681, 1000 AR Amsterdam, Netherlands. Review articles are invited or proposed in writing to the Editors who welcome suggestions for subjects. An outline of the proposed review should first be forwarded to the Editors for preliminary discussion prior to preparation. Submission of an article is understood to imply that the article is original and unpublished and is not being considered for publication elsewhere. For copyright regulations, see below.

Publication. The *Journal of Chromatography* (incl. *Biomedical Applications*) has 40 volumes in 1993. The subscription prices for 1993 are:

J. Chromatogr. (incl. *Cum. Indexes, Vols. 601–650*) + *Biomed. Appl.* (Vols. 612–651):
Dfl. 8520.00 plus Dfl. 1320.00 (p.p.h.) (total *ca.* US$ 5927.75)

J. Chromatogr. (incl. *Cum. Indexes, Vols. 601–650*) only (Vols. 623–651):
Dfl. 7047.00 plus Dfl. 957.00 (p.p.h.) (total *ca.* US$ 4821.75)

Biomed. Appl. only (Vols. 612–622):
Dfl. 2783.00 plus Dfl. 363.00 (p.p.h.) (total *ca.* US$ 1895.25).

Subscription Orders. The Dutch guilder price is definitive. The US$ price is subject to exchange-rate fluctuations and is given as a guide. Subscriptions are accepted on a prepaid basis only, unless different terms have been previously agreed upon. Subscriptions orders can be entered only by calender year (Jan.–Dec.) and should be sent to Elsevier Science Publishers, Journal Department, P.O. Box 211, 1000 AE Amsterdam, Netherlands, Tel. (+31-20) 5803 642, Telefax (+31-20) 5803 598, or to your usual subscription agent. Postage and handling charges include surface delivery except to the following countries where air delivery via SAL (Surface Air Lift) mail is ensured: Argentina, Australia, Brazil, Canada, China, Hong Kong, India, Israel, Japan*, Malaysia, Mexico, New Zealand, Pakistan, Singapore, South Africa, South Korea, Taiwan, Thailand, USA. *For Japan air delivery (SAL) requires 25% additional charge of the normal postage and handling charge. For all other countries airmail rates are available upon request. Claims for missing issues must be made within six months of our publication (mailing) date, otherwise such claims cannot be honoured free of charge. Back volumes of the *Journal of Chromatography* (Vols. 1–611) are available at Dfl. 230.00 (plus postage). Customers in the USA and Canada wishing information on this and other Elsevier journals, please contact Journal Information Center, Elsevier Science Publishing Co. Inc., 655 Avenue of the Americas, New York, NY 10010, USA, Tel. (+1-212) 633 3750, Telefax (+1-212) 633 3764.

Abstracts/Contents Lists published in Analytical Abstracts, Biochemical Abstracts, Biological Abstracts, Chemical Abstracts, Chemical Titles, Chromatography Abstracts, Clinical Chemistry Lookout, Current Awareness in Biological Sciences (CABS), Current Contents/Life Sciences, Current Contents/Physical, Chemical & Earth Sciences, Deep-Sea Research/Part B: Oceanographic Literature Review, Excerpta Medica, Index Medicus, Mass Spectrometry Bulletin, PASCAL-CNRS, Pharmaceutical Abstracts, Referativnyi Zhurnal, Research Alert, Science Citation Index and Trends in Biotechnology.

US Mailing Notice. *Journal of Chromatography* (ISSN 0021-9673) is published weekly (total 58 issues) by Elsevier Science Publishers (Sara Burgerhartstraat 25, P.O. Box 211, 1000 AE Amsterdam, Netherlands). Annual subscription price in the USA US$ 5927.75 (subject to change), including air speed delivery. Application to mail at second class postage rate is pending at Jamaica, NY 11431. **USA POSTMASTERS:** Send address changes to *Journal of Chromatography*, Publications Expediting, Inc., 200 Meacham Avenue, Elmont, NY 11003. Airfreight and mailing in the USA by Publication Expediting.

See inside back cover for Publication Schedule, Information for Authors and information on Advertisements.

© 1992 ELSEVIER SCIENCE PUBLISHERS B.V. All rights reserved.

0021-9673/92/$05.00

No part of this publication may be reproduced, stored in a retrieval system or transmitted in any form or by any means, electronic, mechanical, photocopying, recording or otherwise, without the prior written permission of the publisher, Elsevier Science Publishers B.V., Copyright and Permissions Department, P.O. Box 521, 1000 AM Amsterdam, Netherlands.

Upon acceptance of an article by the journal, the author(s) will be asked to transfer copyright of the article to the publisher. The transfer will ensure the widest possible dissemination of information.

Special regulations for readers in the USA. This journal has been registered with the Copyright Clearance Center, Inc. Consent is given for copying of articles for personal or internal use, or for the personal use of specific clients. This consent is given on the condition that the copier pays through the Center the per-copy fee stated in the code on the first page of each article for copying beyond that permitted by Sections 107 or 108 of the US Copyright Law. The appropriate fee should be forwarded with a copy of the first page of the article to the Copyright Clearance Center, Inc., 27 Congress Street, Salem, MA 01970, USA. If no code appears in an article, the author has not given broad consent to copy and permission to copy must be obtained directly from the author. All articles published prior to 1980 may be copied for a per-copy fee of US$ 2.25, also payable through the Center. This consent does not extend to other kinds of copying, such as for general distribution, resale, advertising and promotion purposes, or for creating new collective works. Special written permission must be obtained from the publisher for such copying.

No responsibility is assumed by the Publisher for any injury and/or damage to persons or property as a matter of products liability, negligence or otherwise, or from any use or operation of any methods, products, instructions or ideas contained in the materials herein. Because of rapid advances in the medical sciences, the Publisher recommends that independent verification of diagnoses and drug dosages should be made.

Although all advertising material is expected to conform to ethical (medical) standards, inclusion in this publication does not constitute a guarantee or endorsement of the quality or value of such product or of the claims made of it by its manufacturer.

This issue is printed on acid-free paper.

Printed in the Netherlands

For Contents, see p. VII

Only one LC will get the most out of your new Mass Spec interface

Since 1985, Isco microbore systems have proved the benefits of 1 mm and capillary HPLC. They'll give you simple, direct interfacing to electrospray and FAB-MS, and to other advanced spectrometers. Plus you'll get manyfold improvement in mass sensitivity, resolution, and sample and solvent economy.

Digital syringe pumps deliver totally pulseless flow, with quartz-locked stability and precision—even at packed-capillary flow rates.

Program precise, reproducible gradients for highest efficiency in demanding separations such as peptide mapping and protein sequencing.

A new programmable absorbance detector gives you dual-wavelength monitoring and spectral scans, and a choice of four microcolumn flow cells with volumes down to 35 nl.

Find out more about how microbore HPLC can solve your special problems. Call **(800)228-4250**, or contact your Isco distributor today.

Isco, Inc.
P.O. Box 5347
Lincoln NE 68505, U.S.A.
Tel: **(800)228-4250**

Isco Europe AG
Brüschstr. 17
CH8708 Männedorf
Switzerland
Fax **(41-1)920 62 08**

ISCO

Distributors • **Australia:** Australian Chromatography Co. • **Austria:** INULA • **Belgium:** Mettler-Toledo S.A. • **Canada:** Canberra Packard Canada, Ltd. • **Denmark:** Mikrolab Aarhus • **Finland:** ETEK OY • **France:** Ets. Roucaire, S.A. • **Germany:** Colora Messtechnik GmbH • **Italy:** Analytical Control Italia S.p.A. • **Japan:** JSI Co. Ltd. • **Korea:** Sang Chung, Ltd. • **The Netherlands:** Beun-de Ronde B.V. • **Norway:** Dipl. Ing. Houm A.S. • **Portugal:** CAMPOS & Ca., Lda. • **Spain:** VARIAN IBERICA, S.L. • **Sweden:** Spectrochrom AB • **Switzerland:** IG Instrumenten-Gesellschaft AG • **UK:** Jones Chromatography Ltd. •

The most useful chiral separation column, ULTRON ES-OVM, for enantiomeric drugs.

Substance	Rs	Substance	Rs	Substance	Rs
Acetylpheneturide	2.74	Disopyramid	2.04	Nisoldipine	2.36
Alimemazine	6.06	Eperisone	1.15	Nitrendipine	1.80
Alprenolol	1.09[1]	Ethiazide	1.42	Oxazepan	2.65[2]
Arotinolol	1.95	Fenoprofen	0.80	Oxprenolol	1.38
Bay K 8644	5.92	Flurbiprofen	1.27	Pindolol	2.04
Benproperine	3.27	Glutethimide	1.36	2-Phenylpropionic acid	0.80
Benzoin	8.41	Glycopyrronium	1.73	Pranoprofen	0.63
Biperiden	3.17	Hexobarbital	1.70	Prenylamine	0.86
Bunitrolol	3.08	Homochlorcyclizine	3.04	Profenamine	3.31
Bupivacaine	1.26	Hydroxyzine	2.15	Promethazine	1.42
Chlormezanone	6.48	Ibuprofen	1.72	Propranolol	1.24
Chlorphenesin	2.23	Ketoprofen	1.37	Terfenadine	2.22
Chlorpheniramine	2.36	Lorazepam	2.55[2]	Thioridazine	0.72
Chlorprenaline	2.34	Meclizine	3.71	Tolperisone	1.50
Cloperastin	2.85	Mepenzolate	1.40	Trihexyphenidyl	5.16
Dimethindene	4.33	Mephobarbital	1.70	Trimipramine	3.69
1,2-Diphenylethylamine	1.74	Methylphenidate	1.13[1]	Verapamil	1.49

NOTE: 4.6×150mm column at room temp. except[1] 6.0×150mm at room temp. and[2] 6.0×150mm at 10°C

From trace analysis for metabolites

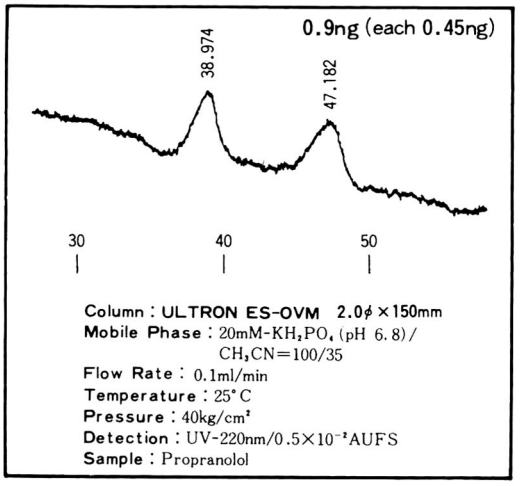

to preparative scale

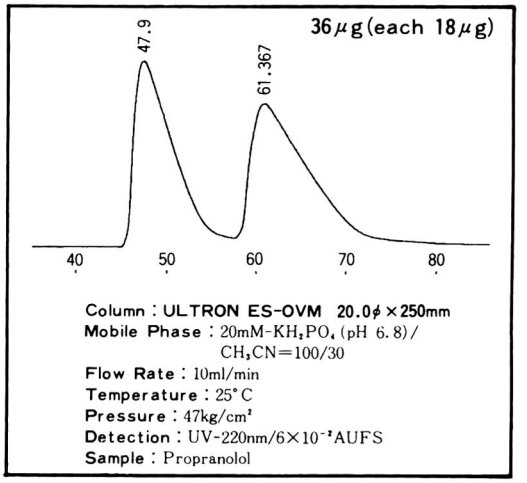

SHINWA CHEMICAL INDUSTRIES, LTD

50 Kagekatsu-cho, Fushimi-ku, Kyoto 612, JAPAN

Phone: 80-75-621-2360 Fax : 80-75-602-2660

Please contact in United States of America and Europe to :

Rockland Technologies, Inc. 538 First State Boulevard, Newport, DE 19804, U.S.A.

Phone : 302-633-5880, Fax : 302-633-5893

This product is licenced by Eisai Co., Ltd.

JOURNAL OF CHROMATOGRAPHY

VOL. 626 (1992)

JOURNAL of CHROMATOGRAPHY

INCLUDING ELECTROPHORESIS AND OTHER SEPARATION METHODS

SYMPOSIUM VOLUMES

EDITORS

E. HEFTMANN (Orinda, CA), Z. DEYL (Prague)

EDITORIAL BOARD

E. Bayer (Tübingen), S. R. Binder (Hercules, CA), S. C. Churms (Rondebosch), J. C. Fetzer (Richmond, CA), E. Gelpí (Barcelona), K. M. Gooding (Lafayette, IN), S. Hara (Tokyo), P. Helboe (Brønshøj), W. Lindner (Graz), T. M. Phillips (Washington, DC), S. Terabe (Hyogo), H. F. Walton (Boulder, CO), M. Wilchek (Rehovot)

ELSEVIER
AMSTERDAM — LONDON — NEW YORK — TOKYO

J. Chromatogr., Vol. 626 (1992)

© 1992 ELSEVIER SCIENCE PUBLISHERS B.V. All rights reserved.

0021-9673/92/$05.00

No part of this publication may be reproduced, stored in a retrieval system or transmitted in any form or by any means, electronic, mechanical, photocopying, recording or otherwise, without the prior written permission of the publisher, Elsevier Science Publishers B.V., Copyright and Permissions Department, P.O. Box 521, 1000 AM Amsterdam, Netherlands.

Upon acceptance of an article by the journal, the author(s) will be asked to transfer copyright of the article to the publisher. The transfer will ensure the widest possible dissemination of information.

Special regulations for readers in the USA. This journal has been registered with the Copyright Clearance Center, Inc. Consent is given for copying of articles for personal or internal use, or for the personal use of specific clients. This consent is given on the condition that the copier pays through the Center the per-copy fee stated in the code on the first page of each article for copying beyond that permitted by Sections 107 or 108 of the US Copyright Law. The appropriate fee should be forwarded with a copy of the first page of the article to the Copyright Clearance Center, Inc., 27 Congress Street, Salem, MA 01970, USA. If no code appears in an article, the author has not given broad consent to copy and permission to copy must be obtained directly from the author. All articles published prior to 1980 may be copied for a per-copy fee of US$ 2.25, also payable through the Center. This consent does not extend to other kinds of copying, such as for general distribution, resale, advertising and promotion purposes, or for creating new collective works. Special written permission must be obtained from the publisher for such copying.

No responsibility is assumed by the Publisher for any injury and/or damage to persons or property as a matter of products liability, negligence or otherwise, or from any use or operation of any methods, products, instructions or ideas contained in the materials herein. Because of rapid advances in the medical sciences, the Publisher recommends that independent verification of diagnoses and drug dosages should be made.

Although all advertising material is expected to conform to ethical (medical) standards, inclusion in this publication does not constitute a guarantee or endorsement of the quality or value of such product or of the claims made of it by its manufacturer.

This issue is printed on acid-free paper.

Printed in the Netherlands

SYMPOSIUM ISSUE

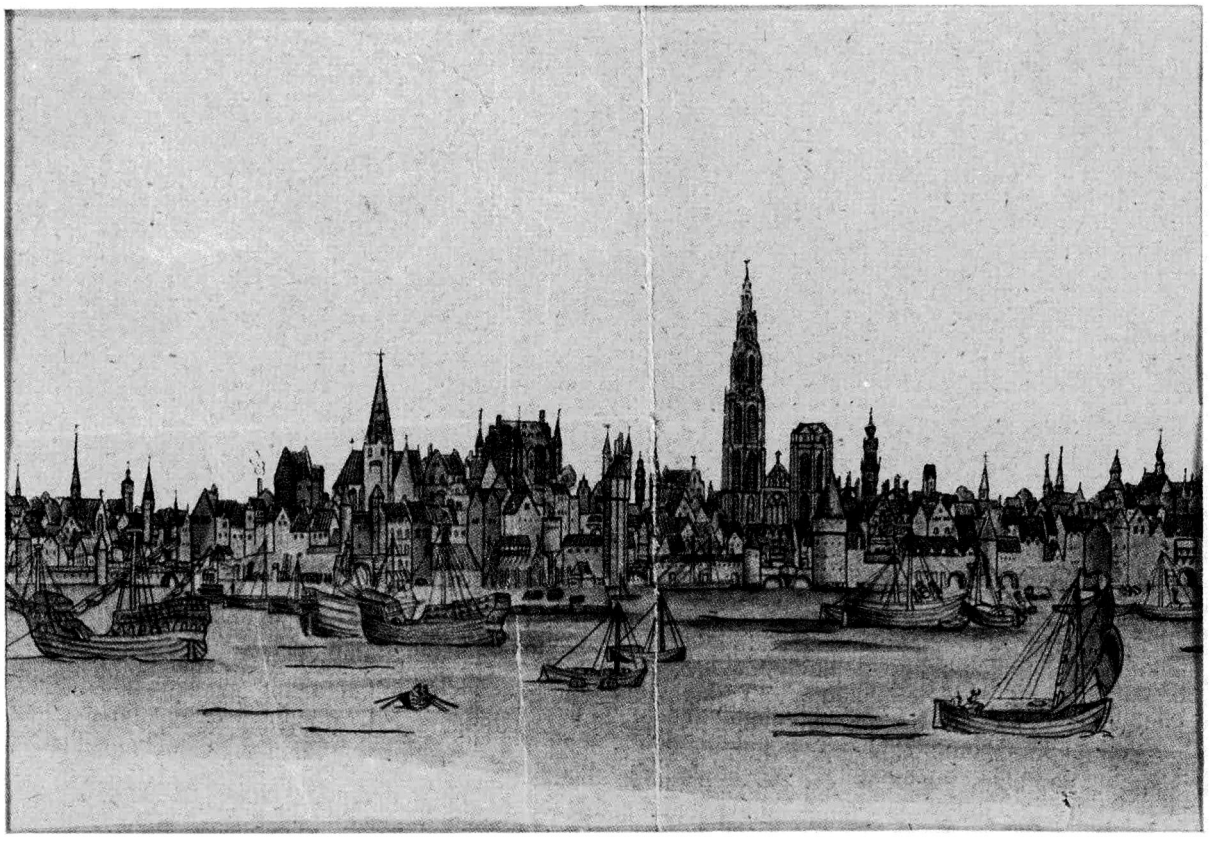

SECOND INTERNATIONAL SYMPOSIUM ON HYPHENATED TECHNIQUES IN CHROMATOGRAPHY

Antwerp (Belgium), February 18–21, 1992

Guest Editor

R. SMITS

(Antwerp)

VOL. 626, NO. 1 JOURNAL OF CHROMATOGRAPHY DECEMBER 16, 1992

CONTENTS

ห้องสมุดกรมวิทยาศาสตร์บริการ
10 มี.ค. 2536

Journal of Chromatography, 626 (1992) 1
Elsevier Science Publishers B.V., Amsterdam

CHROM. 24 579

Preface

The *Second International Symposium on Hyphenated Techniques in Chromatography* (HTC 2) was held at the University of Antwerp (UIA) on February 19th–21st, 1992. Like the previous meeting, held in 1990 in the same place, it was attended by about 170 participants from 17 different countries, mostly from Western Europe and the USA; 32 companies exhibited instruments, books and supplies.

The symposium was preceded by a series of workshops on supercritical fluid extraction–supercritical fluid chromatography, liquid chromatography–gas chromatography, gas chromatography–mass spectrometry, gas chromatography–Fourier transform infrared spectroscopy and gas chromatography–atomic emission detection.

The symposium was organized by the Working Party on Chromatography of the Royal Flemish Chemical Society (KVCV), with the valuable financial support of the Nationaal Fonds voor Wetenschappelijk Onderzoek (NFWO) and an important number of sponsoring companies. The organizing committee [R. Senten, R. Smits (Chairman) and P. van Hee] was aided by an advisory international scientific committee, consisting of F. Adams, K. D. Bartle, C. A. Cramers, K. Grob, D. L. Massart (Chairman) and P. Sandra.

Twenty-five lectures and 40 posters covered the most important fundamental aspects, instrumental developments and applications of the various hyphenated chromatographic techniques. The main topics of the three sessions were hyphenated supercritical fluid, gas and fluid chromatography, but attention was also paid to coupled counter-current and thin-layer chromatography and to capillary electrophoresis. Excellent reviews on the art of hyphenating different techniques were presented by Adams, Bartle, Brinckman, Brinkman, Cortes, Cramers, Fell, Greibrokk, Grob, Markides, Rosset, Sandra and Van der Greef.

This second symposium clearly showed that hyphenated chromatographic methods have evolved from a scientific research subject to a generally applied analytical technique, opening the road to further automation. Therefore, the *Third Symposium on Hyphenated Techniques in Chromatography* (HTC 3), to be held again in Antwerp (February 22nd–25th, 1994), will also be devoted to the design of hyphenated, on- and at-line chromatographic analysers.

(Antwerp, Belgium)

Robert Smits
Symposium Chairman

Journal of Chromatography, 626 (1992) 3–23
Elsevier Science Publishers B.V., Amsterdam

CHROM. 24 443

Review

Developments in multidimensional separation systems

Hernan J. Cortes

The Dow Chemical Company, Analytical Sciences, 1897B Building, Midland, MI, 48667 (USA)

ABSTRACT

Coupled-column systems in a multidimensional mode are increasingly used in order to obtain greater selectivity and sensitivity for the determination of trace components in complex matrices, and to increase the information content of an analysis in the characterization of complex samples. A review of the various strategies used in chromatography to couple orthogonal separation stages is presented, with emphasis on instrumental design and the role of miniaturization.

CONTENTS

1. INTRODUCTION

Single-stage (linear) chromatographic systems offer high resolving power, which is essential for the analysis of complex samples and the determination of trace-level impurities in a wide variety of complex matrices. With efforts placed in obtaining lower limits of detection in increasingly complex samples, stringent demands are being placed on the resolving power of chromatographic systems. Increases in resolution can be achieved by variations in the plate number, N, selectivity, α, or capacity factor, k'; however, adjustment of the capacity factor has a limited influence on resolution, (and only at low values); large numbers of theoretical plates can be realized using the technology available, but because resolution does not increase as greatly by the generation of further plates, increasing column

Correspondence to: Dr. H. J. Cortes, The Dow Chemical Company, Analytical Sciences, 1897B Building, Midland, MI 48667, USA.

length often yields marginal increases in resolution with the corresponding increase of analysis time to unacceptable levels. Since selectivity has the greatest influence on resolution, it is therefore the variable that attracts the most attention.

The limitations of single stage separation systems have been recognized for many years, and in order to describe separations of a multicomponent mixture, Giddings introduced the concept of peak capacity [1], which is defined as the maximum number of components, n, that can be placed side by side in the available separation space with a given resolution which satisfies the analytical goals [2], and is given by the following equation for unit resolution:

$$n = (1 + N^{1/2}/r) \ln (1 + k'_i) \quad (1)$$

where r = the number of standard deviations taken as equaling the peak width (typically 4), and k'_i = the capacity factor of the last peak in a series.

Modern high-resolution chromatographic systems yield peak capacities which are calculated to be in the range of 100–300. These results would appear adequate to resolve components in a mixture where the number of components, m, is less than the peak capacity of the system; however, components in a complex mixture are usually not uniformly distributed, and appear randomly, overlapping each other. Giddings and Davis [3] developed the statistical model of overlap to study the seriousness of said component overlap, which becomes apparent when the number of visible peaks, V, in a chromatogram is estimated by the following equation:

$$V = me^{-m/n} \quad (2)$$

providing that n is chosen as the value corresponding to a resolution of 0.5. Assuming that the number of components in a mixture can be estimated (and in many cases, this cannot be done), and in the case in which the number of components equals the peak capacity of the system used, the maximum number of visible peaks will be equivalent to 37% of the system's peak capacity. Further, the number of peaks in a chromatogram which represent a single component, S, is given by:

$$S = me^{-2m/n} \quad (3)$$

which yields a value of only 18% of the peak capacity, using the conditions described above.

These calculations help us to understand the limitations encountered in the separation of components in a complex matrix, even in cases where single column (linear) chromatographic systems are operated close to the theoretical limits [4].

A practical means of effecting changes in resolution is the introduction of a different fundamental mechanism of interaction by the use of two (or more) separation stages (multidimensional chromatography, or coupled column chromatography). In order to obtain the maximum benefit from multidimensional chromatographic systems, the basic mechanisms controlling separation in each dimension should be different. That is, the system should be non-redundant [5], otherwise, for a column chromatographic system the total peak capacity is given by:

$$n_{tot} = x^{1/2}n \quad (4)$$

where x = number of identical columns used, yielding a coupled system which is only equivalent to a longer linear system. In addition to coupling separation systems with different separation mechanisms, Giddings has suggested the additional requirement that when two components are resolved in the first separation step, they remain resolved throughout the process [3]. A representation of the peak capacity of a planar two-dimensional system is presented in Fig. 1. The maximum peak capacity attainable in a system of this type is given by the product of the peak capacities of each dimension

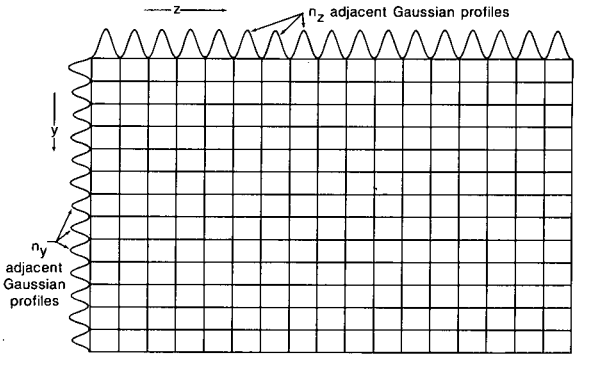

Fig. 1. The peak capacity of a two-dimensional system, represented by the number of boxes is approximately equal to the product of the peak capacities n_z and n_y generated along the two individual axes, as represented by the number of adjacent gaussian profiles [6].

(discounting the additional band broadening of the migrating components in the second dimension [6]). In column chromatography, utilization of the total available separation space would require a large number of secondary columns, so that all the sample cuts taken while eluting in the first dimension could be transferred for subsequent separations. In practice however, only definite fractions of the separation obtained in the first dimension are studied in detail at one time, due in part to the difficulty and awkwardness of a system composed of a multitude of secondary columns. The use of these types of systems is conventionally termed coupled-column chromatography, and their total peak capacities vary according to its design. Total peak capacities can range from $2n$ for two columns of correlated selectivities to a theoretical maximum of n^2 for columns of independent selectivities. A representation of the separation space utilized with such a system is presented in Fig. 2.

Multi-stage separations are historically common in the fields of trace analysis, where samples typically contain a large number and variety of components that can potentially interfere with the analytes of interest. Typically, samples are pretreated to reduce the complexity of the original sample by separating some fraction of the matrix from the analytes of interest. Separation schemes for sample pretreatment can include solvent extractions, the use of small packed beds, membranes, or gravity-flow liquid chromatographic columns, for example. Such schemes, where sample preparation and analytical columns are not physically coupled and manual steps are involved, can be grouped under the class of off-line multidimensional separations. In the practice of off-line multidimensional separations, it is recognized that clean-up techniques such as those described above can be time consuming, operator intensive, and can also be difficult to automate and reproduce. Of greater importance in areas of quantitative trace analysis, is the fact that off-line sample pretreatments can be susceptible to solute loss and contamination.

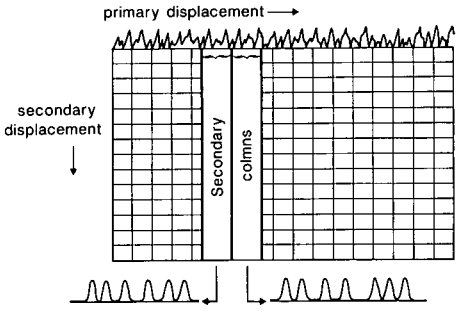

Fig. 2. Superposition of two adjacent secondary columns (represented by wide vertical bars) of a coupled column system on the two-dimensional separation matrix of Fig. 1. The columns are shown diagrammatically with a width proportional to the number of peaks shunted from the primary displacement (column) [6].

An alternative approach to increase in selectivity is the use of several separation stages in an on-line mode, where two (or more) separation systems of relatively high efficiency are coupled together via the use of traps, valves and other means.

2. THE ROLE OF MICROCOLUMNS IN MULTIDIMENSIONAL SEPARATIONS

Coupled column systems can utilize combinations of both packed and open tubular chromatographic columns. Coupled column chromatography has been practiced using gas chromatography (GC), supercritical fluid chromatography (SFC), liquid chromatography (LC), and combinations of these, such as LC–GC, LC–SFC, or LC coupled to capillary zone electrophoresis. Supercritical fluid extractions, although not a chromatographic technique in the rigorous sense, has also been used as a preliminary separation stage with other chromatographic systems. Coupled techniques can benefit from miniaturization. The advantages of using capillary columns for GC, for example, are already well documented [7]. In the following sections, a short review of the various separation modes will be discussed. Due to the large volume of information available in the literature regarding coupled column techniques, this review is not intended to be exhaustive, but is intended to point out the major advantages of each separation strategy and summarize the important contributions, with special emphasis on the use of microcolumns.

3. MICROCOLUMN LIQUID CHROMATOGRAPHY

Miniaturization of an LC system was initially investigated in the 1970s [8–12] with the recognized benefits of reduced consumption of mobile and sta-

ห้องสมุดกลางงานวิทยาศาสตร์บริการ

tionary phases, increased mass sensitivity with concentration-sensitive detectors, high separation efficiencies and posibility of new detection techniques [13–15]. The technique has been reviewed extensively [16–19] and the purpose of this section is to detail the salient merits of microcolumn LC as they apply to the on-line coupling to other separation modes.

The reduction of the internal diameter of the LC column utilized for multidimensional chromatographic applications to microcolumn dimensions (<1.0 mm) introduces various significant advantages to the technique. Elution volumes of microcolumns are more closely matched to capillary column requirements than conventional columns, since successful interfacing requires that broadening of fractions introduced in the second dimension remain minimal. Difficulties in interfacing chromatographic techniques are typically a direct result of the volume and nature of the mobile phase used in the first dimension. The volume of eluent used in microcolumn LC is considerably reduced, which means the solutes of interest are diluted in much less eluent (lower volumetric dispersion). As an example, the peak volume (V_p) eluting from an LC column can be calculated by the following equation [17]:

$$V_p = \pi d_c^2 \varepsilon L(1 + k')/N^{1/2} \quad (5)$$

where d_c = column diameter, ε = column porosity and L = column length. The peak volume of a compound eluting from a typical microcolumn of 25 cm × 250 μm I.D., a column porosity of 0.5 and at a k' of 3 with an efficiency of 25 000 plates can be calculated as *ca.* 0.6 μl; a significant reduction when compared to the peak volume given by a conventional column (4.6 mm I.D.) under the same conditions, *ca.* 200 μl. In practice, the peak volumes observed at the detector are somewhat larger, due to the extra-column band broadening contributions of the injector, connections, and detector cell. Nevertheless, this reduction in peak volume can be critical, as it minimizes the problems encountered in the introduction of large volumes of solvent into other separation techniques, such as capillary GC. Because of this peak volume reduction, much larger sections of the LC chromatogram can be introduced into the subsequent separation stages allowing quantitative transfer of the components of interest, resulting in greater reproducibility and better opportunity for quantitative analyses. Microcolums can be effectively prepared at lengths greater than the conventional 25 cm, and greater total column efficiencies can be obtained [20,21].

The column diameter has been shown to have an effect on the efficiency of packed-column systems [22,23]. Fluctuations in the packing density which may occur across the column diameter [24], and temperature gradients generated due to viscous friction [25], may be detrimental contributions which can be minimized by reducing the column diameter. (Heat generated due to viscous friction is expected to be dissipated faster with reduced diameter columns).

The conditions for packing microcolumns for LC reproducibly have been described [26–29]. Typically, columns are packed using a slurry in a suitable solvent and pressures in the range of 400 to 680 atm. Various techniques have been developed to hold the particles in the column and at the same time, minimize flow resistance, such as the use of glass wool [30], wires [31], porous filters [32] and porous polymer discs [33]. In order to simplify the preparation of bed supports for microcolumns, a porous ceramic frit was developed, which we found to yield acceptable performance in terms of ease of preparation and efficiency of the columns used [34].

A perceived limitation of using microcolumns for LC in the context of coupled column separations is the lower sample capacity of the column, which is proportional to the surface area. The effect of sample mass injected on plate height observed at various capacity factors is illustrated in Fig. 3. The results were obtained at linear velocities above the optimum, and therefore the plate heights observed were not as low as could be theoretically or practically obtained. Higher plate heights were observed for components with lower k', which suggests extra-column band broadening, as these effects are expected to be more apparent at lower values of k'. Little change was observed for up to 300 ng of material introduced.

The maximum volume that can be injected into a micro LC column has been estimated [17], and is in the range of 60–200 nl for columns dimensions normally used. In practice, high volume loads can be applied if the analytes are dissolved in a weaker solvent than the mobile phase (peak focusing). This procedure allows introduction of relatively large

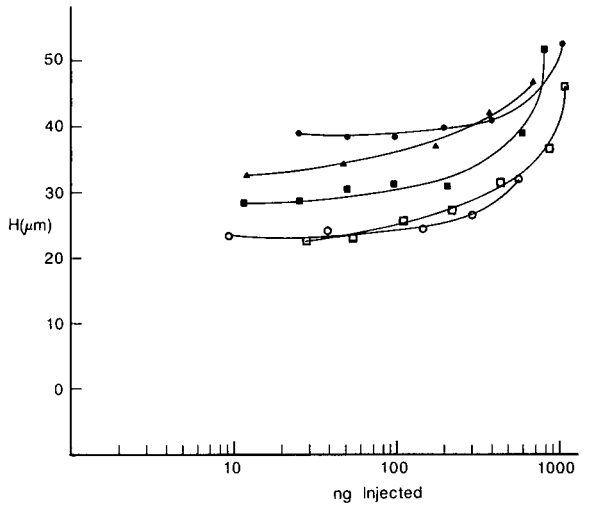

Fig. 3. Plate height (H) *vs.* amount injected at various values of k'. Column: 12 cm × 250 mm I.D. packed with Zorbax ODS. Eluent: acetonitrile–water (70:30). Flow: 5 ml/min. Injection: 60 nl. Detection: 254 nm. ● = Phenol (k' = 0.48); ▲ = acetophenone (k' = 1.45); ■ = benzophenone (k' = 2.33); ○ = biphenyl (k' = 4.23); □ = dibenzofuran (k' = 4.59).

volumes without excessive loss in efficiency, as shown for microcolumns by Duquet *et al.* [35], who demonstrated that 10-μl volumes could be injected into a microcolumn in this manner without serious loss in efficiency. More recently, introduction of 10 ml into a microcolumn without detrimental effects was demonstrated [36].

In the use of microcolumns for LC in multidimensional separations, the microcolumn is used as a highly efficient pre-separation (clean-up) step or a chemical class fractionation, and therefore, a limited decrease in efficiency due to large injection volumes can be tolerated. Problems of peak band broadening and solute overloading in the LC are seldom critical to the subsequent separation stage. Samples which may contain higher-molecular-mass material, or components which may be irreversibly adsorbed can, as a last resort, be introduced into the LC system. In our experience, when the head of LC the column becomes severely contaminated, removing a short section at the front of the column usually restores the column to nearly its original performance. Another alternative is to backflush the LC column to remove undesirable components prior to subsequent injections.

Various modes of coupled column systems have been developed, the advantages and constraints of which are summarized in the following sections.

4. MULTIDIMENSIONAL GAS CHROMATOGRAPHY

The use of multidimensional GC was originally reported in 1963 [37] and has been under development and use since. Typically, two GC columns which can be packed, open tubular, or combinations of both, are coupled together via switching valves or pneumatic control [38]. Due to the large heat capacity of metal valves, and the possibilities of adsorption or catalytic reactions in the metal parts of a valve [39], valveless switching systems are more commonly used and are based on careful balancing of pressures along the system [38] or flow control [40], and are commonly refered to as Deans switching. Some years later, Schomburg and Weeke [41] developed a live-T-interface which reduces some of the problems encountered in balancing pressures along the multidimensional arrangement.

The use of multidimensional chromatography in the gas phase is perhaps the most widely used multidimensional technique due to the following reasons: mobile phase compatibility, availability of a wide range of sensitive and selective detectors, commercially available instrumentation or add-on accessories and conversion kits to carry out switching operations, and highest total theoretical peak capacity when using columns of capillary dimensions. Some of the disadvantages of multidimensional GC are that components must be sufficiently volatile to be transported in the gas phase (although derivatization techniques alleviate some of these problems [42]); the need for a relatively clean sample so as not to deteriorate the performance of the primary column by contamination with non-volatile or highly polar compounds (particularly when the primary separation is performed using a column of capillary dimensions), the lack of selectivity dependance on mobile phase composition and the limited selectivity differences which are obtained when using common stationary phases. For example, separations of components using stationary phases with very different characteristics, such as methylsilicone and cyanopropyl, are still highly correlated by boiling point. For this reason, selectivity tuning [43] should be considered an important tool for the selection of conditions suitable for multidimensional GC. Ex-

amples of coupled column GC in the petroleum [44,45] geochemical [46], and environmental [47] fields illustrate the utility of multidimensional GC [48,49].

5. MULTIDIMENSIONAL LIQUID CHROMATOGRAPHY

In contrast to GC, LC offers extended flexibility, since the mobile phase composition can be adjusted in order to obtain enhanced resolution. The greater selectivity differences between columns which are attainable due to the wide variety of separation modes available, such as for example adsorption, partition, size-exclusion, ion-exchange or affinity chromatography make multidimensional LC a very powerful tool. Highly polar and non-volatile compounds can be separated using most of the above modes, while relatively complex samples can be introduced without severely deteriorating the performance of the system. Some limitations are that the total theoretical peak capacities in multidimensional LC are lower than in multidimensional GC, detection systems are generally not as sensitive or universal as in GC, and mobile phase incompatibilities can limit the applicability of multidimensional LC. Most separation modes can be easily interfaced when the mobile phases used are compatible. The interfacing of normal-phase and reversed-phase systems is particularly difficult, due to the mobile phase immiscibilities. Two approaches have been used to overcome this problem. Sonnefeld *et al.* [50] used a system in which the fraction of interest was transferred from the first (normal-phase) column to a packed precolumn, and the normal-phase eluent was removed by passage of an inert gas and vacuum. Once the solvent was removed, the precolumn was desorbed using a reversed-phase eluent and transfered to the second (reversed-phase) analytical column. More recently Takeuchi *et al.* [51] used a microcolumn in the first dimension and a conventional-size column in the second dimension to interface normal phase and reversed-phase separations. Due to the reduced peak volume generated by the use of microcolumns, solvent removal was not required.

Another example of the flexibility attainable by the use of microcolumns is in the coupling of size-exclusion chromatography (SEC) to reversed-phase chromatography for the determination of polymer additives [52], as illustrated in Figs. 4 and 5. In this case, the use of a conventional-size column in the first dimension would have yielded a fraction containing the additives of interest in a volume of *ca.* 1 ml. Introduction of such a large volume of tetrahydrofuran into an aqueous mobile phase would have yielded broadened and distorted peaks. Because of the lowered volumetric dispersion obtained by the use of microcolumns, the additive fraction obtained was only 6 μl, a volume which was easily introduced into the reversed-phase system without peak shape deterioration or resolution losses.

Examples of multidimensional LC in the petroleum [53], pharmaceutical [54], biomedical [55] and toxicological [56] areas have been presented, and a review of the technique was recently published [57].

6. MULTIDIMENSIONAL LIQUID CHROMATOGRAPHY–CAPILLARY ELECTROPHORESIS

The coupling of LC and capillary electrophoresis (CE) was recently described by Bushey and Jorgenson [58,59]. As CE operates under fundamentally different separation mechanisms, the combination with LC represents a true orthogonal system. A reversed-phase LC system was used in the first dimension, and eluting fractions were introduced and further separated on a CE system, which was used to separate peptide standards and fluorescently labeled peptide fragments from a tryptic digest of ovalbumin [58] and to compare tryptic digest fingerprints of horse heart cytochrome *c* and bovine heart cytochrome *c* [59]. A diagram of the experimental

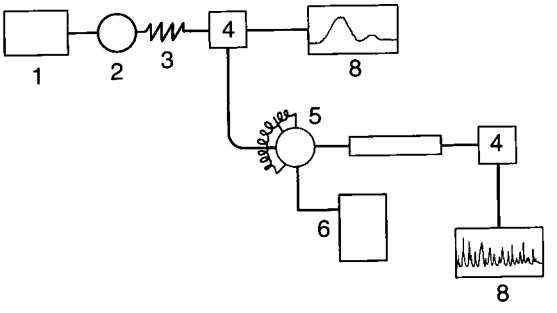

Fig. 4. Schematic diagram of micro SEC–LC system. 1 = Micro LC pump; 2 = injection valve; 3 = micro SEC column; 4 = detector; 5 = switching valve; 6 = LC pump; 7 = LC column; 8 = recording devices [52].

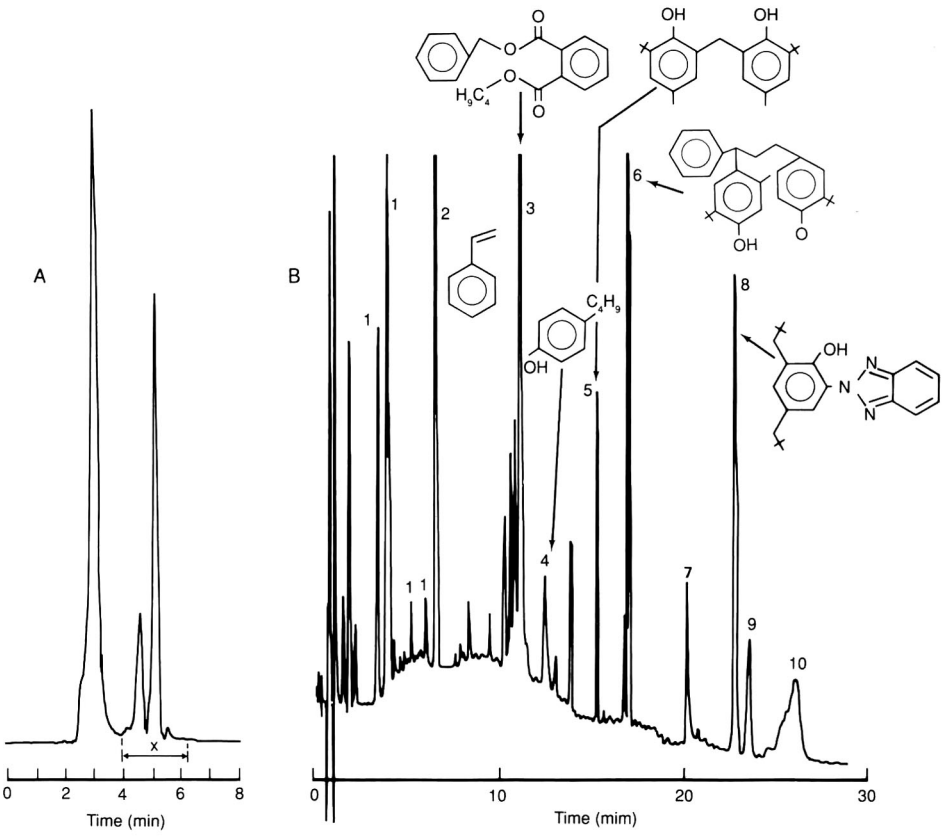

Fig. 5. Micro SEC–LC chromatograms of acrylonitrile–butadiene–styrene sample. (A) Micro SEC. Column: 30 cm × 250 mm I.D. fused silica packed with PL-GEL, 50 Å pore-size, 5 mm particle diameter. Eluent: tetrahydrofuran. Flow: 2.0 ml/min. Injection size: 200 nl. Detection: UV at 254 nm. x = polymer additive fraction transfered to LC system (*ca.* 6 μl). (B) LC chromatogram of introduced fraction. Column: 15 cm × 4.6 mm I.D. Nova-Pak C_{18}. Eluent: acetonitrile–water (60:40) to (95:5) in 15 min gradient. Flow: 1.5 ml/min. Detection: UV at 214 nm. Peaks: 1 = styrene–acrylonitrile oligomers; 2 = styrene; 3 = benzylbutyl phthalate; 4 = nonylphenol isomers; 5 = Vanox 2246; 6 = Topanol CA; 7 = unknown; 8 = Tinuvin 328; 9 = Irganox 1076; 10 = unknown [52].

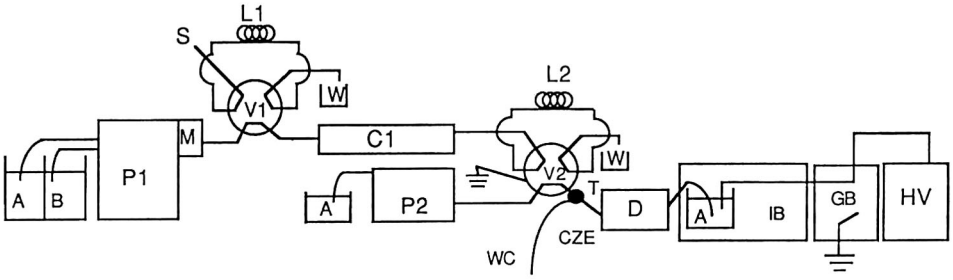

Fig. 6. Schematic of two-dimensional high-performance LC–CE instrumentation. A and B = buffer A and acetonitrile respectively; P1 = Brownlee microgradient syringe pump; M = 52-μl mixer; V1 = Valco six-port manual injection valve; S = injection syringe; L1 = 50-μl loop; C1 = reversed-phase column; P2 = Waters Assoc. Model 6000A piston pump; V2 = grounded six-port electrically actuated Valco valve; L2 = 10-μl loop; CZE = CE capillary; T = Valco low-dead-volume tee; WC = waste capillary; D = fluorescence detector; IB = interlock box; GB = grounding box; HV = Spellman high-voltage power supply; W = waste [59].

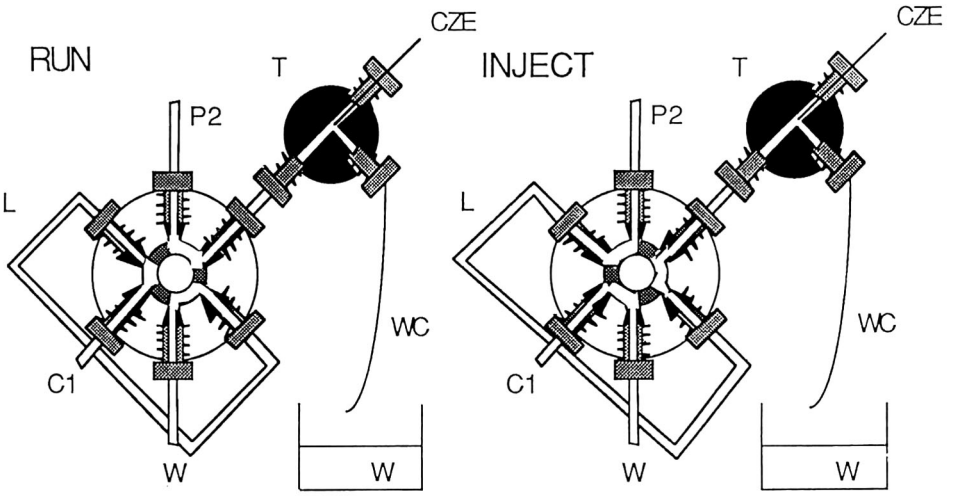

Fig. 7. LC–CE coupling: valve connections. C1 = Reversed-phase (RP) high-performance LC column; P2 = pump 2; L = loop; CZE = capillary electrophoresis fused-silica capillary; WC = waste capillary; T = Valco low-dead volume tee; W = waste [59].

setup is presented in Fig. 6, while a detail of the valving configuration is presented in Fig. 7. In the operation of the system, the LC effluent fills a loop, and the contents are passed through a tee where the end of the CE capillary is positioned. Sample is introduced into the CE system by electromigration. By using reduced diameter capillaries, high voltage drops per unit length could be applied, yielding increased efficiency and shorter analysis times. A three-dimensional representation of the separations obtained is presented in Fig. 8.

7. MULTIDIMENSIONAL SUPERCRITICAL FLUID CHROMATOGRAPHY

Supercritical fluids have physical properties between those of liquids and gases, and as mobile phases for chromatography, solvent strength is closely dependent on density [60]. Therefore, variations in density allow chromatographic behaviour which becomes more "GC-like" or "LC-like" depending on the pressure and temperature conditions chosen. The coupling of SFC to capillary GC (or another SFC) offers an advantage in that supercritical fluids are generally more compatible than liquids, as they typically decompress into gases under GC conditions. However, to a large extent, selectivity is controlled by the stationary phases used. The increased use of polar modifiers [61] and the development of stationary phases with unique characteristics, such as liquid crystalline phases [62] and chiral stationary phases [63], suggest great potential for resolution of complex samples using SFC in a multidimensional mode. Various examples of the application of multidimensional SFC to the separation of a complex matrices have been presented [64–

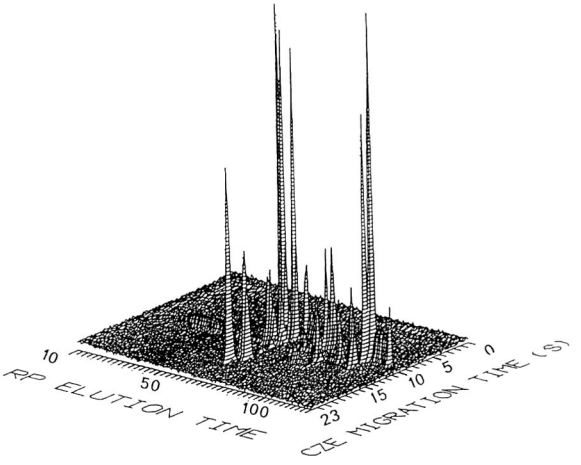

Fig. 8. Three-dimensional plot of horse heart cytochrome *c*. Obtained with 15 μm I.D. capillary. CE injections: −1 kV, 5 s; CE runs: −28 kV, 0.5 min; P1 flow-rate: 20 μl/min; P2 flow-rate: 0.3 ml/min; CE capillary 6.5 cm to detector, 26 cm overall. Eight points per second collected. Every other point displayed for injections 20–245 [59].

66]. Of particular interest, the analysis of a bird gullet extract utilizing columns of capillary dimensions was published [67] as well as the analysis of a complex hydrocarbon matrix using packed microcolumns [68].

8. MULTIDIMENSIONAL LIQUID CHROMATOGRAPHY CAPILLARY GAS CHROMATOGRAPHY

The coupling of a liquid chromatograph to a gas chromatograph in an on-line mode offers another, different perspective on multidimensional separations. As with LC–CE, an orthogonal operation system is realized. Selectivities that are difficult to obtain using gas or liquid phases alone are in principle possible using the wide range of variables available, such as mobile and stationary phases, temperature profiles and detector systems of the two techniques. A system of this type combines the selectivity of LC with the efficiency and sensitivity of GC, yielding high peak capacities. In the application of this technology, the LC can act as an efficient clean up step, yielding a much less complex fraction for subsequent GC analysis, or as a chemical class fractionation step, where group types can be transferred to the GC for individual separation of the components within each class. LC–GC also provides two independent retention data sets, which can be helpful in confirming the identity of unknown components.

Matching LC and GC presents several challenges, since the two separation techniques operate in phases which are in two different physical states, and the relatively large volume of LC effluent must be made compatible with the gas chromatograph. As discussed above, the peak elution volumes of a liquid chromatograph can range from a few microliters when using LC columns of less than 1 mm diameter (microcolumns) up to several milliliters when using conventional size columns. In either case, the volumes introduced are larger than can normally be tolerated in capillary GC using on-column injection techniques. The successful interfacing of LC and GC involves the steps of isolation of the fraction containing the components of interest, transfer of the isolated fraction to the gas chromatograph and volatilization of the solvent and of the components of interest.

The basic approaches which have been used to introduce effluent from a liquid chromatograph to a gas chromatograph are to introduce a sufficiently small volume of the peak of interest from the LC so that the injected profiles of the components of interest are not distorted by the large volumes of solvent [69], to develop introduction techniques which allow large volumes of effluent to be introduced into the GC [70,71] and to reduce the LC column diameter in order to elute the components of interest in a smaller volume [71].

Effluent from the LC system can be directed to the GC system by interposing a switching valve (four- or six-port) between the LC and the GC uncoated inlet/capillary column. The components of interest are bypassed to waste when the valve is in one position, and transferred to the GC injector (or directly to the uncoated inlet) when the valve is switched to the alternate position. After the transfer is complete, the connecting tube between the valve and GC injector may be backflushed to decrease the probability of contamination of the next section transfered from the LC column. If the system does not involve the GC injector, the transfer line is flushed by the eluting mobile phase and backflushing is not required. The nomenclature of "stop-flow introduction" is suggested for the process of interrupting carrier gas flow to the uncoated inlet/capillary GC column arrangement while the LC effluent is introduced. The time period for which carrier gas flow is interrupted can be relatively long, as when the effluent is introduced by the LC pump, or relatively short, as when the effluent is trapped in an external valve loop and introduced via carrier gas flow pushing the contents of the loop into the GC system. In either case the main variables that affect the quality of the results obtained are the introduction temperature of the effluent and the introduction rate. The introduction of solvent into the GC system under conditions in which carrier gas is introduced at the same time as the effluent from the LC system should be considered to be different, and for clarity purposes we suggest the term "simultaneous introduction".

As mentioned above, stop-flow introduction can also be accomplished using a loop injection. A six- or ten-port valve is connected to the LC detector outlet, and the components are introduced into a fixed loop of known volume, corresponding to the volume of the fraction of interest. When the valve is

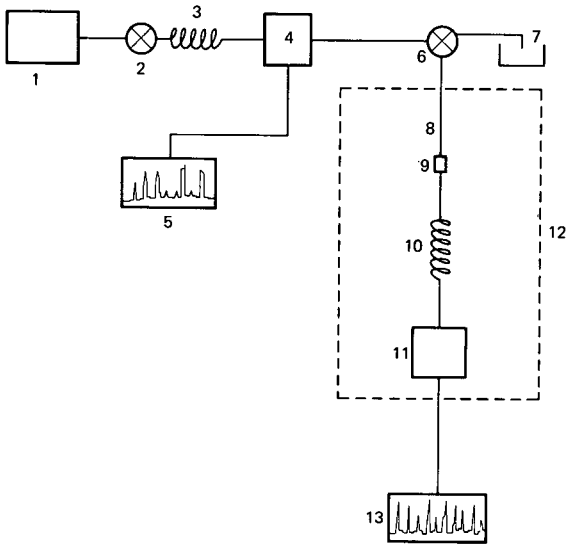

Fig. 9. Schematic diagram of LC–GC system. 1 = pump; 2 = injector; 3 = LC column; 4 = UV detector; 5 = recorder; 6 = switching valve; 7 = waste; 8 = uncoated inlet; 9 = butt connector; 10 = capillary GC column; 11 = detector; 12 = GC oven; 13 = recorder [71].

switched, the carrier gas flushes the sample loop and forces the liquid plug into the GC column. If a ten-port switching valve is used, a second loop can be added to either introduce other components into the GC column or to flush the sample loop if the second loop is filled with solvent in order to decrease contamination.

A schematic diagram of an LC–GC system is presented in Fig. 9, while valving configurations used to couple the two separation systems are presented in Fig. 10.

A number of applications of LC–GC have been published, where the primary separation step is conducted using LC columns of conventional dimensions [72–87]. The ease of use of conventional-size columns for LC demands however an increase in complexity of the interface design [88,89] due to the effluent volumes involved, and precludes the use of reversed-phase (aqueous) systems [90]. Since a large majority of the LC separations performed today are done in the reversed-phase mode, this is an important limitation to the use of conventional size columns in the first dimension. In contrast, the use of microcolumns simplifies the liquid introduction process, allowing introduction of aqueous eluents without the severe difficulties encountered using conventional size columns [91–105]. Examples of such applications are the determination of an insecticide in a supercritical fluid extract of wheat, as shown in Fig. 11, and the determination of a herbicide in soil, presented in Fig. 12.

8.1. Quantitative determination of polymer additives

An example of the power of multidimensional

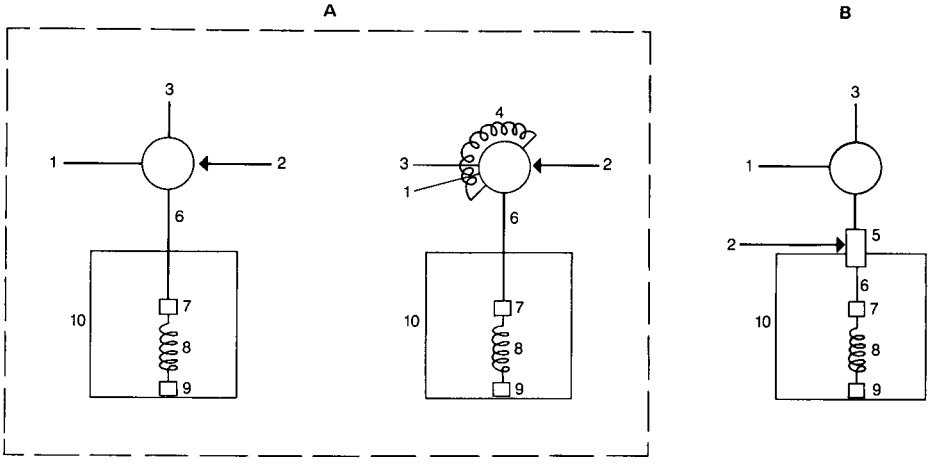

Fig. 10. Representation of LC–GC interfaces. (A) Stopped-flow introduction. (B) Simultaneous introduction. 1 = LC effluent; 2 = carrier gas; 3 = LC waste; 4 = external sample loop (volume equivalent to transfered section); 5 = GC injector; 6 = uncoated inlet; 7 = dead volume free connector; 8 = capillary GC column; 9 = detector; 10 = GC oven [102].

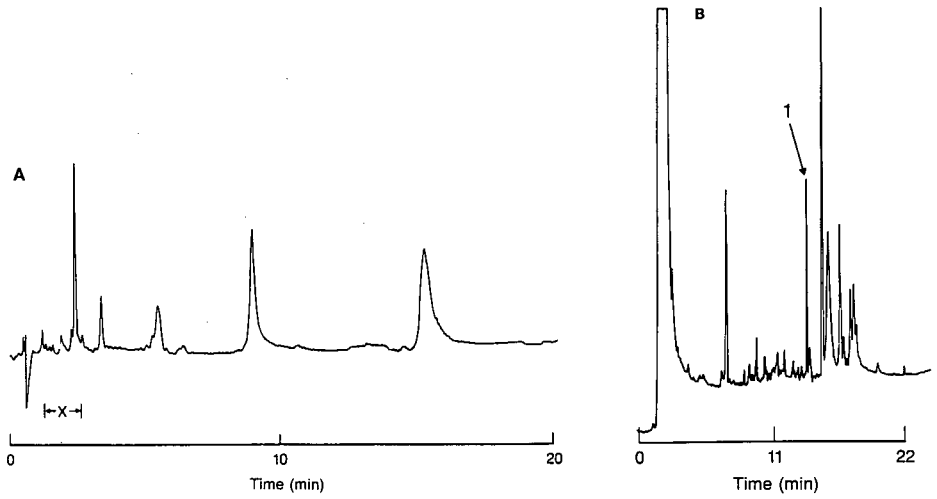

Fig. 11. LC–GC separations of supercritical fluid extract of wheat. (A) Micro LC. Column: 40 cm × 250 μm I.D. fused silica packed with Spherisorb ODS, 5 μm particle diameter; eluent: acetonitrile–water (85:15); flow: 6 μl/min; detection: UV at 214 nm; injection: 60 nl; X = fraction introduced into capillary GC. (B) Capillary GC of introduced fraction. Column: 30 m × 0.25 mm I.D. DB-5, 0.25 μm film thickness; oven uncoated inlet: 5 m × 0.25 mm I.D. undeactivated fused silica; temperature program: 115 to 270°C at 8°C/min; detection: electron capture; carrier: helium at 28 cm/s; peak 1 = chlorpyrifos methyl (50 ng/g) [95].

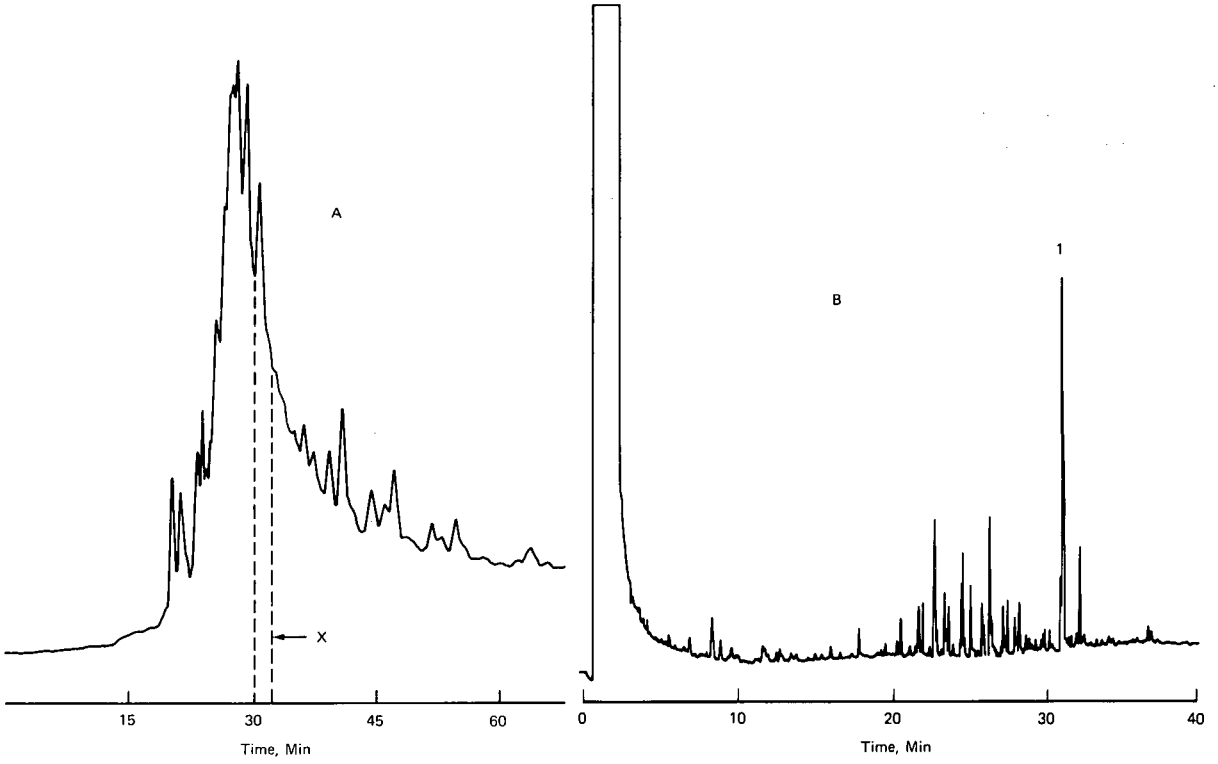

Fig. 12. Chromatograms of soil extract. (A) Micro LC. Column: 105 cm × 250 μm I.D. fused silica packed with Spherisorb ODS, 5-μm particle diameter; mobile phase: methanol–water (90:10); flow: 3.0 μl/min; detection: UV at 214 nm; injection: 200 nl; X = section introduced into the GC. (B) Capillary GC of introduced fraction. Column: 30 m × 0.25 mm I.D. J&W Carbowax, 0.25-μm film; uncoated inlet: 10 m × 0.25 mm I.D.; undeactivated fused silica; oven: 100°C 10 min, 5°C/min to 230°C; carrier: helium at 80 cm/s; detection: flame ionization; peak 1 = 2-chloro-N-isopropylacetanilide (14 μg/g) [92]

separations is in the field of polymer characterization. A variety of additives are typically incorporated into the polymer systems to enhance their enduse performance. Determination of the identity and levels of such additives is typically performed by isolation of the additives via soxhlet extraction, or by dissolving the polymer in a suitable solvent, followed by precipitation of the polymer and analysis of the supernatant using chromatographic techniques and identification via mass spectrometry. However, such sample preparation schemes may not yield accurate quantitative results, due to the solubility dependance of the additives and the probability of coprecipitation with the polymer.

An alternative analysis scheme is to separate the additive fraction from the polymer via microcolumn SEC, followed by on-line introduction into capillary GC with mass spectrometric detection [104]. The techniques developed were applied to a wide variety of commercial polymer products. The main advantage of such a system is that it eliminates the inherent losses when additives are separated from the polymers via other conventional techniques, in addition to minimizing sample analysis times. Typical chromatograms obtained using the technology described are presented in Fig. 13, while Table 1 represents a quantitative comparison of additive concentrations obtained using the precipitation approach and the multidimensional approach. As can be observed, additive losses were experienced using the precipitation approach [105].

8.2. *Characterization of non-volatile compounds*

In order to overcome one of the limitations of on-line coupled LC–GC, which is the requirement that components be sufficiently volatile to be transported in the carrier gas, an interface was designed which would allow the conversion of non-volatile species to volatile fragments. Alternative approaches are the use of off-line treatments such as derivatization [42], or on-line treatments, such as subjecting the analyte to postcolumn reactions [106].

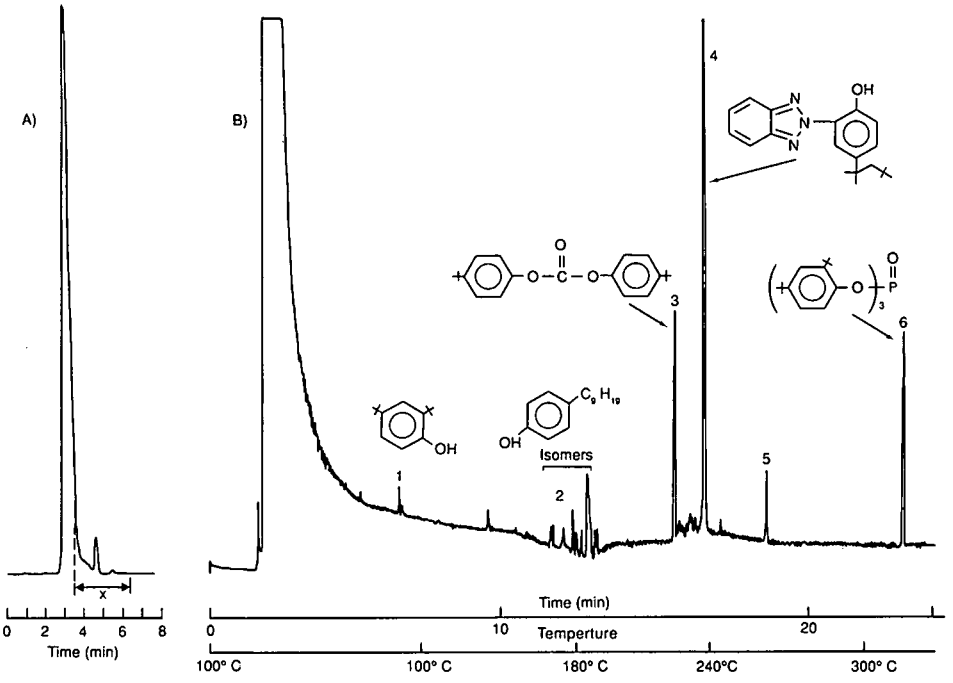

Fig. 13. Chromatograms of polycarbonate sample. (A) Micro SEC. (B) Capillary GC of introduced fraction. Micro SEC conditions as in Fig. 5. Column: 15 m × 0.25 mm I.D. DB-1, 0.25 μm film; uncoated inlet: 5 m × 0.32 mm I.D. deactivated fused silica; Temperature program: 100°C 8 min, 12°C/min to 350°C; detection: flame ionization; X = fraction introduced into capillary GC. Peaks: 1 = 2,4-di-*tert.*-butylphenol; 2 = nonylphenol isomers; 3 = di(4-*tert.*-butylphenyl) carbonate; 4 = Tinuvin 329; 5 = solvent impurity; 6 = Irgaphos 168 (oxidized) [104].

TABLE 1

POLYCARBONATE ADDITIVE ANALYSIS

R.S.D. = Relative standard deviation.

	Concentration (μg/g)	
	Precipitation (R.S.D. %)	Micro SEC–GC (R.S.D. %)
2,4-Di-*tert.*-butylphenol	60 (15)	80 (3.8)
Di-(4-*tert.*-butylphenyl) carbonate	620 (9.0)	630 (4.5)
Irgaphos 168	570 (9.5)	540 (6.3)
Tinuvin 329	2680 (7.9)	3530 (5.1)

The development of a pyrolysis interface to effect a postcolumn treatment of a non-volatile material (in this case a styrene–acrylonitrile copolymer) was published [107]. Fig. 14 represents a diagram of the multidimensional system while Fig. 15 represents details of the interface design.

Polymer characterization, in terms of composition *vs.* molecular mass is valuable information which aids in the understanding of polymerization chemistry. Some of the approaches used to obtain this type of information have included the use of adsorption chromatography [108,109], gradient elution LC [110,111], precipitation chromatography [112] or adsorption chromatography followed by size exclusion [113]. The analysis of compositional and structural heterogeneities of polymers by non-exclusion LC has also been reviewed [114].

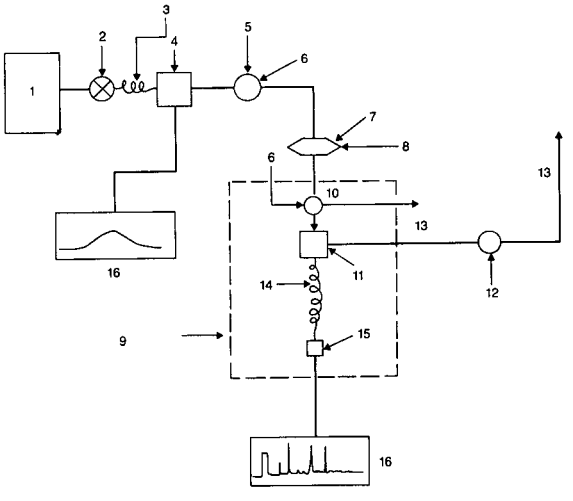

Fig. 14. Schematic diagram of on-line LC–pyrolysis–GC system. 1 = Pump; 2 = injection valve; 3 = micro LC column; 4 = detector; 5 = ten-port switching valve; 6 = carrier gas; 7 = interface; 8 = auxiliary carrier; 9 = GC oven; 10 = four-port switching valve; 11 = splitter; 12 = micro metering valve; 13 = vent; 14 = GC column; 15 = detector; 16 = recorder [107].

The characterization of a styrene–acrylonitrile copolymer was accomplished by separating the polymer via microcolumn SEC, transferring selected fractions of the molecular weight distribution to an interface, and subjecting the polymer in the sections selected to pyrolysis–GC, in order to determine the relative composition of the isolated fractions by the ratio of the monomeric composition obtained upon pyrolysis. A study of the variables influencing reproducibility, such as interface temperature, flow, and pyrolysis ribbon geometry were conducted [107]. Typical chromatograms obtained are presented in Fig. 16.

9. SUPERCRITICAL FLUID EXTRACTIONS

The application of multidimensional chromatography to the analysis of complex matrices helps to minimize sample pretreatment steps. Still, when the matrix to be analyzed is not totally soluble in a particular solvent, such as for example plant tissue, a preliminary step is necessary to obtain a solution suitable for subsequent introduction into the preliminary separation stage. Supercritical fluids offer potential advantages over liquid solvents to meet the sample preparation requirements. The solvent strength of supercritical fluids approach those of liquid solvents while having lower viscosities and higher solute diffusivities. Further, the solvent strength of a supercritical fluid increases with in-

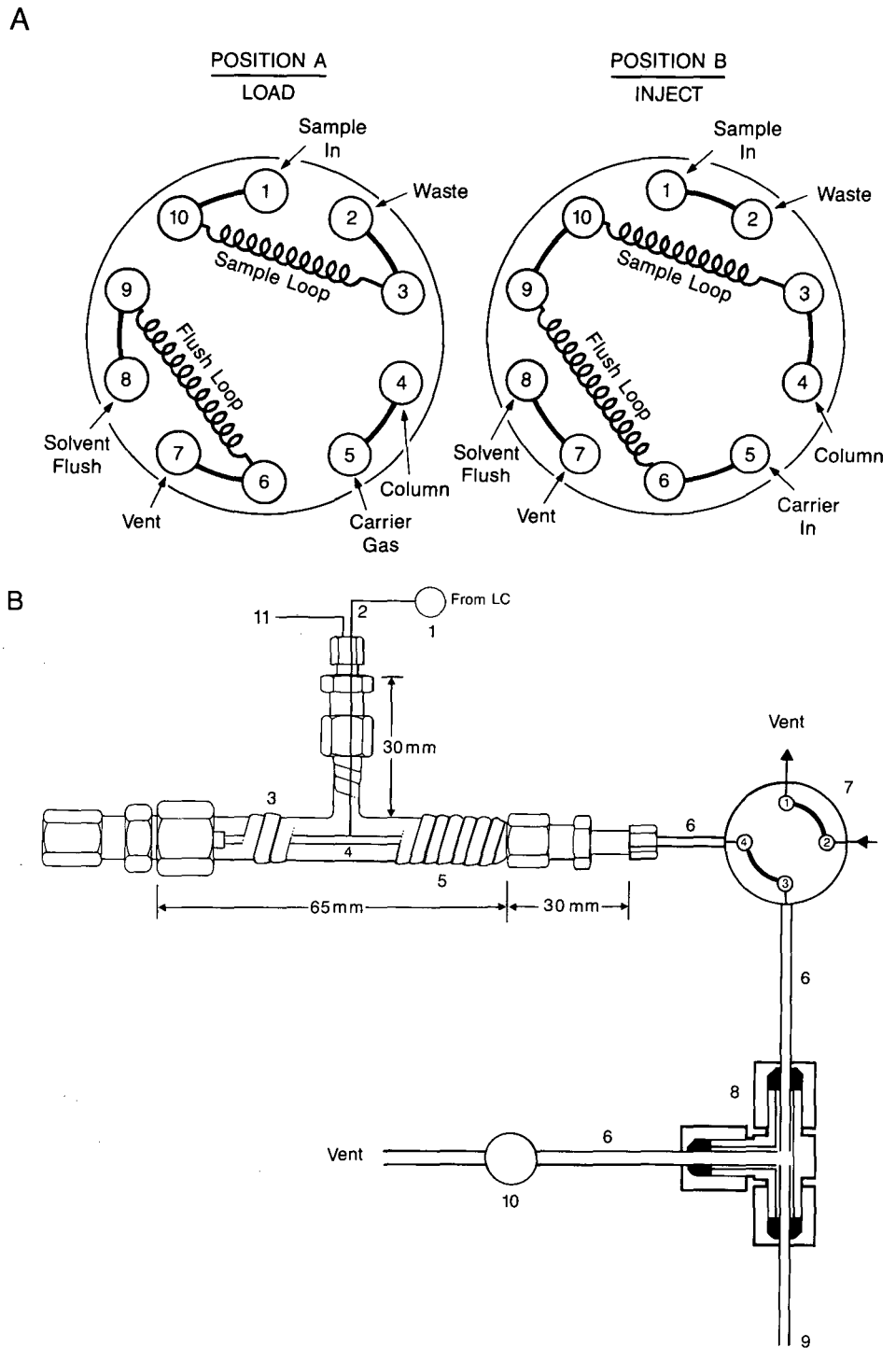

Fig. 15. Diagram of LC–pyrolysis–GC interface. (A) Ten-port switching valve and loop configuration. (B) Glass chamber interface: 1 = ten-port switching valve; 2 = transfer capillary; 3 = glass chamber; 4 = pyrolysis ribbon; 5 = heating tape; 6 = transfer capillaries; 7 = four-port switching valve; 8 = split tee; 9 = capillary GC column; 10 = micrometering valve; 11 = auxiliary carrier gas [107].

creasing density [115,116]. The conditions necessary to extract target analytes can therefore be optimized by varying the extraction pressure, the extraction temperature or both. In addition, many supercritical fluids are gases at standard temperatures and pressures, which simplifies the concentration and collection of extracted analytes.

Supercritical fluids have been used for extraction purposes on an industrial-scale process for several years [117,118] but as a sample preparation technique for chromatography its use is a relatively recent development [119]. Supercritical fluid extraction (SFE) was used in conjunction with thin-layer chromatography [120] and conventional LC [121]. The on-line coupling of SFE to capillary GC [122–126] and capillary SFC [127–132] is experiencing rapid growth and will continue to be studied as a simplified method of sample preparation and analysis. To our knowledge, however, the reported studies on analytical SFE have typically dealt with analyte concentrations in the μg/g range, orders of magnitude higher than necessary to study pesticide residues, for example, which are determined at the ng/g level. Studies were conducted in the SFE of a pesticide from a wheat matrix at these concentrations [95]. It was discovered that the extracts generated for analysis at the ng/g level from this matrix were not sufficiently clean (interference-free) to be analyzed directly by capillary GC alone, and microcolumn LC–GC was required in order to analyze the extracts obtained [95].

When performing SFE off-line, extracted components are typically collected in a solvent, a portion of which is then introduced into a chromatographic system. This approach does not take full advantage of the potential sensitivity increases which can be obtained in an on-line system. For example, if 100% of the analyte of interest can be extracted from the matrix, and no losses of analyte occur during the transfer process, the total mass of analyte extracted will reach the detector, yielding optimal sensitivity. In addition, a system of this type would allow analyses on very small sample sizes.

In order to decrease sample handling steps and to increase the sensitivity of the analyses, a system was developed coupling SFE on-line to microcolumn LC–GC [133]. A schematic diagram of the system developed is presented in Fig. 17, and the impactor

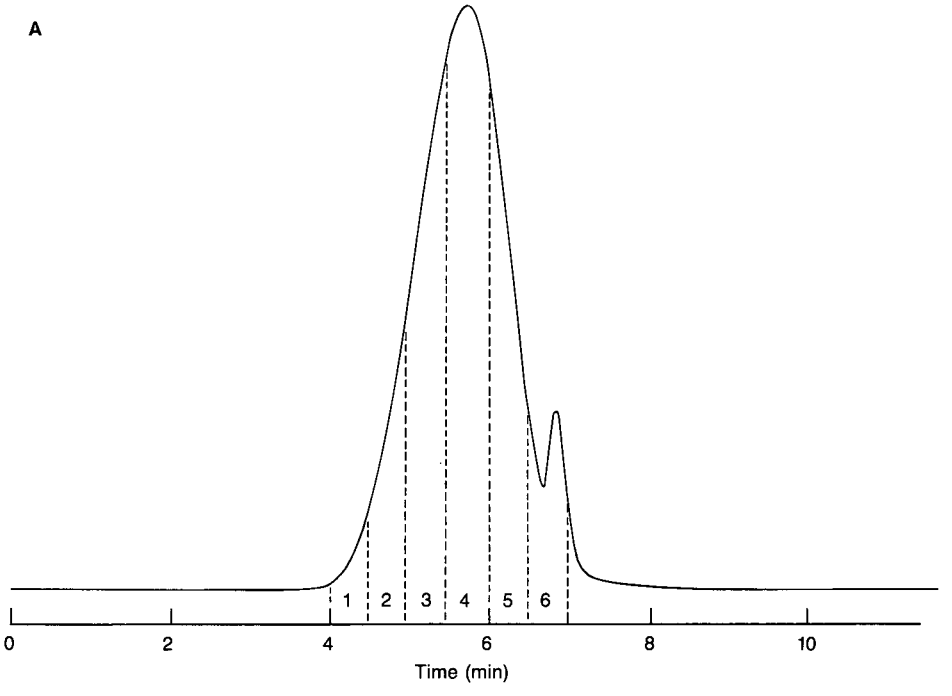

Fig. 16.

(Continued on p. 18)

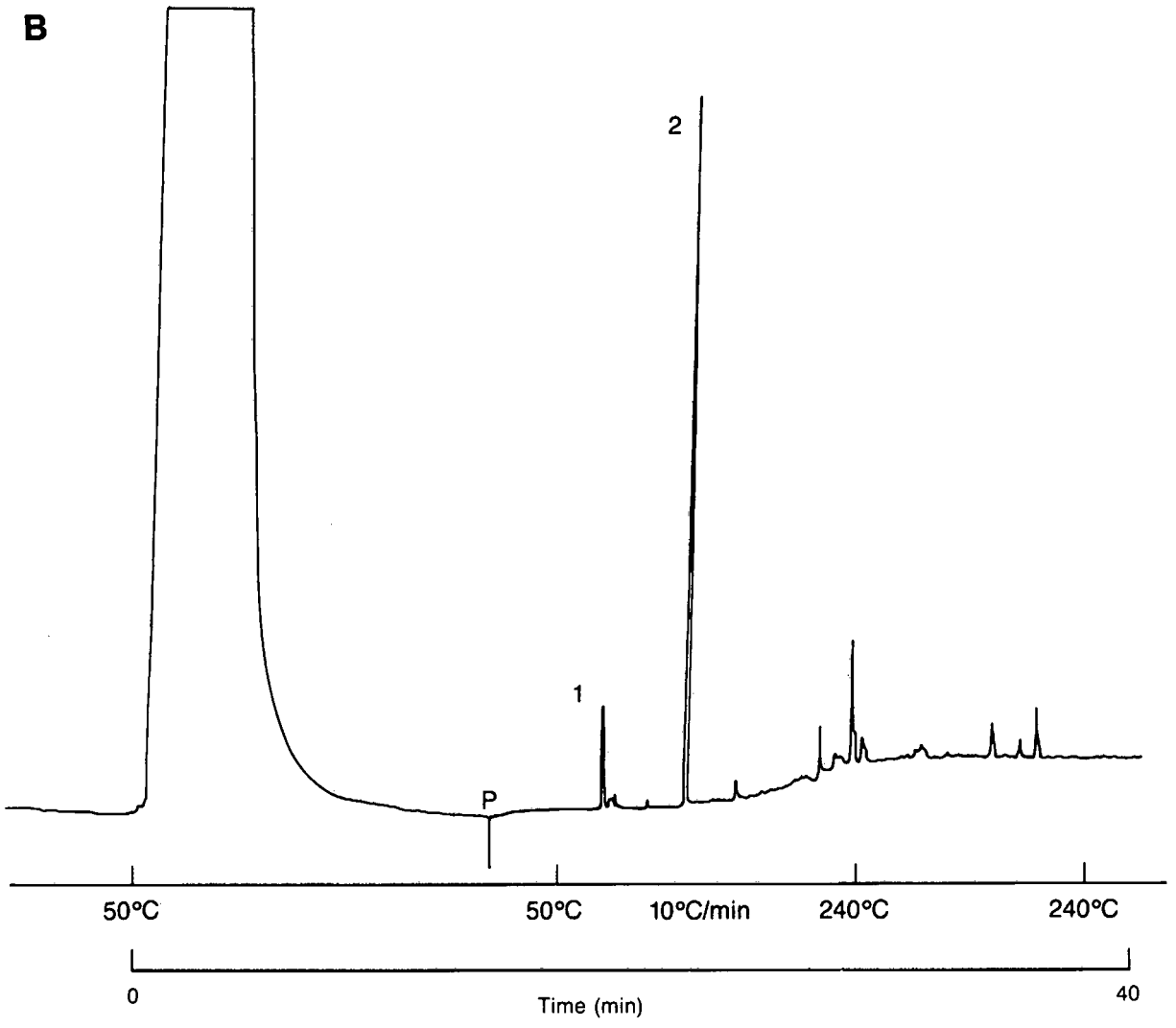

Fig. 16. (A) Micro SEC chromatogram of styrene–acrylonitrile copolymer. Column: 50 cm × 250 μm I.D. fused silica packed with Zorbax PSM-1000, 7-μm particle size; eluent: tetrahydrofuran; flow: 2.0 μl/min; injection: 200 nl; detection: UV at 220 nm. Fractions transferred to the pyrolysis interface are indicated. (B) Pyrolysis–GC chromatogram of introduced fraction from micro SEC. Column: 30 m × 0.2 mm I.D. phenylmethyl silicone, 0.33 μm film; temperature program: 50 to 240°C at 10°C/min; carrier: helium at 60 cm/s; detection: flame ionization. Peaks: 1 = acrylonitrile; 2 = styrene; P = pyrolysis time [107].

interface used is presented in Fig. 18. In the operation of the system, a sample is placed in a vessel and extracted with supercritical carbon dioxide. The extracted components are deposited in the impactor interface as a narrow band by decompressing the fluid into the gas phase via a restrictor and providing a surface for further dissipation of kinetic energy. The deposited material is then transferred to the micro LC column, where the target analyte(s) are separated from the majority of co-extracted interferences. At the appropriate time, the LC fraction containing the components of interest is introduced into the capillary GC system, where further separation and detection takes place. The system was applied to the determination of an insecticide in grass samples at the ng/g level. Reproducibility ex-

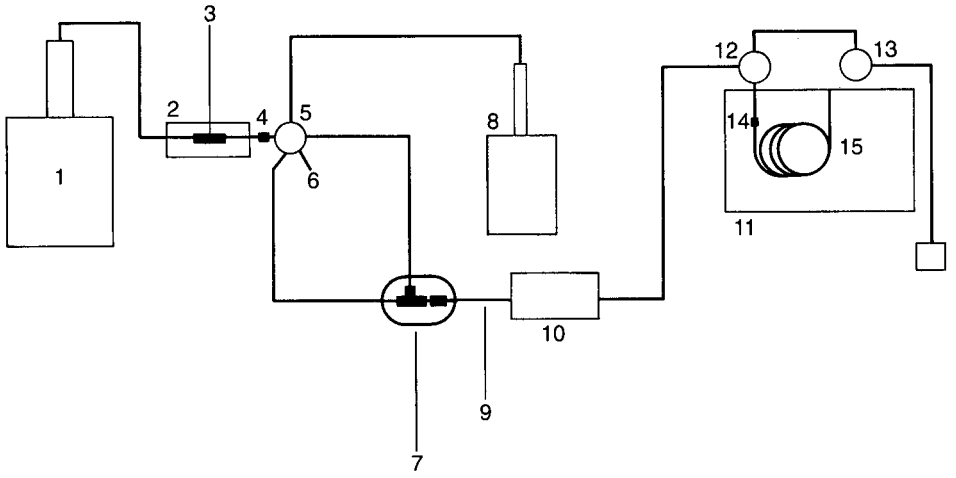

Fig. 17. Schematic diagram of on-line supercritical fluid extraction–microcolumn LC–capillary GC system. 1 = Supercritical fluid pump; 2 = column heater; 3 = extraction vessel; 4 = filter; 5 = switching valve (V1); 6 = vent; 7 = impactor interface; 8 = micro LC pump; 9 = micro LC column; 10 = UV detector; 11 = GC oven; 12 = switching valve (V2); 13 = on–off valve (V3); 14 = uncoated inlet; 15 = capillary GC column [133].

periments yielded R.S.D. values of 10.8% with sample sizes of only 5 mg and total organic solvent usage of less that 100 μl. Representative chromatograms are presented in Fig. 19.

10. MULTIDIMENSIONAL LIQUID CHROMATOGRAPHY–CAPILLARY SUPERCRITICAL FLUID CHROMATOGRAPHY

The coupling of LC to capillary SFC is expected to be of utility in the characterization of complex samples where components of interest are thermally labile, do not contain significant chromophores or do not have sufficient volatility to be analysed by GC. Since capillary columns of 50 μm I.D. are necessary for optimal chromatographic performance, injection volumes are typically in the nanoliter range, yielding limited sensitivity. Alternative sample introduction processes which would allow larger sample volumes into capillary SFC columns have been investigated, such as the use of a dilution chamber [134], solvent venting techniques [135–137], density gradient focusing [138] or solvent backflushing [138].

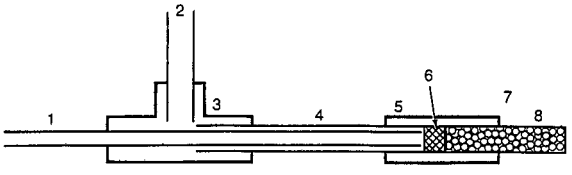

Fig. 18. Schematic diagram of impactor interface. 1 = Linear restrictor; 2 = LC eluent inlet/CO_2 vent; 3 = low-dead-volume tee; 4 = impactor tube; 5 = low-dead-volume union; 6 = impactor; 7 = micro LC column; 8 = packing [133].

Multidimensional LC–SFC has been reported using conventional-size columns in the first dimension, so that a small fraction of the peak of interest was transferred to the SFC, allowing for qualitative results only [139]. More recently, LC–SFC was reported using the dilution chamber approach [140] and combinations of the above techniques [141].

An alternative approach was recently developed [142] which allowed introduction of hundreds of microliters of solvent into capillary SFC columns without detrimental effects on peak shapes and resolution. A schematic diagram of the system is presented in Fig. 20. In the operation of the system, the liquid fraction containing the components of interest eluting from the LC system is introduced into an uncoated inlet, where the solvent is removed by heat and passage of an inert gas. Once the solvent is eliminated, the components of interest which are deposited in the inlet are transferred to the interface by extraction of the inlet with supercritical carbon dioxide. The supercritical carbon dioxide stream is

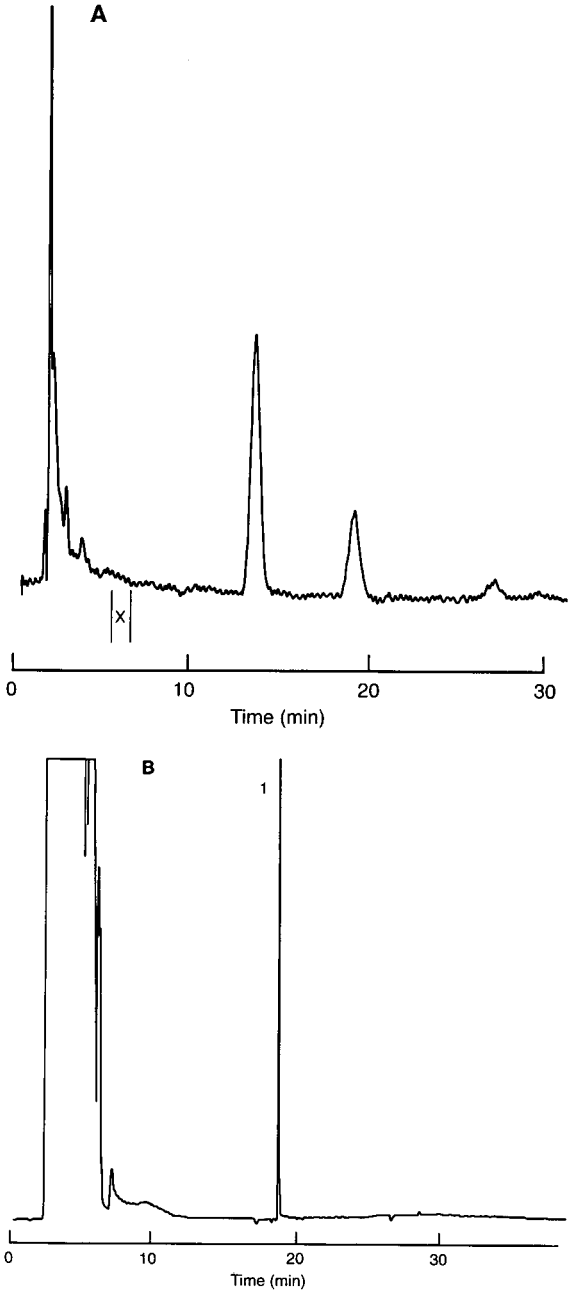

Fig. 19. (A) Micro LC chromatogram of supercritical fluid extract of grass. Column: 20 cm × 250 μm I.D. fused silica packed with Spherisorb ODS; eluent: methanol–water (80:20); flow: 4.1 μl/min; detection: UV at 205 nm; injection: 60 nl; X = fraction introduced into capillary GC. (B) Capillary GC of fraction introduced from Micro LC. Column: 30 m × 0.25 mm I.D. DB-1, 0.25 μm film; program temperature: 115°C 6 min, 8°C/min to 300°C; detection: electron-capture. Peak 1 = chlorpyrifos (160 ng/g) [133].

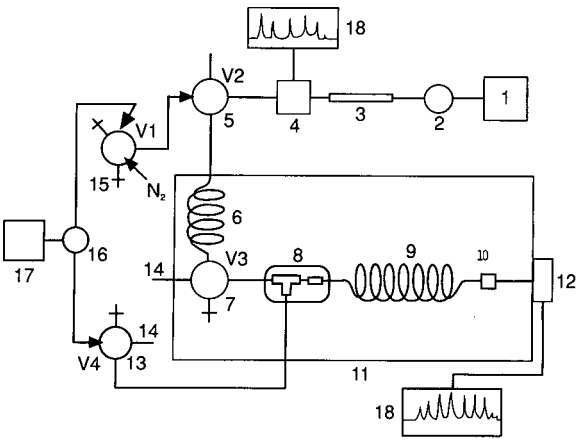

Fig. 20. Diagram of LC–capillary SFC system. 1 = Pump; 2 = injection valve; 3 = micro LC column; 4 = detector; 5 = ten-port switching valve (V2); 6 = capillary inlet; 7 = four-port switching valve (V3); 8 = impactor interface; 9 = capillary SFC column; 10 = frit restrictor; 11 = GC oven; 12 = flame ionization detector; 13 = four-port switching valve (V4); 14 = vents; 15 = ten-port switching valve (V1); 16 = tee; 17 = SFC pump; 18 = recording devices [142].

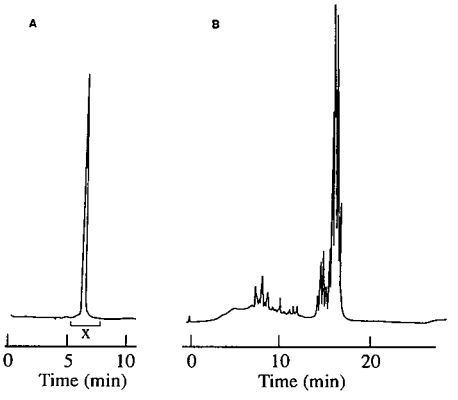

Fig. 21. Chromatograms of pentaerythritol tetrastearate. (A) Micro SEC. Column: 30 cm × 250 μm I.D. PL-GEL, Ångstrom 5 μm particle size; flow: 2.0 μl/min; eluent: tetrahydrofuran; detection: UV at 254 nm; injection size: 60 nl; X = section introduced into capillary SFC. (B) SFC chromatogram of introduced section. Volume introduced: 9 μl; transfer mode; oven temperature 100°C, Program: 100 to 400 atm at 50 atm/min, 5 min final time; Elution mode: column: 10 m × 50 μm I.D. SB-Methyl-100, 0.25 μm film; oven temperature: 100°C, Program: 100 to 400 atm at 15 atm/min, 5 min final time; detection: flame ionization [142].

decompressed though a restrictor, depositing the analytes at the head of the analytical column. When the extraction is completed, the deposited analytes are chromatographed on the SFC system. Chromatograms obtained for pentaerythretol tetrastearate, a polymer additive which is not sufficiently volatile to be analyzed by GC are presented in Fig. 21.

11. CONCLUSIONS

The use of multidimensional separation systems has experienced significant growth in the past decade, as is expected to continue to be a fruitful area of research in the future. A large range of options has only just begun to be considered [2]. The theoretical and practical advantages of multidimensional separation systems are beginning to be fully exploited, and it is expected that growth will continue as more users recognize that multidimensional separations can be the most succesful approach to the solution of difficult separation problems.

The use of microcolumns in multidimensional separations has allowed coupling of seemingly incompatible techniques, as well as operation of systems close to the theoretical limits. The key role played by miniaturization is expected to be fully exploited in the future.

REFERENCES

1 J. C. Giddings, *Anal. Chem.*, 39 (1967) 1927.
2 J. C. Giddings, *Anal. Chem.*, 53 (1981) 945A.
3 J. C. Giddings and R. Davis, *Anal. Chem.*, 55 (1983) 418.
4 J. C. Giddings, in H. J. Cortes (Editor), *Multidimensional Chromatography*, Marcel Dekker, New York, 1990, p. 1.
5 D. H. Freeman, *Anal. Chem.*, 35 (1983) 418.
6 J. C. Giddings, *J. High Resolut. Chromatogr. Chromatogr. Commun.*, 10 (1987) 319.
7 W. Berstch, in H. J. Cortes (Editor), *Multidimensional Chromatography*, Marcel Dekker, New York, 1990, p. 75.
8 V. McGuffin and M. Novotny, *Anal. Chem.*, 53 (1981) 946.
9 D. Ishii, K. Asai, K. Hibi, T. Jonokuchi and M. Nagaya, *J. Chromatogr.*, 144 (1977) 157.
10 T. Tsuda and M. Novotny, *Anal. Chem.*, 50 (1978) 271.
11 D. Ishii, T. Tsuda and T. Takeuchi, *J. Chromatogr.*, 185 (1979) 73.
12 Y. Hirata and M. Novotny, *J. Chromatogr.*, 186 (1979) 521.
13 M. Krejčí, K. Tesařík, M. Rused and J. Pajurek, *J. Chromatogr.*, 218 (1981) 167.
14 S. Folestad, L. Johnson and B. Josefsson, *Anal. Chem.*, 54 (1982) 925.
15 V. McGuffin and M. Novotny, *Anal. Chem.*, 55 (1983) 2296.
16 P. Kucera (Editor), *Microcolumn High-Performance Liquid Chromatography*, Elsevier, Amsterdam, 1984.
17 M. Novotny and D. Ishii (Editors), *Microcolumn Separations*, Elsevier, Amsterdam, 1985.
18 D. Ishii, *Introduction to Microscale High Performance Liquid Chromatography*, VCH, New York, 1988.
19 F. Yang, *Microbore Column Chromatography —A Unified Approach*, Marcel Dekker, New York, 1989.
20 C. Borra, M. Soon and M. Novotny, *J. Chromatogr.*, 385 (1987) 75.
21 M. Dewerdt, C. Dewaele and M. Verzele, *J. High Resolut. Chromatogr. Chromatogr. Commun.*, 10 (1987) 553.
22 K. E. Karlsson and M. Novotny, *Anal. Chem.*, 60 (1988) 1662.
23 R. T. Kennedy and J. W. Jorgenson, *Anal. Chem.*, 61 (1989) 1128.
24 J. C. Giddings, *Dynamics of Chromatography*, Marcel Dekker, New York, 1965.
25 I. Halász, R. Endele and J. Asshouer, *J. Chromatogr.*, 112 (1975) 37.
26 F. J. Yang, *J. Chromatogr.*, 236 (1982) 265.
27 M. Novotny, V. McGuffin, A. Hirose, J. Gluckman, *Chromatographia*, 17 (1983) 303.
28 S. Hoffmann and L. Blomberg, *Chromatographia*, 24 (1987) 416.
29 F. Andreolini, C. Borra and M. Novotny, *Anal. Chem.*, 59 (1987) 2428.
30 T. Takeuchi and D. Ishii, *J. Chromatogr.*, 213, (1981) 25.
31 F. Yang, *US Pat.*, 4 483 773 (1984).
32 S. Folestad, *Ph. D. Thesis*, University of Göteborg, Göteborg, 1985.
33 D. Shelly, J. Gluckman and M. Novotny, *Anal. Chem.*, 56 (1984) 2990.
34 H. J. Cortes, C. D. Pfeiffer, B. E. Richter and T. S. Stevens, *J. High Resolut. Chromatogr. Chromatogr. Commun.*, 10 (1987) 446.
35 D. Duquet, C. Dewaele, M. Verzele and S. McKinley, *J. High Resolut. Chromatogr. Chromatogr. Commun.*, 11 (1988) 824.
36 B. L. Ling, W. Baeyens and C. Dewaele, *J. Microcol. Sep.*, 4 (1992) 17.
37 R. L. Martin, J. C. Winters, *Anal. Chem.*, 35, (1963) 116.
38 D. R. Deans, *Chromatographia*, 1 (1968) 18.
39 H. J. Stan and D. Morowetz, *J. High Resolut. Chromatogr. Chromatogr. Commun.*, 6 (1983) 255.
40 D. J. Abbott, *J. High Resolut. Chromatogr. Chromatogr. Commun.*, 7 (1984) 577.
41 G. Schomburg and F. Weeke, *Chromatographia*, 16 (1982) 87.
42 K. Blau and G. King, *Handbook of Derivatives for Chromatography*, Heyden & Son, London, 1978.
43 P. Sandra and F. David, in H. J. Cortes (Editor), *Multidimensional Chromatography*, Marcel Dekker, New York, 1990, p. 145.
44 W. Jennings, *J. Chromatogr. Sci.*, 22 (1984) 129.
45 P. Van Arkel, J. Beens, H. Spans, D. Gutteriink and R. Verbeek, *J. Chromatogr. Sci.*, 25 (1987) 141.
46 G. Schomburg, F. Weeke and R. Schaefer, *J. High Resolut. Chromatogr. Chromatogr. Commun.*, 8 (1985) 388.

47 R. A. Lunsford and Y. T. Gagnon, *J. High Resolut. Chromatogr. Chromatogr. Commun.*, 10 (1987) 102.
48 G. Schomburg, *LC · GC*, 5 (1987) 304.
49 K. Himberg, E. Sippola and M. Riekkola, *J. Microcol. Sep.*, 1 (1989) 271.
50 W. J. Sonnefeld, W. H. Zoller, W. E. May and S. A. Wise, *Anal. Chem.*, 54 (1984) 723.
51 T. Takeuchi, M. Asai, H. Haraguchi and D. Ishii, *J. Chromatogr.*, 499 (1990) 549.
52 H. J. Cortes, G. E. Bormett and J. D. Graham, *J. Microcol. Sep.*, 4 (1992) 51.
53 P. Hayes and S. Anderson, *J. Chromatogr.*, 437 (1988) 365.
54 A. Walhagen and L. E. Edholm, *J. Chromatogr.*, 473 (1989) 371.
55 P. O. Edlund and D. Westerlund, *J. Pharm. Biomed. Anal.*, 2 (1984) 315.
56 L. Karlsson, *J. Chromatogr.*, 417 (1987) 309.
57 H. J. Cortes, L. D. Rothman, in H. J. Cortes (Editor), *Multidimensional Chromatography*, Marcel Dekker, New York, 1990, p. 219.
58 M. M. Bushey and J. W. Jorgenson, *Anal. Chem.*, 62 (1990) 978.
59 M. M. Bushey and J. W. Jorgenson, *J. Microcol. Sep.*, 2 (1990) 293.
60 P. A. Peaden and M. L. Lee, *J. Chromatogr.*, 259 (1983) 1.
61 E. Klesper and F. P. Schmitz, in C. M. White (Editor), *Modern Supercritical Fluid Chromatography*, Hüthig, Heidelberg, 1988, p. 1.
62 H. C. Chang, K. E. Markides, J. S. Bradshaw and M. L. Lee, *J. Microcol. Sep.*, 1 (1989) 131.
63 D. F. Johnson, J. S. Bradsaw, M. Eguchi, B. E. Rossiter, M. L. Lee, P. Petersson and K. E. Markides, *J. Chromatogr.*, 594 (1992) 283.
64 E. Lundanes and T. Greibrokk, *J. Chromatogr.*, 349 (1985) 439.
65 R. G. Cristensen, *J. High Resolut. Chromatogr. Chromatogr. Commun.*, 8 (1985) 824.
66 R. M. Campbell, N. M. Djordjevic, K. E. Markides and M. L. Lee, *Anal. Chem.*, 60 (1988) 356.
67 I. L. Davies, B. Xu, K. E. Markides and M. L. Lee, *J. Microcol. Sep.*, 1 (1989) 71.
68 K. M. Payne, I. L. Davies, K. D. Bartle, K. E. Markides and M. L. Lee, *J. Chromatogr.*, 477 (1989) 161.
69 R. Majors, *J. Chromatogr. Sci.*, 18 (1980) 571.
70 H. J. Cortes, C. D. Pfeiffer and B. E. Richter, *US Pat.*, 4 935 145 (1990).
71 H. J. Cortes, C. D. Pfeiffer and B. E. Richter, *J. High Resolut. Chromatogr. Chromatogr. Commun.*, 8 (1985) 469.
72 K. Grob Jr., D. Frollich, B. Schilling, H. Neukom and P. Nageli, *J. Chromatogr.*, 55 (1984) 295.
73 F. Munari, A. Trisciani, G. Mapelli, S. Trestianu, K. Grob, Jr. and J. Colin, *J. High Resolut. Chromatogr. Chromatogr. Commun.*, 9 (1985) 601.
74 K. Grob, Jr. and T. Laubli, *J. High Resolut. Chromatogr. Chromatogr. Commun.*, 9 (1986) 593.
75 K. Grob, Jr., E. Muller and W. Meier, *J. High Resolut. Chromatogr. Chromatogr. Commun.*, 10 (1987) 416.
76 E. Noroozian, F. Maris, M. Nielen, R. Frei, G. de Jong and U. A. Th. Brinkman, *J. High Resolut. Chromatogr. Chromatogr. Commun.*, 10 (1987) 17.
77 V. Gianesello, L. Bolzani, E. Brenn and A. Gazzaniga, *J. High Resolut. Chromatogr. Chromatogr. Commun.*, 11 (1988) 99.
78 V. M. A. Hakkinen, M. M. Virolainen and M. L. Riekkola, *J. High Resolut. Chromatogr. Chromatogr. Commun.*, 11 (1988) 214.
79 B. Pacciarelli, E. Muller, R. Schnieder, K. Grob, W. Steiner and D. Frohlich, *J. High Resolut. Chromatogr. Chromatogr. Commun.*, 11 (1988) 135.
80 F. Berthou and Y. Dreano, *J. High Resolut. Chromatogr. Chromatogr. Commun.*, 11 (1988) 706.
81 V. Gianesello, E. Brenn, G. Figini and A. Gazzaniga, *J. Chromatogr.*, 473 (1989) 343.
82 V. M. Hakkinen, K. Grob, Jr. and C. Burki, *J. Chromatogr.*, 473 (1989) 353.
83 K. Grob, M. Lafranchi and C. Mariani, *J. Chromatogr.*, 471 (1989) 397.
84 K. Grob, M. Biedermann and T. Laubli, *J. High Resolut. Chromatogr.*, 12 (1989) 49.
85 K. Grob and M. Lafranchi, *J. High Resolut. Chromatogr.*, 12 (1989) 379.
86 M. Biedermann, K. Grob and W. Meier, *J. High Resolut. Chromatogr.*, 12 (1989) 591.
87 P. Lukkari, J. Hannuksela, M. Mattinen, M. Virolainen, M. A. Hakkinen and M. L. Riekkola, *J. High Resolut. Chromatogr.*, 13 (1990) 170.
88 Th. Noy, E. Weiss, T. Herps, H. van Crutchen and J. Rijks, *J. High Resolut. Chromatogr. Chromatogr. Commun.*, 11 (1988) 181.
89 K. Grob, Jr., H. Schmarr and A. Mosandl, *J. High Resolut. Chromatogr.*, 12 (1989) 379.
90 K. Grob, Jr. and B. Shilling, *J. High Resolut. Chromatogr. Chromatogr. Commun.*, 8 (1985) 726.
91 H. J. Cortes, C. D. Pfeiffer, B. E. Richter and D. E. Jensen, *J. Chromatogr.*, 349 (1985) 55.
92 H. J. Cortes, in F. Yang (Editor), *Microbore Column Chromatography*, Marcel Dekker, New York, 1989, p. 211.
93 H. J. Cortes, C. D. Pfeiffer, G. L. Jewett and B. E. Richter, *J. Microcol. Sep.*, 1 (1989) 28.
94 H. J. Cortes and C. D. Pfeiffer, *Chromatography Forum*, 4 (1986) 29.
95 H. J. Cortes, R. E. Campbell and D. M. Meunier, *J. Microcol. Sep.*, 1 (1989) 302.
96 B. E. Gerhart and H. J. Cortes, *J. Chromatogr.*, 503 (1989) 377.
97 I. L. Davies, M. Raynor, P. Williams, G. Andrews and K. Bartle, *Anal. Chem.*, 59 (1987) 2579.
98 I. L. Davies, K. E. Markides, M. L. Lee, M. W. Raynor and K. D. Bartle, *J. High Resolut. Chromatogr.*, 12 (1989) 193.
99 D. Duquet, C. Dewaele and M. Verzele, *J. High Resolut. Chromatogr. Chromatogr. Commun.*, 11 (1988) 252.
100 A. Pouwelse, D. de Jong and J. H. M. van den Berg, *J. High Resolut. Chromatogr. Chromatogr. Commun.*, 11 (1988) 607.
101 I. L. Davies, M. W. Raynor, D. J. Irwin, K. D. Bartle, M. Tlay, E. Ekinci, H. E. Schwartz, *J. High Resolut. Chromatogr. Chromatogr. Commun.*, 11 (1988) 792.
102 H. J. Cortes, E. L. Olberding and J. H. Wetters, *Anal. Chim. Acta.*, 236 (1990) 173.
103 H. J. Cortes, in H. J. Cortes (Editor), *Multidimensional Chromatography*, Marcel Dekker, New York, 1989, p. 251.

104 H. J. Cortes, B. M. Bell, C. D. Pfeiffer and J. D. Graham, *J. Microcol. Sep.*, 1 (1989) 278.
105 H. J. Cortes, G. E. Bormett and J. D. Graham, *J. Microcol. Sep.*, 4 (1992) 51.
106 T. V. Raglione and R. A. Harwick, *J. Chromatogr.*, 454 (1988) 157.
107 H. J. Cortes, G. L. Jewett, C. D. Pfeiffer, S. Martin and C. Smith, *Anal. Chem.*, 61 (1989) 961.
108 S. Mori, *J. Chromatogr.*, 411 (1987) 355.
109 S. Mori, *Anal. Chem.*, 60 (1988) 1125.
110 G. Glöckner and J. H. M. van den Berg, *J. Chromatogr.*, 384 (1987) 135.
111 M. Danielewicz, M. Kubin and S. Vozka, *J. Appl. Polym. Sci.* 27 (1982) 3629.
112 G. Glökner, *Pure Appl. Chem.*, 55 (1983) 1553.
113 S. Mori, Y. Uno and M. Suzuki, *Anal. Chem.*, 58 (1986) 303.
114 G. Glöckner, *Adv. Polym. Sci.*, 79 (1986) 159.
115 J. C. Giddings, M. N. Meyers, L. McLaren and R. A. Keller, *Science (Washington, D.C.)*, 162 (1968) 67.
116 J. C. Giddings, M. N. Meyers and J. W. King, *J. Chromatogr. Sci.*, 7 (1969) 276.
117 G. M. Schneider, E. Stahl and G. Wilke (Editors), *Extraction with Supercritical Gases*, Verlag Chemie, Weinheim, 1980.
118 E. Stahl, K. W. Quirin and D. Gerard, *Dense Gases for Extraction and Refining*, Springer, Berlin, 1988.
119 M. L. Lee and K. E. Markides, *Analytical Supercritical Fluid Chromatography and Extraction*, Chromatography Conferences Inc. Provo, UT, 1990.
120 E. Stahl and W. Schilz, *Z. Anal. Chem.*, 280 (1976) 99.
121 K. Unger and P. Roumeliotis, *J. Chromatogr.*, 282 (1983) 519.
122 S. B. Hawthorne and D. J. Miller, *J. Chromatogr. Sci.*, 24 (1986) 258.
123 S. B. Hawthorne, D. J. Miller and M. S. Krieger, *Fresenius' Z. Anal. Chem.*, 330 (1988) 211.
124 B. W. Wright, S. R. Frye, D. G. McMinn and R. D. Smith, *Anal. Chem.*, 59 (1987) 680.
125 S. Hawthorne, D. J. Miller and M. S. Krieger, *Anal. Chem.*, 60 (1988) 472.
126 S. Hawthorne, D. J. Miller and M. S. Krieger, *J. Chromatogr. Sci.*, 27 (1989) 347.
127 K. Sugiyama, M. Saito, T. Hondo and M. Senda, *J. Chromatogr.*, 332 (1985) 107.
128 R. J. Skelton, C. C. Johnson and L. T. Taylor, *Chromatographia*, 21 (1986) 4.
129 W. P. Jackson, K. E. Markides and M. L. Lee, *J. High Resolut. Chromatogr. Chromatogr. Commun.*, 9 (1986) 213.
130 Q. L. Xie, K. E. Markides and M. L. Lee, *J. Chromatogr. Sci.*, 27 (1989) 365.
131 M. Andersen, J. T. Swanson, N. L. Porter and B. E. Richter, *J. Chromatogr. Sci.*, 27 (1989) 371.
132 M. Saito, T. Hondo, M. Senda, in H. J. Cortes (Editor) *Multidimensional Chromatography*, Marcel Dekker, New York, 1990, p. 331.
133 H. J. Cortes, L. S. Green and R. M. Campbell, *Anal. Chem.*, 63 (1991) 2719.
134 Y. Hirata, H. Koshiba and T. Maeda, *J. High Resolut. Chromatogr.*, 13 (1990) 619.
135 B. E. Berg and T. Greibrokk, *J. High Resolut. Chromatogr.*, 12 (1989) 322.
136 S. Ashraf, K. D. Bartle, A. A. Clifford, I. L. Davies and R. Moulder, *Chromatographia*, 30 (1990) 618.
137 M. L. Lee, B. Xu, E. C. Huang, N. M. Djordjevic, H. C. Chang and K. E. Markides, *J. Microcol. Sep.*, 1 (1989) 7.
138 Z. Liu, P. B. Farnsworth and M. L. Lee, *J. Microcol. Sep.*, 3 (1991) 435.
139 I. S. Lurie, *LC · GC*, 6 (1988) 1066.
140 Y. Hirata, Y. Kadota and T. Hondo, *J. Microcol. Sep.*, 3 (1991) 17.
141 R. Moulder, K. D. Barle and A. A. Clifford, *Analyst (London)*, 116 (1991) 1293.
142 H. J. Cortes, R. M. Campbell, R. P. Himes and C. D. Pfeiffer, *J. Microcol. Sep.*, 4 (1992) 239.

Journal of Chromatography, 626 (1992) 25–32
Elsevier Science Publishers B.V., Amsterdam

CHROM. 24 407

Review

Hyphenated high-performance liquid chromatography–capillary gas chromatography

Konrad Grob

Kantonales Labor, P.O. Box, CH-8030 Zürich (Switzerland)

ABSTRACT

Coupled chromatographic techniques involve hyphenation at the front end of the main separation step and will increasingly be required for laboratories to carry out routine analyses of increasing complexity in the future. Thousands of samples have been analysed by automated liquid chromatography–gas chromatography (LC–GC), saving around 15 000 h of sample preparation time and allowed determinations which would otherwise have been out of reach for a small government laboratory to be carried out. The techniques presently applied, however, exploit just a small fraction of the possible LC–GC transfer techniques, of the many LC techniques available, and of auxiliary techniques, such as on-line solvent evaporation and on-line solute derivatization.

CONTENTS

1. SOME CONSIDERATIONS ON HYPHENATION

Hyphenation of techniques may occur at the front or at the rear end of the main chromatographic separation step. At the rear end (outlet of the main chromatograph), it involves sophisticated detectors, whereas the purpose of hyphenation at the front end is usually sample preparation or pre-separation —two totally different methods. Hyphenation just means a close relationship between two devices or techniques, any techniques, and basically it does not

Correspondence to: Dr. K. Grob, Kantonales Labor, P.O. Box CH-8030 Zürich, Switzerland.

0021-9673/92/$15.00 © 1992 Elsevier Science Publishers B.V. All rights reserved

even mean on-line coupling. The heterogeneous subject also causes the people involved to be heterogeneous: people involved in sophisticated high technology and "megadollar" equipment have little in common with the "tube artists", directing eluent flows through unfathomable pieces of equipment. So far, the term "hyphenation" does not seem to be a very good choice.

It is difficult to propose a better alternative, however. The term "coupled" is more specific, but also has its limitation: if, for instance, high-performance liquid chromatography (LC) is coupled to capillary gas chromatography (GC), not just two corresponding instruments are merged with tubing connecting the outlet of the first instrument to the inlet of the second. Both techniques are adjusted to each other and the result may strongly differ from their normal way of use. LC, in its normal application, for instance, is mostly used in the reversed-phase mode, with water and salts in the eluent. Many newcomers expect that LC–GC would, therefore, also be reversed phase LC–GC. When hyphenated to GC, however, most applications do not allow reversed-phase LC (*e.g.* because the sample contains too much fat or the derivatives suitable for GC are sensitive to water or alcohols), or there is no advantage in the reversed-phase mode because GC is possible only for relatively non-polar compounds. Adjustment in the hyphenated technique, however, goes further. Smaller LC columns are used with smaller eluent flow-rates, eluents are usually more volatile and requirements on selectivity are often such that no separation is wanted between the members of a class of compounds. This explains why "coupled" is not a particularly suitable choice either: it misses out the fact that the combinations always need adjustment and compromises.

2. ROUTINE ON-LINE LIQUID CHROMATOGRAPHY–GAS CHROMATOGRAPHY

Efforts invested into the development of new techniques must be paid off by time saving during their application and/or by better results. LC–GC has clearly passed this test. It was used in routine analysis from the beginning: Cortes *et al.* [1] brought their first (automated) LC–GC instrument to a production site and let it be operated by untrained users. This allowed a complex method to be performed by non-experts. Gianesello and co-workers [2,3] used several LC–GC instruments for the routine determination of trace amounts of pharmaceuticals in plasma, primarily profiting from a substantially lowered detection limit and a shortened sample preparation procedure.

Working for the government chemist, primarily responsible for the control of foods and drinking water, our laboratory has used LC–GC for many kinds of applications. The largest number of analyses, however, were carried out with four methods: (i) the analysis of mineral oil contamination in foods [4–6]; (ii) determination of sterols in edible oils and fats after cleavage of the esters [7]; (iii) determination of the minor components in oils and fats, leaving the esters intact [8], and (iv) the determination of raffination of oils and fats through the degradation products of sterols and squalene [9]. The first method was used for analysing about 4000 food samples and packaging materials. The latter three methods were used to analyse most of the oils and fats on the Swiss market; summing up the analyses by all three methods, a total of around 2000 is obtained, including 200–300 samples of known origin which served as reference samples.

The previously used (and official) methods for oil analysis involve saponification, a tedious extraction from a soap solution, preparative thin-layer chromatography, derivatization and GC; these widely used methods allow the analysis of about two samples per day per analyst. The proposed method, however, involves making up an oil solution and a derivatization in this solution in two of the three methods; all other steps were replaced by on-line LC. There is no established method for the determination of mineral oil in foods; it is, in fact, difficult to detect about 1–5 ppm of oil by conventional methods. We immersed the sample in pentane and analysed the supernatant by LC–GC.

A conservative estimate shows that about 15 000 working hours were saved by using the LC–GC methods, more than was invested into the development of the technique. In addition, sensitivities were far higher and for sterol analysis the relative standard deviations of the quantitative results were approximately ten times lower, lower, in fact, than those obtained by GC analysis alone when using usual injection [7,10].

3. THE NEED FOR AUTOMATED METHODS

If all three people in our group had carried out the above analyses using conventional, manual methods, the work would have taken about four years—which would, of course, have been considered unacceptable. There was, in fact, not a choice of performing the analyses by one or another method, but whether such control analyses were feasible at all.

At this point it is necessary to explain briefly the situation in a government chemist's laboratory, such as that of the Kanton of Zürich. About 35 people work in the laboratory, which is supposed to be capable of controlling all foods, the water of swimming pools, etc. Olive oils, for instance (about 80 products are available on the local market) are just a very small segment. Owing to their high price, adulteration of olive oils has a long tradition. Easily detectable admixtures, *e.g.* of rape seed oil, however, are now rarely used. The people carrying out the adulteration are well equipped with analytical methods. Harmless components are removed from certain olive oils (by unsavoury chemistry) because control laboratories, such as the government chemists, use them as markers, *e.g.* for the detection of cheaper solvent-extracted oils in pressed oils. Control, therefore, requires methods of increasing complexity, which rapidly overtax the government chemists' laboratories. Together with the necessary blanks, recoveries and confirmations, checking of the 80 olive oils by the conventional sterol method would require about 150 analyses, or 75 days of work for a single person; using LC–GC, the work was carried out in less than 10 days (about 30 analyses during a successful day).

The situation is similar in other fields: the analysis of pesticide residues keeps an unreasonably large proportion of our staff busy. It is boring work, and the results would be better if most of this work was carried out by a hyphenated technique, for example by a kind of a pesticide analyser, the development of which is overdue. Chemistry misused for rearing animals with less feed or providing meat with less fat is another problem: in the Kanton of Zürich, about 1.5 million pigs and cattle are slaughtered every year and each animal is a sample. If 0.1% of these samples were analysed, this would involve 1500 samples a year. With present methods, a few tens of samples are analysed for a small number of chemicals, and this is carried out at the limit of our capabilities. Only hyphenated analysers will be capable of handling the number of samples sufficient for a serious control programme, as long as chromatography is the analytical method.

4. TECHNIQUES FOR TRANSFER FROM LIQUID CHROMATOGRAPHY TO GAS CHROMATOGRAPHY

Routine analysis of large numbers of samples has confirmed usefulness of LC–GC in practice. Only a very small section of the potential of such a technique is, however, used at present; numerous ideas are available, suggesting a broad field into which it could expand. Some of the ideas are discussed here.

4.1. On-column transfer techniques

At present, nearly all LC–GC transfers are carried out by a kind of on-column technique. The eluent is introduced into the oven-thermostated inlet of the GC column, using retention gap techniques, the technique applied by Cortes *et al.* [1], or concurrent eluent evaporation [11,12]. On-column techniques allow extremely precise and accurate results to be produced, but also have two limitations: first, involatile material introduced into the oven-thermostated column rapidly builds up enough retention power to cause peak broadening. As up to several tens of milligrams of sample are injected into the LC part of the system, a very small fraction of the material injected is sufficient to ruin the GC system (one part out of ten thousand probably destroys it at once). Second, water attacks the pre-column if it enters in the liquid phase [13]; some humidity in the eluent (*e.g.* ethyl acetate containing up to 4% water) is sufficient to destroy the deactivation on the uncoated pre-column. Despite some disagreement about whether or not there are GC pre-columns resisting water [14–16], there seems to be little hope for the reliable LC–GC transfer of water-containing eluents by on-column techniques.

4.2. Transfer via programmed temperature vaporizing injector

The use of a programmed temperature vaporizing (PTV) injector for LC–GC transfer has been discussed, but, surprisingly, has not yet been put into practice. A solvent split technique was intended, as used for the syringe injection of large volumes [17].

Vaporization in a PTV injector chamber instead of in an oven-thermostated capillary pre-column allows the introduction of far larger amounts of involatile by-products [18], as the retention power of this material can be overcome by a high temperature. It is expected, furthermore, that a packing, *e.g.* Tenax, would not be attacked by water, enabling the introduction of water-containing eluents. PTV solvent split injection will not, however, be a simple technique for the adjustment of conditions, it will not allow the analysis of volatile solutes, and it will hardly produce results of a precision and reliability comparable with the on-column techniques.

Some of the drawbacks of transfer via the PTV solvent split technique could be overcome by using PTV vapour overflow [19]: instead of driving the eluent vapours out of the vaporizing chamber by a carrier gas flow, the vapours leave it on their own, as a result of their expansion during evaporation. To create the necessary vapour pressure, the vaporizer temperature must exceed the solvent boiling point at the current pressure. PTV vapour overflow largely regulates itself: the vapours escape at a rate corresponding to the evaporation rate and at the end of the evaporation process, the escape automatically stops. This reduces the loss of volatiles, as no carrier gas drives the solutes through the packed bed. Method development should be facilitated as the input flow-rate, the carrier gas flow-rate, and the vaporizer temperature do not need to be adjusted to each other. As an additional advantage, evaporation may occur under reduced pressure, as the carrier gas supply may be cut off during eluent evaporation. Reduced pressures allow using lower vaporizing temperatures, which increases the retention of the volatile components in the injector and reduces the aggressivity of water. The technique has, however, not yet been put into practice.

4.3. Splitless injection of large volumes

Another technique, which has again not been tried for LC–GC transfer, could involve splitless injection with a conventional vaporizing injector and a packed insert [20]. Cooling by the evaporating solvent is exploited to create an island in the normally heated vaporizer, which remains at the solvent boiling point until all the solvent is evaporated. All but the most volatile components remain in this cooled zone until the latter resumes the injector temperature. The solutes are then transferred to the column in the splitless mode. Injection by syringe allows the introduction of at least 500-μl volumes, and a 200-μl injection of water is not the upper limit. The method is simple to handle and resists involatile and aggressive dirt or water.

4.4. Extraction into packed bed: water-containing eluents

Evaporation of large volumes of solvent is always accompanied by a loss of volatile solutes because the solvent vapours act as a carrier gas and advance the solute material, *e.g.* through a retaining packed bed. Losses are, of course, particularly high if the solvent has a high boiling point. If the solute material could first be extracted from the eluent into a solid phase, at least a large proportion of the solvent could be removed without evaporation, avoiding the corresponding losses (although possibly in exchange with losses by poor extraction). This approach is particularly promising for the transfer of water-containing eluents, because it could provide a method for coupling reversed-phase LC to GC without introducing water into the GC system.

Vreuls *et al.* [21] extracted aqueous samples into various packed beds, evaporated the residual water from the packing, and thermally transferred the solute material into the GC system. Tenax was the most thermostable packing material, but alkylated silica gels extracted the aqueous phase better.

Extraction into a solid phase is not necessarily followed by thermal transfer to GC: transfer with a small volume of a convenient solvent may be an interesting alternative because an adsorbent with good extraction properties often has insufficient thermostability. Vreuls *et al.* [22] described the trapping of solutes in a small packed bed followed by transfer to GC with ethyl acetate, using partially concurrent eluent evaporation. This approach seemed to work, but has two problems: as most components of interest will be eluted near the interface between the organic and the aqueous phase, accurate cutting of the transferred fraction is crucial. If the cut is slightly early, the GC system is flooded by water; if it is slightly late, substantial amounts of solute material are lost. The transfer of some water cannot be completely avoided; at best it only involves the water dissolved in the ethyl acetate (which, however, is sufficient to damage the de-

activation of the precolumn when run routinely).

It is the feeling of the author that the basic possibilities for transferring water-containing eluents to the GC system have been determined and that the breakthrough depends only on the ingenious combination of these means. However, the breakthrough has not yet been made.

5. LIQUID CHROMATOGRAPHY FOR COUPLING TO GAS CHROMATOGRAPHY

LC offers an enormous wealth of possibilities to pre-separate or enrich samples. The ingenious hyphenated methods will probably be those with an inventive LC part. LC for LC–GC has been reviewed [23], emphasizing the special requirements of LC if it has to serve sample preparation for GC. Discussion was centred on the use of raw and derivatized silica gel, for which considerable experience is available. Work with size-exclusion chromatography (SEC) is continuing. SEC removes the high-molecular-mass material which disturbs GC and should, therefore, facilitate on-column transfer. An attempt to perform on-line SEC–GC for the determination of chlorinated pesticides in fat-containing foods has been described [24].

The combination of SEC and LC provides pre-separation by two totally different selectivities: SEC removes the molecules larger and smaller than that of interest, whereas LC separates the isolated fraction according to polarity. Owing to the efficient removal of by-products, an on-line combination of the two should enable a trace analyser with a large field of application to be built. Some results in this direction were reported by De Paoli *et al.* [25] for the determination of organophosphorus pesticides in fruits: extracts were pre-separated by a 25 cm × 3 mm I.D. SEC column and filtered through a silica gel column before being transferred to the GC system. As the mobile phase in SEC on a polystyrene-type column could not be weaker than dichloromethane and the fraction from SEC was directly transferred to the silica gel column, the function of the silica gel column was restricted. The first components of interest broke through during introduction of the SEC fraction and the initial bands were broad; the removal of by-products less polar than the insecticides was therefore impossible. The components disturbing the GC were, however, more polar than the pesticides and could be eliminated completely. Detection limits by this SEC–LC–GC method with flame photometric detection were around 1 μg/kg, and there were no peaks other than the insecticides of interest in the gas chromatogram. An on-line eluent evaporator, positioned between the SEC and the LC column, would have allowed heart cutting (see below).

No work has been published on coupling ion-exchange sample enrichment or pre-separation to GC. Ion exchangers strongly and selectively bind some components and are therefore of interest for the determination of acidic and basic components. Such techniques often presuppose, however, on-line derivatization.

5.1. Example: determination of degradation of edible oils

One of the highly successful routine applications of LC–GC is the determination of degradation products from sterols and squalene in edible oils for the determination of whether oils or fats have been refined or subjected to other thermal stress (Fig. 1) [9]. Sterols are dehydroxylated, forming a hydrocarbon with at least two double bonds (3,5-stigmastadiene is the degradation product of sitosterol); squalene isomerization products are formed. Previous methods involved lengthy saponification and

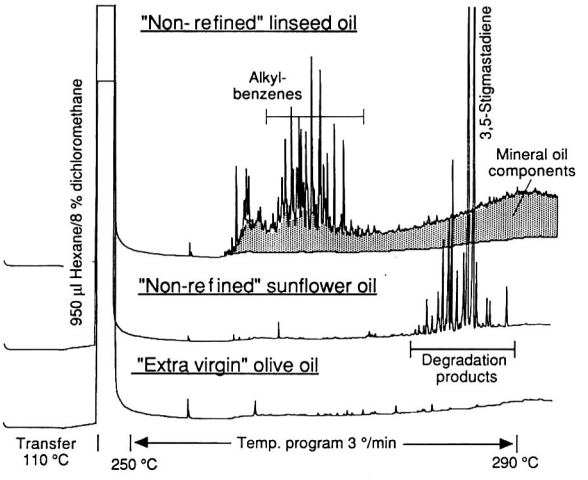

Fig. 1. Example of a routine application of LC–GC determination of degradation products of sterols and squalene in edible oils. For detailed explanation, see text.

clean-up. The LC–GC method reduces sample preparation to making up a 20% solution of the oil in hexane and gives an increased sensitivity by one to two orders of magnitude. LC removes the large amounts of triglycerides and separates the alkenes from alkanes and squalene (which presupposes a high separation efficiency).

For an extra virgin olive oil (bottom chromatogram), only pression and filtration is allowed. In this instance, no degradation products are visible (a small peak corresponds to about 50 μg/kg), confirming the quality of the oil; for most of the olive oils sold in Switzerland, the declaration corresponded to the oil. The sunflower oil sold as non-refined, however, contained a substantial amount (about 30 mg/kg) of degradation products (centre chromatogram) and obviously did not correspond to the declaration. Disregarding the olive oils, hardly more than half of the oils declared as non-refined were what they stated. The cold pressed and non-refined linseed oil (top chromatogram) contained no degradation products, *i.e.* the declaration is not violated. However, the chromatogram shows numerous other peaks, which have nothing to do with the oil: they were identified as alkylbenzenes, which are used, for example, in paints or (after sulphonation) as detergents (about 15 mg/kg referring to the oil). The increase in the baseline is not due to column bleed (dotted area; the real baseline, taken from a blank run, is shown), but to contamination with mineral oil. The *n*-alkanes, removed by LC, ranged from C_{17} to higher than C_{35}. The residues in the fraction shown consist of alkenes with more than one double bond and (primarily) alkyl aromatics with more than one ring. Owing to the enormous number of isomers, no peaks are distinguishable (which is typical for aromatics from mineral oils [26]). The concentration of mineral oil in this linseed oil approached 0.1%; its origin is still unknown.

6. AUXILIARY TECHNIQUES

Standard LC for LC–GC consists of one LC pump, one LC column, two switching valves and the accessory for backflushing the LC column. To this system, however, many steps could be added, which would render the system more versatile. LC–LC–GC has been described for the determination of food irradiation products [27].

6.1. *On-line extraction*

On-line extraction, originating in flow injection analysis, was introduced in GC as a method for analysing organic components in water [28,29]. It allows fully automated on-line water analysis, but could also be used as a first step for analysing other samples.

As there is still no method for the direct transfer of water-containing eluents to a GC system, a number of workers have experimented with on-line extraction aiming at exchanging the solvent. The water-containing eluent was mixed with an organic solvent of low polarity, passed through extraction coils, the organic phase was separated, and finally transferred to the GC system through a loop-type interface [30–33]. Such methods produced interesting results, but might become obsolete as soon as better alternatives become available. Extraction yields are often far below 100% and there usually remains enough water in the organic extract to cause problems in GC.

6.2. *On-line derivatization*

Complex sample preparation procedures can hardly be used without on-line derivatization. There are two important reasons for this: first, enrichment or pre-separation may need to be based on underivatized functional groups of the components of interest or of those to be removed. If the components need to be derivatized before they are amenable to GC, *e.g.* those containing amino or carboxyl groups, derivatization must occur between the LC sample preparation step and GC. Second, samples may be in a matrix not allowing derivatization, *e.g.* in water, which must be removed before derivatization.

There are two options to achieve on-line derivatization: reactions within the LC system, *i.e.* on the LC column or within an interface, or reactions in the inlet of the GC column. Raglione and Hartwick [34] isolated triglycerides from biological samples by LC, methylated them on-line on a cation exchanger (acid catalysis) and analysed the esters by GC. Derivatization in an uncoated GC pre-column was achieved for pentachlorophenol, though not in an LC–GC system. The methyl ester was formed with diazomethane and the acetate with acetanhydride–pyridine [35].

6.3. On-line evaporator

Multiple step LC often creates the problem that the volume of eluent from the first column is excessively large for a direct transfer to the second column. This is particularly true in LC–GC because the first column typically needs to be large to offer the capacity required for removing large amounts of by-products, and the second column should be smaller to produce fractions small enough for easy transfer to GC. In other instances the mobile phase from the first column does not suit the second column, *e.g.* because it is excessively strong (see on-line SEC–LC discussed earlier). To overcome such incompatibilities, an on-line eluent evaporator was constructed [36], evaporating the mobile phase, *e.g.* from a first LC column, but retaining the solutes. When evaporation is completed, the solute material is carried into, *e.g.* a second LC column by a mobile phase suiting the second LC step.

7. LC–GC INSTRUMENTATION

Instrumentation allowing complete automation of LC–GC is needed. Automation is required for the analysis of large numbers of samples, but also because LC often presupposes reproducible chromatographic cycles: retention times may not be sufficiently reproducible otherwise.

Scientists often tend to underestimate the work carried out by instrument manufacturers, perhaps because they have to pay for the instrument. The work carried out by F. Munari at Carlo Erba/Fisons deserves special recognition. Over a number of years a totally new type of instrument has been developed. The first two instruments of this type in this laboratory analysed the many thousands of samples mentioned earlier, often running over weekends. They did their job without major problems, and thus fulfilled the expectations.

This instrument offers a broad range of capabilities, including multitransfer, *i.e.* the transfer of several fractions from a liquid chromatogram to GC, "GC scanning", *i.e.* GC analysis of a larger section of a liquid chromatogram, segment by segment, and LC–GC transfer by peak recognition, adjusting the transfer to the signals observed by the LC detector. It allows automated backflush of the LC column, steps in the LC part (*e.g.* on-line eluent evaporation) to be performed at increased temperature, and a variety of LC–LC techniques. With respect to the more sophisticated techniques discussed here, it is obvious, however, that the development of the "Dualchrom" instrument will not end in the near future: more valves will be needed, additional LC–GC interfaces may need to be integrated, and the software will have to follow these developments.

REFERENCES

1 H. J. Cortes, C. D. Pfeiffer and B. E. Richter, *J. High Resolut. Chromatogr. Chromatogr. Commun.*, 8 (1985) 469.
2 V. Gianesello, L. Bolzani, E. Brenn and A. Gazzaniga, *J. High Resolut. Chromatogr. Chromatogr. Commun.*, 11 (1988) 99.
3 V. Gianesello, E. Brenn, G. Figini and A. Gazzaniga, *J. Chromatogr.*, 473 (1989) 343.
4 K. Grob, M. Biedermann, A. Artho and J. Egli, *Z. Lebensm.-Unters. Forsch.*, 193 (1991) 213.
5 K. Grob, A. Artho, M. Biedermann and J. Egli, *Food Addit. Contam.*, 8 (1991) 437.
6 K. Grob, A. Artho, M. Biedermann, J. Egli, M. Lanfranchi, A. Caramaschi, R. Etter and E. Romann, *Mitt. Geb. Lebensmittelunters. Hyg.*, 83 (1992) 40.
7 M. Biedermann, K. Grob and C. Mariani, *Fat Sci. Technol.*, in press.
8 K. Grob, A. Artho and C. Mariani, *Fat Sci. Technol.*, in press.
9 K. Grob, A. Artho and C. Mariani, *Fat Sci. Technol.*, in press.
10 K. Grob and M. Lanfranchi, *J. High Resolut. Chromatogr.*, 12 (1989) 624.
11 F. Munari and K. Grob, *J. Chromatogr. Sci.*, 28 (1990) 61.
12 K. Grob, *On-Line Coupled LC–GC*, Hüthig, Heidelberg, 1991.
13 K. Grob, H. P. Neukom and Z. Li, *J. Chromatogr.*, 473 (1989) 401.
14 A. Pouwelse, D. de Jong and J. H. M. van den Berg, *J. High Resolut. Chromatogr. Chromatogr. Commun.*, 11 (1988) 607.
15 H. J. Cortes, C. D. Pfeiffer, G. L. Jewett and B. E. Richter, *J. Microcolumn Sep.*, 1 (1989) 28.
16 K. Grob and A. Artho, *J. High Resolut. Chromatogr.*, 14 (1991) 212.
17 W. Vogt, K. Jacob and H. W. Obwexer, *J. Chromatogr.*, 174 (1979) 437.
18 K. Grob, T. Läubli and B. Brechbühler, *J. High Resolut. Chromatogr. Chromatogr. Commun.*, 11 (1988) 462.
19 K. Grob, *J. High Resolut. Chromatogr.*, 13 (1990) 540.
20 K. Grob, S. Brem and D. Fröhlich, *J. High Resolut. Chromatogr.*, in press.
21 J. J. Vreuls, U. A. Th. Brinkman, G. J. de Jong, K. Grob and A. Artho, *J. High Resolut. Chromatogr.*, 14 (1991) 455.
22 J. J. Vreuls, V. P. Goudriaan, U. A. Th. Brinkman and G. J. de Jong, *J. High Resolut. Chromatogr.*, 14 (1991) 475.
23 K. Grob, *Chimia*, 45 (1991) 109.
24 K. Grob and I. Kälin, *J. Agric. Food Chem.*, 39 (1991) 1950.
25 M. De Paoli, M. Barbina, R. Mondini, A. Valentino, A. Pezzoni and K. Grob, *J. High Resolut. Chromatogr.*, in press.

26 K. Grob, M. Biedermann, A. Caramaschi and B. Pacciarelli, *J. High Resolut. Chromatogr.*, 14 (1991) 33.
27 M. Biedermann, K. Grob, D. Fröhlich and W. Meier, *Z. Lebensm.-Unters. Forsch.*, in press.
28 E. Fogelqvist, M. Krysell and L.-G. Danielsson, *Anal. Chem.*, 58 (1986) 1516.
29 J. Roeraade, *J. Chromatogr.*, 330 (1985) 293.
30 P. van Zoonen, G. R. van der Hoff, and E. A. Hogendoorn, *J. High Resolut. Chromatogr.*, 13 (1990) 483.
31 E. C. Goosens, R. G. Bunschoten, V. Engelen, D. de Jong and J. H. M. van den Berg, *J. High Resolut. Chromatogr.*, 13 (1990) 438.
32 G. R. van der Hoff, R. A. Baumann and P. van Zoonen, in P. Sandra (Editor), *Proceedings of the 13th International Symposium on Capillary Chromatography, Riva del Garda, 1991*, Hüthig, Heidelberg, 1991, 536.
33 J. Ogorka, G. Schwinger, G. Bruat and V. Seidel, presented at the *2nd International Symposium on Hyphenated Techniques in Chromatography, Antwerp, Feb. 18–21, 1992.*
34 Th. V. Raglione and R. A. Hartwick, *J. Chromatogr.*, 454 (1988) 157.
35 K. Grob and H. P. Neukom, *J. Chromatogr.*, 295 (1984) 49.
36 K. Grob and B. Tönz, *J. High Resolut. Chromatogr.*, in press.

Journal of Chromatography, 626 (1992) 33–40
Elsevier Science Publishers B.V., Amsterdam

CHROM. 24 431

Review

Recent developments in the use of supercritical fluids in coupled systems

T. Greibrokk

Department of Chemistry, University of Oslo, P.B. 1033 Blindern, 0315 Oslo (Norway)

ABSTRACT

Multi-dimensional systems utilizing supercritical fluids in either chromatography or on-line extraction are reviewed, with the main emphasis on phase transfer, reconcentration and selectivity.

CONTENTS

1. INTRODUCTION

Fractionation or purification of complex samples prior to analysis is usually performed either by extraction or by chromatographic methods. Off-line procedures are often chosen when multiple analyses are required on each sample, but automated on-line multi-dimensional techniques can reduce the analysis time and improve accuracy, reproducibility and detectability [1]. The requirements for multi-dimensional separations were defined by Giddings [2,3], demonstrating that multi-dimensional techniques can lead to extremely high peak resolution. An overview of interfacing methods, with particular emphasis on liquid chromatography–gas chromatography, was presented by Davies *et al.* [4].

The first fractionation step may consist of liquid extraction, solid-phase extraction, supercritical fluid extraction (SFE), chromatography with or without guard columns and other separation methods, such as dialysis, depending on the components of interest. Liquid samples from the first separation step can be transferred to the second mode of sep-

Correspondence to: Dr. T. Greibrokk, Department of Chemistry, University of Oslo, P.B. 1033 Blindern, 0315 Oslo, Norway.

0021-9673/92/$15.00 © 1992 Elsevier Science Publishers B.V. All rights reserved

aration, such as to gas chromatography (GC), supercritical fluid chromatography (SFC), liquid chromatography (LC), thin-layer chromatography or capillary zone electrophoreses, by narrow heart cuts via a sampling valve. An important question is whether the concentration of a narrow cut is high enough for analysis in the second step or if a concentration step is required. This paper discusses opportunities and problems involved with the use of supercritical fluids in multi-dimensional systems, with particular emphasis on phase transfer, reconcentration and selectivity, and demonstrates how some problems have been solved in recent developments.

2. PHASE TRANSFER OF LIQUID SAMPLES

Combining LC and GC is a fairly straightforward technique provided that suitable column dimensions are selected, with narrow-bore LC columns or split-flow systems.

The fraction to be transferred needs to be defined by on-line detection or by retention time. A detector will usually be inserted either directly in the flow line between the first column and the transfer valve (V1) or connected to the waste line (Fig. 1). The first alternative (a) requires an on-column flow-cell in order to limit peak broadening, but gives direct control of the fraction transferred. The second alternative (b) does not require on-column detection and

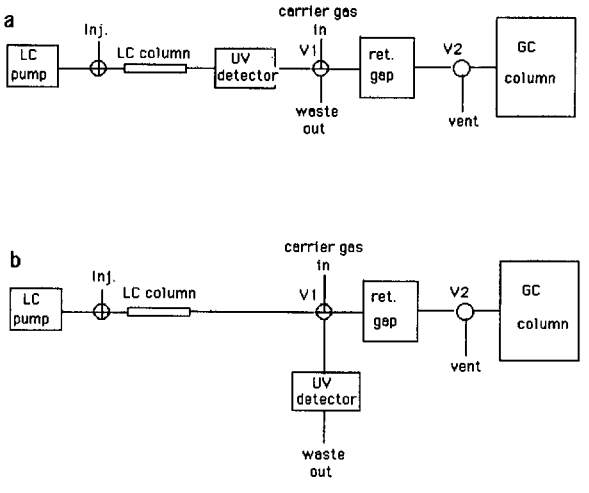

Fig. 1. Scheme of LC–GC with a UV detector (a) in the transfer line or (b) in the waste line.

gives no extra peak broadening but lacks the direct control of the transferred fraction.

After the collection time or volume has been determined, the fraction is eluted directly into a retention gap by the LC pump or is collected in a loop connected to the valve (V1).

With concurrent solvent evaporation [5], large volumes can be transferred to a heated retention gap, 2–20 m long and 0.3 mm I.D., with a pump rate of 20–200 μl/min, as the solvent evaporates as it enters the retention gap. With non-aqueous solvents, millilitre volumes can be transferred [5]. However, low-boiling solutes can only be reconcentrated with partial concurrent evaporation, using long retention gaps.

With the standard retention gap technique the solvent is not removed during the transfer step. With a 50 m × 0.32 mm I.D. retention gap, up to 300 μl of non-aqueous solvents can be injected, utilizing a thick-film column for better reconcentration [6]. Unfortunately, such high-volume injections are not permissible with aqueous solvents, as the surfaces of the retention gaps are not easily wetted by water and as the vapour volume of water is approximately four times higher than that of most non-aqueous solvents. As most LC applications utilize aqueous reverse-phase systems, the transferable volumes are drastically reduced.

With microbore (1 mm I.D.) LC columns, the peak volumes are usually in excess of the volumes that can be handled by conventional splitless or on-column GC injectors. With a 10 cm × 1 mm I.D. column, the peak volume at $k' = 3$ can be calculated to be 6.4 μl (Table 1) and with a 25 cm × 1 mm I.D. column to be 16 μl. However, as the components of interest often do not show up as visible peaks on the first column, but rather are hidden behind other components, the cut must be considerably wider than one calculated peak volume. With a buffer of two peak volumes on each side of the peak, to prevent losses, the corresponding volumes are 32 and 80 μl, respectively. If a relatively broad band ($k'_n - k'_m = 1$) is collected, the corresponding volumes are of the order of 64 and 160 μl (Table 1). The only way to concentrate such volumes is to use concurrent solvent evaporation with slow introduction into a heated retention gap. With packed microcolumns (0.1–0.3 mm I.D.), however, the effluent volumes can be handled with standard

TABLE 1

PEAK VOLUMES FROM PACKED COLUMNS, CALCULATED AS 4 STANDARD DEVIATIONS

Column length, 10 cm; N = 4000; linear flow = 0.14 cm/s.

Column I.D. (mm)	Peak volume (μl)			Flow-rate (μl/min)	Wide cut ($\Delta k'$ = 1)	
	k' = 1	k' = 3	k' = 7		μl	s
1	3.2	6.4	12.8	40	64	96
0.5	0.8	1.6	3.2	10	16	96
0.25	0.2	0.4	0.8	2.5	4	96
0.1	0.05	0.1	0.2	0.4	0.7	96

injection techniques, for example with a sampling valve with a 5-μl loop and a sampling time of 1–2 min.

3. LC–SFC

Compared with capillary GC, the column dimensions required to obtain similar efficiencies are significantly smaller in capillary SFC owing to the less favourable mass transfer properties of supercritical fluids compared with gases. Consequently, the volumes of the retention gaps that can be used in SFC need to be smaller than in GC, in order to avoid peak broadening. The required reduction in inner diameter is difficult to stipulate, as the reconcentration that can be obtained at the column inlet in SFC depends on the density gradient that can be applied.

In LC–SFC (Fig. 2), a selected fraction can be transferred and concentrated as above on a heated retention gap or the solvent can be removed with an inert gas (gas purging) or removed under supercritical conditions on a precolumn [7]. The latter procedure allows volumes up to 1–2 μl to be transferred to 50 μm I.D. columns. During solvent evaporation, the vent valve (V2) has been recommended to be closed towards the SFC column in order to maintain pressure on the column and avoid peak broadening [8].

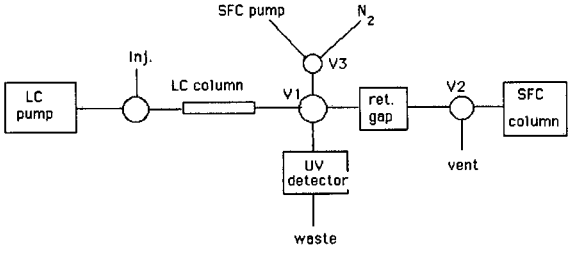

Fig. 2. Scheme of LC–SFC with a UV detector in the waste line and solvent venting valve (V2). The solvent can be removed by gas purging via the switching valve V3.

In a recent demonstration of LC–SFC, utilizing a packed capillary size-exclusion column in the first step, 3–7-μl samples were transferred, the solvent was evaporated with an inert gas on a long retention gap (13 m × 100 μm I.D.) and the components were focused at the inlet of the open-tubular SFC column [9]. Attempts to collect in coated open-tubular precolumns suffered from the disadvantage that solvent which was dissolved in the swollen film was released later, causing disturbances in the chromatograms.

4. PHASE TRANSFER OF SAMPLES IN SUPERCRITICAL FLUIDS

In multi-dimensional systems starting with SFE or SFC, sample fractions in large (millilitre) volumes of carbon dioxide can be collected in a small cold-trap which usually consists of a cooled uncoated retention gap. Samples in carbon dioxide can also be adsorbed in an open-tubular coated precolumn or a packed precolumn. An advantage of SFE over liquid extraction is that a potentially higher selectivity can be obtained, as the density can be chosen at will. Although liquid extraction can be performed with solvents of different solubility, this is significantly more laborious than SFE, where multi-step extractions can be achieved by controlling the pressure and the temperature only, or by a

final step with batch-added solvent [10]. Further, owing to the lower viscosity and higher diffusivity and also the absence of phase separation problems, supercritical fluids often reduce extraction times considerably. Thus, based on these simple physical facts, utilizing a supercritical fluid in the first dimension will often be of significant advantage, whether this is SFE, capillary SFC or packed column SFC.

5. SFC–SFC

The first multi-dimensional SFC was performed on packed columns [11–13]. With valve switching and back-flushing, oil samples were class separated on three coupled microbore columns [11,13], utilizing a flame ionization detector (FID) for quantification. The columns gave good resolution of compound classes due to high selectivity, not high efficiency. The advantages of packed column SFC–SFC are speed and selectivity. Crude North Sea oils were separated into three fractions on three columns and determined within 10–15 min (Fig. 3). The flame ionization detector, however, sets limitations on the total flow into the detector [14]. With packed columns, current detectors require inner diameters not larger than *ca.* 0.5–1 mm for high-speed purposes.

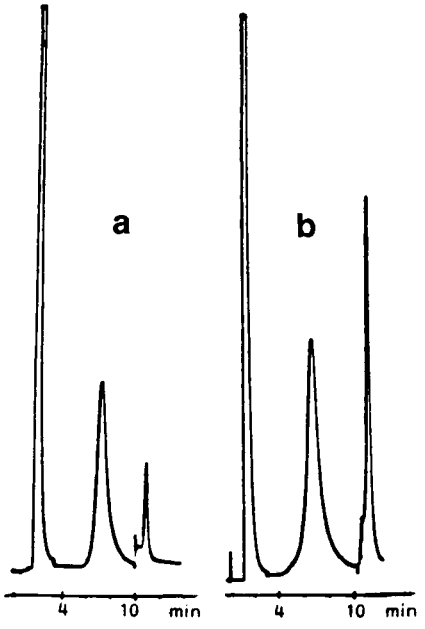

Fig. 3. SFC–SFC class separation of saturates, aromatics and resins in a crude light oil (a) and a crude medium heavy oil (b). From ref. 14, with permission.

For applications requiring high resolution, the last column will normally be a capillary column. In order to obtain high speed and good loadability, a packed narrow-bore column can be included as the first column [15]. The function of the packed column will often be class separation, as shown for coal tar samples [16]. With a rotary valve interface and a cold trap to focus the sample, overloading the capillary column can be avoided. The best resolution on the second column is obtained with a narrow cut from the first column, but there are practical limitations to very narrow heart cuts. Narrow time intervals are difficult to reproduce, and the risk of losing part of the material is considerable. With wider cuts, retention intervals are easier to control, assuming a focusing device is included to avoid overloading the capillary column.

Owing to the limited loading capacity, open-tubular SFC is not necessarily the first choice for the initial separation step. However, if sample concentration is not needed, SFC–SFC with two capillary columns has been demonstrated to give high resolution of narrow heart cuts from complex samples [16]. The total analysis time is increased with a capillary column in the front, although this can be reduced by using a short column at high flow-rates [7].

Sample concentration from the supercritical state is not completely without problems. Pressure reduction from several hundred bar to the lower levels that are needed to deposit the solutes in the retention gap requires a restrictor which is heated to avoid plugging (by solid carbon dioxide or by precipitated sample components), sufficient room for fluid–gas expansion and efficient trapping in the collector. Hence the construction of the restrictor–collector interface is vital to the practical utility of the system, particularly for applications including relatively high-molecular-weight compounds.

6. SFC–GC

By introducing GC in the last dimension, higher chromatographic efficiency is obtained, for applications that allow GC to be used. SFC–GC combinations have been reported for the analysis of fossil

fuel samples with packed SFC columns in the first step [17,18]. With the ability to transfer large effluent volumes to a cold-trap after density-related class separations, the potential of SFC–GC is probably far from being fully developed.

7. SFE–LC

SFE–LC utilizes the advantage of a selective extraction method, but does not always include sufficient resolution in the second dimension. Thus, pesticides in grass were determined at ppb levels with SFE–LC connected to GC with electron-capture detection in a three-dimensional system [19]. The phase transfer from the supercritical state was performed on a linear restrictor (12 μm) and a ceramic frit in a short (4 cm) 0.25 mm I.D. tube at the LC column inlet, venting the carbon dioxide gas to the atmosphere via a three-port connector. The recovery of the insecticide chlorpyrifos was virtually quantitative. Extraction of the same pesticide from wheat required 2% methanol in carbon dioxide for quantitative recoveries [20]. The LC–GC interface was recently shown to be able to transfer larger volumes of liquid, utilizing a modified version of concurrent solvent evaporation [21].

8. SFE–SFC

The most important feature of SFE–SFC is the ability to chromatograph the complete extract, after collection of large extraction volumes on a cold-

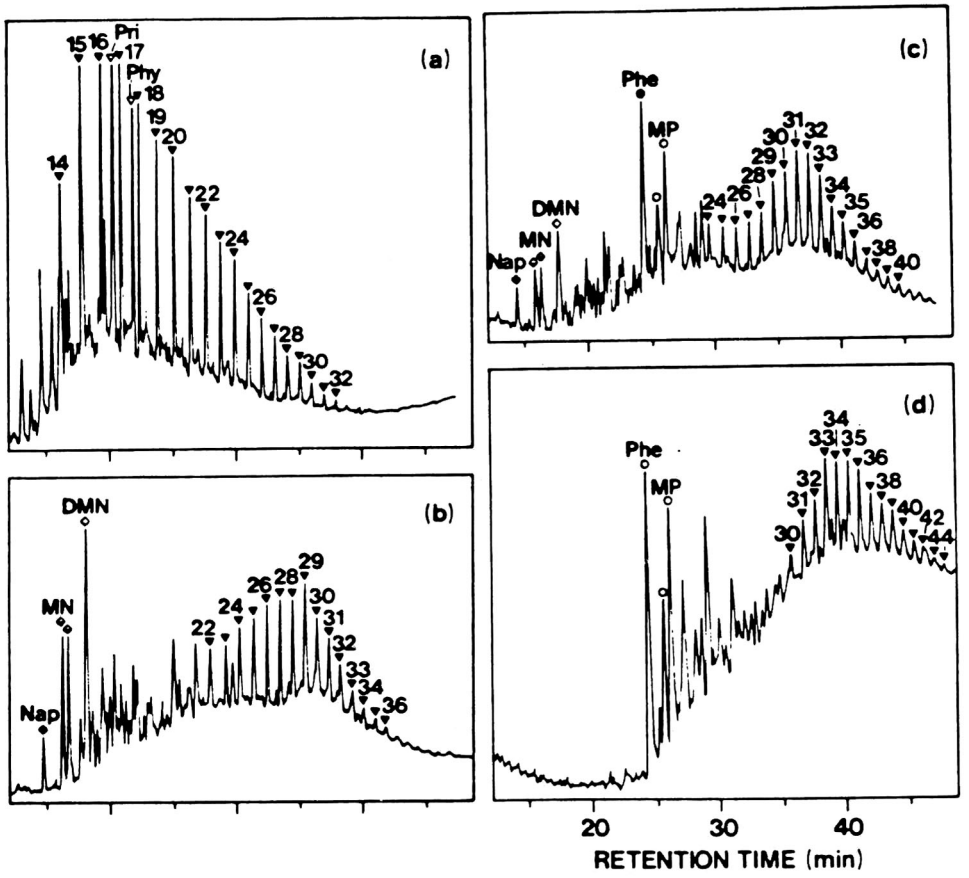

Fig. 4. Capillary SFC of four-stage extraction of Kimmeridge Clay shales with carbon dioxide at (a) 25 MPa and 110°C, (b) 40 MPa and 110°C, (c) 40 MPa and 40°C and (d) 40 MPa, 40°C and CS_2. Peaks: Pri = pristane, Phy = phytane, Nap = naphthalene, MN = methylnaphthalenes, DMN = dimethylnaphthalenes, Phe = phenanthrene, MP = methylphenanthrenes; numbers refer to *n*-alkanes. From ref. 10, with permission.

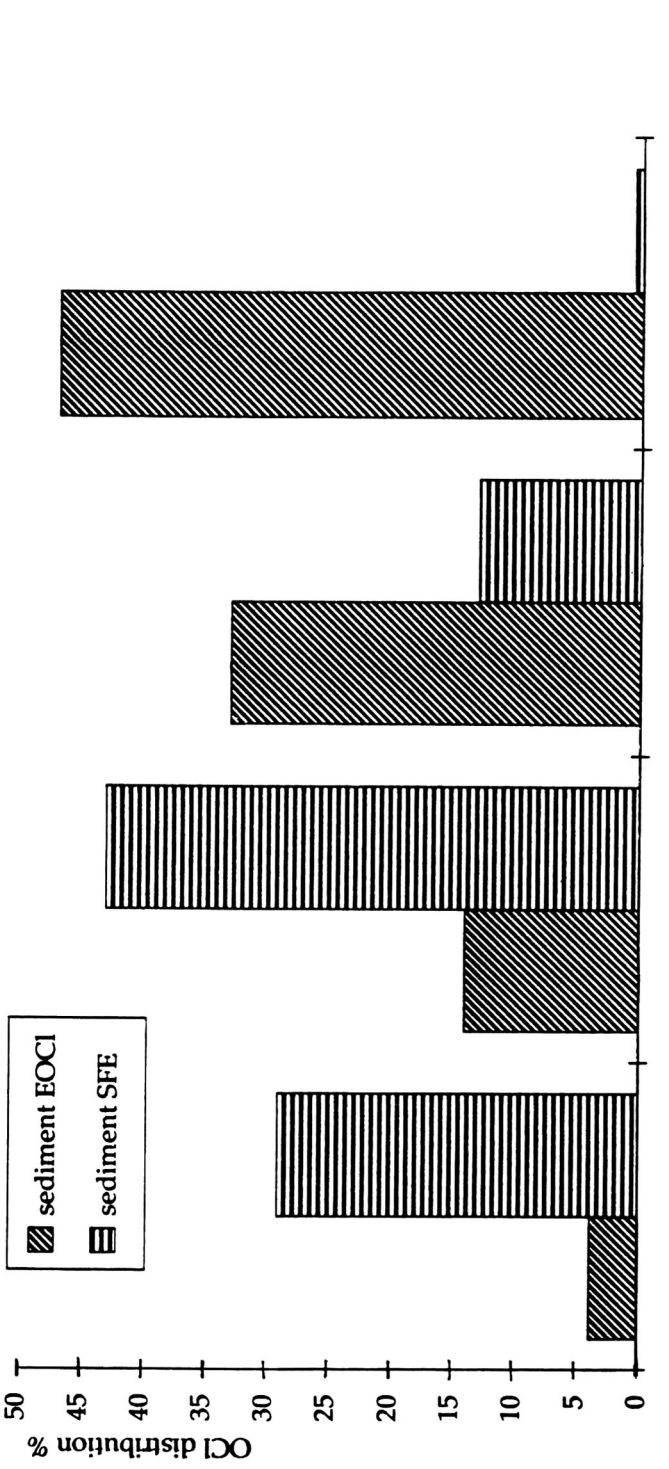

Fig. 5. Polarity distribution of extracts of marine sediments with supercritical CO_2 (sediment SFE) compared with extraction with cyclohexane–isopropanol (sediment EOCl) by elution on silica with the effluents A–D. A = toluene–cyclohexane (1:3); B = diethyl ether–cyclohexane (14:86); C = diethyl ether; D = methanol. From ref. 35, with permission.

trap. Applications utilizing SFE–SFC have been demonstrated in a substantial number of papers with cryotrapping as the most common collection method [22–28], but also with sorbent adsorption as an alternative [27,29–32]. With polar solutes, sorbent trapping may give rise to mass transfer problems, owing to lower desorption rates of polar solutes from adsorbents [27].

An example of the selectivity of SFE was demonstrated by multi-stage extraction of oil shales at different densities (Fig. 4).

9. SFE–GC

SFE–GC, which probably is the most widely applied multi-dimensional technique involving supercritical fluids, was first described by Hawthorne and Miller [33] in 1986. One reason for the instant popularity is that the SFE effluent could simply be depressurized inside the conventional split/splitless injection port, without additional heated transfer lines [33,34]. The advantages of the SFE–GC combination are that the requirements for small retention gaps are less demanding in GC, allowing standard GC dimensions to be used, and that capillary GC in general gives the highest resolution of all the chromatographic techniques. The limits of the SFE–GC combination are usually determined by the limitations set by the chromatographic technique, but often the extraction properties of supercritical carbon dioxide are highly compatible with analytes suitable for GC. As an example, the total content of organic chlorine extracted from marine sediments with plain carbon dioxide was much smaller than that with liquid extraction, particularly of the polar components (Fig. 5). The amount of chlorinated compounds that could be chromatographed by GC, however, was independent of the extraction method [35], demonstrating the selectivity of the extraction and the advantage of not filling up the injector with "dirt".

10. COLD-TRAPS AND SAMPLE TREATMENT

The cold-traps used in SFC–SFC, SFC–GC, SFE–SFC and SFE–GC commonly utilize temperatures of -10 to -50°C. If too high temperatures are chosen, volatile components are lost. If too low temperatures are chosen, water or carbon dioxide may become collected in addition to the solutes, ruining the chromatography after desorption. In order to avoid filling the cold-trap with ice, moist samples should be dried, by freeze-drying or by treating the sample with hydrate formers, such as anhydrous sodium sulphate. Freeze-drying is not compatible with volatile analytes. Hydrate formers have been used on various occasions, but so far no systematic studies have appeared on their ability to withhold the crystalline water under supercritical conditions.

Samples of biological origin and food-related samples often contain considerable amounts of fats, which also have a tendency to fill the cold-trap and overload the column after desorption. The selective extraction of analytes without the fat by adjusting the carbon dioxide density alone is a very tricky procedure and often not possible. A far more practical approach is to add a sorbent with a high fat affinity to the system. Thus, in the extraction of polychlorinated biphenyls (PCBs) from crab hepatopancreas, containing 9% fat [36], the PCBs were virtually selectively extracted by including basic aluminium oxide in a separate vessel in the flow-line after the extractor (Table 2). Thus, treating the sample to increase the adsorption of unwanted sample components introduces the opportunity to improve the selectivity by simple methods. In the future, combinations of SFE and adsorbents are likely to be of value for many applications where high selectivity is required.

TABLE 2

EXTRACTION OF FAT FROM CRAB HEPATOPANCREAS (CONTAINING 9% FAT) WITH CARBON DIOXIDE AT 60°C

The samples were treated with anhydrous sodium sulphate (1:3, w/w), with or without an equal amount of basic alumina. The PCBs were extracted quantitatively at 14.5 MPa. From ref. 36.

Pressure (MPa)	Extracted fat (% of total mass)	
	Na_2SO_4	$Na_2SO_4 + Al_2O_3$
14.5	0.90	<0.01
20	–	0.31
25	2.2	0.44
30	–	0.55
35	4.5	0.60

11. CONCLUSIONS

Automated on-line multi-dimensional separation techniques can reduce analysis times of multi-component samples and improve accuracy, reproducibility and detectability. The use of supercritical fluids in coupled systems is favoured by the lower viscosity and the higher diffusivity of supercritical fluids compared with liquids. Rapid, selective single-stage or multistage extractions can be performed, particularly in combination with the use of selective adsorbents, and coupled to LC, SFC or GC. The consumption of toxic or environmentally hazardous solvents is reduced. Packed column or open-tubular column SFC is coupled to LC or GC depending on solute solubility, selectivity and the efficiency required. Recently developed solvent venting techniques allow increasingly larger volumes of liquid fractions to be transferred to capillary columns. Fractions in supercritical fluids can be transferred to high-resolution columns, either directly or after on-line concentration.

REFERENCES

1 K. D. Bartle, I. Davies, M. W. Raynor, A. A. Clifford and J. P. Kithinji, *J. Microcol. Sep.*, 1 (1989) 63.
2 J. C. Giddings, *Anal. Chem.*, 56 (1984) 1258A.
3 J. C. Giddings, *J. High Resolut. Chromatogr. Chromatogr. Commun.*, 10 (1987) 319.
4 I. L. Davies, M. W. Raynor, J. P. Kithinji, K. D. Bartle, P. T. Williams and G. E. Andrews, *Anal. Chem.*, 60 (1988) 683A.
5 K. Grob Jr. and B. Schilling, *J. High Resolut. Chromatogr. Chromatogr. Commun.*, 8 (1985) 726.
6 K. Grob, Jr., C. Walder and B. Schilling, *J. High Resolut. Chromatogr. Chromatogr. Commun.*, 9 (1986) 95.
7 B. E. Berg, A. M. Flaaten, J. Paus and T. Greibrokk, *J. Microcol. Sep.*, 4 (1992) 227.
8 I. J. Koski and M. L. Lee, *J. Microcol Sep.*, 3 (1991) 481.
9 R. Moulder, K. D. Bartle and A. A. Clifford, *Analyst (London)*, 116 (1991) 1293.
10 T. Greibrokk, M. Radke, M. Skurdal and H. Willsch, *Org. Geochem.*, in press.
11 E. Lundanes and T. Greibrokk, *J. Chromatogr.*, 349 (1985) 439.
12 R. G. Christensen, *J. High Resolut. Chromatogr.*, 8 (1985) 824.
13 E. Lundanes, B. Iversen and T. Greibrokk, *J. Chromatogr.*, 366 (1986) 391.
14 H. Skaar, H. R. Norli, E. Lundanes and T. Greibrokk, *J. Microcol. Sep.*, 2 (1990) 222.
15 I. L. Davies, B. Xu, K. E. Markides, K. D. Bartle and M. L. Lee, *J. Microcol. Sep.*, 1 (1989) 71.
16 Z. Juvancz, K. M. Payne, K. E. Markides and M. L. Lee, *Anal. Chem.*, 62 (1990) 1384.
17 J. M. Levy, J. P. Guzowski and W. E. Huhak, *J. High Resolut. Chromatogr. Chromatogr. Commun.*, 10 (1987) 337.
18 J. M. Levy and J. P. Guzowski, *Fresenius' Z. Anal. Chem.*, 330 (1988) 207.
19 R. M. Campbell, D. M. Meunier and H. J. Cortes, *J. Microcol. Sep.*, 1 (1989) 302.
20 H. J. Cortes, L. Shayne Greene and R. M. Campbell, *Anal. Chem.*, 63 (1991) 2719.
21 H. J. Cortes, R. M. Campbell, R. P. Himes and C. D. Pfeiffer, *J. Microcol. Sep.*, 4 (1992) 239.
22 M. R. Andersen, J. T. Swanson, N. L. Porter and B. E. Richter, *J. Chromatogr. Sci.*, 27 (1989) 371.
23 Q. L. Xie, K. E. Markides and M. L. Lee, *J. Chromatogr. Sci.*, 27 (1989) 365.
24 M. Asraf-Khorassani, M. L. Kumar, D. J. Koebler and G. P. Williams, *J. Chromatogr. Sci.*, 28 (1990) 599.
25 N. J. Cotton, K. D. Bartle, A. A. Clifford, S. Asraf, R. Moulder and C. J. Dowle, *J. High Resolut. Chromatogr.*, 14 (1991) 164.
26 B. Murugaverl and K. J. Voorhees, *J. Microcol. Sep.*, 3 (1991) 11.
27 H. Daimon and Y. Hirata, *Chromatographia*, 32 (1991) 649.
28 S. B. Hawthorne, M. S. Krieger and D. J. Miller, *Anal. Chem.*, 60 (1988) 472.
29 M. Saito, Y. Yamauchi, K. Inomata and W. Kottkamp, *J. Chromatogr. Sci.*, 27 (1989) 79.
30 T. W. Ryan, S. G. Yocklowich, J. C. Watkins and E. J. Levy, *J. Chromatogr.*, 505 (1990) 273.
31 I. J. Koski, K. E. Markides, B. E. Richter and M. L. Lee, *Anal. Chem.*, 64 (1992) 1669.
32 A. Munder, R. G. Christensen and S. A. Wise, *J. Microcol. Sep.*, 3 (1991) 127.
33 S. B. Hawthorne and D. J. Miller, *J. Chromatogr. Sci.*, 24 (1986) 258.
34 S. B. Hawthorne, D. J. Miller and J. J. Langenfeld, *J. Chromatogr. Sci.*, 28 (1990) 2.
35 A. L. Kvernheim, K. Martinsen, G. E. Carlberg, B. E. Berg, M. Fresvig and T. Greibrokk, *Environmental Fate and Effects of Bleach Pulp Mill Effluents. Proceedings of a SEPA Conference, Saltsjøbaden, Stockholm, November 19–21, 1991*, Swedish Environmental Protection Agency, Report No. 4031.
36 H. R. Johansen, G. Becher and T. Greibrokk, *Fresenius' J. Anal. Chem.*, in press.

Journal of Chromatography, 626 (1992) 41–52
Elsevier Science Publishers B.V., Amsterdam

CHROM. 24 522

Review

Hydrodynamic and hydrostatic high-speed countercurrent chromatography and its coupling with various kinds of detectors

Application to biochemical separations

D. Thiébaut and R. Rosset

Laboratoire de Chimie Analytique de l'Ecole Supérieure de Physique et de Chimie Industrielles de la Ville de Paris (URA CNRS 437), 10 Rue Vauquelin, 75231 Paris Cedex 05 (France)

ABSTRACT

A general introduction is given to modern countercurrent chromatography, high-speed countercurrent chromatography using the coil planet centrifuge and centrifugal droplet countercurrent chromatography (centrifugal partition chromatography). The two techniques offer new capabilities for the retention of the liquid stationary phase in the column via a strong centrifugal field and for increased efficiency. Thus, the flow-rate of the mobile phase permits faster separations in comparison with previous techniques such as droplet countercurrent chromatography or rotation locular countercurrent chromatography. Examples are given to show that this is a powerful technique for the preparative-scale separation of natural compounds and it can be coupled to various detection system.

CONTENTS

Correspondence to: Dr. D. Thiébaut, Laboratoire de Chimie Analytique de l'ESPCI, 10 Rue Vauquelin, 75231 Paris Cedex 05, France.

0021-9673/92/$15.00 © 1992 Elsevier Science Publishers B.V. All rights reserved

1. INTRODUCTION

Countercurrent chromatography (CCC) refers to support-free liquid–liquid chromatography with two immiscible solvents. Recently developed instruments allow the liquid stationary phase to be kept in the column while the mobile phase is pumped through it at high flow-rate, because a strong centrifugal field is created by the motion of the column. Thus, the separation time is much lower than in previous techniques such as droplet countercurrent chromatography (DCCC).

The main features of interest of modern CCC arise from the use of a liquid stationary phase instead of a solid phase: adsorption or degradation of solutes by the solid phase are avoided, the stationary phase is more stable to acidic or basic conditions than silica-based supports, the volume ratio of the stationary phase to the total column volume is much higher than that in reversed-phase HPLC [1], giving higher column capacity and limiting column overloading, and the volume of the stationary phase can be easily fixed by the operator. Dirty samples or complex matrices can be accepted without clean-up; total recovery of the sample is ensured because both the mobile and the stationary phases are liquids and can be collected after the separation. This makes CCC very attractive for preparative-scale chromatography and competitive with preparative-scale HPLC [2].

From an economical point of view, only the cost of the solvents has to be considered; the consumable operating cost of preparative CCC per gram of product is much lower than that of preparative HPLC [2].

Numerous types of CCC apparatus have been developed over the past 25 years, mostly as prototypes by Ito. In our opinion, too much different apparatus combined with a complicated original technique discouraged newcomers to the field, leading to very poor development of this technique. Here, only the commercially available modern and fast systems that have been used in our laboratory will be considered: a hydrostatic equilibrium system (HSES) known as centrifugal partition chromatography (CPC) or centrifugal droplet CCC (CDCCC) where the "locular column" is arranged in a centrifuge; and hydrodynamic equilibrium systems (HDES) in which the coiled column (or two or three columns in series) has a planetary motion, promoting mixing and settling of the two phases. The latter type of system is generally refered as Ito's machine, coil planet centrifuge (CPC) or high-speed countercurrent chromatography (HSCCC).

As in modern liquid chromatography, on-line detection is of major importance for monitoring the HSCCC column effluent and will be discussed here.

This paper also presents some recent advances in CCC from the points of view of separations and loadability. For convenience, HSES and HDES will be treated separately and briefly presented. More details concerning the fundamentals, instrumentation and applications of CCC can be found in books and other papers [1,3–8]. Special issues of the *Journal of Liquid Chromatography* have also been published on this topic (see ref. 1) and one is actually in preparation. Curiously, only a few papers have dealt with the chromatographic fundamentals of HSCCC or comparison with HPLC and are also of interest [3,4,9,10]. Basics and major references concerning CDCCC can be found in ref. 8.

2. HYDRODYNAMIC EQUILIBRIUM SYSTEM: THE COIL PLANET CENTRIFUGE (HIGH-SPEED COUNTERCURRENT CHROMATOGRAPHY)

2.1. Principle and apparatus

2.1.1. Column and rotation. The HDES apparatus exhibits a complex motion of the column that has to be described for a better understanding of the technique.

The column (Fig. 1) consists of a PTFE multilayer coiled column rotating around its own axis. The radius (r) of the coiled column depends on the number of layers. During rotation, an Archimedean effect is experienced by the contents of the column, which migrate toward the head of the column; this effect is assumed to be responsible for the retention of one liquid phase (the stationary phase) in the column. The column is also rotating around the axis of revolution of the system to lead to a planetary motion defined as type IV by Mandava and Ito [3]. The revolution radius is R. The ratio r/R is defined as the parameter β, which generally varies between 0.25 and 0.75 depending on the apparatus and the number of layers of PTFE tubing constituting the column.

Owing to this motion, the movement of a layer of

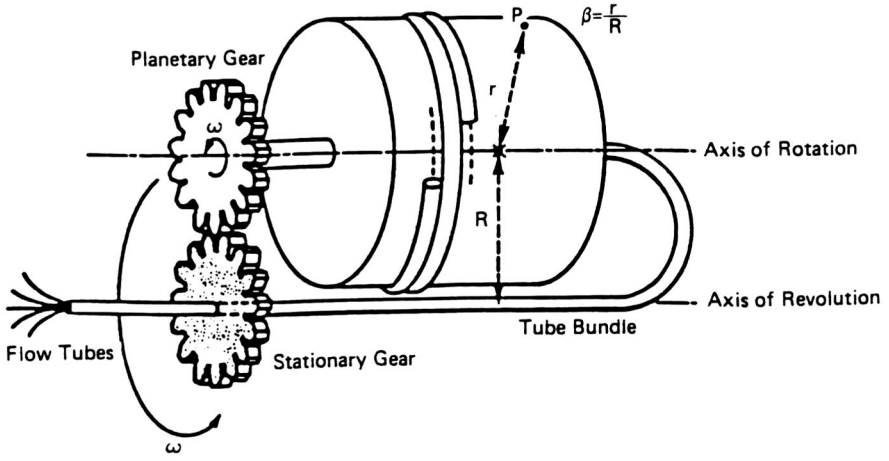

Fig. 1. Schematic diagram of an HSCCC column. The column rotates around its axis at angular velocity ω and around the main axis at ω. Flow tubes are placed in the central axis and the column axis to avoid twisting and breaking; hence no rotational seal is required.

the column can be represented as shown in Fig. 2. When β exceeds 0.5, the trajectory exhibits a loop where the force field is much lower (or is zero for $\beta = 0.25$) than in the opposite case. This difference in force field leads to two different behaviours of a two-phase system in the CCC column: when the force field is strong, the two phases are separated (settling step); when the intensity of the field is low (in the loop), mixing of the two phases occurs [4]; this can lead to the formation of droplets depending on the properties of the solvents [11]. Thus, during revolution, mixing and decantation steps are automatically produced that simulate a series of separating funnels.

2.1.2. Solvent systems. In CCC, there are three main criteria for selecting a solvent system to perform separations. First, solvent systems have to be composed of two immiscible phases; second, their selectivity towards samples of interest has to be sufficient to lead to separations with good resolution; and third, the stationary phase must be retained in the column when applied in a CCC unit.

The most important criterion is the second one. Depending on the polarity of the solutes to be separated, one will select a hydrophobic or non-aqueous, hydrophilic or intermediate solvent system (trends are given in Table 1). Generally, the systems are based on two immiscible solvents and the partitioning of the solutes in the two phases is adjusted by addition of one or two solvents (modi-

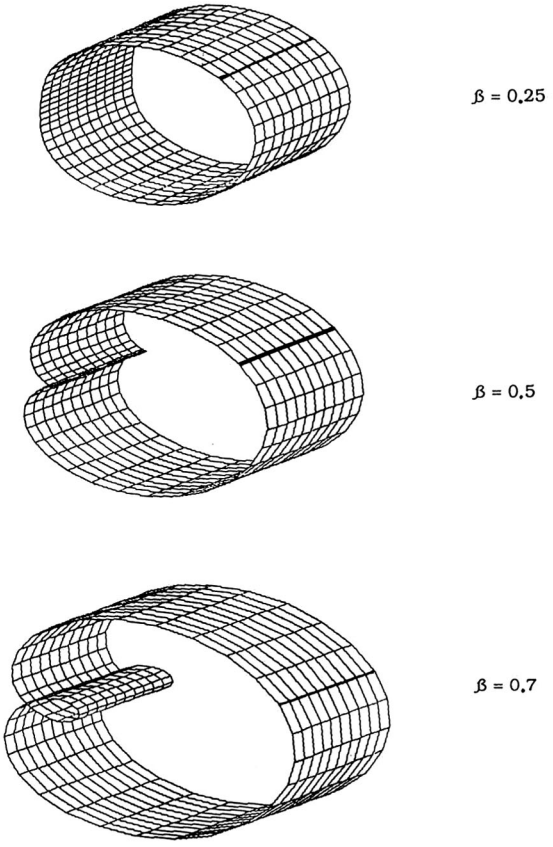

Fig. 2. Motion of a layer of the column in a coil planet centrifuge. In the small loop, at high β values, mixing of the two phases occurs. At the opposite of this small loop, settling is observed.

TABLE 1

GENERAL TRENDS FOR SELECTING SOLVENT SYSTEMS FOR COUNTERCURRENT CHROMATOGRAPHY AS A FUNCTION OF POLARITY OF SOLUTES

Pumping direction of mobile phase *versus* density of the mobile phase and solvent system classification in a coil planet centrifuge.

	Polarity of solutes		
	Non-polar	Medium polarity	Polar
System of solvent (Ito's classification)	Non-aqueous or hydrophobic	Intermediate	Hydrophilic
Pumping direction of the lighter (L) and heavier (H) phases in the coil planet centrifuge	L: tail-to-head H: head-to-tail	$B > 0.25$ as hydrophobic $B < 0.25$ as hydrophilic	L: head-to-tail H: tail-to-head
Basic solvents	Hydrocarbons–acetonitrile, methanol (or water)	Chloroform–methanol–water	Butanol–ethanol–water
Modifiers	Methyl acetate Ethyl acetate Dichloromethane Ethanol	Ethyl acetate Propanol Acetic acid	Methanol Acetone Acetic acid

fiers) that dissolve in the two phases. The pH can also be controlled. Evaluation of the selectivity of different solvent systems can be done by determination of the partition coefficients (K) of the components; K is the ratio of the concentration in the stationary phase to that in mobile phase. TLC, HPLC, UV absorptiometry, etc., can be used to determine K. A high selectivity (α) between adjacent solutes ($\alpha = K_2/K_1$) is needed [1] ($\alpha \approx 1.5$–2 at $K \approx 1$) and is easily obtained [12] to ensure separations require only 1000–2000 theoretical plates in the CCC column.

The two previous points have to be considered for any CCC separation. However, in HSCCC, the third criterion is very important because the behaviour of the stationary phase depends on the nature of the solvents used to form the system: one must check the class to which the system belongs before operation in order to obtain maximum retention of the stationary phase by pumping the mobile phase in the right way depending on the material chosen as the stationary phase (Table 1); calculation of settling velocity and of capillary wavelength [13] can be of major interest for systems for which the behaviour in the HSCCC column is unknown.

Moreover, in CCC the resolution can be expressed as

$$R_s = 2\ V_s \cdot \frac{K_2 - K_1}{w_1 + w_2} \quad (1)$$

where V_s is the volume of stationary phase in the column, K_i the partition coefficient of solute i and w_i the peak base width (in volume units). The higher is V_s in CCC (and in CDCC), the higher is the resolution between adjacent peaks. Hence V_s must also be considered for optimizing resolution in CCC [9].

Finally, to achieve on-line detection, a stable stationary phase retention is also required, which sometimes can be difficult [14,15].

2.1.3. Apparatus. In HDES apparatus, the Ito coil planet centrifuge (PC, Potomac, MD, USA), the use of rotary seals is avoided by placing the flow tubes in the central and column axis to make connections between the injection valve, the column and the detector. In this model, the column is balanced by a counterweight (Fig. 3). More recently, apparatus have been developed by Pharmatech (Baltimore, MD, USA), Models 800, 2000 and 3000, SFCC (Eragny, France), Model CPHV 2000 (not avail-

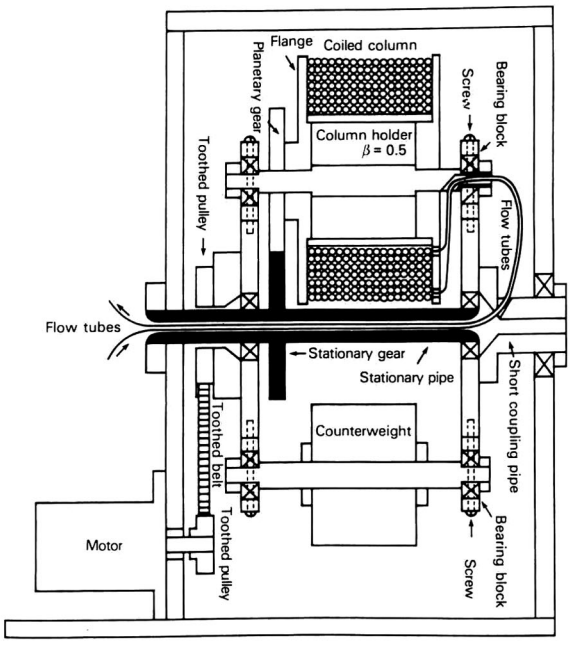

Fig. 3. Schematic diagram of a single-column coil planet centrifuge. A counterweight is used to equilibrate the system.

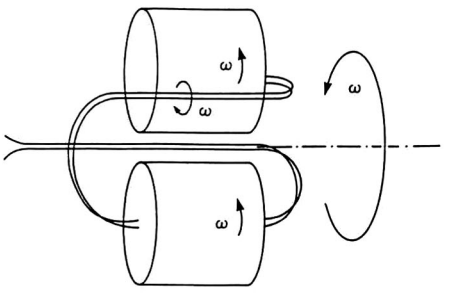

Fig. 4. Schematic diagram of a two-column coil planet centrifuge. The columns balance each other and no counterweight is required.

able), and SEAB (Villejuif, France), Model Kromaton, where two or three columns are connected in series and balance each other (Fig. 4); to avoid breaking of the flow tubes between two adjacent columns, they must be placed in a counter-rotating axis. Generally, HSCCC columns are not thermostated, except the Model CPHV 2000. Pumps and injectors are identical with those in analytical or semi-preparative HPLC.

Generally, UV detection is performed off-line, after laborious collection of fractions; on-line detection is to be preferred for high-speed separations but it can be difficult because bleeding of the stationary phase can occur and a difference in temperature may exist between the column and the detector, leading to demixing of the two phases in the detection cell [14]. Hence other detection methods can be used, such as evaporative light-scattering detection, which removes the solvents before the solutes enter the detection cell [15], or fluorescence detection; mass spectrometry [16–18] and FTIR spectrometry [19] have been applied in several applications coupled to HSCCC. Several devices have also been proposed to enhance on-line UV detection: heating of the transfer line between detection cell and column [14] to reduce the difference in temperature; installation of a pressure restrictor after detection to avoid bubble formation in the detection cell [14]; and prior detection, addition of a solvent (such as 2-propanol) to the column effluent that increases the miscibility between the stationary phase and the mobile phase in case of bleeding of the stationary phase [15,20]; an extra pump (pulse-free) and a mixing chamber are required.

In the next section, several examples are given to demonstrate the use of on-line detectors with HDES–HSCCC.

2.2. *Applications*

Several applications of HSCCC are presented here with special emphasis devoted to the separation of pristinamycin macrolide antibiotics. Table 2 gives general fields of applications of HSCCC (also valid for CDCCC).

Pristinamycins are macrolide antibiotics active on Gram-positive microorganisms (Fig. 5). An extract of fermentation medium can be injected directly into the HSCCC column, leading to a raw separation, the polar stationary phase retaining the ballast (which is yellow). The solvent system chloroform–ethyl acetate–methanol–water (2.5:1.5:3:2, v/v) can produce fractions containing up to 60% of PIIB compared with 9% in the sample. Fig. 6 shows the chromatograms obtained by HSCCC by injecting 500 mg of raw extract (dissolved in the aqueous stationary phase to obtain 50 ml). Chromatogram (a) is a first fractionation: peak compression occurs owing to selection of the stationary phase as the solvent for

TABLE 2

GENERAL APPLICATIONS OF COUNTERCURRENT CHROMATOGRAPHY

H = Heavier phase; L = lighter phase; MS = mass spectrometry; TLC = thin-layer chromatography; UV and Visible = absorptiometry in ultraviolet or visible region; on-/off-line = effluent is continuously monitored on-line but off-line detection is also performed on collected fractions; n.a. = data not available.

Application	Solvent system	Mobile phase and detection	Ref.
Insecticides Demeton	Pentane–methanol–water (6:5:1)	H TLC of fractions	21
Herbicides Triazines	Hexane–ethyl acetate–methanol–water (8:2:5:5)	L UV 254 nm MS off-line	22
Terpenes Triterpenes	Hexane–acetonitrile–methanol–water (5:5:4:2)	H n.a.	7
Antibiotics Arizonins	Hexane–ethyl acetate–methanol–water (1:1:1:1, 2:3:3:2 or 2:5:3:2)	L n.a.	3
Various antibiotics	Chloroform–methanol–water	H	3, 4, 7
Norerythromycins	*n*-Heptane–benzene–2-propanol–acetone–buffer (5:10:3:2:5) or carbon tetrachloride (or chloroform)–methanol–buffer (1:1:1)	H TLC	23
Steroids Hydrocortisone	Hexane–dichloromethane–methanol–water (1:4:1.7:0.8)	H n.a.	3
DNP-amino acids	Chloroform–0.1 *M* hydrochloric acid–acetic acid (2:1:2)	L/H UV of fractions	24
Hormones Indole auxins	Hexane–ethyl acetate–methanol–water (3:7:5:5)	H UV 260 nm on-/off-line	25
Alkaloids Digitonin	Chloroform–methanol–acetic acid–water (5:3:1:3)	H n.a.	3, 7
Tannins	*n*-Butanol–0.1 *M* sodium chloride (1:1)	L UV 280 nm	26
Dipeptides	*n*-Butanol–acetic acid–water (4:1:5)	H/L UV 280 nm on-/off-line	27
Purine and pyrimidines	*n*-Butanol–phosphate buffer (pH 6.5) (1:1)	L UV off-line	24
Proteins Bombesin	*n*-Butanol–dichloroacetic acid–water (100:1:100)	H UV 280 nm on-/off-line	28
Cholecystokinin analogue	*n*-Butanol–0.2 *M* ammonium acetate (pH 9)	L UV 280 nm HPLC of fractions	29
Pigments Dyes	*n*-Butanol–ethanol–water (10:1:5)	L n.a.	7
Methyl violet	Chloroform–water–acetic acid (2:1:2)	H Visible/MS off-line	30
Catecholamines Noradrenaline Dopamine	*n*-Butanol–barium chloride (saturated solution, pH 6.5) (1:1)	L UV 278 nm	31

the samples [12]; the second chromatogram is obtained by re-injecting the collected fraction into the HSCCC system and leads to 85% purity of PIIB. Pristinamycins were detected on-line ELSD. On-line spectrofluorimetry was also used for the detection of PI in analytical-scale HSCCC (Fig. 7). The selectivity of the solvent system was obtained by adding formic acid to the previous one. Stable detection was

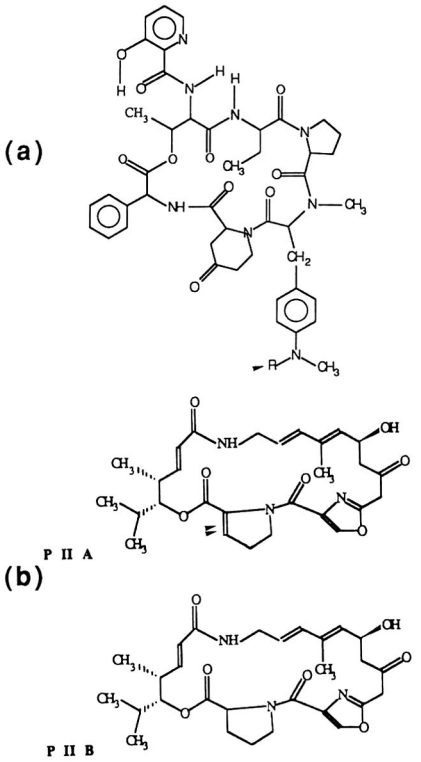

Fig. 5. Structures of (a) pristinamycins IA (R = CH_3) and B (R = H) and (b) pristinamycins IIA and B.

ensured by using specific detection. UV detection with similar conditions of solvents and flow-rate required addition of 2-propanol to the column effluent prior to detection [15].

Using a 1-l column and the aqueous phase as the mobile phase to increase capacity factors and resolution, injections of 11 g of sample treated as for preparative HPLC were made. Comparisons with preparative HPLC demonstrated that HPLC is twice as fast but much more expensive: the solvent consumption is five times higher in HPLC (without considering the cost of the stationary phase). The final purities of PIIB were 92.3% and 91.6% for preparative HPLC and preparative CCC, respectively [2,32].

As Figs. 6 and 7 show, analytical separations performed by HSCCC approach HPLC separations from the point of view of efficiency, resolution and separation time; thus, mass spectrometry on-line with HSCCC can be a powerful tool for the identifi-

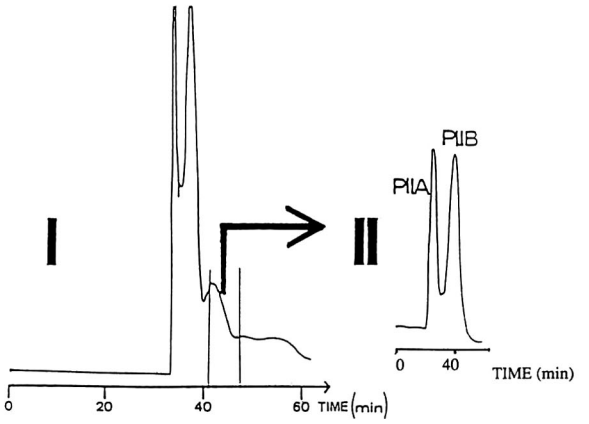

Fig. 6. Direct two-step purification of raw extract of pristinamycins from fermentation medium. After the first separation, the fraction containing PIIA and B is collected and re-injected into the countercurrent chromatograph. PIIB recovered is of 85% purity. Conditions: column, volume 300 ml, 700 rpm (PC high-speed countercurrent chromatograph); solvent system, chloroform–methanol–ethyl acetate–water (2.5:3:1.5:2, v/v); mobile phase, organic phase; flow-rate, 4 ml/min; detection, evaporative light scattering detector at 40°C; sample, 500 mg of raw extract dissolved in the stationary phase to obtain peak compression; volume injected, 50 ml.

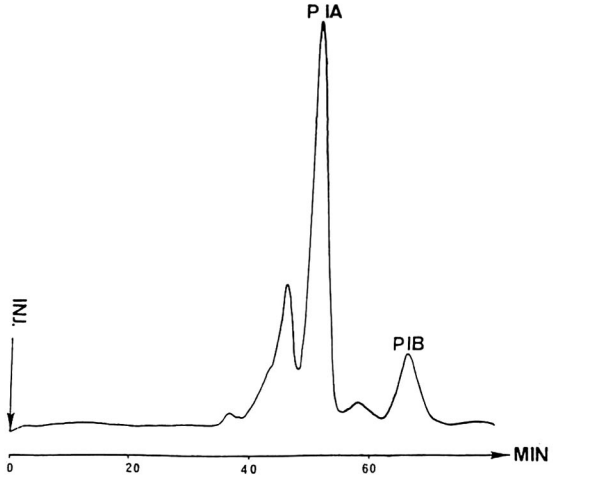

Fig. 7. Separation of pristinamycins IA and IB by countercurrent chromatography with fluorescence detection. Conditions as in Fig. 6 except 0.4% formic adid added to the solvent system and mobile phase flow-rate 2 ml/min; sample injected, mixture containing 79% of PIA and 11% of PIB dissolved in 450 μl of mobile phase. Fluorescence detection, excitation at 365 nm, emission at 415 nm, 2 mV full-scale.

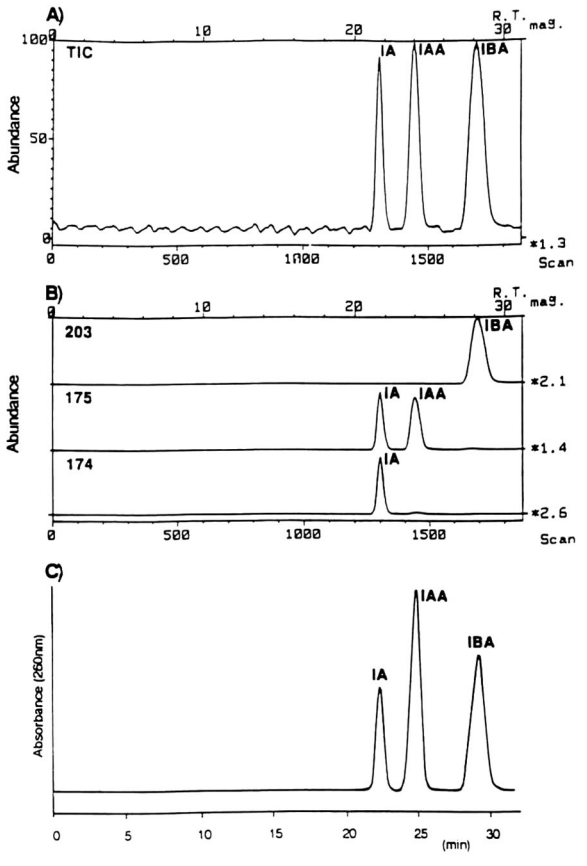

Fig. 8. High-speed countercurrent chromatograms of indole auxins: (A) total ion current and (B) mass chromatograms obtained by electron impact mass spectrometry using splitting of column effluent before frit interfacing to the mass spectrometer; (C) UV trace. Solutes, IA = indole-3-acetamide; IAA = indole-3-acetic acid; IBA = indole-3-butyric acid. From ref. 18.

cation of compounds. This is demonstrated in Fig. 8; separation of indole auxins has been achieved using HSCCC on-line with electron impact mass spectrometry using a frit interface for introducing the column effluent after splitting [18].

3. HYDROSTATIC EQUILIBRIUM SYSTEM: CENTRIFUGAL DROPLET COUNTERCURRENT CHROMATOGRAPHY (CENTRIFUGAL PARTITION CHROMATOGRAPHY)

Centrifugal droplet countercurrent chromatographic or centrifugal partition chromatographic

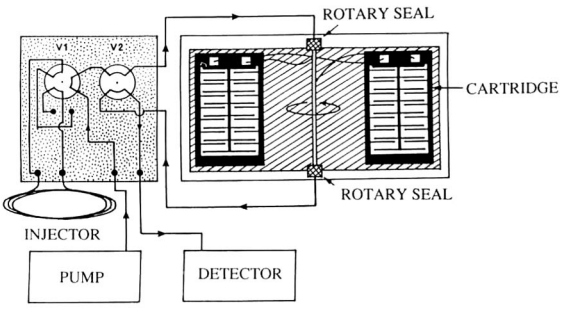

Fig. 9. Schematic diagram of centrifugal droplet countercurrent chromatograph. Two rotary seals are used to connect the injection valve and detector to the column placed in a centrifuge. Ascending or descending modes are selected using a valve located in the injection module. Two to twelve cartridges can be placed in the centrifuge to vary the column volume from 40 to 240 ml.

instruments are manufactured by Sanki Engineering (Kyoto, Japan). The Model LLN is shown in Fig. 9. Rectangular PTFE cartridges engraved with channels and ducts (Fig. 10) are connected in series with capillary tubing and arranged in a circle in a centrifuge to constitute the "column". Two to twelve cartridges can be mounted in the rotor to give 800 to 4800 partition channels and a total volume ranging from 20 to 240 ml. Preparative cartridges can also be placed in the centrifuge to give 480 partition channels and a total volume of 900 ml. The

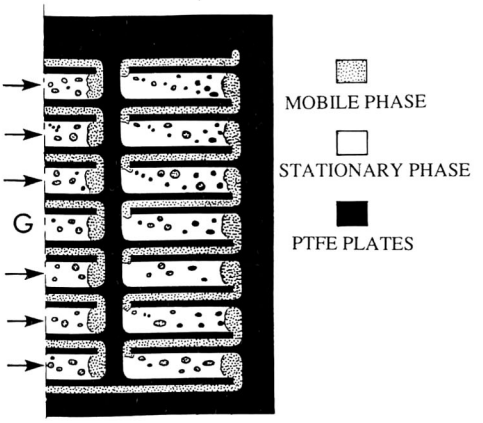

Fig. 10. Schematic diagram of channels in a cartridge of a centrifugal droplet countercurrent chromatograph. In the descending mode, the heavy mobile phase flow in the same direction as the centrifugal field indicated by an arrow; in the ascending mode, the direction of the flow is reversed.

centrifuge can be thermostated. This model is actually being replaced with a new system with a fixed volume of 240 ml equiped with a single disc engraved with 2136 partition channels.

The complete apparatus, including pumps, injection valve and detector, is very similar to an HSCCC system, except for the column. The column is connected to the pump and to the detector via two rotary seals and can be rotated at *ca.* 700–1500 rpm.

Using a selection valve, two elution modes can be performed: in the descending mode the heavier (lower) phase is used as the mobile phase and flows through the lighter (upper) phase used as the stationary phase; the mobile phase has the same direction as the centrifugal field (the channels are parallel to the direction of the centrifugal field); in the ascending mode the upper phase is the mobile phase and the lower phase is the stationary phase. In the ascending mode, the motion of the droplets of the mobile phase is the contrary of the direction of the centrifugal field G (Fig. 10).

Owing to excellent stationary phase retention in the column, original two-phase systems can be used such as aqueous systems or systems having a low interfacial tension in which it is difficult to retain the stationary phase in HDES apparatus. Thus, on-line detection is generally easy to perform after CPC separation. When selecting a solvent system, one does not need to worry about retention of the stationary phase; the only requirement is to obtain a high selectivity in order to achieve resolution of the mixture to be separated with a plate number close to 1000.

The main drawback of CPC is related to the HSES, where partitioning occurs between droplets of the mobile phase dispersed in the stationary phase without promotion of mixing by the motion of the column. Hence the efficiency of the HSES is limited and lower than that of HDES apparatus where the column motion creates mixing/settling sequences.

In CPC, the pressure drop in the system also has to be considered [33]; mainly, it depends on the square of the angular velocity, the flow-rate and the viscosity of the mobile phase. When viscous solvents are used at elevated rotational speed, the pressure drop can exceed the mechanical resistance of the PTFE cartridges. Hence the maximum pressure allowed in CPC has been fixed at 60 bar by the manufacturer; users have to maintain the pressure within this limit by reducing the flow-rate of the mobile phase or the rotational speed of the column. The former can lengthen the duration of separation and reduce the efficiency because the variation of efficiency *versus* the mobile phase flow-rate exhibits

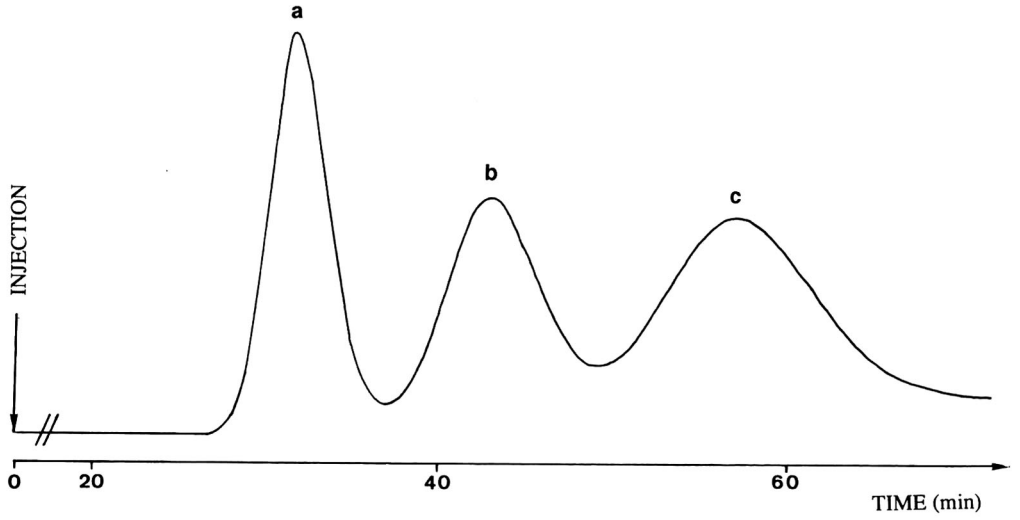

Fig. 11. Separation of phenol derivatives by centrifugal droplet countercurrent chromatography. Conditions: column, six cartridges, 120 ml, 900 rpm; solvent system and mobile phase as in Fig. 6, flow-rate, 2 ml/min; pressure, 43 bar; sample injected, 1 ml of 1 g/l solution dissolved in the mobile phase; detection, UV at 270 nm. a = 2,3-Di-*tert.*-butylphenol, b = *o*-cresol, c = 4-ethylresorcinol.

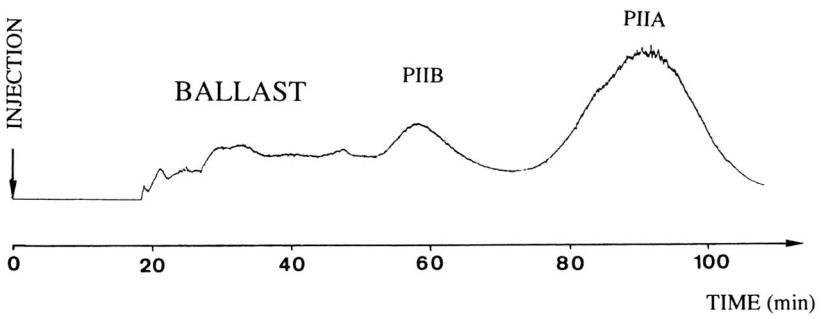

Fig. 12. Centrifugal droplet countercurrent chromatogram of pristinamycins II. In comparison with the separations in Figs. 6 and 7, the mobile phase is the aqueous phase and the composition has been changed to improve the selectivity to compensate for the lower efficiency. Conditions: column, 120 ml (six cartridges), 800 rpm; solvent system, chloroform–methanol–ethyl acetate–water (2:3:2:2, v/v); mobile phase flow-rate, 5 ml/min; pressure drop, 30 bar; detection, evaporative light scattering detector at 40°C; sample, 400 mg of extract dissolved in the stationary phase; volume injected, 8 ml.

a minimum at 1–2 ml/min [34] instead of a maximum in HPLC; thus, flow-rates of 3–5 ml/min are preferred; the latter can be a prejudice for the volume of the stationary phase retained in the column and, consequently, for the resolution, R_s (eqn. 1).

Three examples of applications of CPC are presented in Figs. 11–13. The separation of phenol derivatives summarizes the points developed here concerning efficiency (theoretical plates), pressure drop (43 bar), easy on-line detection (2-propanol is not required after the separation to obtain sensitive and stable detection; it was required for a similar separation by HSCCC [15]). The semi-preparative and preparative capabilities of CPC are demonstrated in Figs. 12 and 13. In Fig. 12, using six analytical cartridges, 400 mg of pristinamycin extract can be injected to lead to more than 92% purity PIIB (more than 95% purity of PIIA). In comparison with Figs. 6 and 7, the solvent system has been changed to enhance the selectivity in order to compensate for the lower efficiency of CDCCC compared with HSCCC. An increase in ethyl acetate content allows the selectivity to be high enough to lead to baseline separation with only a few hundred theoretical plates and one does not have to worry about the stationary phase retention in the column. This was not the case in HSCCC, where a solvent system containing more chloroform was preferred to ensure stable retention of the mobile phase [12]. Fig. 13 shows an example of preparative-scale purification of 130 g of a mixture containing dihomo-γ-linolenic acid performed with a 7-l centrifugal partition chromatograph. Other examples of applications can be found in ref. 8.

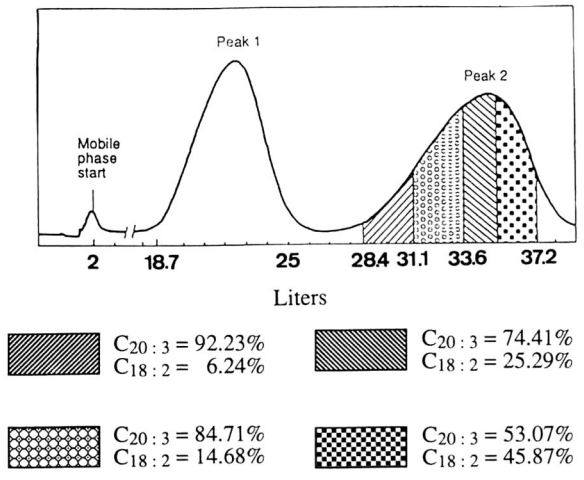

Fig. 13. Preparative centrifugal droplet countercurrent chromatogram of ethyl dihomo-γ-linolenate. Conditions: column, 7 l, 700 rpm; solvent system, hexane–acetonitrile; mobile phase, acetonitrile; flow-rate, 150 ml/min; detection, UV at 210 nm; sample, 130 g of a mixture containing 17.08% of ethyl dihomo-γ-linolenate dissolved in 400 ml of 75% stationary phase–25% mobile phase. Peak 1 is a mixture of ethyl linolenate and ethyl arachidonate. Peak 2 was analysed by gas chromatography: percentages of ethyl dihomo-γ-linolenate ($C_{20:3}$) and ethyl linoleate ($C_{18:2}$) are indicated for the four fractions collected. From ref. 1.

A promising application of CPC for the determination of partition coefficients should also be pointed out because an excellent correlation between shake-flask and CPC measurement of K has

been reported [35,36]. HSCCC has also been used for this purpose [37].

4. CONCLUSION

CCC has already received numerous applications, mostly for the separation or fractionation of natural compounds because raw samples are easily accepted. Generally, the amount injected is a few hundred milligrams for a 300-ml column volume. Results on pristinamycins show that a higher input can be obtained after studying the sample medium. Thus, CCC can compete with preparative HPLC because similar resolution and purity are obtained. It has also been demonstrates that this is a powerful technique for fractionation prior to separation by CCC or preparative HPLC [38] and it can be used for extraction purposes [39,40] (centrifugal partition chromatography with a "modular column volume" is very convenient for extraction). Recognition of CCC by the US Food and Drug Administration is also expected for the determination of octanol–water partition coefficients.

The commercial systems described here offer reliability. Very high selectivity of solvent systems associated with a higher efficiency per unit time than previous CCC techniques such as DCCC permit separations to be completed in less than 1 h instead of days. Nevertheless, more studies of the fundamentals of this technique are required for a better understanding of the mechanism of retention of the stationary phase (HSCCC) and for optimization of separations; the effects of the volume and repartition of the stationary phase in the CCC column, linear velocity of the mobile phase, rotational speed, partition coefficient, etc., on efficiency and resolution (and loadability) have to be clearer than at present. Work is in progress in many laboratories. Difficulties arise from the complex motion of the column used for HSCCC.

When the mechanisms involved in CCC are better understood, the technique should be improved to approach the efficiency per unit time of HPLC.

5. LIST OF ABBREVIATIONS

CCC	Countercurrent chromatography
CPC	Centrifugal partition chromatography
DCCC	Droplet countercurrent chromatography
ELSD	Evaporative light-scattering detection
FTIR	Fourier transform infrared
G	Centrifugal field
HDES	Hydrodynamic equilibrium system
HPLC	High-performance liquid chromatography
HSCCC	High-speed countercurrent chromatography
HSES	Hydrostatic equilibrium system
K	Partition coefficient
MS	Mass spectrometry
MP	Mobile phase
PI, PII	Pristinamycins I and II, respectively
r	Rotation radius
R	Revolution radius
R_s	Resolution
TLC	Thin-layer chromatography
UV	Ultraviolet
V_s	Volume of stationary phase
w_1	Peak base width of solute i
α	Selectivity
β	Ratio of rotation radius to revolution radius

REFERENCES

1 A. P. Foucault, *Anal. Chem.*, 63 (1991) 569A.
2 S. Drogue, D. Thiébaut and R. Rosset, presented at the *19th International Symposium on Chromatography, September 1992, Aix en Provence, France.*
3 N. B. Mandava and Y. Ito (Editors), *Countercurrent Chromatography, Theory and Practice*, Marcel Dekker, New York, 1988.
4 W. D. Conway (Editor), *Countercurrent Chromatography, Apparatus, Theory and Practice*, VCH, New York, 1990.
5 A. Foucault and R. Rosset, *Analusis*, 16 (1988) 157.
6 Y. Ito, Y. W. Lee, W. D. Conway and M. Knight (Editors), *J. Chromatogr.*, 538 (1991).
7 J. B. McAlpine and J. E. Hochlowski, in G. H. Wagman and R. Cooper (Editors), *Natural Products Isolation (Journal of Chromatography Library*, Vol. 43), Elsevier, Amsterdam, 1989, Ch. 1.
8 M.-C. Rolet, D. Thiébaut and R. Rosset, *Analusis*, 20 (1992) 1.
9 O. Bousquet, A. P. Foucault and F. Le Goffic, *J. Liq. Chromatogr.*, 14 (1991) 3343.
10 J.-M. Menet, M.-C. Rolet, D. Thiébaut, R. Rosset and Y. Ito, *J. Liq. Chromatogr.*, in press.
11 J.-M. Menet, *Diplôme d'Etudes Approfondies*, Université Pierre et Marie Curie, Paris, 1991.
12 S. Drogue, M.-C. Rolet, D. Thiébaut and R. Rosset, *J. Chromatogr.*, 593 (1992) 363.
13 J.-M. Menet, D. Thiébaut, R. Rosset, J. E. Wesfreid and M. Martin, presented at *Pittsburgh Conference, New Orleans, 1992*, Abstract 389.

14 H. Oka and Y. Ito, *J. Chromatogr.*, 475 (1989) 229.
15 S. Drogue, M.-C. Rolet, D. Thiébaut and R. Rosset, *J. Chromatogr.*, 538 (1991) 91.
16 Y. W. Lee, R. D. Voykser, Q. C. Fang, C. E. Cook and Y. Ito, *J. Liq. Chromatogr.*, 11 (1988) 153.
17 Y. W. Lee, R. D. Voykser, T. W. Pack, C. E. Cook, Q. C. Fang and Y. Ito, *Anal. Chem.*, 62 (1990) 244.
18 H. Oka, Y. Ikai, N. Kawamura, J. Hayakawa, K. Harada, H. Murata, M. Suzuki and Y. Ito, *Anal. Chem.*, 63 (1991) 2861.
19 R. J. Romañach and J. A. de Haseth, *J. Liq. Chromatogr.*, 11 (1988) 133.
20 D. E. Shaufelberger, *J. Liq. Chromatogr.*, 12 (1989) 2263.
21 Y. W. Lee and C. E. Cook, *J. Liq. Chromatogr.*, 8 (1985) 2253.
22 N. B. Mandava, Y. Ito and J. M. Ruth, *J. Liq. Chromatogr.*, 8 (1985) 2221.
23 J. B. McAlpine, J. S. Tuan, D. P. Brown, K. D. Grebner, D. N. Whittern, A. Buko and L. Katz, *J. Antibiot.*, 40 (1987) 1115.
24 Y. Ito, J. Sandlin and W. G. Bowers, *J. Chromatogr.*, 244 (1982) 247.
25 N. B. Mandava and Y. Ito, *J. Liq. Chromatogr.*, 7 (1984) 303.
26 L. J. Putman and L. G. Butler, *J. Chromatogr.*, 318 (1985) 85.
27 J. Sandlin and Y. Ito, *J. Chromatogr.*, 348 (1985) 131.
28 M. Knight, Y. Ito, P. Peters and C. DiBello, *J. Liq. Chromatogr.*, 8 (1985) 2281.
29 M. Knight, Y. Ito, J. Sandlin and A. M. Kask, *J. Liq. Chromatogr.*, 9 (1986) 791.
30 H. M. Fales, L. K. Pannel, A. E. Sokoloski and P. Carmeci, *Anal. Chem.*, 57 (1985) 376.
31 A. Weisz, S. P. Markey and Y. Ito, *J. Chromatogr.*, 383 (1986) 132.
32 S. Drogue, D. Thiébaut, R. Rosset and J.-L. Janicot, in preparation.
33 A. Berthod and D. W. Armstrong, *J. Liq. Chromatogr.*, 11 (1988) 547.
34 A. Berthod and D. W. Armstrong, *J. Liq. Chromatogr.*, 11 (1988) 567.
35 A. Berthod and D. W. Armstrong, *J. Liq. Chromatogr.*, 11 (1988) 1187.
36 A. Berthod, Y. I. Han and D. W. Armstrong, *J. Liq. Chromatogr.*, 11 (1988) 141.
37 P. Vallat, N. El Tayar, B. Testa, I. Slacanin, A. Marston and K. Hostettmann, *J. Chromatogr.*, 504 (1990) 411.
38 R. Vanhaelen-Fastre, B. Diallo, M. Jaziri, M.-L. Faes, J. Homes and M. Vanhaelen, *J. Liq. Chromatogr.*, 15 (1992) 697.
39 Y. Ito, *J. Chromatogr.*, 207 (1981) 161.
40 Y. Ito, in N. B. Mandava and Y. Ito (Editors), *Countercurrent Chromatography, Theory and Practice*, Marcel Dekker, New York, 1988, p. 377.

Journal of Chromatography, 626 (1992) 53–58
Elsevier Science Publishers B.V., Amsterdam

CHROM. 24 527

Dramatic advances in on-line Fourier transform IR detection for capillary supercritical fluid chromatography

Timothy J. Jenkins, Muammer Kaplan, George Davidson, Michael A. Healy and Martyn Poliakoff

Department of Chemistry, University of Nottingham, University Park, Nottingham, NG7 2RD (UK)

ABSTRACT

We have shown that a flow cell Fourier transform (FT) IR detector for capillary supercritical fluid chromatography (cSFC) can give minimum detection limits which are much lower than any previously reported for on-line cSFC–FT-IR. The system was tested using a range of analytes. The following reproducible values were obtained, using supercritical CO_2 as the mobile phase: 2 ng for a polycyclic aromatic hydrocarbon (pyrene) —a rather weak infrared absorber, 95 pg for caffeine —a strong infrared absorber, and *ca.* 20 pg for the organometallic complex (mesitylene)chromium tricarbonyl —which has some intense infrared absorptions. These figures represent an improvement by a factor of at least 25 on comparable data in the literature. For caffeine a linear dynamic range of more than three orders of magnitude was established for this system.

INTRODUCTION

Supercritical fluids are fascinating and unique media. In the region of a phase diagram above the critical temperature and pressure the physical properties are in many ways intermediate between those of a gas and a liquid. In particular, the viscosity and diffusivity are gas-like, while the density and solvent strength approach those of liquids. This combination of properties has led to the use of supercritical fluids in chromatography (see, for example, ref. 1).

Supercritical fluid chromatography (SFC) has some of the characteristics of gas chromatography (GC) and some of high-performance liquid chromatography (HPLC), and these characteristics have ensured for SFC a particular niche, whereby a significant range of samples which are inaccessible to GC and HPLC can profitably be studied. Thus, the solvent properties of supercritical fluids, and the relatively low tempeatures at which SFC can be carried out, together with chromatographic efficiencies approaching those of GC, mean that high-resolution chromatography can be performed on high-molecular weight and/or thermally labile compounds (see, for example, ref. 2).

In many of the reported applications of SFC, the detection systems employed have been flame ionisation detection (FID) and UV detection, the latter usually at a fixed wavelength. Such detectors can be extremely sensitive, but they have one very serious drawback. They do not provide any direct information on the identities of the species present in any analyte mixture. All that can be achieved is comparison of retention times with those of standard substances, and this technique is only applicable when the likely identities of the analytes are known in advance.

Fourier transform (FT) IR spectroscopy is greatly superior to UV or FID detection in that a very high proportion of analytes possess characteristic infrared spectra, and therefore the spectroscopic identification of individual species is possible [3]. However, there are compensating disadvantages in the use of FT-IR detection. The chief among these

Correspondence to: Dr. George Davidson, Department of Chemistry, University of Nottingham, University Park, Nottingham, NG7 2RD, UK.

0021-9673/92/$05.00 © 1992 Elsevier Science Publishers B.V. All rights reserved

is that the intensity of infrared absorption is very much less than that in the UV region, and this imposes severe restrictions on the design of any FT-IR detector. It has, however, been possible to make use of FT-IR detection in GC [4], although there remain problems in GC–FT-IR associated with the need to maintain the flow cell at a high enough temperature. HPLC–FT-IR is subject to very serious restrictions, because most of the available liquid mobile phases are themselves strong infrared absorbers, and the use of concentration–gradient elution methods makes effective subtraction of solvent spectra virtually impossible. Hence, on-line HPLC–FT-IR has a very limited potential.

Two very convenient supercritical fluids, however, CO_2 and xenon, leave regions of the infrared spectrum free of absorption. Indeed xenon possesses no infrared absorptions at all and therefore leaves the whole infrared range free [5]. There are two principal means by which FT-IR spectra can be obtained from SFC analyte mixtures: solvent-elimination and on-line methods. Both have been described in some detail by Taylor and Calvey [6]. The former technique, as the name implies, involves removal of the solvent and deposition of solid analyte on a moving substrate, which can then be subjected at leisure to FT-IR analysis [7]. The resulting spectra can then be matched to condensed-phase spectral library data [8,9] for species identification.

On-line SFC–FT-IR involves recording the spectrum of an analyte while still in the (supercritical) mobile phase, and here the chief problem is that the cell used to record the spectra must be of small volume compared to the volume of mobile phase containing a single chromatographic peak. For packed-column SFC this is not so difficult, but for capillary SFC (preferred in many cases for reasons to be discussed below) the technical problems in constructing an on-line flow cell for FT-IR detection are formidable. Nevertheless, there have been a number of published reports of such systems [10,11]. Good signal-to-noise ratios are attainable despite the limited number of FT-IR scans that can be carried out in the time taken to scan across a chromatographic peak. A possible modificatin of the on-line SFC–FT-IR method is to use a stopped-flow technique. The mobile phase can be switched from the FT-IR cell to a by-pass line and the spectrum recorded later [12].

Although FT-IR alone is very useful for identifying unknown analyte spectra, no single detection technique can give enough information for unambiguous speciation in all possible analytical mixtures. It is, therefore, our aim to construct a "multiply-hyphenated" analytical system, with sequential UV, FT-IR, FID and/or mass spectrometric detection [13]. The resultant data would be vastly more informative than results obtainable from any single detection technique. It has been decided to use capillary SFC (cSFC) as the method of choice, despite the more stringent volume requirements for the FT-IR cell, as pressure-programming is much easier than with packed-column SFC. Capillary columns also enable very high chromatographic efficiencies to be achieved, and the flow-rates are to be preferred when using expensive and/or toxic mobile phases.

The first stage in developing such a system has been to construct an on-line cSFC–FT-IR system, with a flow-cell FT-IR detector. In order that the analytical system should be compatible with standard chromatographic equipment, care was taken to design the cell so that it could be used in existing commercial FT-IR spectrometers. The cell development has been described in detail [5], together with some preliminary results [14], showing that excellent FT-IR spectra and chromatograms (reconstructed from measurements of total infrared absorption overtime) can be obtained.

We wish now to report some further significant developments with this apparatus: (1) determination of minimum detection limits with on-line cSFC–FT-IR for several types of analyte; and (ii) establishment of the linear dynamic range [15] of amounts of material which can be determined by cSFC–FT-IR.

RESULTS AND DISCUSSION

Experimental

The cSFC–FT-IR system, see Fig. 1, used a Brownlee Microgradient pump (Anachem) for delivery and pressure programming of the mobile phase. The outlet of the pump was connected via a length of stainless steel tubing (1.6 mm O.D. × 0.25 mm I.D.) to the injection valve. This was a Valco C14W two-position switching valve (Anachem) with an internal loop of 100-nl volume and was lo-

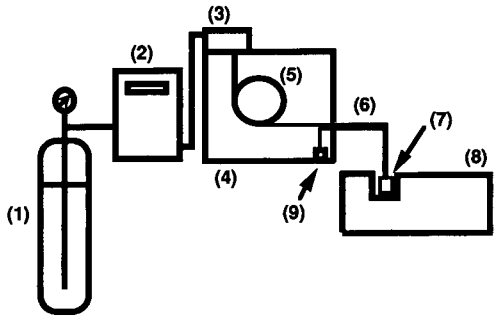

Fig. 1. A schematic diagram of the cSFC–FT-IR system. 1 = Mobile phase cylinder, 2 = syringe pump, 3 = injection valve, 4 = GC oven, 5 = capillary column, 6 = capillary transfer line, 7 = FT-IR flow cell, 8 = FT-IR spectrometer, 9 = flame ionisation detector.

cated on the door of an 8500 GC-oven (Perkin-Elmer). The SFC capillary column (Lee Scientific, from Dionex, Camberley, UK), was installed inside the GC oven and connected directly to the valve. Samples of 100 nl were introduced onto the column by direct injection. The column outlet was connected to a 50 cm × 50 μm I.D. uncoated, deactivated fused-silica capillary transfer line (S.G.E., Milton Keynes, UK) using a zero dead-volume butt-connector (S.G.E.) which passed through the oven wall and was connected to the FT-IR flow-cell.

Two differnt flow cells were used in the experiments described in this paper. Their volumes were 980 nl (path length 5 mm) and 500 nl (path length 4.5 mm), respectively. The cell in use was installed in the sample compartment of a 1760-X FT-IR spectrometer (Perkin-Elmer) fitted with an mercury cadmium telluride detector. After the flow cell a second transfer line was used to return eluent to the GC-oven. This transfer line was butt-connected to a frit restrictor (Lee Scientific) which was then interfaced to the flame ionisation detector of the GC. Following injection IR data were collected using the standard GC–IR software of the spectrometer.

The mobile phase was SFC grade CO_2 (Air Products, Rotherham, UK). Caffeine (Aldrich, Gillingham, UK) and pyrene (B.D.H., Poole, UK) were both of 99% purity, and used without further purification.

Detection limits with cSFC–FT-IR

The sensitivity of any detection technique can be defined in a number of ways, but a convenient concept is that of the injected minimum detectable quantity (IMDQ), as defined originally by Griffiths [16]. The IMDQ for any substrate is defined as that quantity which gives a detector response with a signal-to-noise (S/N) ratio of approximately 3, which can be regarded as the minimum acceptable value for clear identification of a peak.

Among detection techniques that have been used for SFC, the following are the best reported values for IMDQ: (i) scanning UV detection, approximately 3 pg for naphthalene and anthracene [17]; (ii) fluorescence detection, also approximately 3 pg for pyrene [18]; and (iii) electron capture detection, in favourable cases the most sensitive of the techniques reported, 270–640 fg for several polychlorinated biphenyls [19]. Such figures, however, are only attainable in favourable cases for each of these techniques and is important to be able extend the number of detection methods so as to encompass the widest possible range of analytes.

As FT-IR is generally regarded as a less sensitive chromatographic detection technique than, for example, UV, it is important to determine the minimum detection limits for analytes by this method and to show that these are small enough to enable FT-IR detection to play a significant role in SFC detection. As indicated in the Introduction, there have been two distinct approaches to interfacing FT-IR with SFC: on-line flow-cell detection [10], and solvent elimination [6]. The latter is clearly inappropriate for "multi-hyphenation" of detection methods, although in principle it can be made more sensitive, as it is possible to carry out a very large number of FT-IR scans to improve signal-to-noise ratios. One report [7] of such an experiment showed that 1.4 ng of indole-3-acetic acid, after 1000 scans, gave a clear spectrum, with a signal-to-noise ratio for the carbonyl stretching mode (νC=O) of approximately 20.

In order to achieve our goal of "multiple-hyphenation", however, it is necessary to use on-line FT-IR detection. This is, of course, restricted to rather a small number of scans, as the spectrum has to be recorded during the time it takes for a chromatographic peak to pass through the cell. Under such conditions, the lowest reported value for the injected minimum detectable quantity (IMDQ) for strong infrared absorber is 2.5 ng for caffeine, where the strongest νC=O band had a signal-to-noise ratio of approximately 3 [11].

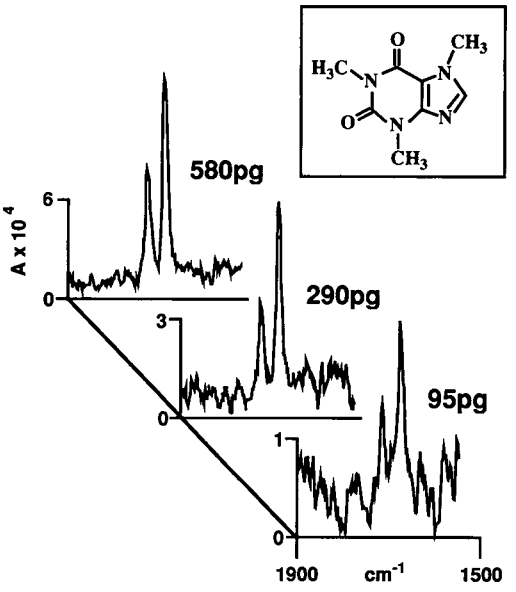

Fig. 2. FT-IR spectra of the νC=O region for caffeine in supercritical CO_2. The injected quantities of caffeine are shown for each spectrum. Experimental conditions: column: 10 m × 50 μm I.D.; stationary phase: 5% phenyl-substituted polymethylsiloxane; temperature: 100°C; mobile phase: CO_2; program: linear pressure ramp from 90 to 400 atm at 10 atm/min; injection: 100 nl direct, solution in dichloromethane; detection: FT-IR flow cell (500 nl) at 25°C.

Using the Nottingham on-line cSFC–FT-IR apparatus, we have recorded the FT-IR spectrum of caffeine in the νC=O region (1500–1900 cm^{-1}) for a range of injected quantities. Fig. 2 shows the spectra obtained for injected amounts of 580, 290 and 95 pg of caffeine in supercritical CO_2 as the mobile phase. In each case the background CO_2 spectrum had been subtracted, and the resulting spectra show clearly the expected two νC=O bands of caffeine. Witj an injected quantity of 95 pg, the signal-to-noise ratio is reaching the lowest acceptable limits, and so in this experiment we can regard 95 pg as the IMDQ for caffeine. This represents a dramatic improvement on any published results (*i.e.* by a factor of more than 25).

It was also decided to investigate the IMDQ for a species which is a much weaker infrared absorber than caffeine, and a polycyclic aromatic hydrocarbon (PAH) was chosen, specifically pyrene. The only report of an estimated IMDQ for on-line cSFC–FT-IR detection of PAHs [10] suggested that the value was approximately 100 ng. The FT-IR spectra of a range of injected quantities of pyrene are shown in Fig. 3, with a characteristic peak, due to an out-of-plane C–H deformation of the hydrocarbon, at 847 cm^{-1}. With the accepted definition of IMDQ, *i.e.* S/N not less than 3, this figure shows that 3 ng of pyrene can be detected by cSFC–FT-IR with supercritical CO_2 as the mobile phase. Although approximately 30 times better than previous results by this technique for PAHs, this quantity is still some three orders of magnitude worse than can be achieved by scanning UV detection for such a molecule [17], and FT-IR will not be the method of choice for detection of low levels of PAHs. However, use of supercritical xenon as the mobile phase enables strong infrared bands of PAHs *ca.* 700 cm^{-1}, which are highly characteristic of individual species, to be detected in cSFC–FT-IR [14], and this will be of use in differentiating PAHs with similar UV spectra.

Many transition-metal carbonyl and organometallic complexes find use as catalyst materials, and the detection of residues of such compounds is likely to become an analytical priority. In order to test the feasibility of detecting small quantities of an organometallic complex, we have determined the IMDQ for (η-mesitylene)chromium tricarbonyl, $(1,3,5\text{-}C_6H_3Me_3)Cr(CO)_3$. In common with all other transition metal carbonyl complexes, this possesses very strong infrared absorptions in the $\nu \equiv O$ range (1800–2000 cm^{-1}), and Fig. 4 shows the cSFC-FTIR spectra from injected quantities of

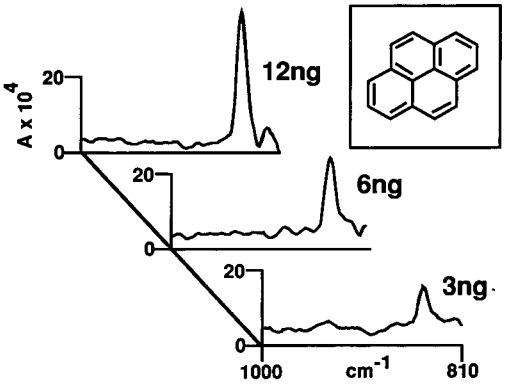

Fig. 3. FT-IR spectra of pyrene in the out-of-plane C–H deformation region. The injected quantities are shown for each spectrum. Experimental conditions as for Fig. 2.

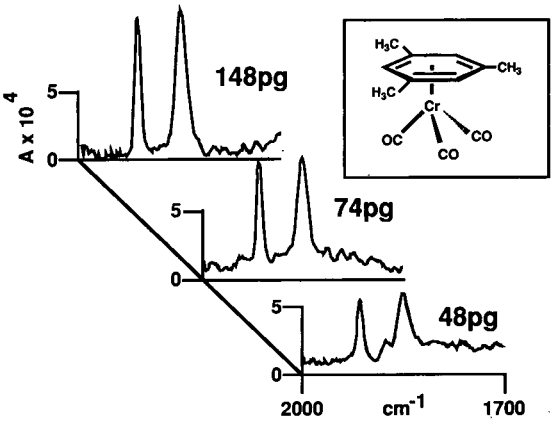

Fig. 4. FT-IR spectra of (mesitylene)chromium tricarbonyl in the carbonyl stretching region. The injected quantities are shown for each spectrum. Experimental conditions as for Fig. 2.

mesitylenechromium tricarbonyl down to 48 pg. The spectrum of the 48 pg sample has a S/N ratio of about 6, and so in this case we can estimate the IMDQ at approximately 20–25 pg. Thus cSFC–FT-IR is potentially a very powerful method for the detection of small residual amounts of transition metal carbonyl complexes.

Our results show that, with careful design of an FT-IR flow cell, it is possible to make on-line FT-IR a very versatile and sufficiently sensitive detection method for cSFC. In addition, as has already been shown [14,20], and further discussed below, the resulting FT-IR spectra are invaluable for identification of unknown species in an analyte mixture.

Linear dynamic range of cSFC–FT-IR

In order to be of use in the quantitative determination of analytes, any detection system used in chromatography should have a wide linear dynamic range, *i.e.*, the detector should respond linearly to concentration changes for a given species. Infrared absorption is subject to the Lambert-Beer Law, *i.e.*, the absorbance is directly proportional to the concentration of the absorbing substance and the path length of the cell. The later is fixed in our cell, and so absorbance at any given wavenumber corresponding to a vibrational mode of the analyte should depend linearly on the concentration.

Shah *et al.* [11] showed that the Lambert-Beer law was obeyed for caffeine in supercritical CO_2 for injected amounts of 2.5 to 50 ng, for a range of just over one order of magnitude. As part of the same series of experiments which was reported in the previous section, to determine the IMDQ value for caffeine using our FT-IR flow cell, we injected amounts of caffeine from 95 pg to 170 ng, *i.e.*, over a range of more than three orders of magnitude. Fig. 5 is a Lambert-Beer law plot for the $\nu C{=}O$ peak of caffeine at 1675 cm^{-1}, showing that the linear dynamic range available for this FT-IR detection method covers at least three orders of magnitude. Extension to significantly larger amounts of material is limited only by the capacity of the chromatographic column employed, and by moving to packed capillary or even packed columns for the chromatographic separation the linear dynamic range will be extendable by several further orders of magnitude.

Quantitative determination of amounts of analyte is clearly possible using a cSFC–FT-IR system, for analytes which possess at least one strong absorption band in the infrared range. The present experiment used supercritical CO_2 as the mobile phase, for which some parts of the infrared spectrum are inaccessible due to CO_2 absorption. As we

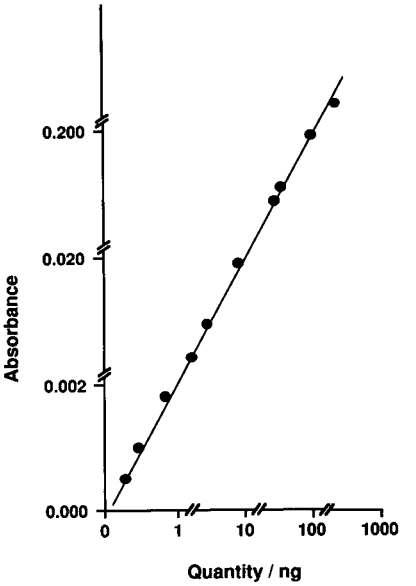

Fig. 5. Plot of the absorbance of the 1675 cm^{-1} ($\nu C{=}O$) band of caffeine *versus* quantity injected for cSFC analysis over the range 95 pg to 170 ng.

have shown previously [2], supercritical xenon is a superior mobile phase from this point of view, as it has no infrared absorptions, leaving the whole range available for observation of solute peaks.

CONCLUSION

We have demonstrated that on-line FT-IR detection following cSFC can lead to very much lower minimum detectable quantities than had previously been reported. These were 2 ng for pyrene, less than 100 pg for caffeine, and approximately 20 pg for (mesitylene)chromium tricarbonyl. In addition, the FT-IR detection has a linear dynamic range of at least three orders of magnitude, limited for larger amounts only by the column capacity.

Our results show that cSFC–FT-IR, with its very great potential for the identification of large numbers of individual analytes, is limited very much less by sensitivity constraints than had been thought. It is proposed in future work to extend the system in two principal ways. The first is to include a variable-wavelength UV detector, to obtain UV spectra of the individual components, and a mass spectrometer, to produce a "multiply-hyphenated" analytical system, cSFC–UV–FT-IR–MS. Secondly, it will be possible to use the wealth of spectroscopic information that will be generated by this sequence, in conjunction with the appropriate spectral libraries. To identify components for a very wide range of analyte mixtures. In the long term, the development of an expert system will covert such a procedure into an analytical technique of unprecedented power and generality.

ACKNOWLEDGEMENTS

We are grateful to Perkin-Elmer Ltd. and British Petroleum for their generous support of the Nottingham Analytical Group, and to the government of the Republic of Turkey (for financial support of M.K.). We thank Professor J. J. Turner and Dr. S. M. Howdle for helpful discussions, and Messrs. D. R. Dye, J. M. Whalley and J. G. Gamble for invaluable technical assistance.

REFERENCES

1 C. M. White (Editor), *Modern Supercritical Fluid Chromatography*, Hüthig, Heidelberg, Germany, 1988.
2 M. L. Lee and K. E. Markides (Editors), *Analytical Supercritical Fluid Chromatography and Extraction*, Chromatography Conferences, Provo, UT, 1990.
3 K. D. Bartle, M. W. Raynor and P. R. Griffiths, in M. L. Lee and K. E. Markides (Editors), *Analytical Supercritical Fluid Chromatography and Extraction*, Chromatography Conferences, Provo, UT, 1990, pp. 245–263.
4 T. Hirschfeld, *Appl. Spectrosc.*, 39 (1985) 1086.
5 T. J. Jenkins, *Ph. D. Thesis*, University of Nottingham, 1991.
6 L. T. Taylor and E. M .Calvey, *Chem. Rev.*, 89 (1989) 321.
7 P. R. Griffiths, S. L. Pentoney, G. L. Pariente and K. L. Norton, *Mikrochim. Acta*, 3 (1987) 47.
8 M. W. Raynor, K. D. Bartle, I. L. Davies, A. Williams, A. A. Clifford, J. M. Chalmers and B. W. Cook, *Anal. Chem.*, 60 (1988) 427.
9 M. W. Raynor, I. L. Davies, K. D. Bartle, A. A. Clifford, A. Williams, J. M. Chalmers and B. W. Cook, *J. High Resolut. Chromatogr. Chromatogr. Commun.*, 11 (1988) 767.
10 M. W. Raynor, A. A. Clifford, K. D. Bartle, C. Reyner, A. Williams and B. W. Cook, *J. Microcol. Sep.*, 1 (1989) 101.
11 S. Shah, M. Ashraf-Khorassani and L. T. Taylor, *Chromatographia*, 25 (1988) 631.
12 M. W. Raynor, K. D. Bartle, A. A. Clifford, M. Cleary and B. W. Cook, unpublished results.
13 M. Poliakoff, G. Davidson, M. A. Healy, T. J. Jenkins, M. Kaplan and M. R. Simmonds, in M. A. McHugh (Editor), *Proceedings 2nd Int. Symposium on Supercritical Fluids, Boston, MA, May 20–22, 1991*, Department of Chemical Engineering, Johns Hopkins University, Baltimore, MD, 1991, p. 447.
14 M. A Healy, T. J. Jenkins and M. Poliakoff, *Trends. Anal. Chem.*, 10 (1991) 92.
15 H. H. Hill, Jr., in M. L. Lee and K. E. Markides (Editors), *Analytical Supercritical Fluid Chromatography and Extraction*, Chromatography Conferences, Provo, UT, 1990, p. 193.
16 P. R. Griffiths, in J. R. Ferraro and L. J. Basile (Editors), *Fourier Transform Infrared Spectroscopy*, Vol. 1, Academic Press, New York, 1978, p. 143.
17 S. R. Weinberger and D. J. Borhop, *J. Microcolumn Sep.*, 1 (1989) 90.
18 J. C. Fjeldsted, B. E. Richter, W. P. Jackson and M. L. Lee, *J. Chromatogr.*, 279 (1983) 423.
19 H.-C. K. Chang and L. T. Taylor, *J. Chromatogr. Sci.*, 28 (1990) 29.
20 P. R. Griffiths, S. L. Pentoney, A. Giorgetti and K. H. Shafer, *Anal. Chem.*, 58 (1986) 1349A.

Journal of Chromatography, 626 (1992) 59–69
Elsevier Science Publishers B.V., Amsterdam

CHROM. 24 322

Flame-based thermionic detection coupled on-line with microcolumn liquid chromatography

I. Optimization of the system

Ch. E. Kientz and A. Verweij

Prins Maurits Laboratory TNO, P.O. Box 45, 2280 AA Rijswijk (Netherlands)

G. J. de Jong* and U. A. Th. Brinkman

Department of Analytical Chemistry, Free University, De Boelelaan 1083, 1081 HV Amsterdam (Netherlands)

ABSTRACT

A thermionic detector originally developed for gas chromatography was coupled with microcolumn (0.3 mm I.D.) liquid chromatography. For coupling, an interface used previously for flame photometric detection was used. Minor modifications to the burner head and detector were necessary. The eluent and analyte introduction were studied by varying parameters such as the air, hydrogen and helium gas flow-rates and the rubidium source–burner rim distance. To obtain stable eluent and analyte introduction, a minimum flame length of about 6 mm was required. A near-stoichiometric H_2:O_2 ratio was found to give optimum detector sensitivity; the optimum rubidium source–burner rim distance and hydrogen flow-rate were mutually dependent. The system was used for the determination of organophosphorus compounds, *e.g.*, the pesticide dichlorvos and its polar non-volatile metabolite dimethylphosphoric acid and the herbicide glyphosate. For the analytes tested, the detection limit was 10–20 pg/s of phosphorus.

INTRODUCTION

The on-line combination of miniaturized liquid chromatography (LC) with flow-rates of 1–50 μl/min and phosphorus-selective gas chromatographic (GC) detectors has been achieved by several groups [1–10]. In miniaturized LC coupled with thermionic detection (TID), one can distinguish between work carried out with flame-based and flameless TID. The use of flameless TID in combination with 0.7 mm I.D. packed microbore columns and an evaporation-type interface was described by Brinkman and co-workers [1–3]. In their work examples were presented of trace-level organophosphorus pesticide determinations in tomato, onion and sediment samples.

Novotny and co-workers [5,6] described the coupling of a laboratory-made dual-flame thermionic detector with micro-LC with the use of an interface based on concentric nebulization of the mobile phase solvent and solutes. In later work, nebulization was carried out orthogonally to improve the determination of larger molecules. With this approach, the nebulizing efficiency was significantly increased for larger molecules; organophosphorus species having molecular masses (M_r) of >500 could now be detected. As more (organic) effluent

Correspondence to: Professor U. A. Th. Brinkman, Department of Analytical Chemistry, Free University, De Boelelaan 1083, 1081 HV Amsterdam, Netherlands.

* Present address: Solvay Duphar BV, Analytical Development Department, P.O. Box 900, 1380 DA Weesp, Netherlands.

0021-9673/92/$05.00 © 1992 Elsevier Science Publishers B.V. All rights reserved

was introduced into the flame compared with concentric nebulization, the flame temperature increased and an increase in background signal was observed. As a result, the detection limits remained similar to those obtained with the former version of the TID instrument. For the less volatile dimethylthiophosphinic ester of estradiol (M_r = 456) the detection limit was ten times higher than for trimethyl phosphate. A linear dynamic range of two, instead of the earlier three, decades was obtained due to a bipolar orientation at high concentrations. More recently, the same group returned to concentric nebulization and the system was optimized for nitrogen-containing species [7]. Unfortunately, no further work has been published on their micro-LC–TID coupling.

There is still a need for selective phosphorus detection in LC using an interface principle which makes the system suitable for various types of application, *i.e.*, independent of analyte volatility and/or polarity. In addition, real samples often contain non-volatile matrix compounds which make detection impossible or reduce the lifetime of systems based on evaporation owing to blocking of the heated capillary. In this work, the use of a direct-introduction-type interface originally developed for the detection of non-volatile solutes in micro-LC with flame-photometric detection (FPD) [9,10] was coupled to a commercially available TID instrument. Technical aspects such as detector and interface modification and the optimization of the interface and TID parameters are discussed. Further, it is demonstrated that the system can handle non-volatile compounds in combination with both aqueous and organic LC eluents.

EXPERIMENTAL

Materials

All solvents were of HPLC grade from Merck (Darmstadt, Germany). PRP-X100 polymeric anion-exchange material, with a particle size of 10 μm (Hamilton, Reno, NV, USA), was used as the column packing material. Methylphosphonic acid (MPA), dimethyl methylphosphonate (DMMP) and dimethylphosphoric acid (DMP) were synthesized at the Prins Maurits Laboratory TNO. Glyphosate and dichlorvos were obtained from Dr. S. Ehrenstorfer (Augsburg, Germany).

Apparatus

The chromatographic system consisted of a Phoenix Model 20 CU pump (Carlo Erba, Milan, Italy), a Valco sample injection valve (VICI, Schenkon, Switzerland) with a 60-nl internal volume and a thermionic detector (Carlo Erba). The various fused-silica connection tubings (0.02–0.3 mm I.D.) were supplied by Chrompack (Middelburg, Netherlands).

The microcolumns (0.3 mm I.D., fused silica) were packed with PRP-X100 according to the procedure of Gluckman *et al.* [11]. The column performance was tested using a Spectroflow 783, UV detector (Kratos, Ramsey, NJ, USA) assembled with a laboratory-made 40-nl micro UV flow cell [12].

Detector modification. The thermionic detector (Fig. 1A) consists of four major parts: the detector base body (1) with insulation (a) and the glass burner tip (b); the actual detector (2), which contains the

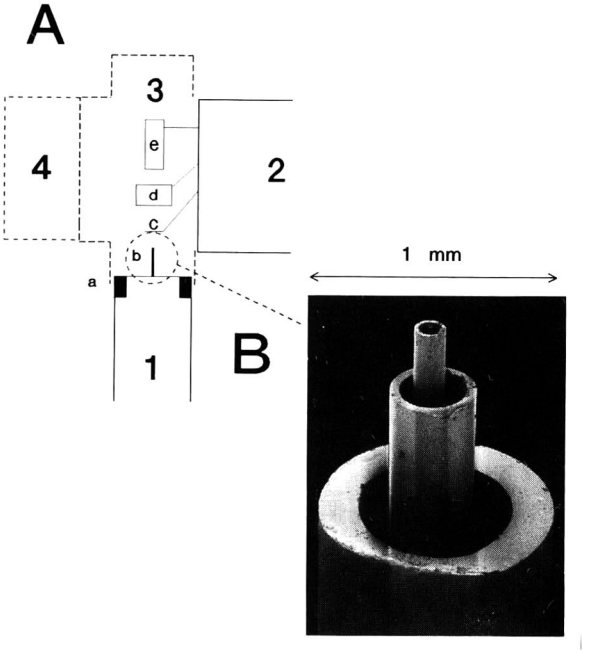

Fig. 1. (A) Thermionic detector used for micro-LC: 1 = base body with (a) insulation and (b) interface tip; 2 = actual detector which contains the electronics, (c) the electrode, (d) Rb source and (e) collector; 3 = detector housing; 4 = U-shaped aluminium block. (B) Interface tip with eluent introduction capillary (0.1 mm I.D. fused silica), fused-silica capillary (0.32 mm I.D.) providing the helium flow and 0.7 mm I.D. burner rim glass tube.

electronics, the electrode (c), the rubidium (Rb) source (d) and the collector (e); the aluminium detector housing (3), which covers the collector, the Rb source and electrode, and prevents atmospheric interferences during detector operation; and an external heating unit mounted in a laboratory-made U-shaped aluminium block (4).

In GC, the thermionic detector is heated via the detector base body which supports the housing and is placed in the heating unit of the gas chromatograph. To maintain liquid introduction when working in the LC mode, it is necessary to have a relatively cold detector base to prevent too early evaporation of the eluent. As a consequence, to avoid condensation of vapour, an external heating unit was mounted in a U-shaped aluminium block, which fits on to the detector housing. To prevent heat transfer from the housing to the base body, insulation (1, a) was inserted between both parts.

Burner head modification. The original metal flame jet also acts as a polarizing electrode and is therefore electrically insulated from the base body. Because of the direct flame contact and the insulation from the base body, the metal flame jet is probably too hot to maintain liquid flow when a 100 μm I.D. fused-silica capillary is put through the jet for LC effluent introduction. Clogging of the fused-silica capillary by non-volatile analytes occurred especially when working with relatively low-boiling eluents (60–100°C). Therefore, the flame jet was removed from the flame tip assembly, leaving an opening suitable for inserting a modified burner tip. The new glass burner tip was situated 6 mm above the base, *i.e.*, at the same height as the original flame jet. To prevent an electrical short-circuit between the electrodes and the top of the metal detector base, a 3-mm thick silicon ring was placed on top of the detector base.

Burner tip modification. The specially designed burner tip, developed in order to combine micro-LC with FPD [9], contains a 100 μm I.D. fused-silica (eluent introduction) capillary which is connected directly with the microcolumn. This capillary was placed in a 320 μm I.D. fused-silica capillary which is used for helium addition. Both capillaries were mounted in a 0.7 mm I.D. metal tube which is used for hydrogen addition. Modification of the metal tube of the FPD interface was necessary to prevent an electrical short-circuit between the electrodes and the interface: a glass tube (20 mm × 1.3 mm O.D. × 0.7 mm I.D.) was mounted with 1-cm shrinking Teflon on the end of the metal tube; this provides sufficient electrical insulation. Additionally, the use of glass prevents heat transfer to the lower part of the fused-silica LC eluent introduction capillary. The tip of the glass tube, which is also the burner rim, is shown in Fig. 1B. The hydrogen flow is introduced through the glass tube of the interface causing the flame to originate at the glass tube outlet. The original hydrogen flow inlet is, therefore, not used. The tip of the glass tube, *i.e.*, the burner rim, was used throughout this study as a reference point for measuring flame lengths, fused-silica tip positions and Rb source–burner rim distances.

The air flow was introduced through its original inlet mounted in the detector base.

Temperature measurement. Flame temperatures were measured with the use of a laboratory-made platinum *versus* platinum–10% rhodium thermocouple (2 mm × 0.1 mm O.D.) insulated with a 100 mm × 1.4 mm O.D. ceramic rod. The temperature range of this thermocouple extends to 1700°C as derived from standard calibration tables for thermocouples [13].

RESULTS AND DISCUSSION

Optimization of the total LC–interface–flame-based TID system with liquid LC eluent introduction into the diffusion flame is complicated because of the multivariate nature of the problem. Therefore, in this study, the optimization of the interface and the thermionic detector were considered separately. Further, one should realize that parameters such as the various gas flow-rates and the position of the Rb source and the eluent introduction capillary relative to the burner rim may all affect the analyte introduction into the flame. Therefore, a volatile test compound, DMMP, was selected which shows a TID response that is, to a first approximation, independent of the mode of introduction (liquid or vapour) and is therefore very suitable for studying the detector characteristics. The TID response of the corresponding free acid, MPA, on the other hand, will depend strongly on the mode of introduction and/or interface operation: MPA was therefore selected as a second test solute.

In order to study the influence of the different parameter settings on the analyte introduction visually, preliminary variation of each parameter was carried out with an open system, *i.e.*, without using the detector housing [see Fig. 1 (3)]. In this case the surrounding atmospheric air maintains a relatively constant hydrogen-to-oxygen (H_2:O_2) ratio in the flame owing to the high flammability of hydrogen [14]. Hence with the use of an open system the air flow-rate is eliminated as a parameter.

All open- and closed-system optimization studies were carried out using flow-injection analysis (10 μl/min) with methanol as carrier stream. Next, the total analytical system was tested under chromatographic conditions.

Optimization of interface

The influence of the liquid eluent and analyte introduction on the flame characteristics was the first parameter to be studied. A hydrogen flow-rate of 30 ml/min, as used in the GC mode of operation, results in a small flame only 2–3 mm high. This flame is too small to accept liquid flow-rates without causing flame instability. Therefore, it was elongated by increasing the hydrogen flow-rate until regular flame combustion was again obtained. The minimum flame length required to achieve this was about 6 mm; it needed a hydrogen flow-rate of *ca.* 60 ml/min.

The use of helium cooling is required to prevent overheating of the fused-silica tip, which becomes visible as glowing of the tip as a result of a vortex flow around the burner rim. On increasing the helium flow-rate, F, over the range 0–150 ml/min, a linear decrease in the tip temperature, T, was observed over the range 1100–500°C, *viz.*, $T = -4F + 1115$, with a correlation coefficient, r, of 0.996 ($n = 6$). According to our experience, under normal operating conditions, *i.e.*, when the detector housing is closed, helium flow-rates of less than 200 ml/min are preferred in order to avoid an unstable flame which is easily extinguished. At a helium flow-rate of *ca.* 100 ml/min the flame becomes colourless, indicating that direct contact of the flame with the glass burner tip is avoided and that cooling is efficient. This result is independent of the hydrogen flow-rate in the range tested, *viz.*, 40–300 ml/min.

The positions of the tip of the LC eluent introduction capillary and the helium-cooling capillary were varied relative to the burner rim position at fixed flow-rates of 60 ml/min of hydrogen and 100 ml/min of helium. The TID responses of DMMP and MPA were measured as a function of these fused silica outlet–burner rim positions. If the LC eluent introduction capillary protruded 5 mm or more above the burner rim, with the helium-cooling capillary at the same height as the burner rim, the non-volatile MPA could not be detected at all, while the volatile methyl derivative, DMMP, gave a constant high signal. Under these conditions, the interface probably operates in the evaporation mode, that is, effluent evaporation is complete, which causes the non-volatile MPA to be deposited in the capillary. For lower positions of the tip of the LC eluent introduction capillary, *i.e.*, for protruding distances from 5 to 0 mm above the burner rim, the MPA signal increased. For tip positions of 0–0.5 mm, the same signal was found for both test compounds. It was also found that the tip of the helium-cooling capillary should not protrude further than the LC eluent introduction capillary; it was positioned *ca.* 0.2–0.3 mm above the burner rim.

Obviously, the introduction of non-volatile test compounds into the flame is complete when the LC eluent introduction capillary outlet is positioned close to the burner rim and just above the tip of the capillary through which the helium gas flow exits.

Optimization of TID

Initial experiments with the open detector system were carried out in order to measure more accurately the distances between the Rb source and burner rim and, additionally, to verify the eluent and analyte introduction stability. The hydrogen and helium flow-rates were 80 and 100 ml/min, respectively. The optimum Rb source–burner rim distance was found to be 7 mm. Optimum signal-to-noise ratios (S/N) for both MPA and DMMP were obtained with the flame coming very close to the Rb source without enveloping it (as indicated by glowing of the Rb source). In the latter situation, the noise level increased dramatically.

Next, the Rb source–burner rim distance was set at 7 mm and the hydrogen flow-rate was varied between 60 and 130 ml/min. With the free acid MPA it was observed that solute introduction remained stable without clogging of the LC eluent introduction

capillary for a hydrogen flow-rate of at least 60 ml/min. The S/N was maximum at *ca.* 80 ml/min. The mutual dependence of the optimum source–rim distance and hydrogen flow-rate was demonstrated by slightly increasing the hydrogen flow-rate, *i.e.* by 10–15 ml/min; this immediately resulted in a 25-fold increase in the noise level. However, on increasing the Rb source–burner rim distance (by *ca.* 0.5 mm), the earlier low noise level was again obtained and the S/N was restored to its original value. The result was found to be independent of the introduction of additional air via the detector base, as was to be expected on the basis of the high flammability of hydrogen in (ambient) air.

Next, the detector was closed and the air flow-rate was varied over the range 120–300 ml/min. On the basis of the S/N, the optimum air flow-rate was found to be 200 ml/min. Compared with the open system discussed above, the S/N increased 15-fold owing to the reduced noise level. The lower noise level observed with the closed system is probably due to the absence of dust particles which are abundantly present in the laboratory atmosphere. This agrees with findings of McWilliam [15] in his early studies on the use of the flame ionization detector for GC. With the closed system and the above conditions, an optimum source–rim position similar to the above, *viz.*, 7–8 mm, was found for both analytes (Fig. 2).

Two-parameter studies. The combined influence of the air flow-rate and the Rb source position on analyte signal, noise and background at constant hydrogen flow-rate, expressed as H_2:O_2 ratio, was studied using methanol as carrier stream (Fig. 3). It is evident from the data that signal (Fig. 3A), noise (Fig. 3B) and background (Fig. 3C) all reach maximum values when the H_2:O_2 ratio is about 2, *i.e.*, is near-stoichiometric. Although the essentially similar profiles of analyte signal and noise plots suggest the lack of a distinct optimum S/N, closer observation reveals that such an optimum does exist in the H_2:O_2 range 1.9–2.1 (Fig. 4).

For a more exact determination of the above optimum, experiments were carried out using calibrated hydrogen and air flow-rates. With hydrogen

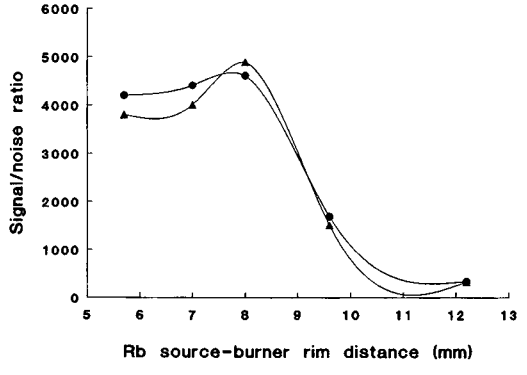

Fig. 2. Dependence of signal-to-noise ratio on Rb source–burner rim distance. Analytes: ▲ = DMMP; ● = MPA. Flow-rates: hydrogen, 80 ml/min; air, 200 ml/min; helium, 100 ml/min. Eluent: methanol at 10 μl/min.

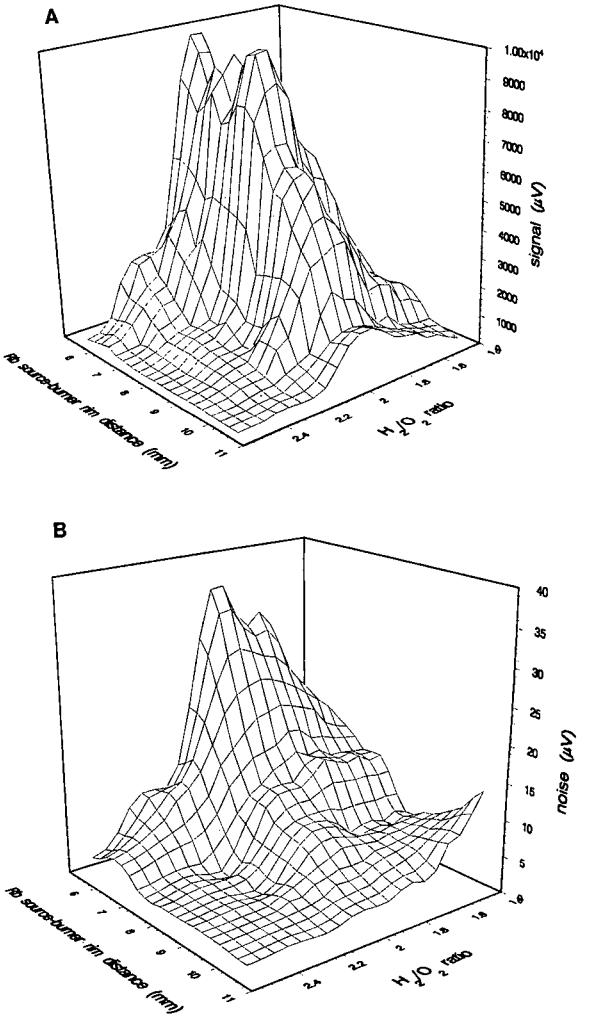

Fig. 3.

(Continued on p. 64)

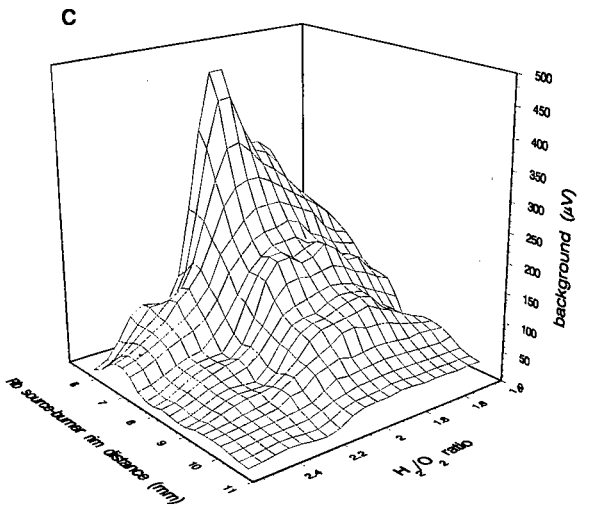

Fig. 3. Dependence of (A) signal, (B) noise and (C) background on Rb source–burner rim distance and H_2:O_2 ratio. Flow-rates: hydrogen, 125 ml/min; helium, 100 ml/min. Eluent: methanol at 10 μl/min. Analyte: DMMP.

flow-rates of 78, 88, 110 and 118 ml/min and varying air flow-rates, maximum S/N values were found at 200, 225, 280 and 304 ml/min of air, respectively, *i.e.*, at stoichiometric H_2:O_2 ratios of 1.95 ± 0.01. In daily practice, an elegant experimental method to find the optimum air flow-rate is to start with an excess of hydrogen and then to increase the air flow-rate slowly up to the level where the background (see Fig. 3C) just starts to increase.

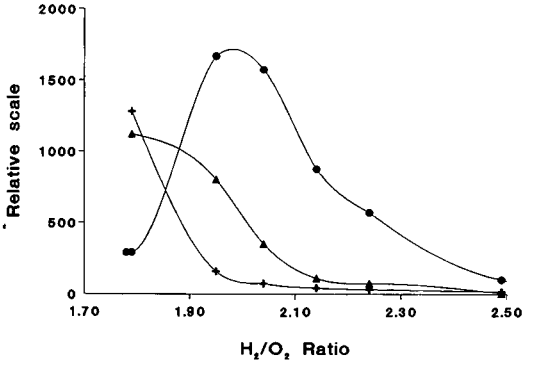

Fig. 4. Dependence of (▲) signal, (+) noise and (●) signal-to-noise ratio on H_2:O_2 ratio (cross-section of Fig. 3 at Rb source–burner rim distance of 8 mm). Flow-rates: hydrogen, 125 ml/min; helium, 100 ml/min. Eluent: methanol at 10 μl/min. Analyte: DMMP.

Next, the combined influence of the Rb source–burner rim distance and the hydrogen flow-rate was studied at a constant H_2:O_2 ratio of 1.95. DMMP was used as test compound and methanol as carrier stream. As is shown in Fig. 5A, the analyte signal increased on decreasing the source–rim distance, especially when working at higher hydrogen (and of course, air) flow-rates. Nevertheless, the best S/N values were obtained at relatively large source–rim distances of 7–12 mm, the exact value depending on

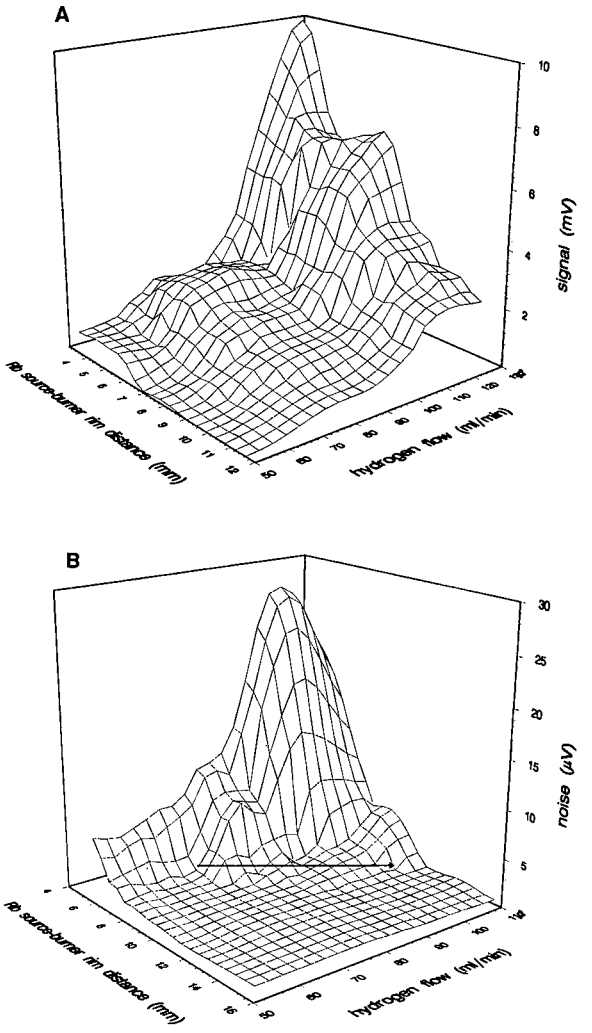

Fig. 5. Dependence of (A) signal and (B) noise on Rb source–burner rim distance and hydrogen flow-rate. H_2:O_2 ratio, 1.96; helium flow-rate, 100 ml/min. Eluent: methanol at 10 μl/min. Analyte: DMMP.

both the hydrogen and air flow-rates. This can be explained by the noise profile shown in Fig. 5B. As a consequence, the best S/N values are obtained by following the arrow drawn in the latter figure.

Influence of the carrier stream. The influence of the methanol flow-rate was studied with the Rb source–burner rim distance set at 8 mm and the H_2:O_2 ratio at 1.95 (80 ml/min of hydrogen and 200 ml/min of air). The methanol flow-rate was varied between 3 and 15 μl/min. As is evident from Fig. 6, a distinct S/N optimum occurs for both DMMP and MPA at a methanol flow-rate of 10 μl/min. Because the flame length depends on the (combustible) methanol flow-rate, as will be shown in Part II [16], a flow-rate of 10 μl/min was applied throughout this study.

As it is our aim to set up an on-line LC–interface–TID system, finally the nature of the carrier stream was varied. The S/N level for DMMP remained essentially the same when hexane was used instead of methanol as the LC carrier stream. However, when water was used as solvent, also at the flow-rate of 10 μl/min, the baseline became less stable and an increase in the noise level by a factor of 4 was observed. The baseline instability was found to be due to irregular solvent introduction into the flame and will be discussed in more detail in Part II [16]. The detector noise could be reduced and stable carrier stream introduction restored by an increase of 0.5 mm in the distance between the LC eluent introduction capillary and the burner rim. These findings are in agreement with our results on the use of the micro-LC–FPD system with aqueous LC eluents [9].

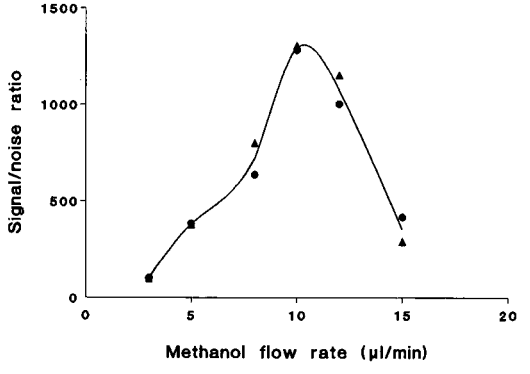

Fig. 6. Dependence of signal-to-noise ratio on methanol flow-rate. Test compounds: ● = DMMP; ▲ = MPA. For further conditions, see text.

With water instead of methanol, the experiment in Fig. 3 was repeated, *i.e.*, the Rb source–burner rim distance and the H_2:O_2 ratio were simultaneously varied, while maintaining a constant hydrogen flow-rate. In contrast to the results with methanol, with water the background current remained low (< 150 pA) and the noise essentially constant (3 ± 1 μV), independent of the Rb source–rim distance and the air flow-rate. This essentially different situation results in a less complicated optimization which is exclusively based on the TID response observed. The influence of water on the signal was essentially the same as with methanol (data not shown), *e.g.*, a maximum occurred at an H_2:O_2 ratio of *ca.* 2; the steep decrease at smaller Rb source–burner rim distances of less than 7 mm was not observed, however, with methanol, where the noise and signal keep increasing (see Fig. 5A and B). This explains that the maximum S/N values were found to be essentially the same with both solvents. However, under the same gas flow and carrier stream conditions, the optimum source–rim distance is 7 mm with water and 9 mm with methanol. This will be discussed in more detail below.

For the separation of inorganic phosphorus-containing acids or acidic organophosphorus compounds, which typically are target components for our LC–interface–TID system, aqueous LC eluents to which volatile acids or salts have been added are usually necessary. Therefore, the optimization of the system was repeated using a micro PRP-X100 anion-exchange column and aqueous–organic eluents containing organic acids or salts. On the basis of the above results, the detector parameters were set as indicated in Table I.

The influence on the TID performance of both the Rb source–burner rim distance and the percent-

TABLE I

PARAMETER SETTINGS FOR MICRO-LC–INTERFACE–TID

Parameter	Value
Hydrogen flow-rate	120 ml/min
Air flow-rate	300 ml/min
Helium flow-rate	100 ml/min
Rb source–burner rim distance	Varied
LC eluent flow-rate	10 μl/min

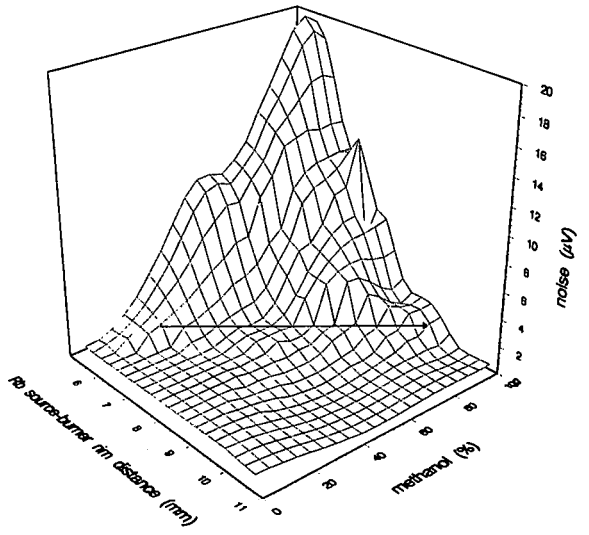

Fig. 7. Dependence of noise on Rb source–burner rim distance and percentage of methanol in LC eluent. Hydrogen flow-rate, 125 ml/min; H_2:O_2 ratio, 1.96. Helium flow-rate, 50 ml/min. Eluent: aqueous 0.6% formic acid, with varying methanol content (0–100%); flow-rate, 10 μl/min.

age of methanol in the aqueous 0.6% formic acid used as the LC eluent was studied. The data presented in Fig. 7 show that on increasing the methanol content from 0 to 95% (v/v) the noise increases dramatically. The three-dimensional plot in Fig. 7 helps to explain the different optimum Rb source–burner rim distances of *ca.* 7 and 9 mm found experimentally when using water and pure methanol as carrier stream, respectively. As discussed above, the most striking difference between the use of water and methanol is the constancy of the noise observed with the former solvent, irrespective of the Rb source–burner rim distance and/or the H_2:O_2 ratio (at a constant hydrogen flow-rate) selected. In other words, on increasing the percentage of methanol in the eluent, the noise will increase and the optimum S/N values will be found when following the full line in Fig. 7. To a first approximation, this line indicates the optimum Rb source–burner rim distance for each methanol–water eluent composition.

Electrode collector polarization. For GC analysis, the manufacturers recommend that the thermionic detector be used with a −300 V polarization electrode potential, with +300 V as an alternative. Both options were studied using 60-nl injections of *ca.* 7 mg/ml of DMMP in methanol. The less conventional positive electrode potential resulted in a six-fold increased S/N ratio compared with the negative electrode potential. The background measured relative to that without LC eluent introduction was the same in both experiments (*ca.* 20 nA). It was decided to use the positive polarization mode in all further work.

TABLE II

INFLUENCE OF ELUENT COMPOSITION ON THERMIONIC DETECTOR NOISE

Eluent: methanol–water (100:0 → 0:100) with or without added (I) ammonium oxalate, (II) ammonium acetate or (III) formic acid.

LC eluent				Noise (μV) at Rb source–burner rim distance of		
Methanol (%)	I (*M*)	II (*M*)	III (*M*)	7.5 mm	8.5 mm	9.5 mm
0				2.0	1.6	1.8
0			0.11	1.6	1.6	1.6
0	0.15			1.6		
0		0.25		1.5		
30			0.11	1.5		
50			0.11	2.0	0.2	0.2
60		0.05				0.4
70		0.15				1.7
80		0.05				0.6
90		0.05				0.5
95		0.05				0.3
95			0.11	4.9	2.3	0.2
100				5.3		0.01

TABLE III

DETECTION LIMITS (pg/s) OF ANALYTES IN MICRO-LC–TID

Eluent[a]				Analyte[b]		
M	W	F	A	MPA	DMMP	DMP
0	100	0.5	–	140	160	–
50	50	0.5	–	90	100	80
80	20	0.3	0.2	90	–	100
100	–	–		45	50	50

[a] Composition in vol.%: M, methanol; W, water; F, formic acid (98–100%); A, ammonia (25%).
[b] MPA, methylphosphonic acid; DMMP, dimethyl methylphosphonate; DMP, dimethylphosphoric acid.

Analytical data

Detector noise. The detector noise under different eluent conditions and Rb source–burner rim distances is shown in Table II. The noise level is seen to be essentially constant at a methanol concentration of 60–95% with or without 0.05 *M* ammonium acetate added. The noise level increases by at least a factor of 3 when the salt concentration is increased to 0.15 *M*. Similar noise levels in the range 1.5–2.0 μV are observed in pure water and for low modifier contents (0–30% methanol), also in the presence of salts (ammonium oxalate or ammonium acetate). Obviously, the system is suitable for both reversed-phase and ion-exchange chromatography, provided that the ionic strength of the eluent is relatively low. At higher modifier contents (30–100%) the noise depends on the Rb source–burner rim distance as discussed above. The lowest noise level was observed when using pure methanol as an eluent at the optimum Rb source–rim distance of *ca.* 9 mm.

Detector sensitivity. The sensitivity of the micro-LC–TID system was studied by injecting solutions of DMMP, MPA and DMP in various eluents. The detection limits of the analytes determined at S/N = 2 are summarized in Table III. The results indicate that the micro-LC–TID system is more suitable for use with organic than with aqueous eluents. The detection limits in aqueous eluents containing ammonia or formic acid generally are about double those obtained with micro-LC–FPD [12]. With pure methanol as eluent, and also with hexane [17], the micro-LC–TID system shows a sensitivity of 10–20 pg/s of phosphorus, which is similar to that of the micro-LC–FPD system. Compared with GC or supercritical fluid chromatography [18], there is, however, a loss of sensitivity of about two orders of magnitude. This is a result of the 100-fold higher noise level caused by the introduction of the LC eluent.

Applications

The applicability of the system was tested by separating and detecting polar organophosphorus compounds such as DMP and glyphosate. These compounds are difficult to analyse because they are highly polar, and therefore difficult to extract from aqueous samples or biological fluids, and non-volatile; in addition, they do not possess suitable chromophores or fluorophores. The increasing use of biodegradable organophosphorus pesticides has stimulated interest in the determination of their degradation products or metabolites. The primary breakdown products are substituted dialkyl(thio) organophosphorus acids.

DMP is the major and most hydrophilic metabolite in animals of a number of commercially available insecticides including dichlorvos (DDVP) [19], monocrotophos and mevinphos [20]. Generally, GC is used after laborious isolation, clean-up and diazoalkane derivatization [21,22]. With the micro-LC–TID system DDVP and DMP can be simultaneously determined without previous derivatization, *viz.*, on a PRP-X100 fused-silica capillary column. Owing to the hydrophobic and strong anion-exchange properties of the packing material, the compounds can be separated with an eluent containing 93% methanol and 0.5 *M* ammonium acetate (Fig. 8).

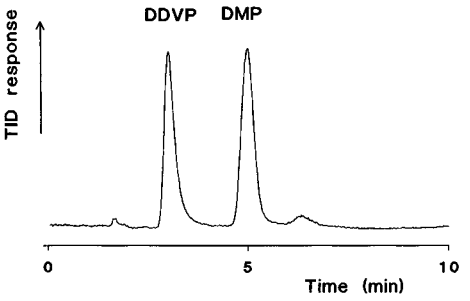

Fig. 8. Micro-LC–TID separation of dichlorvos (DDVP) and its major metabolite DMP. Column: PRP-X100 (200 mm × 0.32 mm I.D.). Eluent: methanol–0.05 *M* ammonium acetate (93:7) at 10 μl/min.

Glyphosate is a broad-spectrum herbicide marketed by Monsanto under the trade name Roundup. It has widespread application, *e.g.*, for potatoes, wheat, barley and asparagus. In soil the residual herbicide is readily adsorbed on soil particles where it undergoes microbial degradation to ammonia and carbon dioxide [23]. Extraction using organic solvents is an onerous task because of its polar and amphoteric character; the best results are obtained with water [24]. Determination is done by GC after extensive clean-up and derivatization [23–27] or by LC after pre- or post-column derivatization [28–33]. The practicality of direct analysis is demonstrated in Fig. 9 for an aqueous soil extract which was spiked with *ca.* 1 ppm of glyphosate. After filtration, 2 μl of the extract were injected directly on to the PRP-X100 column using methanol–water–formic acid (30:70:1) as eluent. The example shows that a large-volume injection of 2 μl has no adverse

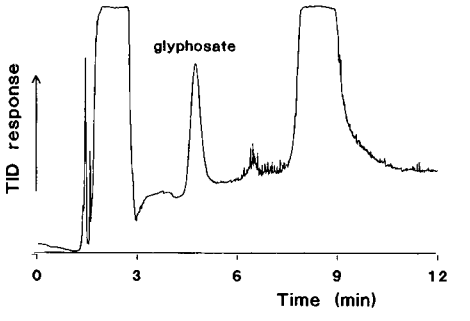

Fig. 9. Micro-LC–TID separation of an aqueous soil extract spiked with 1 ppm of glyphosate. Column: PRP-X100 (150 mm × 0.32 mm I.D.). Eluent: methanol–water–formic acid (30:70:1) at 10 μl/min. Amount injected: 2 μl.

effects on system performance: the glyphosate peak shape is satisfactory. This may be explained by a focusing effect of the sample solution. The spikes just after the glyphosate peak are caused by a small amount of air which was introduced during injection. The detection limit of the herbicide in soil was 200 ppb under the present conditions.

CONCLUSIONS

The systematic study of the present micro-LC–TID system has shown that careful optimization of the various gas flow-rates and of the Rb source position is required. The H_2:O_2 ratio should be near-stoichiometric, with the exact value depending slightly on the type of eluent used, and the flame length should be at least *ca.* 6 mm. The micro-LC–TID system can be used with purely organic and with aqueous solvents. In addition, the presence of salt concentrations of up to 0.2 *M* can be tolerated. Under suitable chromatographic conditions detection limits of about 100 pg/s of analyte can be obtained for alkylphosphonic and alkylphosphoric acids. As an application, the simultaneous determination of organophosphorus pesticides and their polar (acidic) degradation products has been reported.

ACKNOWLEDGEMENT

The authors are grateful to Bart Zegers for experimental assistance and helpful discussions.

REFERENCES

1 U. A. Th. Brinkman and F. A. Maris, *LC · GC Int.*, 1 (1987) 45.
2 F. A. Maris, R. J. van Delft, R. W. Frei, R. B. Geerdink and U. A. Th. Brinkman, *Anal. Chem.*, 58 (1986) 1634.
3 J. C. Gluckman, D. Barcelo, G. J. de Jong, R. W. Frei, F. Maris and U. A. Th. Brinkman, *J. Chromatogr.*, 367 (1986) 35.
4 D. Barcelo, F. A. Maris, R. W. Frei, G. J. de Jong and U. A. Th. Brinkman, *Int. J. Environ. Anal. Chem.*, 30 (1987) 95.
5 V. L. McGuffin and M. Novotny, *Anal. Chem.*, 55 (1983) 2296.
6 J. C. Gluckman and M. Novotny, *J. Chromatogr.*, 314 (1984) 103.
7 J. C. Gluckman and M. Novotny, *J. Chromatogr.*, 333 (1985) 291.
8 Ch. E. Kientz and A. Verweij, *Int. J. Environ. Anal. Chem.*, 30 (1987) 255.

9 Ch. E. Kientz, A. Verweij, H. L. Boter, A. Poppema, R. W. Frei, G. J. de Jong and U. A. Th. Brinkman, *J. Chromatogr.*, 467 (1989) 385.
10 Ch. E. Kientz, A. Verweij, G. J. de Jong and U. A. Th. Brinkman, *J. High Resolut. Chromatogr.*, 12 (1989) 793.
11 J. C. Gluckman, A. Hirose, V. L. McGuffin and M. Novotny, *Chromatographia*, 17 (1984) 3039.
12 Ch. E. Kientz and A. Verweij, *J. High Resolut. Chromatogr. Chromatogr. Commun.*, 3 (1988) 294.
13 D. R. Lide (Editor), *CRC Handbook of Chemistry and Physics*, CRC Press, Boca Raton, FL, 72nd ed., 1991–92, p. 15-1.
14 R. A. Strehlow (Editor), *Fundamentals of Combustion*, Robert E. Kreiger Publishing, Huntington, NY, 1979.
15 I. G. McWilliam, *Chromatographia*, 17 (1983) 241.
16 Ch. E. Kientz, A. Verweij, G. J. de Jong and U. A. Th. Brinkman, *J. Chromatogr.*, 626 (1992) 71.
17 Ch. E. Kientz, J. P. Langenberg, G. J. de Jong and U. A. Th. Brinkman, *J. High Resolut. Chromatogr. Chromatogr. Commun.*, 7 (1991) 460.
18 J. G. J. Mol, B. N. Zegers, H. Lingeman and U. A. Th. Brinkman, *Chromatographia*, 32 (1992) 203.
19 D. H. Hutson and E. C. Hoadley, *Xenobiotica*, 2 (1972) 107.
20 K. I. Beynon, D. H. Hutson and A. N. Wright, *Residue Rev.*, 47 (1973) 55.
21 M. T. Shafic, D. E. Bradway, H. F. Enos and A. R. Yobbs, *J. Agric. Food Chem.*, 21 (1973) 625.
22 D. Blair and H. R. Roderick, *J. Agric. Food Chem.*, 24 (1976) 1221.
23 M. L. Rueppel, B. B. Brigtwell, J. Schaefer and J. T. Marvel, *J. Agric. Food Chem.*, 25 (1977) 517.
24 R. A. Guinivan, N. P. Thompson and W. B. Wheeler, *J. Assoc. Off. Anal. Chem.*, 65 (1982) 35.
25 J. N. Seiber, M. M. McChesney, R. Kon and R. A. Leavitt, *J. Agric. Food Chem.*, 32 (1984) 681.
26 C. L. Deyrub, S. Chang, R. A. Weintraub and H. A. Moye, *J. Agric. Food Chem.*, 33 (1985) 944.
27 R. N. Dibyendu and K. K. Samir, *J. Agric. Food Chem.*, 37 (1989) 441.
28 H. Roseboom and C. J. Berkhoff, *Anal. Chim. Acta*, 135 (1982) 373.
29 R. L. Glass, *J. Agric. Food Chem.*, 31 (1983) 280.
30 H. A. Moye, C. J. Miles and S. J. Scherer, *J. Agric. Food Chem.*, 31 (1983) 69.
31 T. E. Archer and J. D. Stokes, *J. Agric. Food Chem.*, 32 (1984) 586.
32 J. E. Cowell, J. L. Kunstman, P. J. Nord, J. R. Steimetz and G. R. Wilson, *J. Agric. Food Chem.*, 34 (1986) 955.
33 L. G. M. Th. Tuinstra and P. G. M. Kienhuis, *Chromatographia*, 24 (1987) 696.

Journal of Chromatography, 626 (1992) 71–80
Elsevier Science Publishers B.V., Amsterdam

CHROM. 24 389

Flame-based thermionic detection coupled on-line with microcolumn liquid chromatography

II. Characterization of the system

Ch. E. Kientz and A. Verweij

Prins Maurits Laboratory TNO, P.O. Box 45, 2280 AA Rijswijk (Netherlands)

G. J. de Jong* and U. A. Th. Brinkman

Department of Analytical Chemistry, Free University, De Boelelaan 1083, 1081 HV Amsterdam (Netherlands)

ABSTRACT

Flame length and temperature measurements were used to study the influence of various parameter settings in thermionic detection coupled on-line with microcolumn liquid chromatography (micro-LC). In the present system both the rubidium source temperature and the interface performance depend strongly on the flame dimensions and gas flow-rates. When optimizing signal-to-noise ratios, the influences of the flame length, the rubidium source–burner rim distance and the hydrogen and air flow-rates are mutually dependent. When changing the micro-LC eluent composition from pure water to pure methanol, the noise and background are increasingly determined by chemi-ionization reactions.

INTRODUCTION

In a earlier study, thermionic detection (TID) with an instrument developed for gas chromatography (GC) was coupled to microcolumn liquid chromatography (micro-LC) [1]. For coupling, an interface was used that had earlier been designed for micro-LC with flame photometric detection [2,3]. This required minor modifications to both the interface and detector. The system was optimized by varying parameters such as the air, hydrogen and helium gas flow-rates, the rubidium (Rb) source–burner rim distance (see Fig. 5), the methanol content of the aqueous LC eluent and the eluent flow-rate. A minimum flame length of *ca.* 6 mm was found to be required to obtain stable eluent introduction and regular flame combustion; a near-stoichiometric H_2:O_2 ratio was found to give optimum detector sensitivity. The optimum Rb source–burner rim distance and the position of the eluent introduction capillary depended on the nature of the eluent. Mixtures of water and methanol were used; the highest sensitivity was obtained with pure methanol as eluent.

From the literature on GC–TID systems [4,5], it is well known that the operating mechanism of the detector is complicated and still awaits full elucidation. Spectroscopic [6] and mass spectral [7] studies are the best approaches to investigate the reaction products formed and to elucidate the reaction mechanisms involved. From studies on flame-based

Correspondence to: Professor U. A. Th. Brinkman, Department of Analytical Chemistry, Free University, De Boelelaan 1083, 1081 HV Amsterdam, Netherlands.

* Present address: Solvay Duphar BV, Analytical Development Department, P.O. Box 900, 1380 DA Weesp, Netherlands.

0021-9673/92/$05.00 © 1992 Elsevier Science Publishers B.V. All rights reserved

GC–TID it is known that the main factors affecting detector response are the temperature of both the flame and the alkali metal source [5]. When coupling micro-LC with a thermionic detector, the flame has an additional purpose: the temperature that is created by the flame is essential to transport the eluent and analytes into the flame [1], that is, temperature distribution and flame shape will largely determine the micro-LC-TID performance. The influence of the burner configuration, the detector gas flow-rates and the eluent introduction on the height and shape of and temperature distribution in the flame should therefore be well understood.

In this paper we attempt to explain the results of the optimization discussed in Part I [1] and briefly summarized above. To achieve this end, the influence of LC eluent introduction and detector gas flow-rate variation on the flame length and temperature distribution in different parts of the system (interface tip, flame, Rb source) was carefully investigated.

EXPERIMENTAL

Materials

All solvents were of HPLC grade from Merck (Darmstadt, Germany). PRP-1 polymer (10 μm) (Hamilton, Reno, NV, USA) was used as the column packing material. Dimethyl methylphosphonate was synthesized at the Prins Maurits Laboratory TNO. L-α-Lysophosphatidylethanolamine was supplied by Sigma (St. Louis, MO, USA).

Apparatus

The chromatographic system consisted of a Phoenix 20 CU pump (Carlo Erba, Milan, Italy), a Valco sample injection valve (VICI, Schenkon, Switzerland) with a 60-nl internal volume and a thermionic detector (Carlo Erba). The various fused-silica connection tubings (0.02–0.3 mm I.D.) were supplied by Chrompack (Middelburg, Netherlands).

The 150 mm × 0.3 mm I.D. fused-silica microcolumn was packed with PRP-1 according to the procedure of Gluckman *et al.* [8]. The column performance was tested using a Spectroflow 783 UV detector (Kratos ABI Analytical, Ramsey, NJ, USA) assembled with a laboratory-made 40-nl micro-UV flow cell [9].

The detector and interface were described in detail in Part I [1].

Flame measurement

The colourless hydrogen–air flame was made visible with the use of a small piece of sodium glass. Its height was measured against a dark background.

Flame temperatures were measured with the use of a laboratory-made platinum *versus* platinum–10% rhodium thermocouple (2 mm × 0.1 mm O.D.) insulated with a 100 mm × 1.4 mm O.D. ceramic rod. The temperature range of this thermocouple extends to 1700°C (*cf.* standard calibration tables for thermocouples [10]).

RESULTS AND DISCUSSION

Flame characteristics

From the literature on flame combustion [11], it is well known that the simplest form of diffusion flame will occur when a fuel jet flows from a small-diameter burner tube into air of about the same velocity in a wider concentric tube. The majority of the burners used in flame-based GC detectors such as the thermionic and flame photometric detector are constructed according to this principle. The flame originates at the rim of the burner tube, which in this study was the inner glass tube of the modified interface–burner head. It is also known that the shape of the flame surface is determined by the rapidity of the mixing of hydrogen and air and depends on whether air is in excess (overventilated flame; the surface is closed) or is deficient (underventilated flame; the surface has the shape of a cup, called an open or inverted flame shape).

Depending on the gas flow-rates used, mixing takes place by means of laminar or turbulent diffusion. With the hydrogen flow-rates generally applied in GC detector burners, the diffusion flames are laminar (Reynolds number <2000). With laminar flames mixing is controlled by molecular diffusion. The length (L, cm) to achieve a specified, degree of mixing is directly proportional with the volumetric flow (V, cm^3/s) and inversely proportional to the diffusion coefficient of hydrogen in air (D, 0.63 cm^2/s). The flame length can be derived from the relationship [11]

$$L = V/\pi D \quad (1)$$

which indicates that the flame length is independent of the burner diameter if the flame is laminar. We checked the validity of eqn. 1 for small flames (length 2–25 mm) in an experiment in which the flame length (visible by the yellow emission of the sodium glass) was measured at different hydrogen flow-rates for burner diameters of 0.5–1 mm I.D. Fig. 1 shows that the values calculated from eqn. 1 are close to those observed experimentally. It also shows that the presence of the fused-silica capillary placed inside the 0.7 mm I.D. burner tip of the interface (without solvent introduction into the flame) does not change the flame length.

The influence of the helium flow-rate (60–150 ml/min) and air flow-rate (from ambient to *ca.* 600 ml/min) on the flame shape was negligible; the flame shape remained essentially the same with a length of 9.0 ± 0.5 mm and a maximum diameter of 4 ± 0.5 mm (hydrogen flow-rate 95 ml/min).

In this study, increasing the methanol flow-rate (range 0–15 μl/min) caused a linear increase in temperature as measured at different positions of 5–12 mm above the burner rim, *i.e.*, partly in and partly above the flame (Fig. 2). The flame length also increased linearly when increasing the flow-rate of methanol. However, it remained constant when introducing increasing amounts of water, aqueous 0.5 *M* ammonium acetate or 0.5 *M* ammonium formate in the range of 5–15 μl/min. The increase in the flame temperature due to methanol introduction was found to be independent of the hydrogen flow-rate used (Fig. 3). On introducing water, the temperature profile was the same as for the reference measurements without solvent introduction, again irrespective of the hydrogen flow-rate used (Fig. 3).

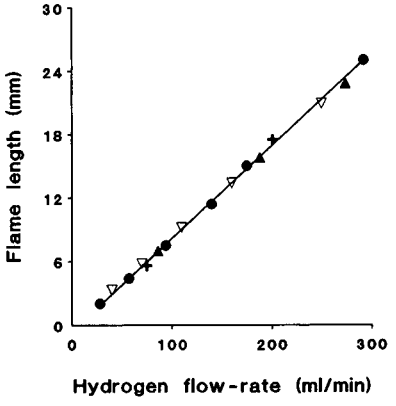

Fig. 1. Influence of hydrogen flow-rate on flame length for different internal diameters of the burner of (▲) 0.5, (●) 0.7 (interface–burner head) and (+) 1 mm. ▽ = data calculated according to eqn. 1. Air, ambient.

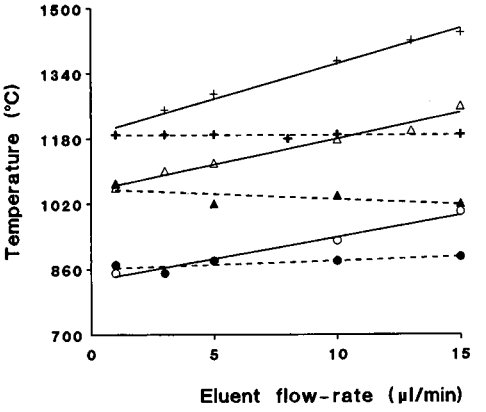

Fig. 2. Influence of the LC eluent flow-rate on temperature measured at various heights above the burner rim: + = 5; ▲ = 7; △ = 8; ● = 10; ○ = 12 mm. Eluent: ———, methanol; – – –, water. Flame length, 9 mm; hydrogen flow-rate, 95 ml/min; helium flow-rate, 100 ml/min; air, ambient.

Fig. 4 shows the relationship between the temperature in and above the flame (flame length 9 mm) measured at various heights above the burner rim when introducing either methanol or water at a constant flow-rate of 10 μl/min. The results are compared with the temperature distribution without

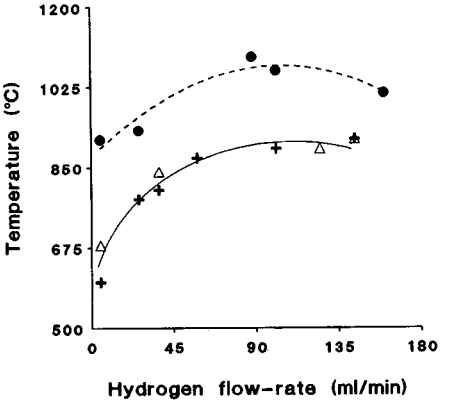

Fig. 3. Influence of LC eluent (methanol) on the flame temperature measured at various hydrogen flow-rates. Temperature measured at 10 mm length above the burner rim; helium flow-rate, 100 ml/min, air, ambient; LC eluent flow-rate, 10 μl/min. Reference temperature measurements were made without eluent introduction. + = Reference; ● = methanol; △ = water.

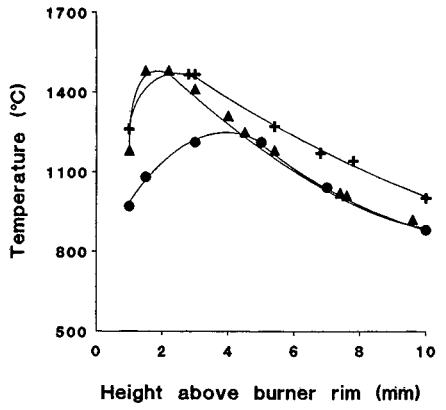

Fig. 4. Influence of LC eluent (methanol or water) on flame temperature at various lengths above the burner rim. The reference temperature measurement was made without eluent introduction. LC eluent flow-rate, 10 μl/min; flame length, 9 mm; hydrogen flow-rate, 95 ml/min; helium flow-rate, 100 ml/min; air, ambient. ▲ = Reference; + = methanol; ● = water.

solvent introduction. Obviously, for heights above the burner rim of over 3 mm the excess of heat released by the combustion of methanol causes a temperature increase. With water as solvent the temperature measured at heights above the burner rim of over 5 mm is the same as without solvent introduction. At lower heights low temperatures are found compared with the flame temperature without solvent introduction. This may be due to conversion of liquid water into gas, and suggests that the solvent leaves the interface capillary as a liquid.

Interface operation

It is interesting to compare the phenomena observed on solvent introduction into the interface used in this study (Fig. 5) with those reported for direct liquid introduction interfaces and thermospray units in mass spectrometry [12–15]. According to Vestal and co-workers [13,14], a thermospray unit can be described as a supersonic jet of vapour with entrained particles or droplets, generated by applying enough heat to a capillary to effect partial vaporization of a liquid as it passes through the capillary. With linear flow velocities of about 80–150 cm/s and a *ca.* 0.1 mm I.D. capillary, the typical thermospray operating point occurs between 150 and 250°C. In our study the temperature measured at the tip of the helium-cooling capillary outlet (see

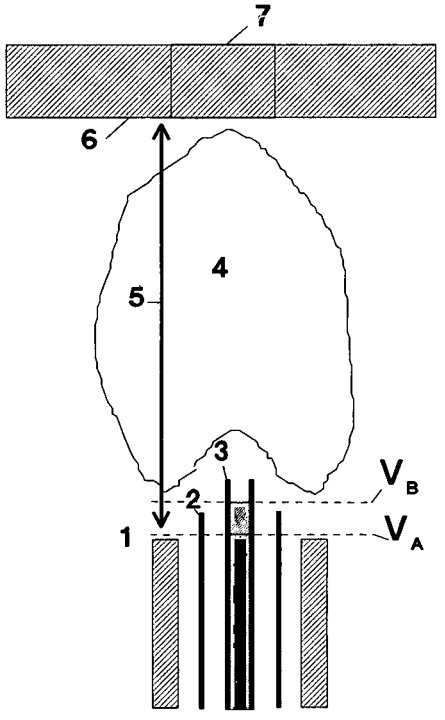

Fig. 5. Schematic diagram of interface configuration (not drawn to scale). 1 = Burner rim; 2 = 0.32 mm I.D. fused-silica helium introduction capillary; 3 = 0.1 mm I.D. eluent introduction capillary; 4 = flame; 5 = Rb source–burner rim distance; 6 = Rb source; 7 = Rb source cavity; V_A–V_B = vaporization zone. For further details, see text.

No. 2 in Fig. 5) proved to be 700°C at a helium flow-rate of about 100 ml/min [1], which is much higher than the temperature quoted above. Moreover, with the interface used in this study, which also contains a *ca.* 0.1 mm I.D. eluent introduction capillary (No. 3 in Fig. 5), the linear solvent flow velocity is only *ca.* 2 cm/s. In conclusion, the interface does not operate as a thermospray and complete vaporization is expected to occur.

For direct liquid interfaces, according to Arpino and Beaugrand [15] the volume flow-rate of vaporization, F (ml/min), in the capillary is

$$F = \frac{\pi P_v}{\rho} \cdot \frac{d_0^2}{2}\left(\frac{M}{2\pi RT}\right)^{1/2} \quad (2)$$

where P_v is the saturated vapour pressure of the LC eluent at temperature T, d_0 is the diameter of the liquid introduction capillary, M and ρ are the molecular weight and the density of the liquid,

respectively, and R is the gas constant. Assuming the temperature at V_A (see Fig. 5) to be 100°C, one can calculate from eqn. 2 that the vaporization rate of water is at least ten times higher than the input of 10 μl/min. As a consequence, vaporization might occur prematurely, *i.e.*, deep inside the capillary, causing non-volatile analytes to be deposited in the capillary. However, the position of the solvent meniscus in the eluent introduction capillary, which was observed to be continuously fluctuating between V_A and V_B, *i.e.*, within the vaporization zone, shows that the helium cooling prevents vaporization to occur deeper than about 0.5–1 mm inside this capillary. The observed fluctuation of the vaporization zone suggests a plug-type solvent introduction into the flame[a].

The above suggestion is supported by the relatively low flame temperature measured close to the exit of the eluent introduction capillary in the case of water (see Fig. 4). Such interface operation should allow the introduction of even distinctly non-volatile analytes into the flame. As an illustration of the potential of the present system to handle such analytes, an LC–TID trace for the phospholipid L-α-lysophosphatidylethanolamine is shown in Fig. 6.

At constant eluent flow-rate, the position of the vaporization zone V_A–V_B (Fig. 5) depends on the vapour pressure of the solvent and the temperature. With an eluent having a low vapour pressure and low specific heat capacity such as water, V_A–V_B will be situated high up in the capillary or even above the outlet of the eluent introduction capillary. Consequently, the LC eluent will leave the capillary as a liquid flowing over its tip, as was indeed observed by us, and will not be introduced into the flame. In order to prevent this, the capillary has to be moved into a higher temperature position. In Fig. 4 it was shown that the maximum temperature occurs *ca.* 2 mm above the burner rim. In other words, the capillary has to be moved closer to the flame. This explains the necessity to increase the eluent introduction capillary–burner rim distance (by *ca.* 0.5 mm) when using water instead of methanol, as was discussed previously [1]. Actually, proper interface operation can also be restored while maintaining the initial eluent introduction capillary–burner rim distance, *viz.*, by changing the temperature of the gas mixture surrounding the capillary. On decreasing the helium gas flow-rate, F, from *ca.* 100 to *ca.* 50 ml/min, the temperature, T at the capillary tip will increase from *ca.* 700 to *ca.* 900°C, as can be calculated from the relationship $T = -4F + 1115$ [1]. In other words, changing the helium flow can be used to optimize eluent introduction when the eluent composition and hence the boiling point of the mixture have been changed.

Thermionic detector operation

In order to study the influence of the detector gas flow-rates on the TID characteristics, a volatile test compound, dimethyl methylphosphonate (DMMP), was selected because it shows a TID response that is independent of the mode of introduction (liquid or vapour) into the flame.

Hydrogen flow-rate. As shown in eqn. 1, at a constant air flow-rate the flame length and, con-

[a] The fluctuation of the vaporization zone can be tentatively explained as follows. When the meniscus has retracted inside the capillary to V_A, the pressure is atmospheric (P_0), because the pressure inside the detector may be assumed to be equal to the outside pressure. The solvent delivered at V_A evaporates completely and the vapour pressure above the solvent starts to increase (P_v). Owing to expansion (a flow of 10 μl/min of water produces 12 ml/min of vapour) and the steep temperature increase (from 100°C, which is the eluent boiling point at P_0, to 700°C), the pressure increase (P_0 to P_V) is dramatic [10]. The increasing pressure reduces the vaporization rate, the solvent becomes overheated and the vaporization zone moves to V_B. At V_B the pressure is assumed to have been reduced sufficiently (because the gas column is pushed out of the capillary by the solvent moving from V_A to V_B) to release the overheated solvent volume between V_A and V_B, restoring the vaporization zone to V_A and reducing the pressure to P_0.

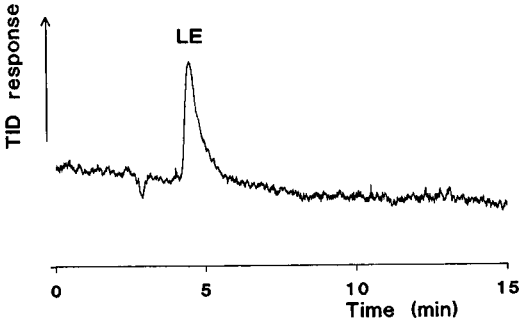

Fig. 6. Micro-LC–TID of 10 ng of L-α-lysophosphatidylethanolamine (LE). Column, 150 mm × 0.32 mm I.D. packed with PRP-1; eluent, methanol–water–formic acid (95:5:0.5); flow-rate, 8 μl/min.

sequently, the position of the high-temperature zone in the flame depend on the hydrogen flow-rate. That is, varying the hydrogen flow-rate results in (i) a different flame–Rb source distance (a 50–100 ml/min increase of the hydrogen results in an about 4 mm increase of the flame length as calculated from eqn. 2), (ii) a different H_2:O_2 ratio and (iii) an inverted flame shape, if hydrogen is in excess. These changes should be carefully considered when interpreting the results obtained on varying the hydrogen flow-rate.

The influence of the hydrogen flow-rate on the analyte signal, and the noise, signal-to-noise (S/N) ratio and temperature measured in the cavity of the Rb source is shown in Fig. 7. Increasing the hydrogen flow-rate from 80 to 100 ml/min (this range corresponds with an H_2:O_2 ratio slightly over the stoichiometric value of 2.0) gave a distinct decrease of both signal and noise. However, the Rb source surface temperature (data not shown) and the temperature in the Rb source cavity (see Fig. 7) just above the flame remained essentially constant. This may indicate that the analyte signal, and also the noise level (see next section), is primarily determined by chemi-ionization reactions in the flame, and not by the temperature. Recently, using mass spectrometry, Bombick and Allison [4] found that PO_3^- is the most abundant ion produced by the interaction of organophosphorus compounds with a hot alkali-ceramic bead. The PO_3^- ion may well be the charge carrier that causes the TID response [4]. For the reductive mode of the flame as used with the flame photometric detector, it is well known that the neutral molecule HPO is responsible for the green phosphorus emission. Possibly, when there is an excess of hydrogen, part of the PO_3^- ions is converted into neutral HPO molecules, which will result in a lower signal.

At low hydrogen flow-rates the flame is overventilated and will be relatively hot (see next section and Fig. 8). However, it will also be short (see eqn. 1). Therefore, the temperature of the reaction gas mixture in the cavity of the Rb source decreases and there is a simultaneous strong decrease in signal (Fig. 7); this suggests a dependence of analyte signal on temperature. In other words, a decreasing hydrogen flow-rate causes a lower flame position; this in its turn results in a decreased Rb source temperature and a correspondingly lower signal. The noise, however, remains essentially constant and the S/N ratio will consequently decrease sharply. These results concerning overventilated flames confirm the mutual dependence of the optimum Rb source–rim distance and the hydrogen flow-rate discussed previously [1].

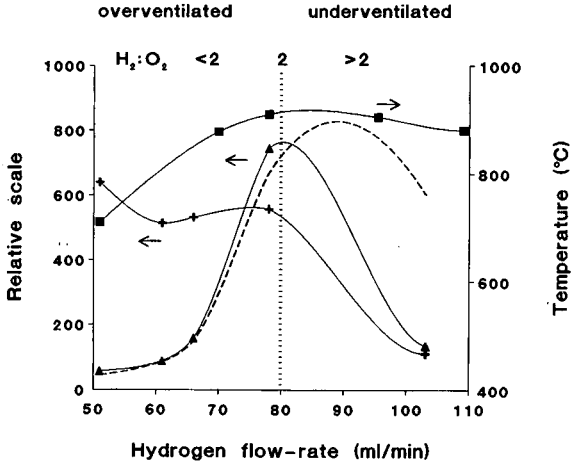

Fig. 7. Influence of hydrogen flow-rate on signal, S/N ratio, noise and Rb source cavity temperature. Air flow-rate, 200 ml/min; eluent, methanol; flow-rate, 10 μl/min. ▲ = Signal; + = noise; ■ = Rb source cavity temperature. Dashed line, S/N ratio.

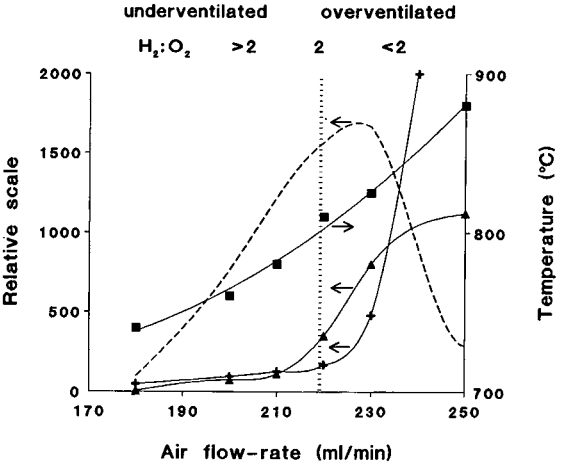

Fig. 8. Influence of air flow-rate on signal, noise, S/N ratio and Rb source cavity temperature. Hydrogen flow-rate, 88 ml/min; analyte, DMMP; eluent, methanol; flow-rate, 10 μl/min. ▲ = Signal; + = noise; ■ = Rb source cavity temperature. Dashed line, S/N ratio.

Air flow-rate. When varying the air flow-rate (at a constant hydrogen flow-rate of 95 ml/min), the flame length will remain constant, as discussed in the section on the flame characteristics. That is, whereas a hydrogen flow-rate variation changes both flame length and H_2:O_2 ratio, in the case of an air flow-rate variation only the H_2:O_2 ratio will vary; consequently, a change in the Rb source cavity temperature is expected. In Fig. 8 (eluent methanol) the influence of the air flow-rate on analyte signal, noise, S/N ratio and Rb source cavity temperature is shown. The optimum S/N ratio at an air flow-rate of 220–230 ml/min (hydrogen flow-rate 88 ml/min) corresponds to a H_2:O_2 ratio of *ca.* 1.95. As shown in Fig. 8, the temperature increases with increasing air flow-rate up to at least 250 ml/min. The detector noise is relatively low and constant above the stoichiometric H_2:O_2 ratio, *i.e.*, when oxygen is deficient. Just below the stoichiometric ratio (air flow-rate >220 ml/min), the analyte signal, noise level (and background; data not shown) start to increase sharply. On further increasing the air flow-rate (H_2:O_2 ratio decreasing from 2 to 1.5), the analyte signal decreases but the noise and background remain relatively high, as shown in Fig. 7, here and Fig. 3A–C in ref. 1. This means that, with methanol as eluent, the noise level essentially determines the optimum S/N ratio.

With water instead of methanol (data not shown), the background and noise remained constant over the total air flow-rate range of 150–300 ml/min (H_2:O_2 ratio from 3 to 1.5). Here the noise is probably the result of the eluent introduction. This suggests that the strong increase of noise and background is the result of the presence of organic molecules (methanol) in the LC eluent, *i.e.*, of the formation of organic ions due to chemi-ionization:

$$CH + O \rightarrow CHO^+ + e^- \quad (3)$$

followed by a charge-exchange reaction:

$$CHO^+ + H_2O \rightarrow H_3O^+ + CO \quad (4)$$

The hydronium ion, H_3O^+, is known to be the dominant ion in hydrocarbon flames [9]. It may decay by reactions such as:

$$H_3O^+ + e^- \rightarrow H_2O + H \quad (5)$$

Eqns. 3 and 4 may explain the relationship between the formation of organic ions and the flame mode when using methanol as eluent.

In the case of overventilation, eqn. 3 shows the initiation of the reaction via the presence of oxygen radicals. The hydrogen radicals formed according to eqn. 5 will be consumed by oxygen [5]:

$$H + O_2 \rightarrow OH + O \quad (6)$$

In other words, overventilation causes the formation of ions and thus increases the noise and background. On the other hand, when the flame is underventilated and hydrogen is in excess, the oxygen radicals will be consumed and hydrogen radicals will be formed, as shown in the equations [5]

$$O + H_2 \rightarrow OH + H \quad (7)$$

$$OH + H_2 \rightarrow H_2O + H \quad (8)$$

This may explain the sharp decrease in noise and background observed when the H_2:O_2 ratio is above the stoichiometric value of 2.0; the consumption of oxygen radicals by hydrogen according to eqns. 7 and 8 prevents the initiation reaction (eqn. 3) from occurring and, consequently, the formation of CHO^+ and H_3O^+ ions.

Hydrogen/air flow-rate ratio. The above results indicate that when keeping the H_2:O_2 ratio constant at the stoichiometric ratio, varying the hydrogen flow-rate will simply result in a change in flame length (see eqn. 1). That is, the simultaneous variation of the hydrogen and air flow-rates over not too large a range has a similar effect as varying the Rb source–burner rim distance. Alternatively, when the flame length and the Rb source–burner rim distance are simultaneously increased to the same extent, the position of the flame boundary relative to the Rb source, and hence the Rb source temperature, is expected to remain essentially constant. This will result in a relatively constant S/N ratio, as was indeed observed previously [1] for a simultaneous hydrogen and Rb source–burner rim distance increase of *ca.* 10 ml/min and *ca.* 0.5 mm, respectively (using adjusted air flow-rates to maintain a constant H_2:O_2 ratio of 1.95).

In contrast to the above, an increase in the S/N ratio occurred when the hydrogen (and air) flow-rates and the Rb source–burner rim distance were simultaneously increased over a much wider range. Fig. 9 shows the increase in the S/N ratio (see arrow) on simultaneously increasing the Rb source–burner rim distance by 6 mm and the hydrogen flow-rate by 70 ml/min (a 70 ml/min increase corresponds to a 6

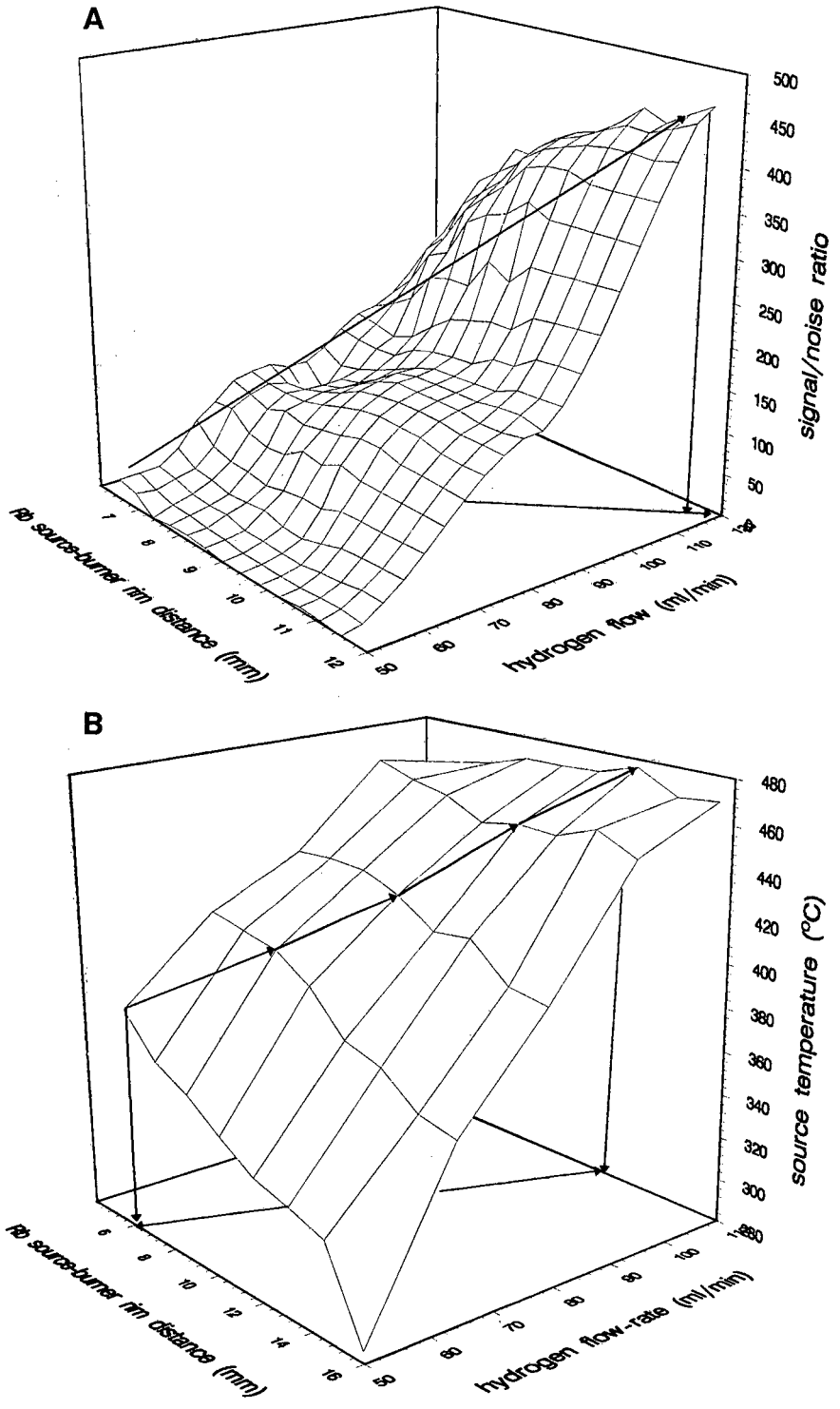

Fig. 9. (A) Dependence of signal-to-noise ratio on hydrogen flow-rate and Rb source–burner rim distance. H_2:O_2 ratio, 1.95. (B) Dependence of Rb source temperature on hydrogen flow-rate and Rb source–burner rim distance. H_2:O_2 ratio, 1.95.

mm increase in flame length; *cf.* eqn. 1). The data presented in Fig. 5A (analyte signal) and Fig. 5B (noise) in ref. 1 may be used to explain why the S/N ratio decreases dramatically both in front of and behind the triangular plane shown in Fig. 9A here. There is a marked parallellism between the optimum S/N ratio plot in Fig. 9A and the plot illustrating the Rb source temperature increase (Fig. 9B). The increase in the source temperature is probably the result of the increased thermal energy of the flame, which is directly proportional with the hydrogen flow-rate.

It should be added that the present detector configuration requires modification to allow convenient handling of some of the large flames and Rb source–burner rim distances used above.

CONCLUSIONS

The characterization of the micro-LC–TID system attempted in this paper clearly shows that the temperature of the Rb source depends strongly on the flame dimensions and gas flow-rates used. A high temperature of the surface and cavity of the Rb source appears essential to obtain a strong analyte signal. The flame should come close to the Rb source without, however, enveloping it, because this will cause a dramatic increase in the noise level. In other words, the optimum distance essentially equals the flame length.

As the flame length depends on the hydrogen flow-rate, provided the H_2:O_2 ratio is <2, the Rb source–burner rim distance and hydrogen flow-rate are mutually dependent. Further, the analyte signal depends strongly on the hydrogen and air flow-rates, and reaches its maximum at a H_2:O_2 ratio close to the stoichiometric value, *i.e.*, in the range 1.90–2.05. These results hold true for all methanol water mixtures irrespective of their composition. However, on increasing the methanol content of an aqueous–organic eluent, the flame length will increase. The concomitant increase in noise and background is probably the result of chemi-ionization reactions rather than temperature effects. Self-evidently, if the methanol content of an eluent is increased, the Rb source–burner rim distance will have to be increased in order to maintain optimum conditions.

The configuration of the present interface with its continuously fluctuating vaporization zone allows the introduction of both volatile and non-volatile analytes into the flame, that is, it meets the main demand required of an interface between an LC separation and a GC-type detection system.

Finally, considering the situation from a practical point of view, one should realize that the mutual dependence of almost all parameters involved, hydrogen and air flow-rates, Rb source–burner rim distance and nature of the solvent, results in a system that is sensitive to small changes in operating conditions. Careful optimization of the system is therefore required, especially when the chromatographic conditions are changed. Uncoupling the regulation of the Rb source temperature and the flame temperature by introducing an external heating unit will certainly result in a less complicated system. In view of the promising analytical results already obtained with the present system, this will be an interesting subject for future studies on micro-LC–TID. Its implementation should facilitate the use of thermionic detection in LC.

ACKNOWLEDGEMENTS

The authors are greatful to A. C. van de Berg and C. J. de Ruiter for helpful discussions.

REFERENCES

1 Ch. E. Kientz, A. Verweij, G. J. de Jong and U. A. Th. Brinkman, *J. Chromatogr.*, 626 (1992) 59.
2 Ch. E. Kientz, A. Verweij, H. L. Boter, A. Poppema, R. W. Frei, G. J. de Jong and U. A. Th. Brinkman, *J. Chromatogr.*, 467 (1989) 385.
3 Ch. E. Kientz, A. Verweij, G. J. de Jong and U. A. Th. Brinkman, *J. High Resolut. Chromatogr.*, 12 (1989) 793.
4 G. Guiochon and C. L. Guillemin (Editors), *Quantitative Gas Chromatography*, Elsevier, Amsterdam, 1988.
5 M. Dressler (Editor), *Selective Gas Chromatographic Detectors*, Elsevier, Amsterdam, 1986.
6 P. van de Weijer, B. H. Zwerver and R. J. Lynch, *Anal. Chem.*, 60 (1988) 1380.
7 D. D. Bombick and J. Allison, *J. Chromatogr. Sci.*, 27 (1989) 612.
8 J. C. Gluckman, A. Hirose, V. L. McGuffin and M. Novotny, *Chromatographia*, 17 (1984) 3039.
9 Ch. E. Kientz and A. Verweij, *J. High Resolut. Chromatogr. Chromatogr. Commun.*, 3 (1988) 294.
10 D. R. Lide (Editor), *CRC Handbook of Chemistry and Physics*, CRC Press, Boston, MA, 72nd Ed., 1991–92, p. 15-1.
11 B. Lewis, *Combustion, Flames and Explosions of Gases*, Academic Press, Orlando, FL, 1987, p. 479.

12 A. P. Bruins and B. F. H. Drenth, *J. Chromatogr.*, 271 (1983) 271.
13 C. R. Blakley and M. L. Vestal, *Anal. Chem.*, 55 (1983) 750.
14 M. L. Vestal and G. J. Fergusson, *Anal. Chem.*, 57 (1985) 2378.
15 P. J. Arpino and C. Beaugrand, *Int. J. Mass Spectrom. Ion Processes*, 64 (1985) 275.

Journal of Chromatography, 626 (1992) 81–86
Elsevier Science Publishers B.V., Amsterdam

CHROM. 24 542

Chemical ionization with gaseous ammonia for normal-phase liquid chromatographic–thermospray mass spectrometric applications

R. G. J. van Leuken and G. T. C. Kwakkenbos

FA Department, DSM Research, P.O. Box 18, 6160 MD Geleen (Netherlands)

ABSTRACT

Addition of gaseous ammonia to a thermospray ion source, followed by filament-on ionization, provides chemical ionization reagent ions. The abundance of reagent ions is sufficient to obtain spectra which contain predominantly $[M+NH_4]^+$ ions. The advantage of this method of ionization lies in normal-phase LC–MS applications, where "traditional" ionization methods such as volatile buffer, filament-on or discharge-on ionization yields either no ionization or too much fragmentation, making identification very difficult or impossible. After modification of a Finnigan TSQ 70 ion source, the source pressure and effluent flow were optimized. The formation of $[M+NH_4]^+$ ions is dependent on the voltage applied to the repeller electrode. Low voltages yield spectra with predominantly $[M+NH_4]^+$ ions, whereas high voltages yield spectra showing mostly fragmentation and a small percentage of chemical ionization. The formation of the $[M+NH_4]^+$ ion of cyclohexanone is linear over two decades ranging from 0.2 to 20 ng of the compound injected into a normal-phase column. Higher concentrations give rise to a deviation of the linear relationship. Quantitative results are obtained, with a repeatability of 8% (R.S.D.).

INTRODUCTION

Liquid chromatography coupled with a thermospray interface and mass spectrometry (LC–TSP–MS) is a powerful technique for the conformation analysis and identification of polar, thermolabile and non-volatile compounds in target analysis. In TSP ionization there are three different approaches: buffer, filament-on and discharge-on ionization, each of which has its own advantages and disadvantages [1–3]. When buffer ionization is applied, the molecules of interest are ionized with aqueous solutions of ammonium buffers, as a result of either the pH of the buffer solutions (depending on the pK_a values of the compounds) or molecule–ion interactions in the ion source. Filament-on ionization and discharge-on ionization are effected by means of a beam of electrons and a plasma of ions created by an electric field, respectively.

A repeller electrode pushes these ions in the direction of the mass separator. As TSP is a "soft" ionization technique, mainly $[M+H]^+$ and $[M+NH_4]^+$ ions are formed. Depending on the repeller voltage some fragmentation occurs [3]. Therefore, the mass spectrum is dependent on both the ionization technique and repeller voltage.

Reversed-phase high-performance liquid chromatography (RP-HPLC) is the most commonly used LC technique [4]. In RP-HPLC an apolar stationary phase (*e.g.*, C_8 or C_{18}) is used in combination with a polar mobile phase *e.g.*, an aqueous buffer solution. Depending on the application, a certain percentage of organic modifier (*e.g.*, methanol or acetonitrile) is added to the mobile phase. Buffer ionization in RP-HPLC is easily applicable and normally yields mass spectra with few fragment ions. Owing to the higher electrical field applied in filament-on and discharge-on ionization, more frag-

Correspondence to: R. G. J. van Leuken, FA Department, DSM Research, P.O. Box 18, 6160 MD Geleen, Netherlands.

0021-9673/92/$05.00 © 1992 Elsevier Science Publishers B.V. All rights reserved

ment ions are found in the mass spectra obtained with these methods.

Normal-phase (NP) HPLC involves a combination of a polar stationary phase (usually modified silica) and an apolar mobile phase such as dichloromethane or *n*-hexane. Sometimes a polar modifier (*e.g.*, 2-propanol) is added to reduce the analysis time. As these apolar mobile phases are not miscible with aqueous solutions, buffer ionization is difficult to apply. For structure elucidation, $[M+H]^+$ and $[M+NH_4]^+$ ions are very useful, but in NP-HPLC, only filament-on ionization and discharge-on ionization can be applied.

The use of buffer ionization with a double-beam thermospray LC–MS interface for apolar mobile phases has been demonstrated for both LC–MS [5] and GPC–MS [6]. Increased sensitivity has been reported for both NP–HPLC–TSP applications [7] and ammonia CI of ketones [8].

When gaseous ammonia is used, mainly $[M+NH_4]^+$ ions are formed [9]. The applicability of gaseous ammonia as an ionization gas in normal-phase LC–TSP–MS will be demonstrated via the analysis of two compounds of interest in the production of polyamides, *viz.*, cyclohexanone and cyclohexanol [10].

EXPERIMENTAL

Source block modification

A slight modification to the source block was necessary to supply gaseous ammonia, as shown in Fig. 1. This was be done by making a new inlet between the aperture for the discharge electrode and the vaporizer entrance hole of the source of a TSQ-70 mass spectrometer (Finnigan MAT, San Jose, CA, USA). In this way ammonia could enter the source block via the cartridge heater and the discharge electrode opening.

The ammonia was fed through the standard available calibration gas/reagent gas inlet. A 3.18-mm stainless-steel tube was provided between the calibration gas/reagent gas inlet and the extra inlet.

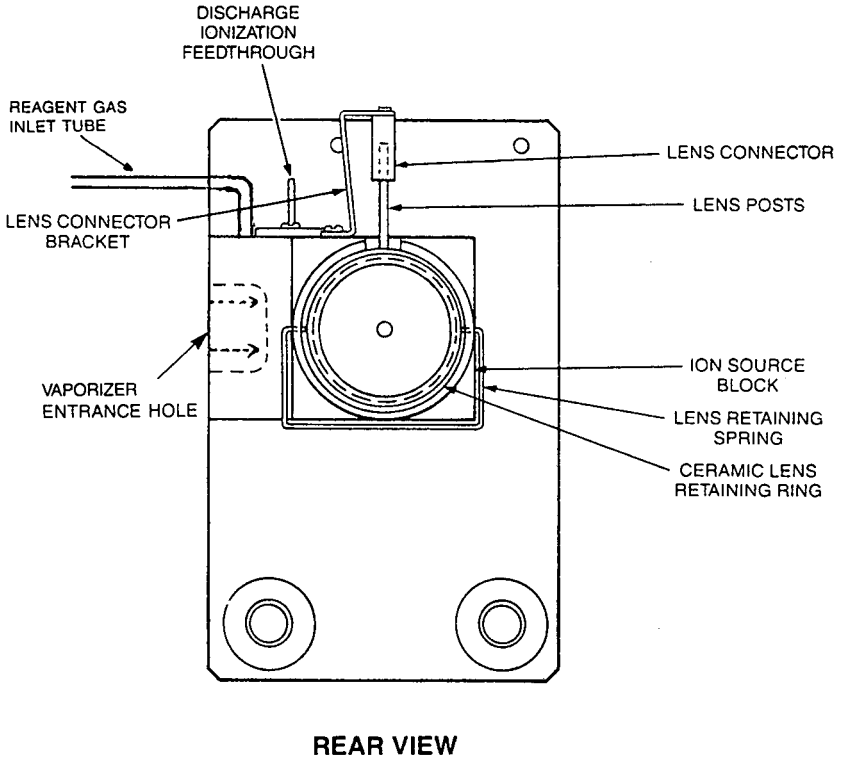

Fig. 1. Position of the reagent gas inlet tube in the modified TSP ion source. (Reprinted with permission from Finnigan MAT Benelux, Veenendaal, Netherlands.)

Instrumentation

The chromatographic system consisted of a Gilson (Villiers-le-Bel, France) Model 305 pump, a Rheodyne (Cotati, CA, USA) Model 7125 injection valve with a 20-μl loop and a Finnigan MAT TSQ-70 triple quadrupole mass spectrometer equipped with a thermospray interface. The column used was a LiChrosorb 10-Diol (250 × 4.6 mm I.D., 5 μm) from Chrompack (Middelburg, Netherlands). The flow-rate was 1 ml/min. The eluent was *n*-hexane–2-propanol (1000:15, v/v). The separations were carried out at ambient temperature. To maintain an optimum source pressure, post column addition of the eluent was effected with a Gilson Model 302 pump for discharge-on experiments only. The solution was added to the column effluent by a Lee (Frankfurt, Germany) visco-jet micromixer. The repeller voltage and ion source pressure were varied, depending on the experiment, and are indicated in the figures.

The vaporizer temperature, discharge voltage, electron energy, electron current and the source temperature were kept at 71°, 450 V, 600 eV, 50 μA and 190°C, respectively. The electron multiplier was operated at 2 kV. Scanning was performed from relative molecular mass 40 to 440 with a scan time of 1 s. Selected ion monitoring (SIM) was used for the determination of cyclohexanone at m/z = 116 ($[M+NH_4]^+$).

Chemicals

Cyclohexanone was obtained from DSM (Geleen, Netherlands), [$^2H_{11}$] cyclohexanol and cyclohexanol from Aldrich (Brussels, Belgium), HPLC-grade *n*-hexane and 2-propanol from Merck (Darmstadt, Germany) and gaseous ammonia from Hoek Loos (Amsterdam, Netherlands).

RESULTS AND DISCUSSION

Modification and optimization of the mass spectrometer

Chemical ionization with gaseous ammonia (NH_3-CI) is possible in both the filament-on and discharge-on modes. After ionization of the ammonia molecules, the ions can react with the compounds of interest. Discharge-on with postcolumn addition of effluent can also be used for ionization, but it causes a large increase in chemical noise due to clustering and fragmentation. The signals of the ions formed by ammonia (m/z 18 and 35) and 2-propanol (m/z 78) were selectively removed from the scan table, resulting in a very low noise level compared with buffer or discharge-on ionization. Hence the signal-to-noise ratios are much better with NH_3-CI.

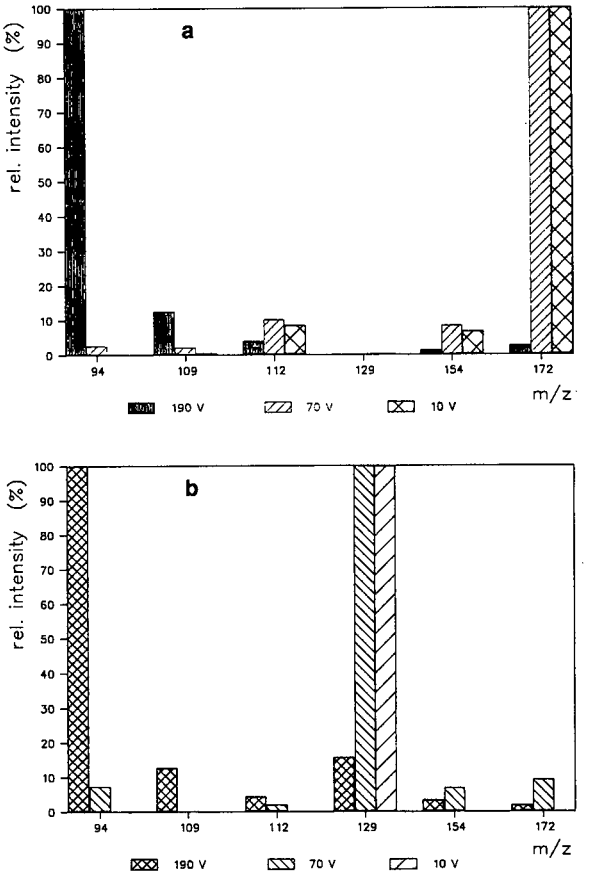

Fig. 2. Relative intensities of characteristic ions of [$^2H_{11}$]cyclohexanol at different repeller voltages. (a) Discharge-on; (b) NH_3-CI/filament-on ionization.

In our experiments we used an ion source pressure of about 120 Pa (0.9 Torr). This was achieved by supplying 67–80 Pa (0.5–0.6 Torr) of ammonia to the ion source (filament-on) or post column addition of 0.5 ml/min of effluent (discharge-on). An ion source pressure of 120 Pa (0.9 Torr) proved to give an optimum yield of ammonium ions. Below 107 Pa (0.8 Torr) instability of the signals occurred.

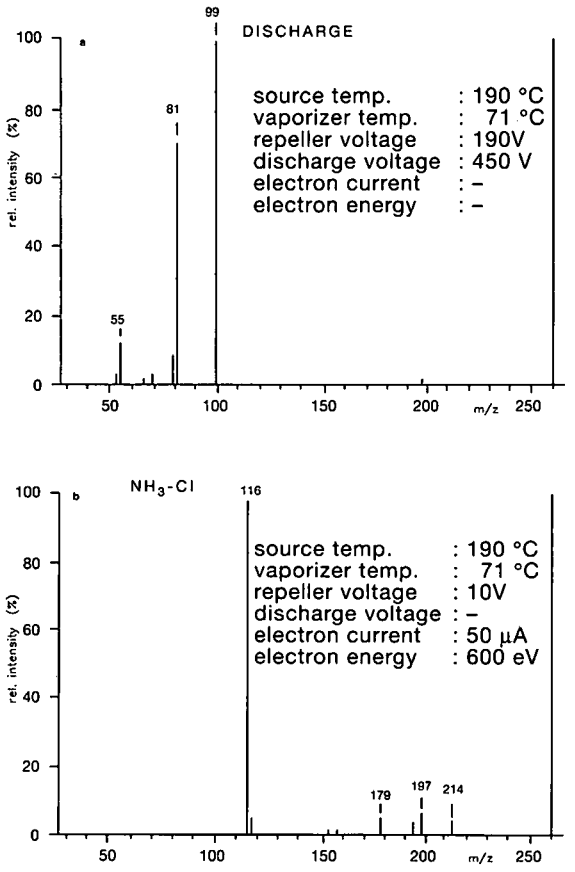

Fig. 3. (a) Discharge-on and (b) NH_3-CI/filament-on ionization spectra from cyclohexanone.

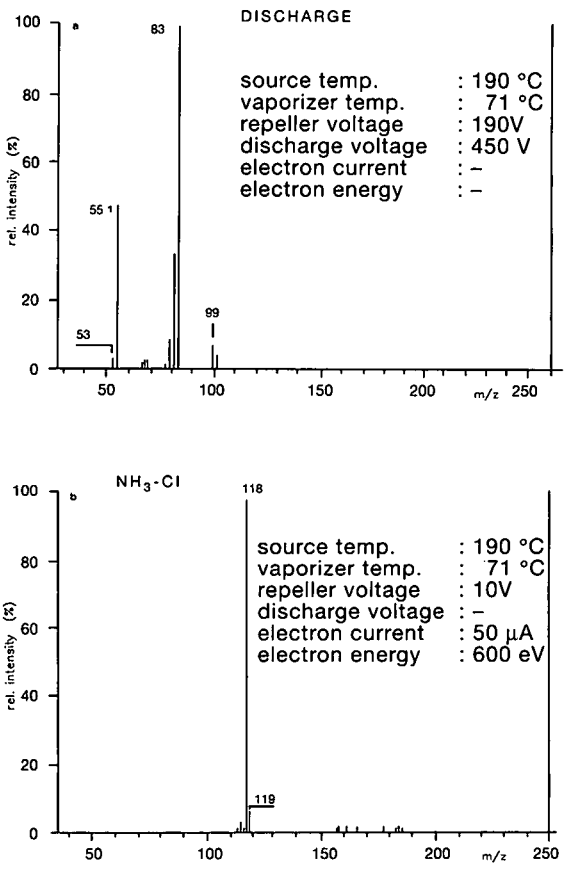

Fig. 4. (a) Discharge-on and (b) NH_3-CI/filament-on ionization spectra from cyclohexanol.

Dependence of mass spectra on repeller voltage

The mass spectra of $[^2H_{11}]$cyclohexanol were investigated at different repeller voltages, both with discharge-on ionization and with NH_3-CI. The relative intensities of the characteristic ions formed are shown in Fig. 2. A decrease in repeller voltage in the discharge-on mode results in less fragmentation and more cluster ion formation. These cluster ions are $[2M+H]^+$ at m/z 223, $[M+C_3H_7OH_2]^+$ at m/z 172 and $[M+C_3H_7]^+$ at m/z 154. The $[M+NH_4]^+$ ion with m/z 129 is the base peak obtained by NH_3-CI at low repeller voltages, as is shown in Fig. 2b.

As demonstrated in Fig. 2, the molecular mass can be obtained from NH_3-CI at low repeller voltages and structural information from discharge-on experiments at high repeller voltages.

Discharge-on ionization versus ammonia chemical ionization

For both discharge-on ionization and NH_3-CI, mass spectra were recorded under the optimum conditions. The spectra of cyclohexanone, cyclohexanol and $[^2H_{11}]$cyclohexanol are shown in Figs. 3, 4 and 5, respectively. Table I gives the formulae of the ions detected. As can be seen in Figs. 3–5, fragmentation occurs with discharge-on ionization at high repeller voltages, whereas an intense $[M+NH_4]^+$ ion is obtained with NH_3-CI at low repeller voltages. Owing to the relatively high concentration of cyclohexanone, cluster ions are present in the mass spectrum (Fig. 3b). These cluster ions are $[2M+NH_4]^+$ at m/z 214, $[2M+H]^+$ at m/z 197, $[2M+NH_4-H_2O]^+$ at m/z 196 and $[2M+H-H_2O]^+$ at m/z 179.

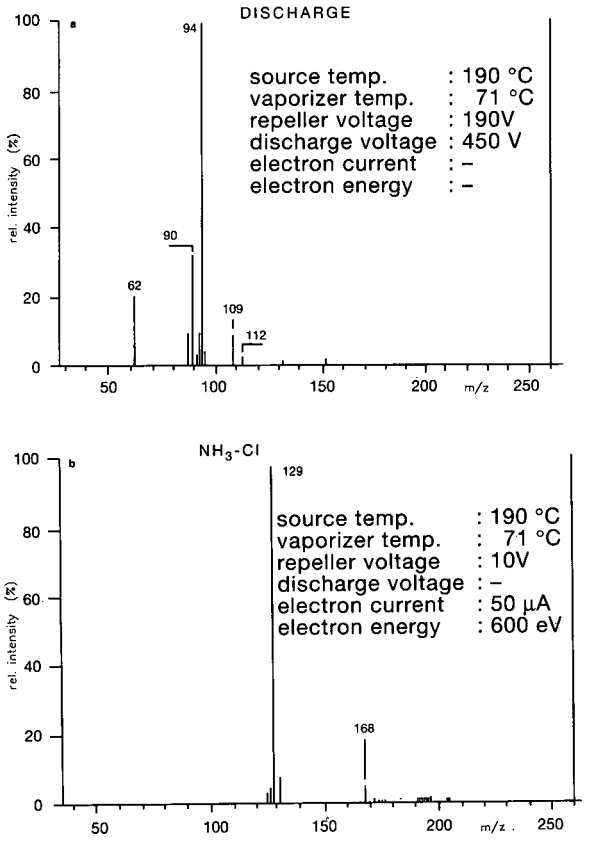

Fig. 5. (a) Discharge-on and (b) NH_3-CI/filament-on ionization spectra from $[^2H_{11}]$cyclohexanol.

Quantitative analysis

A linear relationship (r^2 = 0.999) was found over the range 0.2–20 ng of cyclohexanone. A detection limit of 200 pg of cyclohexanone was found at a signal-to-noise ratio of 3. The repeatability of the method, calculated from repeated injections of 0.8 mg/l of cyclohexanone, is 8.0% (R.S.D.) (n = 11).

CONCLUSIONS

Through a simple modification of the ion source of a Finnigan MAT TSQ-70 mass spectrometer, ionization with gaseous ammonia was made possible for normal-phase LC–TSP–MS applications.

Ionization with gaseous ammonia, in the filament-on mode and at low repeller voltages, results in spectra with predominantly the $[M+NH_4]^+$ peak. Upon additional discharge-on ionization, without NH_3 and at a high repeller voltage, fragment ions are obtained. Hence information on both molecular mass and structure of the compound of interest is obtained in normal-phase LC separations. Structure elucidation of unknown structures thus becomes much easier, provided there is little background interference, as in our case.

Scanning from low masses (*e.g.*, m/z 20), which is a problem with other ionization techniques, is possible.

Chemical ionization with ammonia is very sensitive. In the SIM mode, a detection limit of 200 pg of cyclohexanone (signal-to-noise ratio = 3) was found. Quantitative analysis also gives good results. The calibration graphs are linear over two decades. The repeatability is 8.0% (R.S.D.).

TABLE I

CHARACTERISTIC IONS FROM CYCLOHEXANONE, CYCLOHEXANOL AND $[^2H_{11}]$CYCLOHEXANOL OBTAINED BY DISCHARGE-ON IONIZATION

Cyclohexanone		Cyclohexanol		$[^2H_{11}]$Cyclohexanol	
m/z	Ion	m/z	Ion	m/z	Ion
99	$[M+H]^+$	101	$[M+H]^+$	112	$[M+H]^+$
97	$[C_6H_9O]^+$	99	$[C_6H_{10}OH]^+$	109	$[C_6{}^2H_{10}OH]^+$
		83	$[C_6H_{11}]^+$	94	$[C_6{}^2H_{11}]^+$
81	$[C_6H_9]^+$	81	$[C_6H_9]^+$	90	$[C_6{}^2H_9]^+$
79	$[C_6H_7]^+$	79	$[C_6H_7]^+$		
55	$[C_4H_7]^+$	55	$[C_4H_7]^+$	62	$[C_4{}^2H_7]^+$
53	$[C_4H_5]^+$	53	$[C_4H_5]^+$		

REFERENCES

1 A. L. L. Duchateau, B. H. M. Munsters, G. T. C. Kwakkenbos and R. G. J. van Leuken, *J. Chromatogr.*, 552 (1991) 605.
2 D. Barceló, J. M. Bayona, G. Durand, I. Tolosa and M. Valls, presented at the *7th International Symposium on Liquid Chromatography–Mass Spectrometry, Montreux, October 31–November 2, 1990.*
3 W. H. McFadden and S. A. Lammert, *J. Chromatogr.*, 385 (1987) 201.
4 S. P. Cepa, in *Proceedings of the 38th ASMS Conference on Mass Spectrometry and Allied Topics, Tuscon, AZ, June 3–8, 1990*, pp. 357–358.
5 L. Bütfering, G. Schmelzeisen-Redeker and F.W. Röllgen, *J. Chromatogr.*, 394 (1987) 109–116.

6 W. J. L. Genuit and J. J. de Boer, presented at the *12th International Mass Spectrometry Conference, Amsterdam, August 26–30, 1991.*
7 D. Barceló, G. Durand, R. J. Vreeken, G. J. de Jong and U. A. Th. Brinkman, *Anal. Chem.*, 62 (1990) 1696–1700.
8 P. Rudewicz and B. Munson, *Anal. Chem.*, 57 (1985) 786–789.
9 P. J. Rudewicz, *Ph.D. Thesis*, University of Delaware, University Microfilms, Ann Arbor, MI, 1985.
10 V. Z. Fridman and E. D. Mikhal'chenko, *Khim. Promst. (Moscow)*, 21 (1989) 168–170.

Journal of Chromatography, 626 (1992) 87–96
Elsevier Science Publishers B.V., Amsterdam

CHROM. 24 544

On-line coupled reversed-phase high-performance liquid chromatography–gas chromatography–mass spectrometry

A powerful tool for the identification of unknown impurities in pharmaceutical products

Jörg Ogorka, Gerhard Schwinger and Guy Bruat

Sandoz Pharma Ltd., Analytical Research and Development, P.O. Box, 4002 Basle (Switzerland)

Volker Seidel

Institut für Pharmazeutische Chemie, Universität Graz, Schubertstrasse 1, 8010 Graz (Austria)

ABSTRACT

An alternative approach to HPLC–MS involving direct coupling of reversed-phase HPLC to GC–MS is described for the identification of unknown impurities in pharmaceutical products. Conventional-sized reversed-phase HPLC (column of 4.6 mm I.D., flow-rate 2 ml/min) was coupled to GC–MS. Liquid sample volumes of 500 μl were transferred. In contrast to LC–MS coupling techniques, the proposed method technique experiences no problems with low-molecular-mass solutes or any buffer salts in the reversed-phase LC eluent. An example illustrating the use of this technique in analytical research and development in the pharmaceutical industry is presented. An unknown impurity observed in the HPLC of a stressed sample of a pharmaceutical product was identified by directly transferring the LC fraction of interest to a GC–MS system. The transfer problems arising from the content of water and buffer salts in the LC eluent were circumvented by on-line coupling of liquid–liquid extraction by means of a sandwich-type phase separator, which was coupled to a loop-type LC–GC interface. It is shown that this technique can be improved by lowering the extraction temperature below the freezing point.

INTRODUCTION

In the pharmaceutical industry, there is a great demand for on-line coupling of reversed-phase HPLC to MS, because by this means structural information about unknown impurities observed in HPLC during the development of pharmaceutical products can be obtained in a very economical way. Therefore, LC–MS has become well established in analytical research and development in most pharmaceutical companies. Nevertheless, LC–MS coupling techniques show clear limitations when solutes of interest have a certain volatility and when the LC eluent contains non-volatile buffer salts (such as the commonly used phosphate buffer). In contrast, LC–GC–MS, using the instrumental set-up presented here, experiences no problems with low-molecular-mass solutes (with the exception of very volatile compounds, eluting at a temperature less than *ca.* 80°C above the transfer temperature in GC [1]) or any buffer salts in the LC eluent. Hence, LC–GC–MS is a valuable complement to common LC–MS.

As reversed-phase HPLC clearly dominates over normal-phase HPLC in pharmaceutical analysis, there is a particular interest in transferring aqueous LC fractions to GC columns. In our approach, the

Correspondence to: J. Ogorka, Sandoz Pharma Ltd., Analytical Research and Development, P.O. Box, 4002 Basle, Switzerland.

0021-9673/92/$05.00 © 1992 Elsevier Science Publishers B.V. All rights reserved

transfer problems arising from the content of water and buffer salts in the LC eluent were circumvented by on-line coupling of liquid–liquid extraction by means of a sandwich-type phase separator, as described by Van Zoonen *et al.* [2]. The on-line connected laboratory-made LC–GC interface was set up according to Grob and Stoll [3]. The technique applied for sample introduction into the GC column was concurrent eluent evaporation [4].

Van Zoonen *et al.* [2] reported that the extraction efficiency of their on-line liquid–liquid extraction device was *ca.* 65%. We tried to improve the yield of the organic phase with the same device by cooling the phase separator. Initial results obtained with this approach are presented in this paper. In addition, we present an example illustrating the use of LC–GC–MS for analytical research and development in the pharmaceutical industry.

EXPERIMENTAL

The instrumental set-up for LC–GC–MS is shown in Fig. 1.

Instrumental set-up

For the HPLC system, a Kontron (Zürich, Switzerland) Model 420 pump, a manual injection valve (Rheodyne, Berkeley, CA, USA) and a Kontron Uvicon 725 detector were used. The extraction solvents were delivered by a separate Kontron Model 420 pump via a 100 mm × 4.6 mm I.D. column packed with 5-μm Spheri 5 silica (Brownlee Labs., Applied Biosystems, Santa Clara, CA, USA) serving as a restriction only. LC eluents and the extraction solvent were mixed together in a Valco (Houston, TX, USA) 0.75 mm I.D. T-piece and pushed through a 3 m × 0.8 mm I.D. PTFE capillary, which was connected to a sandwich-type phase separator (purchased from the Free University of Amsterdam, Amsterdam, Netherlands).

The phase separator was cooled by a Haake (Karlsruhe, Germany) F3C cryostat filled with polyethylene glycol. As indicated in Fig. 1, the UV detector was installed either before or after the liquid–liquid extraction unit, depending on whether it was intended to detect the solutes in the LC eluent or in the extract. A needle valve restrictor was used to regulate the flow of the organic extract.

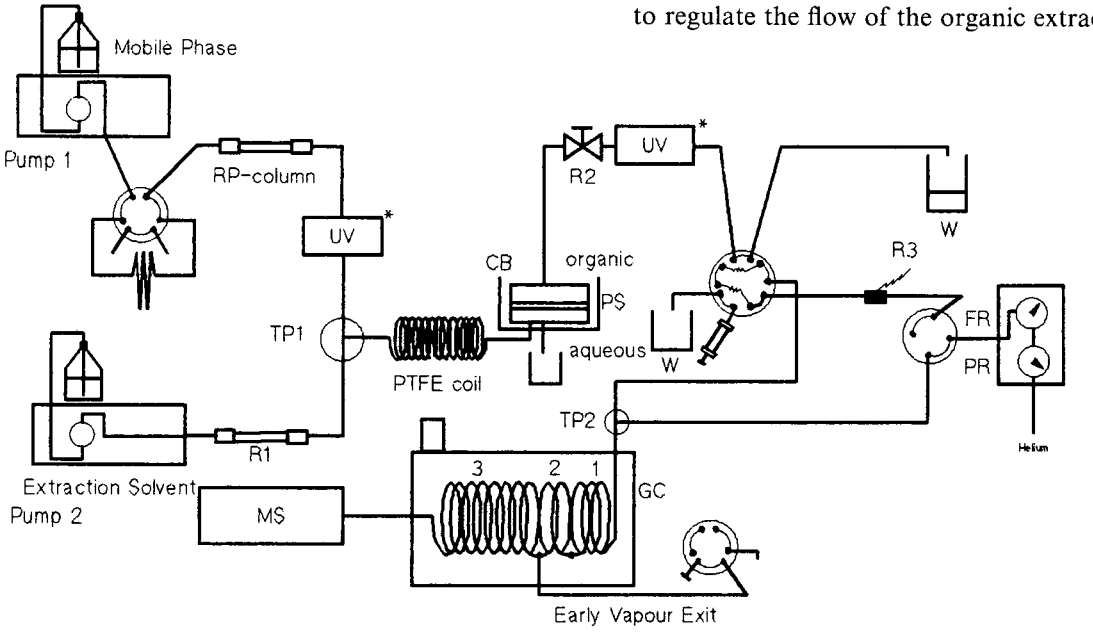

Fig. 1. Instrumental set-up for on-line coupled LC–GC–MS. 1 = Retention gap; 2 = retaining precolumn; 3 = analytical capillary; R1 = LC column (restriction); FR = flow regulator; R2 = needle valve restrictor; R3 = capillary (0.075 mm I.D.); PS = phase separator (sandwich type); CB = cooling bath; PR = pressure regulator; W = waste; TP1 = T-piece 1; TP2 = T-piece 2; UV = UV detector. * = The position of the UV detector is either before or after the liquid–liquid extraction unit. During the transfer of the LC extract to the GC column the UV detector is installed behind the extraction unit.

The LC–GC interface consisted of a Valco ten-port valve, equipped with a 500-μl sample loop. The other two valves were Rheodyne (Berkeley, CA, USA) six-port valves. As described by Grob and Stoll [3], serially connected pressure and flow regulators [Porter (Hatfield, PA, USA) 8286 and Porter DFC 1400, respectively] regulated the carrier gas. T-piece 2 in Fig. 1 was a glass press-fit connector.

A Hewlett-Packard (Palo Alto, CA, USA) Model 5890 gas chromatograph equipped with a Hewlett-Packard Model 5971A mass-selective detector was used. The GC–MS interface was an open-split connection (ratio *ca.* 1:11) with a 50 cm × 0.11 mm I.D. fused-silica capillary.

Chromatographic conditions

LC separations were performed on a 125 mm × 4.0 mm I.D. LiChroCART RP-18 (5 μm) column (Merck, Darmstadt, Germany) using methanol–tetrahydrofuran–water (50:5:45, v/v/v) as eluent at a flow-rate of 2.0 ml/min. UV detection was performed at 230 nm.

After on-line liquid–liquid extraction with *n*-pentane (for conditions, see below), 500 μl of the extract, cut by the loop, were transferred to the GC–MS system. Hence always the total LC peak was transferred.

The oven temperature of the gas chromatograph during transfer was 75°C, leading to an observed maximum pressure of 1.8 bar. The early vapour exit (see Fig. 1) was kept open for 7.95 min after start of the transfer and was closed subsequently.

Gas chromatographic separation was carried out on a 15 m × 0.32 mm I.D. DB-17 fused-silica capillary, 0.5 μm film thickness (J&W Scientific, Folsom, CA, USA), the head of which was connected to a retaining precolumn (3 m × 0.32 mm I.D. DB-17 fused-silica capillary 0.5 μm film thickness) via a Y-shaped press-fit connector, the third leg of which was connected to the temporarily opened early vapour exit (see above). A 3 m × 0.32 mm I.D. fused-silica retention gap, deactivated by phenyldimethylsilylation (J&W Scientific), was connected to the retaining precolumn and left the GC oven through a small hole. It was connected to the LC–GC interface via T-piece 2. The oven temperature was initially kept at 75°C for 10 min, then increased to 260°C at 15°C/min. After termination of the transfer, the pressure of the carrier gas was 1.1 bar.

MS conditions

The ionization mode was electron impact (EI) (70 eV). The filament was switched off for 10 min after start of the transfer.

On-line coupled liquid–liquid extraction

The experimental parameters for on-line coupled liquid–liquid extraction which have an influence on the yield of organic phase were studied. The LC flow-rate was set to 2.0 ml/min. The maximum flow-rate of the organic extract that was achievable without causing turbidity due to non-separated water was measured as functions of the composition of the LC eluent, of the kind of extraction solvent used and of the temperature of the phase separator. The extraction solvents tested were *n*-pentane, *n*-hexane and dichloromethane.

Solvents

Methanol, acetonitrile (both of LiChrosolv grade), dichloromethane, *n*-pentane, *n*-hexane and tetrahydrofuran (all of analytical-reagent grade) were obtained from Merck. The water used was obtained with a Milli-Q water purification system (Millipore).

RESULTS AND DISCUSSION

Liquid–liquid extraction studies

Two common reversed-phase mobile phase systems (methanol–water and acetonitrile–water) were investigated with respect to their suitability for on-line liquid–liquid extraction. The extraction solvents tested were *n*-pentane, *n*-hexane and dichloromethane. Attempts were made to establish what the limits of the concentration of organic solvent in the LC eluent were. In addition, the effect of temperature on the phase separation was studied, aiming at high extraction efficiences even for mobile phases with a high percentage of organic component. It had been expected that lowering the temperature of the phase separator could have a beneficial effect on phase separation, mainly for two reasons: (1) the stability of emulsions is known to be bad at low temperatures and (2) the miscibility of aqueous solutions with alkanes or dichloromethane decreases

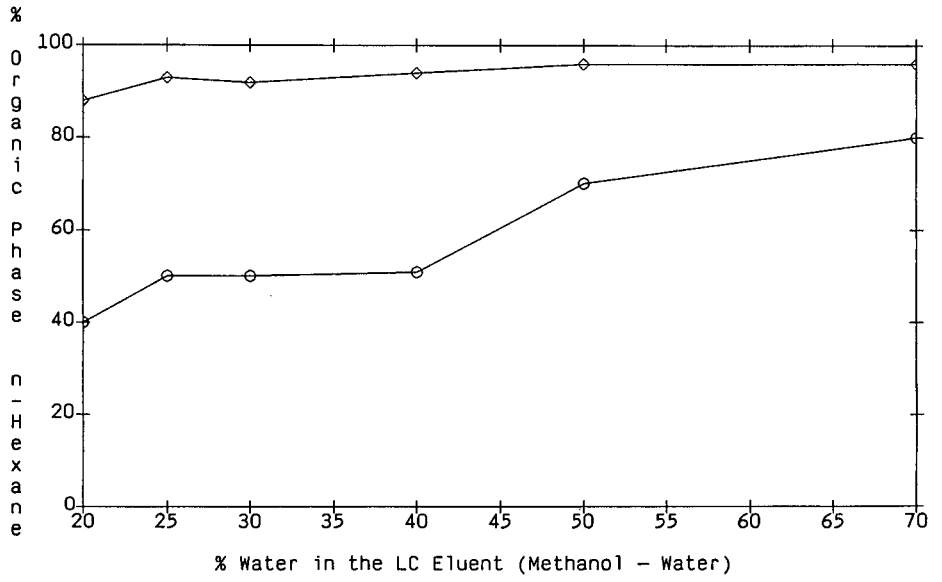

Fig. 2. Extraction solvent *n*-hexane: yield of organic phase *vs.* ratio of water + methanol in the LC eluent. ◇ = −15°C; ○ = room temperature.

on lowering the temperature. It was felt that the extraction process itself should not be affected by our manipulations as the analyte transfer from the aqueous to the organic phase is assumed to take place in T-piece 1 and the subsequent section of the PTFE capillary (see Fig. 1), both being exposed to room temperature. Only the sandwich-type phase separator is immersed in the cooling bath.

This work was focused on the influence of temperature on the yield of organic phase as a function of the water content in the LC eluent. The extraction yield itself (yield of analyte) will be investigated in a separate study.

As expected, the results of this preliminary study show that the yields of organic phase are generally higher with a higher percentage of water in the LC eluent. The positive influence of low temperature during phase separation on the yield of organic phase was demonstrable in all instances, with the exception of aqueous acetonitrile eluents containing high percentages of acetonitrile (*ca.* 70%), which were extracted with *n*-pentane.

In detail, the following results were obtained:

LC eluent methanol–water

Extraction solvent n-hexane (Figs. 2 and 3). Using *n*-hexane as an extraction solvent, methanol–water eluents can be extracted well, even with proportions of methanol in the region of 80%, on cooling the phase separator to −15°C (Fig. 2). The yields of organic phase are in the range 88–96%.

Extraction solvent dichloromethane (Fig. 5). Using dichloromethane as an extraction solvent is very problematic with methanol–water eluents. Even a concentration of 50% methanol results in a yield of organic phase of only 15%.

The recommended temperature of the phase separator is −20°C.

LC eluent acetonitrile–water

Extraction solvent n-pentane (Fig. 4). Using *n*-pentane as an extraction solvent, the yield of organic phase depends strongly on the percentage of acetonitrile in the LC eluent: the higher the percentage of acetonitrile, the lower is the yield. The influence of the temperature on the yield of organic phase is less pronounced for acetonitrile–water than for methanol–water eluents. Cooling the phase separator below 0°C does not have any beneficial effect on the extraction yield. Whereas the extraction of LC eluents containing *ca.* 30% of acetonitrile always gives a constant yield below 0°C, just the opposite

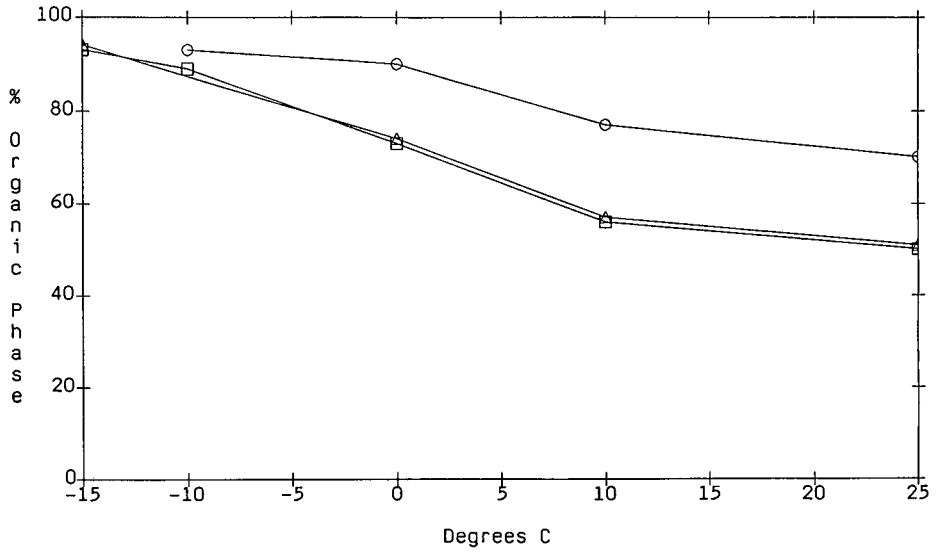

Fig. 3. Extraction solvent *n*-hexane: dependence of the yield of organic phase on the temperature of the phase separator. Methanol–water: ○ = 50:50; △ = 60:40; □ = 75:25.

occurs with LC eluents containing a high proportion of acetonitrile (70%): the yield of organic phase decreases drastically when the temperature is lowered to −20°C.

Extraction solvent dichloromethane (Fig. 5). With respect to the suitability of dichloromethane as an extraction solvent, the situation looks much better for acetonitrile–water than for methanol–water eluents. The extraction of an eluent containing 70% of acetonitrile still results in a yield of organic phase of 60%.

A prerequisite for satisfactory phase separation is

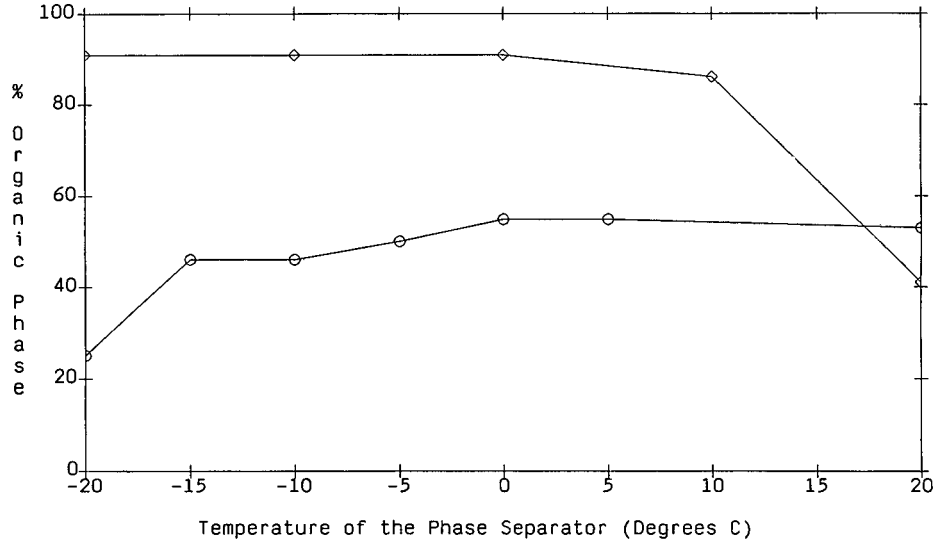

Fig. 4. Extraction solvent *n*-pentane: dependence of the yield of organic phase on the temperature of the phase separator. Acetonitrile concentration: ◇ = 30%; ○ = 70%.

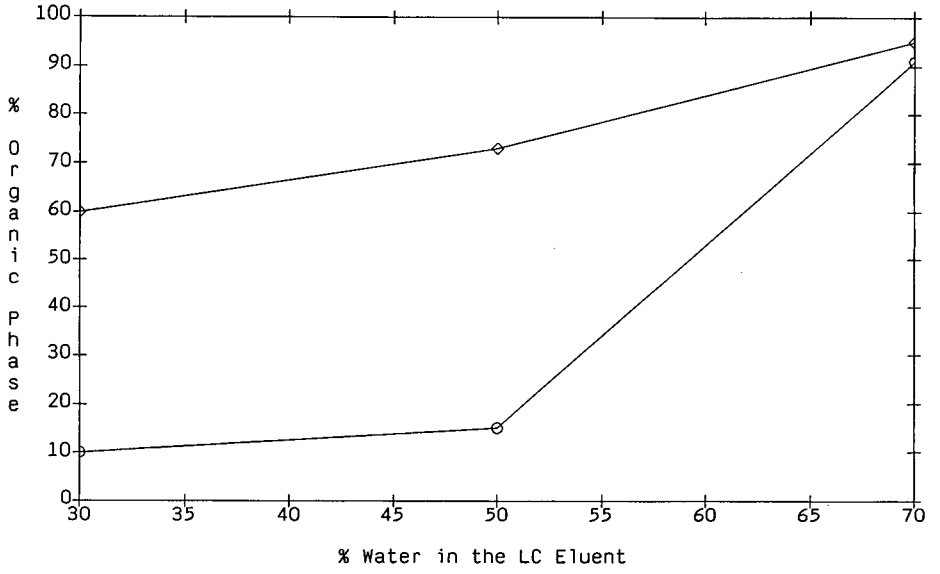

Fig. 5. Extraction solvent dichloromethane: yield of organic phase *vs.* percentage of water in the LC-eluent. ◇ = Acetonitrile–water; ○ = methanol–water.

cooling of the phase separator to −20°C. This applies with all ratios of water and acetonitrile, in contrast to the anomalous behaviour of *n*-pentane extractions (see above).

Transfer of aqueous LC fractions of a particular drug product

The value of LC–GC–MS in the pharmaceutical industry is illustrated by the following example. Particular stress samples of a liquid formulation of a particular drug substance (concentrate for infusion) showed an unusual degradation product giving peak 2 in reversed-phase HPLC (Figs. 6–8). For reasons which are not yet clear, the application of HPLC–MS did not give a mass spectrum that was of any use for the identification of the component of interest. In contrast, the application of LC–GC-MS resulted in a high-quality EI mass spectrum of this unknown degradation product of the active ingredient (Fig. 8), which led to the proposal of a structure for this substance. In the same way, peak 1 (a known degradation product) and peak 3 (active ingredient) were cut and transferred on-line to the GC–MS system (Figs. 6 and 7). The corresponding mass spectra were of similar quality and were in accordance with the known structures of the substances.

The eluent of the reversed-phase system, which had been elaborated for the analysis of the drug product, was methanol–tetrahydrofuran–water (50:5:45, v/v/v). This eluent was also amenable to liquid–liquid extraction. The extration solvent used was *n*-pentane and the phase separator was cooled to *ca.* −20°C. At higher temperatures, the yield of organic phase decreased dramatically.

The volumes of the LC fractions transferred were 500 μl. In accordance with the work of Grob and co-workers, current eluent evaporation [3,4] again proved to be a powerful technique that focuses solutes to narrow bands, even when extremely large sample volumes are transferred to a capillary GC column. As a result, sharp GC peaks were obtained (Figs. 6–8). When such large liquid sample volumes are applied to a GC column, one has to cope with the vast amount of vapour created during the sample transfer. The following measures were taken in order not to affect the functioning of the mass spectrometer: (a) the major part of the solvent vapour was split off by the temporarily opened "early vapour exit", and (b) the filament of the MS ion source was temporarily switched off (for 10 min); it

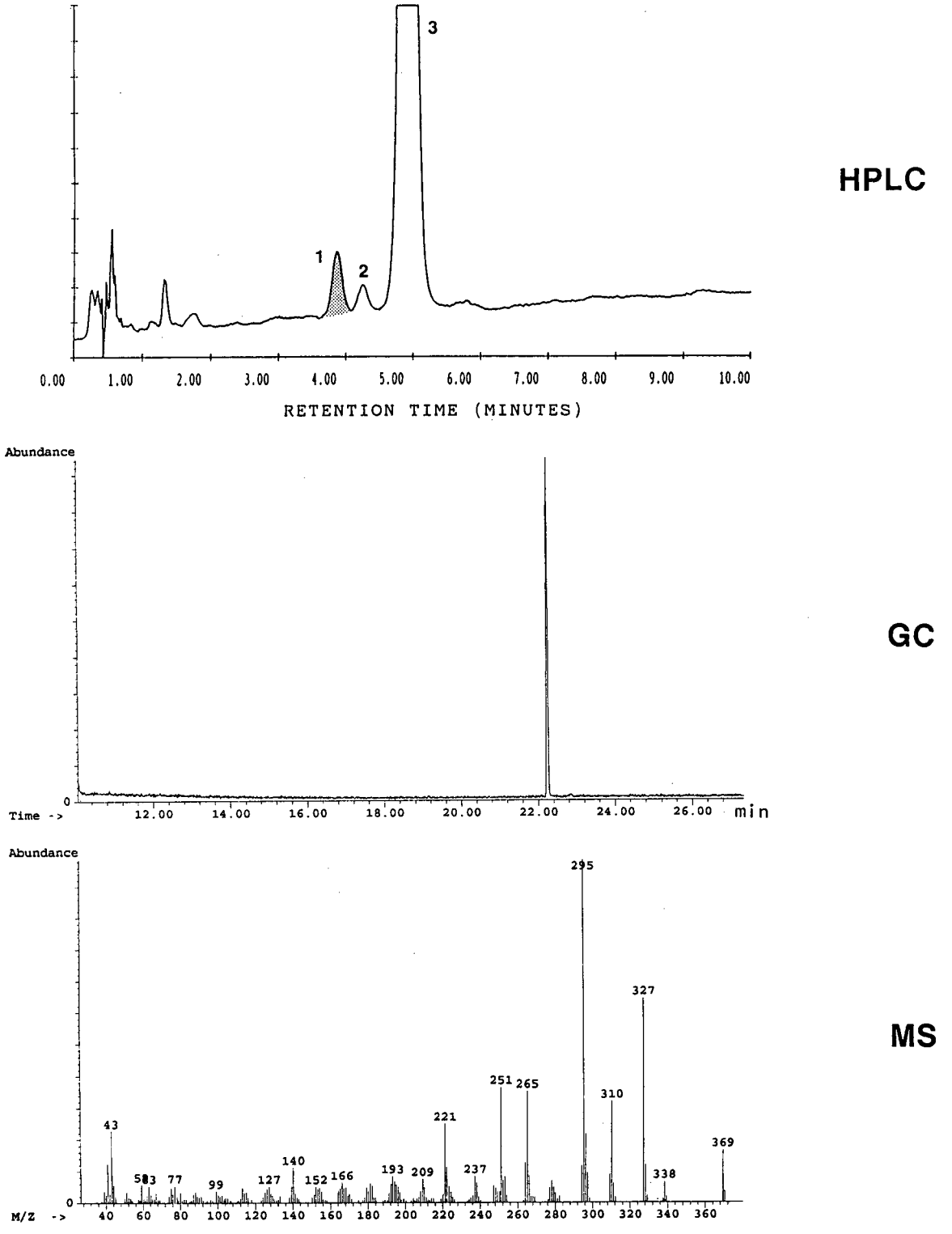

Fig. 6. LC–GC–MS: transfer of an LC fraction (1) of a stressed sample of a drug product. Peaks: 1 and 2 = degradation products; 3 = active ingredient.

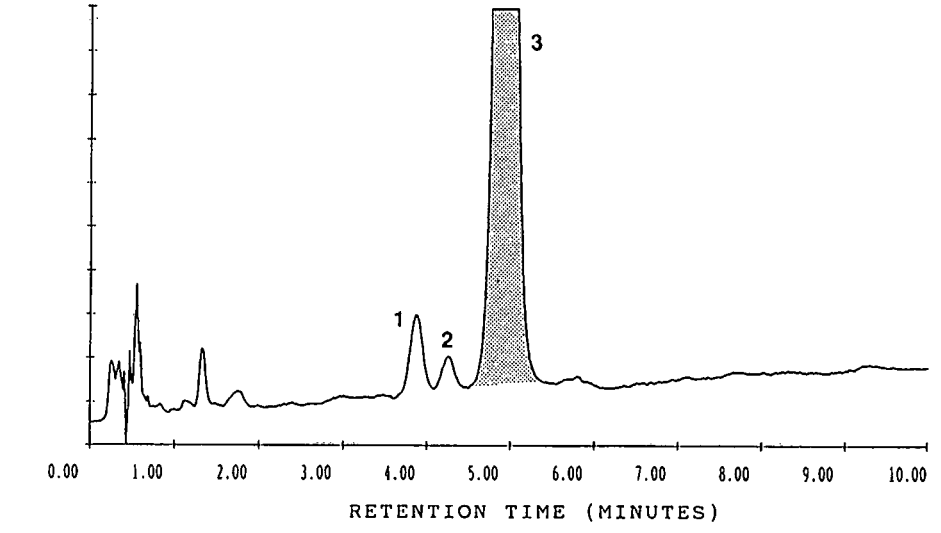

HPLC

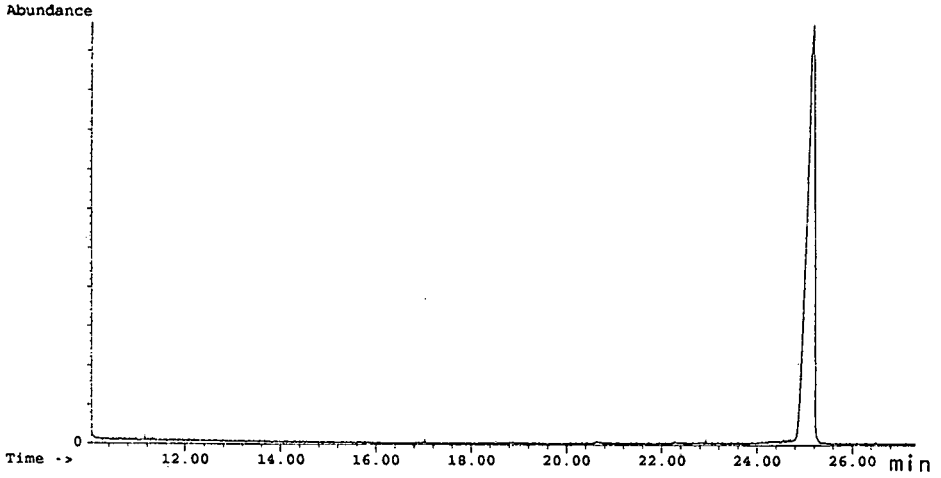

GC

MS

Fig. 7. LC–GC–MS: transfer of an LC fraction (3) of a stressed sample of a drug product. Peaks: 1 and 2 = degradation products; 3 = active ingredient.

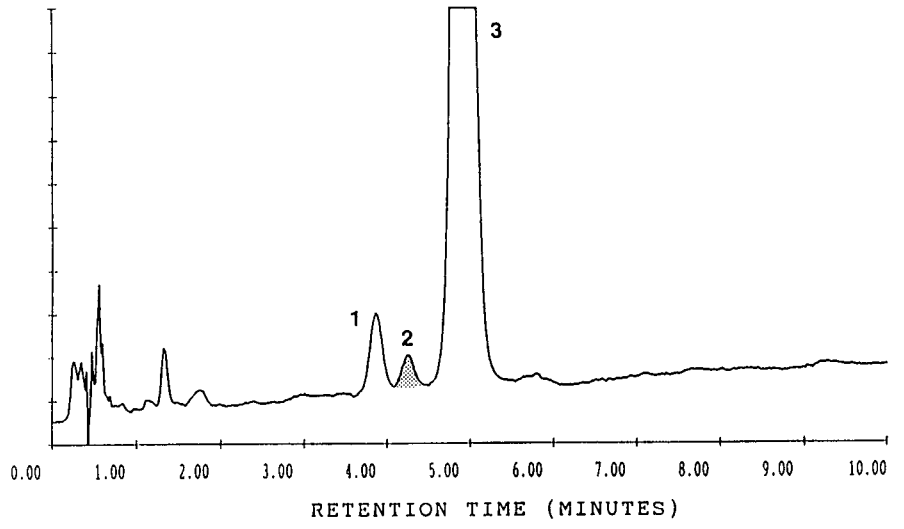

HPLC

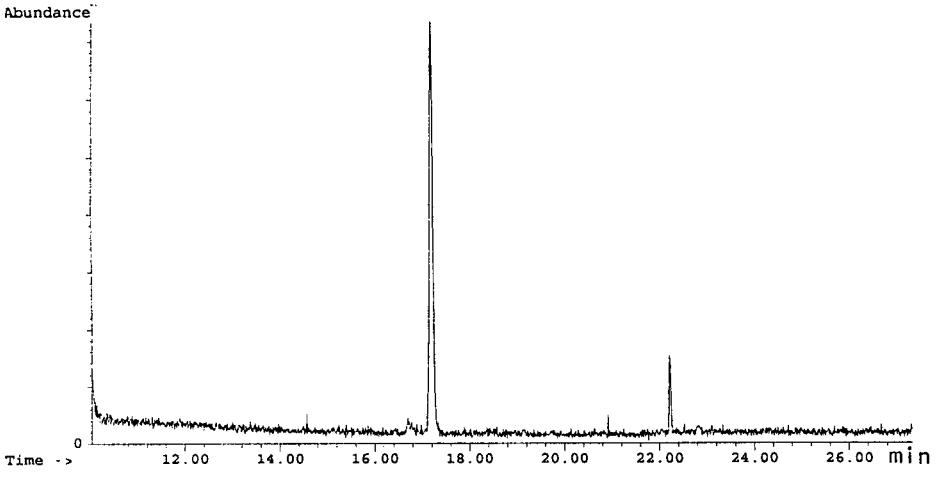

GC

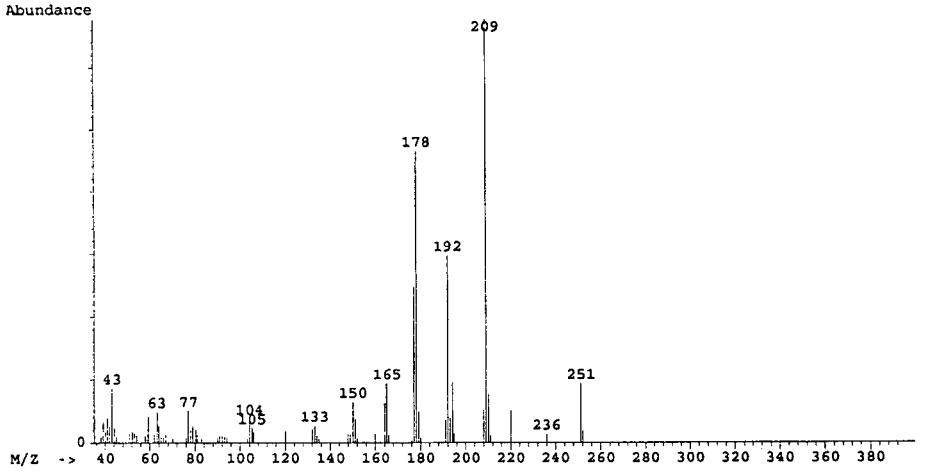

MS

Fig. 8. LC–GC–MS: transfer of an LC fraction (2) of a stressed sample of a drug product. Peaks: 1 and 2 = degradation products; 3 = active ingredient.

took *ca.* 8 min after the start of the transfer of the LC fraction until the temporarily collapsed vacuum in the ion source was re-established.

CONCLUSIONS

From the results obtained by the application of the technique described, the following can be concluded.

Degradation products that occurred in stressed samples of a particular drug product (concentrate for infusion) during development can easily be identified by LC–GC–MS. No problematic isolation steps are necessary, as LC, cutting of the LC fraction of interest, liquid–liquid extraction and transfer to a GC–MS system take place on-line.

Even poorly resolved LC peaks can be selectively transferred to the GC–MS system. The result is one GC peak and one mass spectrum per component. This fact can also be utilized for proving peak purity (see Fig. 6).

As the LC peaks of interest are completely transferred the sensitivity of the method is good.

In contrast to all known LC–MS techniques, LC–GC–MS yields true EI mass spectra of components in reversed-phase LC. The appearance of a spectrum obtained from a large LC fraction does not differ from that obtained from a small sample volume as usually used in GC–MS (0.5 μl). This allows library searching, which could be an aid in the identification of unknown compounds.

Transfer volumes of 500 μl of aqueous LC eluents do not create any problem with the technique described. Hence conventional-sized HPLC (flow-rate of *ca.* 2 ml/min) can be coupled to capillary GC–MS.

REFERENCES

1 K. Grob, *On-Line Coupled LC–GC*, Hüthig, Heidelberg, 1991, p. 37.
2 P. van Zoonen, G. R. van der Hoff and E. A. Hogendoorn, in P. Sandra and G. Redant (Editors), *11th International Symposium on Capillary Chromatography*, Hüthig, Heidelberg, 1990, p. 187.
3 K. Grob, Jr., and J. M. Stoll, *J. High Resolut. Chromatogr. Chromatogr. Commun.*, 9 (1986) 518.
4 K. Grob and Th. Läubli, *J. High Resolut. Chromatogr. Chromatogr. Commun.*, 10 (1987) 435.

Journal of Chromatography, 626 (1992) 97–107
Elsevier Science Publishers B.V., Amsterdam

CHROM. 24 521

Pharmaceutical applications of high-performance liquid chromatography interfaced with Fourier transform infrared spectroscopy

James E. DiNunzio

Bristol-Myers Squibb, Pharmaceutical Research Institute, 100 Forest Avenue, Buffalo, NY 14213 (USA)

ABSTRACT

Application of the solid-phase extraction interface for high-performance liquid chromatography coupled with Fourier transform infrared spectroscopy to problems of pharmaceutical interest is described. A diagram of the interface and description of its use is given. Application of the system to the identification of isomers and degradation products in active ingredients, and contaminants in product excipients are described. The advantages of the use of the solid-phase extractor interface, and its use in on-column and on-extractor preconcentration to increase sensitivity are described.

INTRODUCTION

Infrared (IR) spectroscopy is a powerful technique for the identification of organic compounds. The ability to obtain structural information on compounds, along with its simplicity make it the technique for choice for many qualitative determinations. Furthermore, Fourier transform infrared (FT-IR) spectroscopy is sensitive enough to allow the technique to be used for trace analysis.

The qualitative attributes of FT-IR compliment those of chromatography, which is essentially a quantitative method, and substantial effort has been devoted to interfacing these techniques. While success has been achieved in coupling gas chromatography with FT-IR, less success has been achieved with high-performance liquid chromatography (HPLC). The major problem with HPLC–FT-IR is the interference caused by the liquid mobile phase. This is particularly true for reversed-phase chromatography, which accounts for the large majority of HPLC separations, because water and commonly used polar organic solvents present in the mobile phase strongly absorb in the IR spectral region.

The interface is the critical component in the HPLC–FT-IR system, and the success or failure of the technique is determined almost exclusively by its performance. HPLC–FT-IR interfaces can be classified into two general categories; continuous and analyte capture type. Continuous techniques employ some type of flow cell in order to introduce the analyte into the spectrometer. Three types have been employed: the conventional flow cell using a polymer or lead spacer to set the cell path length [1], the cylindrical cell [2], and the attenuated total reflectance (ATR) flow cell [3]. For direct measurement of reversed-phase HPLC eluents the attenuated total reflectance cell has been used with some success [3–5].

Continuous methods using aqueous mobile phase elimination have been utilized for HPLC–FT-IR. Taylor and co-workers [6–8] have developed a liquid–liquid extraction interface for use with reversed-phase HPLC. In this approach the analytes were extracted from the mobile phase by mixing

Correspondence to: Dr. J. E. DiNunzio, Bristol Myers Squibb Co., Pharmaceutical Research Institute, 100 Forest Avenue, Buffalo, NY 14213, USA.

post-column with a stream of IR transparent, water immiscible solvent. The immiscible solvent, typically CCl_4, C^2HCl_3 or $CHCl_3$, was separated from the segmented eluent stream by a membrane separator, and passed through a flow cell for detection.

Although continuous HPLC–FT-IR systems are advantageous in that they can provide real time chromatographic information, the real usefulness of the HPLC–FT-IR lies in its ability to provide spectral information on analytes. To this end techniques employing analyte capture have been very successful. In general, two basic analyte capture approaches have been employed. In the deposition technique the eluent is deposited on a continuously moving, IR transparent, inert substrate from which the eluent can be easily removed by evaporation. The substrate containing the individually captured analytes is transferred to the spectrometer for spectral analysis. In the solid-phase extraction technique the analytes are collected on a solid adsorbent from which the mobile phase can be eliminated by evaporation. The analytes are eluted from the adsorbent material with an IR transparent solvent and transferred to the spectrometer for spectral analysis. Of these two techniques the deposition method has been the most popular, and some significant advances have been made recently.

The deposition techniques are based on the work of Kuehl and Griffiths [9] and Jinno and co-workers [10–14]. In these original works systems for normal-phase HPLC were described.

Kalasinsky and co-workers [15,16] used a post-column system which converted water to acetone and methanol by reaction with 2,2-dimethyloxypropane. The analytes were then collected by deposition of a nebulized, reacted stream of eluent onto a KCl substrate. This system was used with both microcolumns and packed columns, with detection limits around 1 μg when diffused reflectance analysis was employed.

Analyte capture by deposition on a reflective surface is a technique which shows great potential for development into a sensitive analytical method [17–21]. These techniques which typically employ evaporation of the mobile phase using a heated evacuated chamber, allow spectra to be obtained at very low levels. Identification quality spectra at the 0.5 ng level have been reported [21].

An alternate to the deposition methods for analyte capture based on post-column solid-phase extraction has been described [22,23]. In this technique the analyte of interest was extracted on a small column after post-column dilution of the mobile phase with water. The extractor column was dried with nitrogen and the analyte eluted into a conventional flow cell with an IR transparent solvent. Because of the concentration effect of the post-column extraction, sub-microgram quantities of analyte could be detected, with microgram quantities used to obtain identifiable spectra.

The purpose of this paper is to describe the application of the solid-phase extractor HPLC–FT-IR interface for pharmaceutical applications. Application of the system to the identification of isomers and degradation products in active ingredients, and contaminants in product excipients are described. The advantages of the use of the solid-phase extractor interface, and its use in on-column and on-extractor preconcentration to increase sensitivity are described.

EXPERIMENTAL

The chromatographic system used was a Waters (Milford, MA, USA) Model 204 HPLC with two Model M6000 pumps, a Model 680 gradient controller, a Model 440 absorbance detector, and a Model 712 WISP autoinjector. Chromatographic data collection was performed on a Hewlett-Packard (Valley Forge, PA, USA) HP-3350A LAS computer.

The IR spectrometer used was a Nicolet Instruments (Madison, WI, USA) Model 20DXC with a deuterated triglycine sulfate (DTGS) detector. Spectral acquisition was performed on a Model 620 workstation. Data processing was accomplished using Nicolet DXFTIR software. No beam condenser or spectral enhancement devices were used in this work.

The HPLC–FT-IR interface consisted of a Waters M6000 pump for pumping the IR transparent solvent through the extractor, an LKB 2150 HPLC pump (Paramus, NJ, USA) for pumping the mobile phase diluent (water for reversed-phase separations), a Valco Instruments (Houston, TX, USA) 6-port, 2-position valve, a Valco Instruments 12-port manifold valve, a Valco Instruments 10-port, 2-position valve, and a Valco Instruments serial

valve interface. A Specac micro flow cell (Aries, Concord, MA, USA) with lead spacers and CaF_2 windows was used to introduce the sample into the spectrometer. Extractor columns, 20 × 2 mm I.D. (Upchurch Scientific, Oak Harbor, WA, USA), were packed with C_{18} packing (PrepSep C18, Fisher Scientific, Pittsburgh, PA, USA).

All solvents used were HPLC grade and filtered through type HVLP membrane filters (0.45 μm) (Millipore, Bedford, MA, USA) prior to use.

RESULTS AND DISCUSSION

Although many different interface configurations have been developed for HPLC–FT-IR, no one system has been shown to be generally applicable for reversed-phase chromatography. This is demonstrated by the fact that while there has been a significant amount of work done in this area, there are few publications on applications of the technique to actual analytical problems. No one design can be recommended for general use. The selection of a particular interface configuration will depend on the particular application.

Table I lists those parameters which should be considered in selecting an HPLC–FT-IR interface. Of the practical considerations, the amount of automation required of the system to handle the analytes and the expertise of the analyst are most important in deciding on the type of interface required for a particular application. As shown above some of the interface designs are complicated to use. Therefore, these designs require a high skill level for an analyst. Also, the complicated nature of these interfaces makes them more expensive and time consuming for analysis.

From a chemical perspective, it is the analyte stability and sensitivity requirements which determine the choice of interface design. In cases where unstable analytes are being determined, the selection of the interface design can be critical. Most of the deposition interfaces use elevated temperature to aid in mobile phase evaporation. Also transfer of the substrate from the deposition apparatus to the spectrometer can expose the analyte of oxygen, light, and moisture under uncontrolled conditions. These may not be acceptable in some situations. This is the case in our laboratory where we routinely work with labile compounds.

TABLE I

PARAMETERS FOR INTERFACE SELECTION

Practical	Time
	Cost
	Analyst expertise
	Manual *vs.* automated
	Instrumentation availability
Chemical	Analyte stability
	Sensitivity required

Sensitivity requirements of the assay also determine the interface design selection. One of the major design objectives of HPLC–FT-IR instrumentation has been to lower the detection limit as far as possible. While high sensitivity may be required for some applications, it has placed severe limitations on the use of the technique. There are many situations where the analyst is not concerned with detecting a low absolute amount of analyte, such as ng of pg quantities, but with detecting a low relative amount, such as % or μg/g levels. This is true in the pharmaceutical industry, where it is required to identify impurities and degradation products in drug substances and finished products. These analytes are present in the sample at levels as low as 0.05% (w/w). At these levels the analyte may be below the limit of identification of all but the most sensitive HPLC–FT-IR interface. However, design of the separation may make it possible to have μg or even mg quantities of analyte introduced into the spectrometer after separation. This gives the analyst a choice of utilizing one of the simpler, but less sensitive interfaces. This has been the case in our laboratory.

Based on the above considerations the post-column solid-phase extraction interface was developed and used in our laboratory to investigate a variety of problems. This system was chosen for the following reasons. First, the system is automated so that it can be simply operated by selection of menu items from an in-house written program. Second, it allows the analyte to be automatically transferred from the chromatograph to the spectrometer. This minimizes analyte exposure to oxygen, light or heat. Third, the system is capable of the required sensitivity to obtain spectra of impurities and degradation products. Fourth, the system does not require dedicated instrumentation.

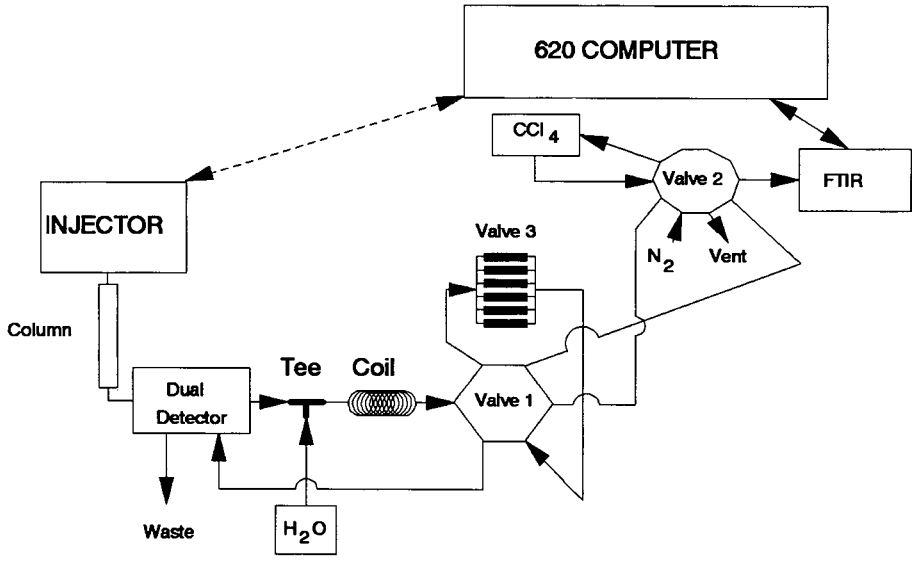

Fig. 1. Diagram of the automated solid-phase extraction interface for HPLC–FT-IR.

Fig. 1 shows a schematic diagram of the HPLC–FT-IR system used in our laboratory. It is designed so that the chromatograph and spectrometer can be operated independently. This has the advantage of allowing chromatographic analyses or other operations (*i.e.*, solvent change over, separation development) to be performed on the chromatographic side while spectral data acquisition and manipulation is being performed on the spectrometer. The system could be controlled entirely from the spectrometer side, if desired.

The extractor interface consists of three valves and a solenoid switch, each of which can be controlled independently by either the chromatograph or the spectrometer. Two pumps are incorporated into the interface. Water is introduced with one

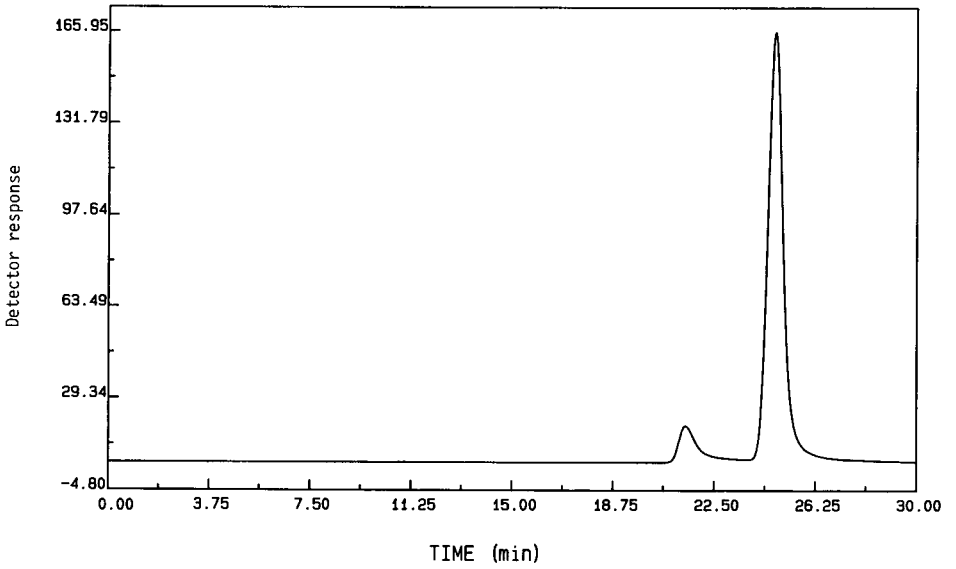

Fig. 2. Chromatogram of homosalate. Mobile phase: acetonitrile–water (70:30, v/v). *y*-Axis in arbitrary units.

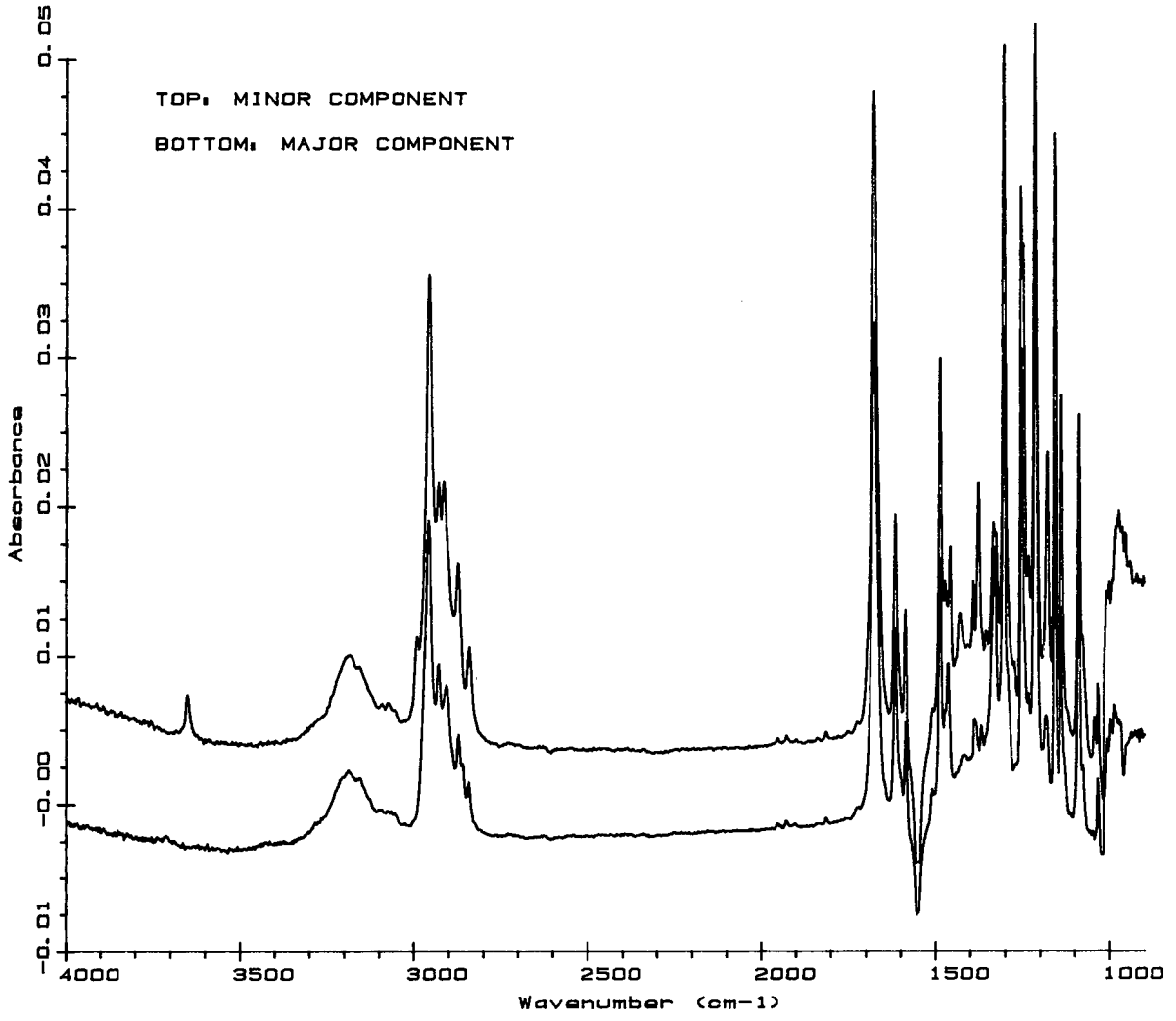

Fig. 3. Overlay spectra of homosalate components.

pump into a mixing tee connected to the outlet of the column. This is used to dilute the reversed-phase eluent to allow extraction of the analyte on the reversed-phase packing of the extractor. A short mixing coil of about 10 cm of 0.8 mm I.D. stainless steel tubing is used to increase mixing of the mobile phase with the water diluent. The second pump is used to continuously pump the IR transparent solvent used to elute the extracted analytes from the extractor. In order to conserve solvent it is normally recycled back to the solvent reservoir.

For normal operation the system is used as follows. Several initial chromatograms are obtained in order to optimize the separation and determined the retention times of the analytes of interest. The extractor manifold is then conditioned by passing solvent through each extractor for some pre-determined time. This is typically done for 3 min at a flow-rate of 1 ml/min of eluent plus 2 ml/min of water from the diluent pump. The conditioning cycle is controlled by the spectrometer. Analyte extraction is performed by injection of the sample on the column and switching to the extractor manifold prior to the pre-determined retention time of the

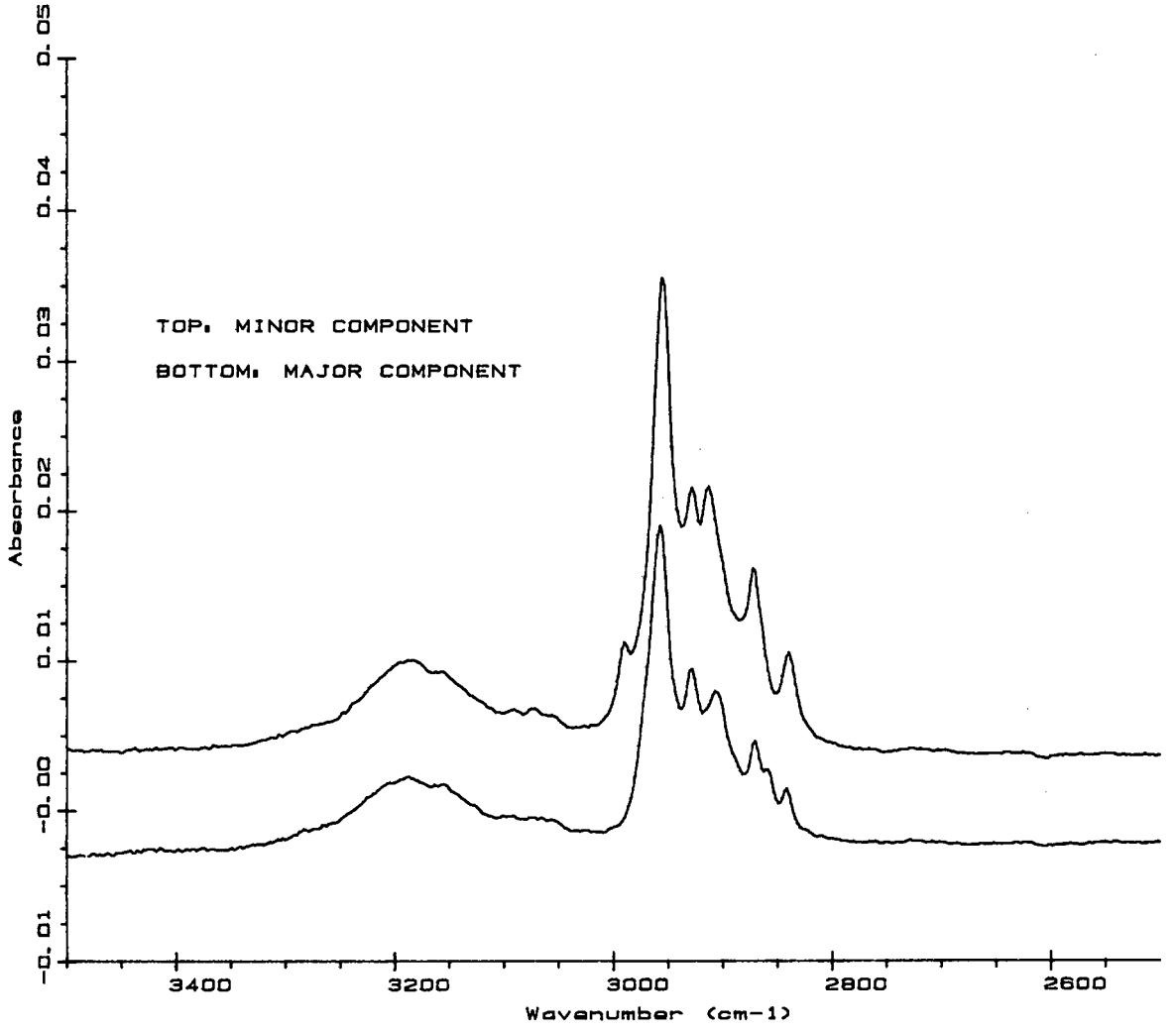

Fig. 4. C–H stretching region of spectra of homosalate components.

peaks of interest. This operation is controlled by the chromatograph. Although an absorbance detector is used on the chromatograph, is is not used to trigger valve switching. It is used initially to determine the retention times of the analytes of interest. It is also used during the extraction operation to determine the extraction efficiency by monitoring the flowing stream into and out of the manifold.

After extraction of the analytes control of the interface is done by the spectrometer. First, the manifold is dried by passing nitrogen at $6.1 \cdot 10^5$ Pa through each extractor. A short pressure equilibration cycle is built into the program in order to release trapped nitrogen from the manifold. At this point the analytes are ready for spectral analysis. This is accomplished by individually back-flushing each extractor with an IR transparent solvent in order to elute the analyte and introduce it into the flow cell. At this point spectra are obtained and saved for later analysis. Typically, thirty coadded scans at 4 cm^{-1} resolution are obtained for each sample.

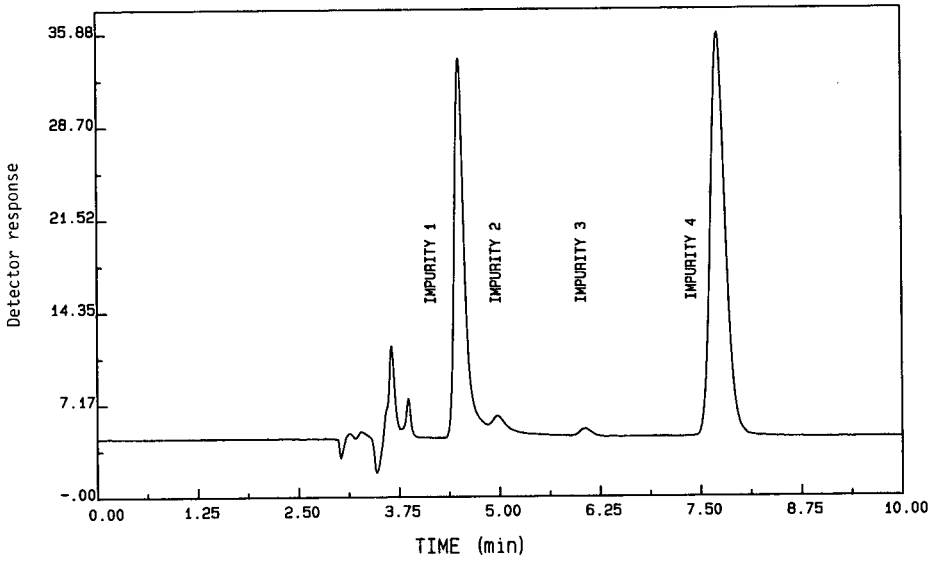

Fig. 5. Chromatogram of impurities in propylene glycol. Chromatographic conditions: acetonitrile–water (25:75, v/v), at time = 0 go to acetonitrile–water (90:10, v/v) in 5 min, hold 12 min. *y*-Axis in arbitrary units.

Applications

3,3,5-Trimethylcyclohexyl 2-hydroxybenzoate (Homosalate) is an ester of salicylic acid. This compound is important in the dermatological and cosmetic product areas because it is the reference compound required for the United States FDA Sunscreen Monograph [24] method for the determination of Sunscreen Protection Factors (SPF) for topically applied sunscreen products. Fig. 2 shows a chromatogram of this material. Upon reversed-phase separation of homosalate two peaks are observed. Although these peaks have similar UV spectra, the absorbance ratios differ slightly. Also, lot to lot and sample to sample variations in the ratio of the two components have been observed. The amount of the lesser component can vary by as much as 100%.

The solid-phase extractor interface was used to obtain IR spectra of the two components in order to identify them. Fig. 3 shows an overlay of the spectra obtained for the two components. These closely matching spectra indicate that both are isomers of homosalate. This was later confirmed by molecular mass determination of each component by LC–mass spectrometry (MS).

Fig. 4 shows an expanded view of these overlaid spectra in the C–H stretching region where the main differences between the two are observed. Inspection of the spectra in this region shows that there are three sets of doublets. For both components two of these doublets are observed at nearly the same frequencies and correlate well with known C–H stretching modes [25]. The methylene C–H stretch is observed at 2928 and 2840 cm^{-1}. The methyl C–H stretch is observed at 2957 and 2872^{-1}.

A third set of C–H stretching bands is observed in the two spectra, but they do not appear at the same frequency in the two spectra. In the major component's spectrum these are observed at 2906 and 2859 cm^{-1}. In the minor component's spectrum these bands are shifted to 2990 and 2913 cm^{-1}.

Homosalate is a substituted cyclohexane with two methyl groups in the 3 position and one in the 5 position of the ring. These methyl groups and the methylenes of the cyclohexane ring are the only aliphatic C–H groups on the molecule. Therefore, the methylene C–H stretching must arise from the cyclohexane CH_2. The other two doublets must arise from the methyl substituents on the ring.

The differences in these spectra suggest that these components are conformational isomers of cyclo-

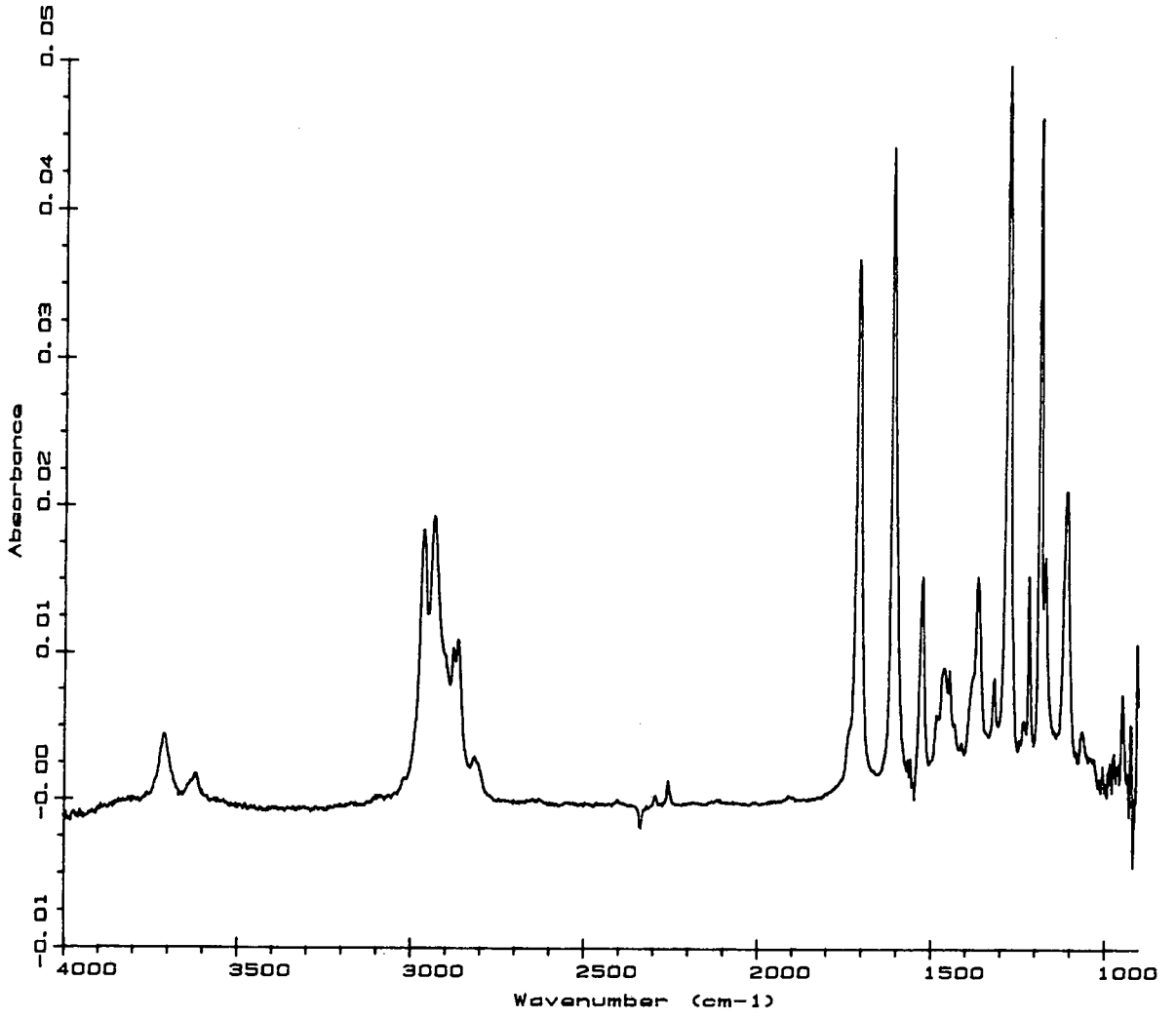

Fig. 6. Spectrum of impurity 4 in propylene glycol.

hexane. The spectra clearly indicate that these components differ in the cyclohexane portion of the molecule. The shift of the methyl C–H stretch could be the result of steric effects between an axial methyl group and the bulky salicylate group occupying the axial position on the cyclohexane ring in one component compared to its presence in the equatorial position in the other component. However, exact assignment of the structure to the components cannot be made with the data available.

Another application in which HPLC–FT-IR is useful is for the identification of impurities in product excipients. Fig. 5 shows a chromatogram of impurities in a sample of propylene glycol. At least four impurities are seen in the chromatogram. These are not observed in chromatograms of clean propylene glycol. Based on the chromatographic response of the impurities it was concluded that the propylene glycol was contaminated at a very low level. No detectable spectra could be obtained for single injections of up to 100 μl of 1:1 dilution of propylene glycol in water. Therefore a preconcentration technique was employed to obtain the IR spectra of impurities.

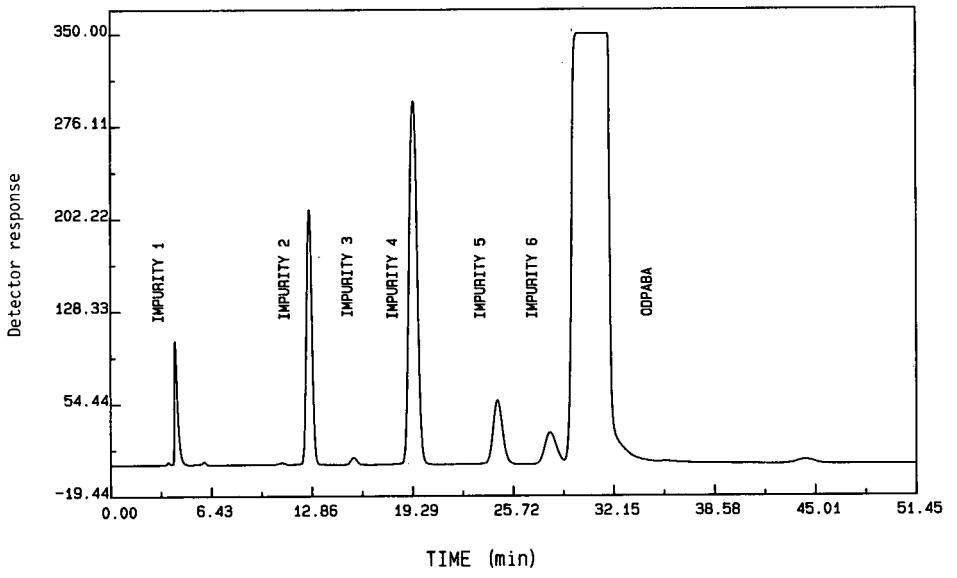

Fig. 7. Chromatogram of impurities in octyl dimethyl *p*-aminobenzoate. Mobile phase: tetrahydrofuran–water (55:45, v/v). *y*-Axis in arbitrary units.

The following procedure was used for this analysis. The procedure employed on-column concentration of the impurities by making nine 200-μl injections of 1:1 propylene glycol in water. The impurities were eluted by gradient elution, and three of the four impurities captured on the extractor. This process was repeated four times, so that a total of 36 injections were collected on the extractor interface. The extractor was dried under nitrogen for 7 min, and the impurities eluted into the spectrometer using CCl_4.

Fig. 6 shows the spectra obtained for impurity 4. Clearly a spectrum which is suitable for identification is obtained using the preconcentration technique outlined above. Based on this spectrum impurity 4 was determined to be octyl dimethyl *p*-aminobenzoate (ODPABA). This was confirmed by matching retention times of the impurity with that of a sample of ODPABA, and by molecular mass determination by LC–MS.

Analysis of the contaminated propylene glycol found ODPABA to be present at a concentration of 19.4 μg/g. Identification of this impurity at this low level demonstrates how the extraction interface can be used to identify low levels of impurities in product excipients. This is an important area of application in the pharmaceutical industry.

ODPABA is a chemical of some significance in dermatology. It is used as an active ingredient in topical sunscreen formulations. *p*-Aminobenzoate (PABA) and its derivatives can undergo degradation to produce impurities [26,27] which may be biologically active [28,29]. Although it has been replaced in many products by other sunscreen actives, it is still used in a variety of topical sunscreen formulations.

Fig. 7 shows a reversed-phase chromatogram of ODPABA. Several components, the largest of which is at about 1%, can be seen in this chromatogram. The HPLC–FT-IR extraction interface was used in the identification of degradation products in ODPABA.

Fig. 8 shows the IR spectra obtained for two of the components in ODPABA. Both spectra contain absorption bands characteristic of amines. The spectra for impurity 4 show bands at 3440, 2820 and 1272 cm^{-1}. These are indicative of an aromatic molecule containing a secondary amine [25]. The spectra for impurity 2 show bands at 3500, 3408, 1622 and 1272 cm^{-1}. These are indicative of an aromatic molecule containing a primary amine [25]. Furthermore, the rest of the spectra of these two components match that of ODPABA, indicating that the basic structure of the molecules is the same.

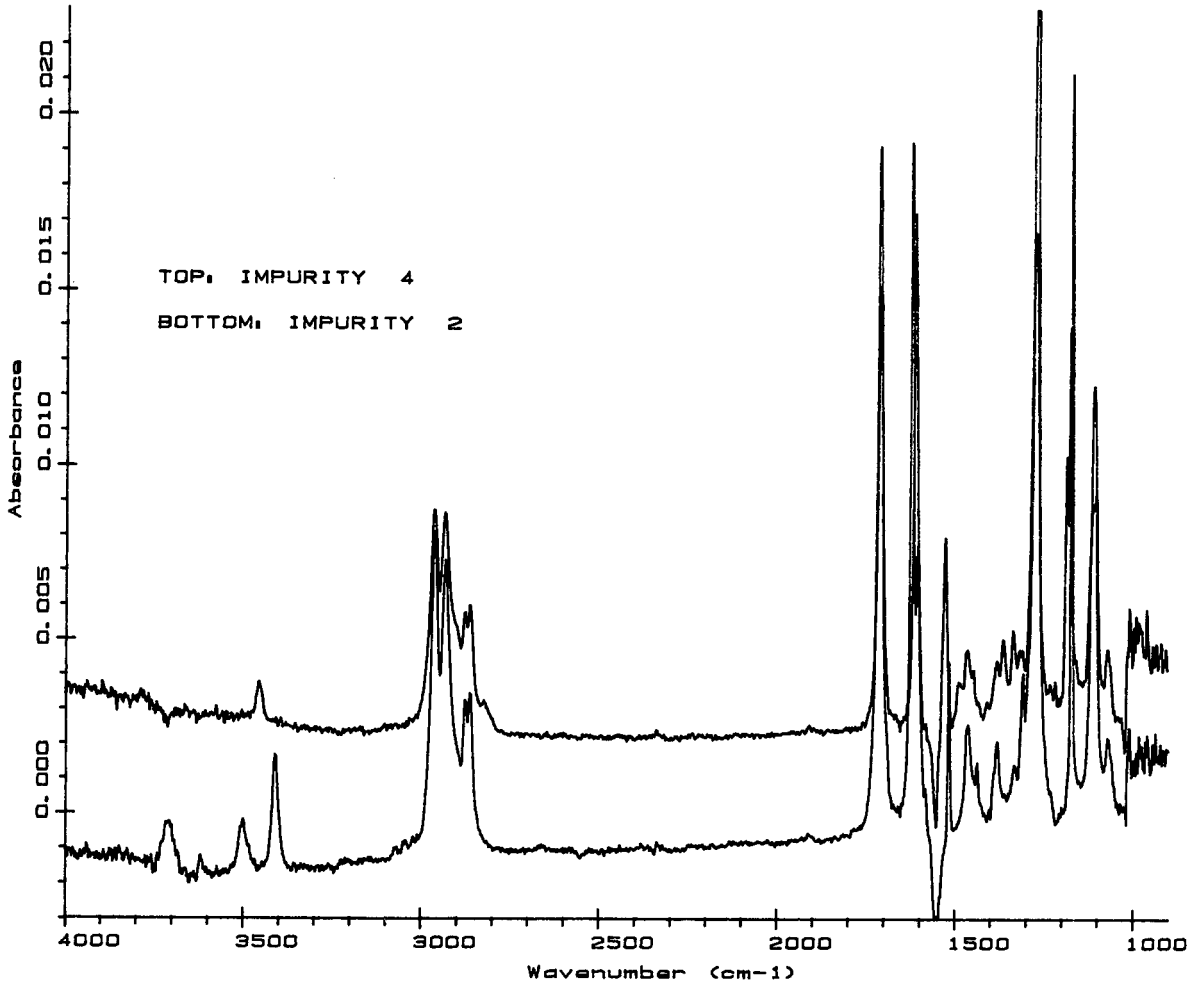

Fig. 8. Overlay spectra of impurities in octyl dimethyl *p*-aminobenzoate.

Based on these spectra impurity 2 was identified as the primary amine degradation product of ODPA-BA, octyl PABA, and impurity 4 was identified as the secondary amine degradation product of OD-PABA, octyl N-methylPABA. These observations were later confirmed by LC–MS.

CONCLUSION

HPLC–FT-IR with a solid-phase extraction interface has been used successfully to investigate a number of problems of pharmaceutical interest. The system has been used to identify isomers, trace contaminants, and degradation products in active ingredients and product excipients. Its ability to provide high quality spectra make it useful for identification and structure elucidation of components in mixtures. Although the solid-phase extractor may not be the ideal interface for every situation, its ease of use and its flexibility make it well suited for the problems described above.

REFERENCES

1 K. L. Kizer, A. W. Mantz and L. C. Bonar, *Am. Lab.*, 7 (5) (1975) 85.

2 C. C. Johnson and L. T. Taylor, *Anal. Chem.*, 56 (1984) 2642.
3 M. Sabo, J. Gross, J. Wang and I. E. Rosenberg, *Anal. Chem.*, 57 (1985) 1822.
4 P. T. Mc Kittrick, N. D. Danielson and J. E. Katon, *J. Liq. Chromatogr.*, 14 (1991) 377.
5 B. E. Miller, N. D. Danielson and J. E. Katon, *Appl. Spectrosc.*, 42 (1988) 401.
6 C. C. Johnson, J. W. Hellgeth and L. T. Taylor, *Anal. Chem.*, 57 (1985) 610.
7 J. W. Hellgeth and L. T. Taylor, *Anal. Chem.*, 59 (1987) 295.
8 S. Shah and L. T. Taylor, *LC–GC*, 7 (1989) 340.
9 D. Kuehl and P. R. Griffiths, *J. Chromatogr. Sci.*, 17 (1980) 471.
10 K. Jinno and C. Fujimoto, *J. Chromatogr.*, 506 (1990) 443.
11 K. Jinno and C. Fujimoto, *J. High Resolut. Chromatogr. Chromatogr. Commun.*, 4 (1981) 532.
12 K. Jinno and C. Fujimoto and D. Ishii, *J. Chromatogr.*, 239 (1982) 625.
13 K. Jinno and C. Fujimoto and Y. Hirata, *J. Chromatogr.*, 258 (1983) 81.
14 C. Fujimoto, T. Oosuka and K. Jino, *Anal. Chim. Acta*, 178 (1985) 159.
15 K. S. Kalasinky, J. A. S. Smith and V. F. Kalasinksy, *Anal. Chem.*, 57 (1985) 552.
16 V. F. Kalasinsky, K. G. Whitehead, R. C. Kenton, J. A. S. Smith and K. S. Kalasinsky, *J. Chromatogr. Sci.*, 25 (1987) 273.
17 J. J. Gagel and K. Biemann, *Anal. Chem.*, 58 (1986) 2184.
18 J. J. Gagel and K. Biemann, *Anal. Chem.*, 59 (1987) 1266.
19 J. J. Gagel and K. Biemann, *Mikrochim. Acta.*, 2 (1987) 185.
20 R. Robertson, J. A. DeHaseth and R. F. Browner, *Mikrochim. Acta.*, 2 (1987) 199.
21 A. J. Lange, P. R. Griffiths and D. J. Fraser, *Anal. Chem.*, 63 (1991) 782.
22 R. G. Messerschmidt, *Proc. SPIE Int. Soc. Opt. Eng.*, 553 (1985) 432.
23 C. D. Wilcox and R. M. Phelan, *J. Chromatogr. Sci.*, 24 (1986) 130.
24 *Federal Register*, 43 (166) (1978) Part 352.
25 N. B. Colthup, L. H. Daly and S. E. Wiberley, *Introduction to Infrared and Raman Spectroscopy*, Academic Press, New York, 1975.
26 A. W. Garret, *Drug Cosmet. Ind.*, 146 (6) (1989) 12.
27 H. Flindt-Hansen, C. J. Nielsen and P. Thune, *Photodermatology*, 5 (1988) 257.
28 F. P. Gasparro, *Photodermatology*, 2 (1995) 151.
29 H. J. Chow, R. L. Yates and J. A. Wenniger, presented at the *Conference on Advances in the Biology and Chemistry of N-Nitroso and Related Compounds, Omaha, Nebraska, 1988.*

Journal of Chromatography, 626 (1992) 109–116
Elsevier Science Publishers B.V., Amsterdam

CHROM. 24 215

Chromatographic determination of the position and configuration of isomers of methyl oleate hydroperoxides

Renzo Bortolomeazzi and Lorena Pizzale

Istituto di Tecnologie Alimentari, Università di Udine, Via Marangoni 97, 33100 Udine (Italy)

Giovanni Lercker

D.I.S.T.A.M., Università di Firenze, Via Donizetti 6, 50144 Firenze (Italy)

ABSTRACT

Oxygen can react with organic substrates (RH) to yield hydroperoxides, which in many instances are the first products of oxidation to be analytically isolated. A study of the structure of hydroperoxides could elucidate the reaction mechanisms activated during the first steps of oxidation processes. The simplest structural model used in the study of oxidation mechanisms of fats is methyl oleate. In this work the structures of methyl oleate hydroperoxides (MOHPs) were determined by gas chromatography–ion-trap detector mass spectrometry (GC–ITD-MS) of the corresponding hydroxystearates (MSHs). The hydroperoxides were reduced to methyl hydroxyoctadecenoates (MOHs), which were separated into the *cis* and *trans* fractions by argentation thin-layer chromatography. By hydrogenation of the double bond the *cis*- and *trans*-MOHs were reduced to MSHs for GC–ITD-MS analysis. Methods to isolate and determine the positional isomers of MOHPs were tested. The analytical techniques used were preparative high-performance liquid chromatography and GC–ITD-MS, solid-phase extraction–GC–ITD-MS and direct GC–ITD-MS.

INTRODUCTION

To understand the oxidation processes of unsaturated fractions of fatty substances, it is necessary to determine the relative composition and the concentration of the isomers of methyl oleate hydroperoxides (MOHPs). These isomers are defined with respect to double bond position and configuration, and peroxide group position.

The separation of MOHPs can be conveniently carried out only by liquid chromatography (LC) or high-performance liquid chromatography (HPLC), because they are thermally labile and chemically unstable. However, by using these techniques it is not possible to separate *cis* from *trans* isomers.

Grosh [1] described a method for the separation of MOHPs using HPLC, but the individual determination of *cis* and *trans* isomers for the MOHP system is limited to the use of gas chromatography (GC)–mass spectrometry (MS) and GC–nuclear magnetic resonance techniques [2,3]. The data obtained with these techniques are in agreement but, due to a lengthy sample preparation and to instrumental requirements, these techniques cannot be used for the analysis of a large number of samples.

This paper describes the HPLC separation of hydroxyoctadecenoates (MOHs) obtained from the reduction of MOHPs following the separation of isomers into *cis* and *trans* fractions by argentation thin-layer chromatography (TLC).

EXPERIMENTAL

Materials and reagents

Methyl oleate standard (> 99%) was supplied by Nu-Chek-Prep (Elysian, MI, USA). Reagents and solvents (analytical or HPLC grade) were supplied by Carlo Erba (Milan, Italy).

Solid-phase extraction (SPE) columns (Bond

Correspondence to: Dr. G. Lercker, D.I.S.T.A.M., Universita di Firenze, Via Donizetti 6, 50144 Firenze, Italy.

0021-9673/92/$05.00 © 1992 Elsevier Science Publishers B.V. All rights reserved

Elut, Analytichem International, Varian, CA, USA) packed with 500 mg of silica were used.

HPLC

A Varian Model 5040 liquid chromatograph equipped with a Varian CDS 401 data system and a Varian UV 50 detector operating at 212 nm was used. The column (15 cm × 4.6 mm I.D.) was a Spherisorb CN (alkylnitrile) of 3 μm particle size (Phase Separations, Deeside, UK). Separations were performed under isocratic conditions at a flow-rate of 1.5 ml/min, using a solution of 0.3% anhydrous ethanol in *n*-hexane as the mobile phase.

GC and GC–ion-trap detector mass spectrometry

A Carlo Erba Model Mega 5160 high-resolution gas chromatograph equipped with a split–splitless injector and a flame ionization detector was used. The fused-silica column was an SP 2340 column (Supelco, Bellefonte, PA, USA), 30 m × 0.32 mm I.D., 0.2 μm film thickness, and the temperature ranged from 80 to 240°C with a gradient of 5°C/min. The carrier gas (helium) flow-rate was 1.6 ml/min and the split ratio 1:80 (v/v). The injector and detector temperatures were 230 and 240°C, respectively.

For GC–ion-trap detector mass spectrometric (ITD-MS) analysis a Varian 3400 capillary gas chromatograph, coupled to a Varian Saturn ion-trap detector, was used. The fused-silica column was a DB-5 column (5% phenylmethyl) (J&W, Folsom, CA, USA), 30 m × 0.255 mm I.D., 0.25 μm film thickness. The oven temperature was programmed from 220 to 300°C with a gradient of 5°C/min. The injection was in the split mode (split ratio 1:70) with helium as the carrier gas at a flow-rate of 1 ml/min. The injector, transfer line and manifold temperatures were 300, 300 and 320°C, respectively. The filament emission current was 10 mA. Samples were injected as trimethylsilyl (TMS) derivatives.

Preparation and isolation of MOHP

Before carrying out the oxidation process, the methyl oleate standard was purified by passing through an alumina (neutral) liquid chromatographic column (2 cm × 1 cm I.D.), using hexane as the elution solvent.

The oxidation step was carried out by transferring 1 g of methyl oleate in a PTFE-lined screw-cap tube and placing it in oven at 80°C for about 120–140 h. The sample was then dissolved in 1 ml of *n*-hexane and loaded onto a SPE silica column previously conditioned with 5 ml of *n*-hexane. The column was eluted with 10 ml of *n*-hexane (fraction 1) and with 5 ml of an *n*-hexane–diethyl ether (1:1, v/v) mixture (fraction 2).

Fraction 1 contained the main part of non-reacted methyl oleate, whereas fraction 2 contained MOHPs together with other polar products of the oxidation. Fraction 2 was loaded on a silica gel TLC plate, 20 × 20 cm, 0.25 mm thickness and eluted with an *n*-hexane–diethylether (65:35, v/v) mixture. The band corresponding to MOHPs, visualized under UV light (254 nm) after spraying with a 0.2% ethanolic solution of 2,7-dichlorofluorescein sodium salt, was scraped off, extracted with chloroform and evaporated under nitrogen flow.

Reduction of MOHPs

MOHPs were reduced to the corresponding MOHs in 1 ml of methanol by adding a spatula tip of solid $NaBH_4$ [4]. After the disappearance of bubbles (about 30 min), the solution was acidified with 2–3 drops of 6 *M* HCl and its volume reduced under a stream of nitrogen. After the addition of 0.5 ml of water, hydroxides were extracted twice with 2 ml of diethyl ether. The ether extract was dried with anhydrous Na_2SO_4 and evaporated to dryness under a flow of nitrogen.

Argentation thin-layer chromatography

MOHs were separated on a TLC plate, 15 × 20 cm, 0.25 mm thickness, impregnated with silver nitrate [5]. The two fractions were detected by viewing under UV light after spraying the plate with the 2,7-dichlorofluorescein solution. The two bands corresponding to *trans* and *cis* isomers were extracted with chloroform and evaporated to dryness under a nitrogen flow.

HPLC and GC–ITD-MS

MOHPs, the corresponding MOHs and the two *trans* and *cis* isomer fractions, were analysed by HPLC (Fig. 1). The *cis* and *trans* isomer mixtures of MOHs were fractionated into the single isomers by collecting the corresponding peaks at the outlet of the HPLC detector cell.

To confirm the structure of the eight positional

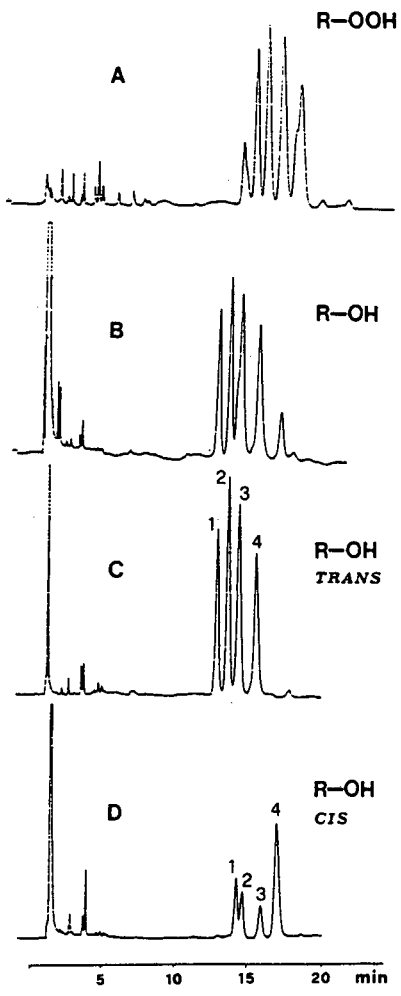

Fig. 1. HPLC chromatograms of (A) MOHPs; (B) MOHs; (C) *trans*-MOHs and (D) *cis*-MOHs.

and *cis*/*trans* isomers of MOHs, each single compound was analysed by GC–ITD-MS as the TMS ether. Using a similar procedure their corresponding methyl stearate hydroxides (MSHs), obtained by hydrogenation of each single MOH isomer using platinum as catalyst [2], were analysed.

For quantitative purposes the *trans* and *cis* isomer mixtures were analysed by GC–ITDMS with the same procedure before and after hydrogenation.

Preparation of the TMS ethers

The samples were silylated with about 0.1 ml of a pyridine–hexamethyldisilazane–trimethylchlorosilane (5:2:1, v/v) mixture, by storing them for 30 min at room temperature in a desiccator. After evaporation to dryness under nitrogen flow the samples were redissolved in 30–50 μl of benzene.

RESULTS AND DISCUSSION

For the collection of polar compounds from a methyl oleate peroxidation mixture we used an SPE column, which allows the elimination of the largest portion of non-reacted methyl oleate. This clean-up step made the improved isolation of the MOHP fraction from low oxidized systems possible.

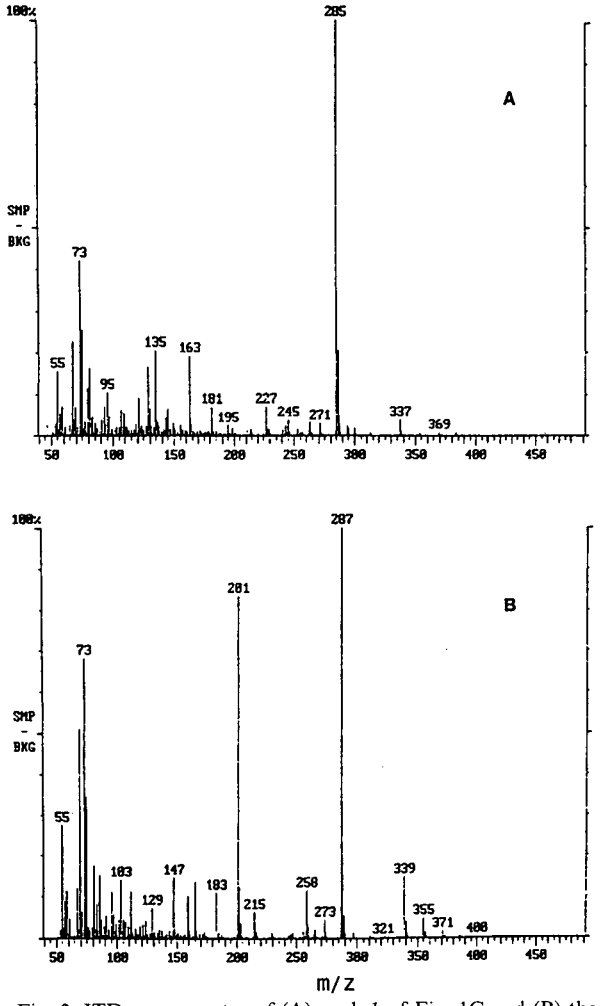

Fig. 2. ITD mass spectra of (A) peak 1 of Fig. 1C and (B) the same compound after hydrogenation.

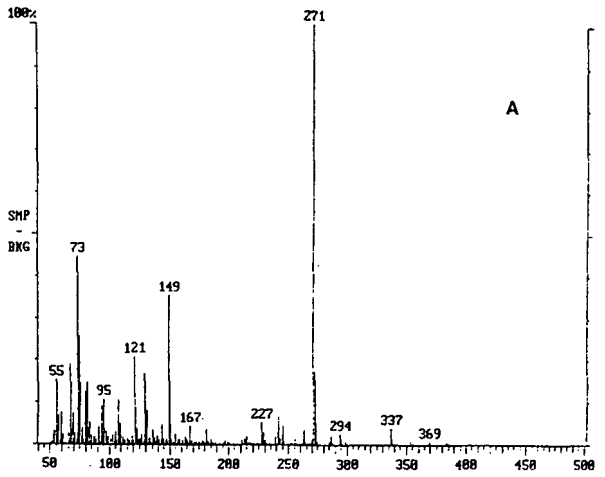

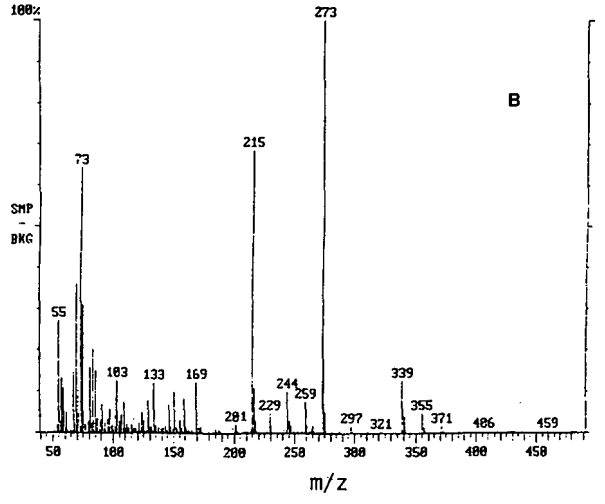

Fig. 3. ITD mass spectra of (A) peak 2 of Fig. 1C and (B) the same compound after hydrogenation.

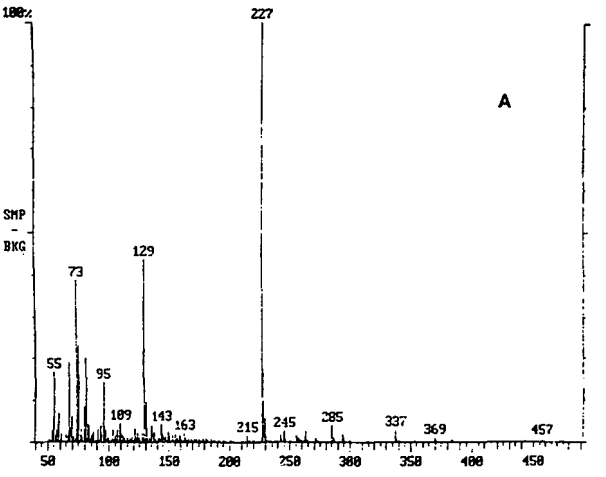

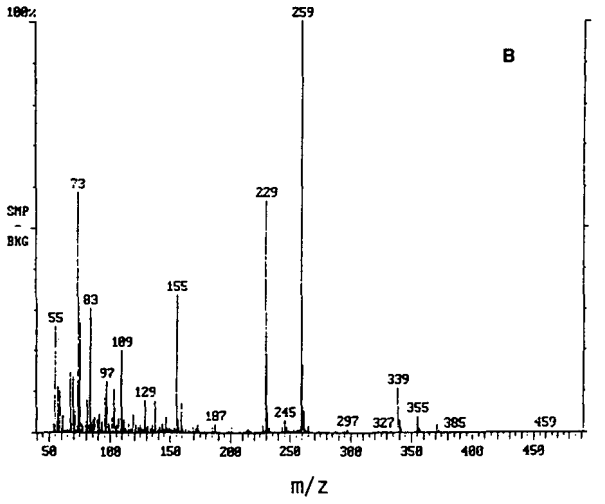

Fig. 4. ITD mass spectra of (A) peak 3 of Fig. 1C and (B) the same compound after hydrogenation.

The HPLC chromatograms showing the separation of the MOHPs, the corresponding MOH and the *trans* and *cis* isomers mixture are presented in Fig. 1.

Similarly to what was observed for silica HPLC columns [6], with the alkylnitrile HPLC column it was not possible to separate either the eight MOHP isomers or the corresponding MOHs. In contrast, the *trans* isomers, and to a lesser degree the *cis* isomers, were fairly well resolved. This separation allowed the collection of each single isomer as it eluted from HPLC instrument.

In Figs. 2–5, the ITD mass spectra of peaks 1–4 in the HPLC chromatogram (Fig. 1C) of the *trans*-MOHs are shown. The corresponding spectra of peaks 1–4 in the HPLC chromatogram (Fig. 1D) of the *cis*-MOHPs are shown in Figs. 6–9.

The mass spectra of the four *trans* isomers of MOHs showed a very intense peak (base peak) at *m/z* 285, 271, 227 and 241, respectively. These ions are characteristic of MOH positional isomers, and have the –OH group in the 11, 10, 9 and 8 position, respectively. They originate from the homolytic cleavage of the C–C bond next to the –O–TMS

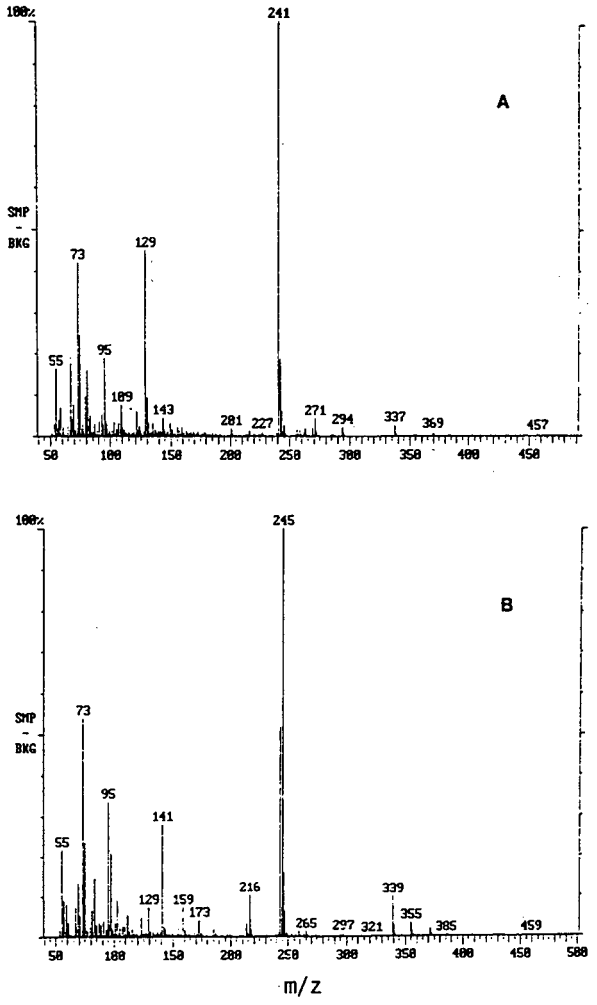

Fig. 5. ITD mass spectra of (A) peak 4 of Fig. 1C and (B) the same compound after hydrogenation.

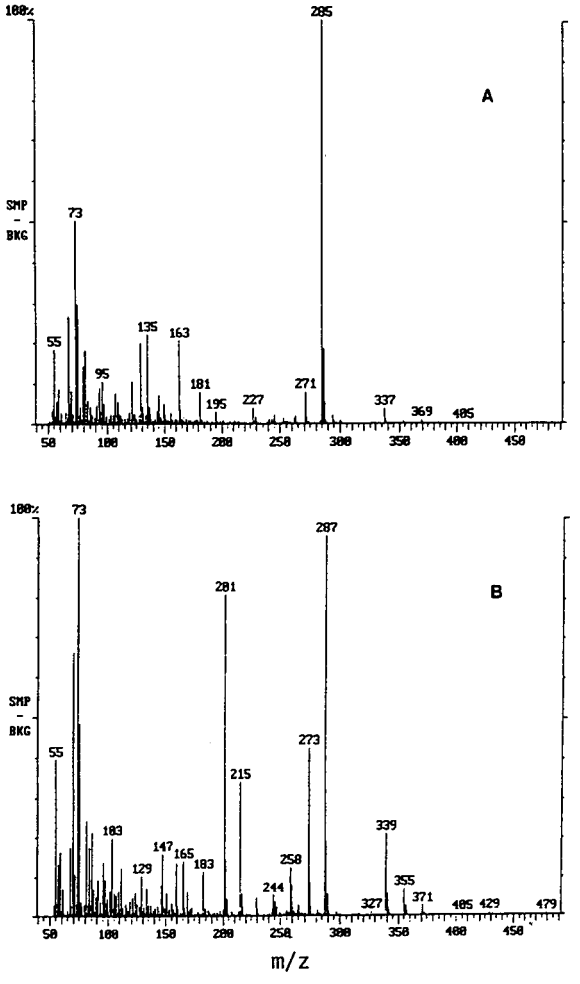

Fig. 6. ITD mass spectra of (A) peak 1 of Fig. 1D and (B) the same compound after hydrogenation.

group (α bond) on the opposite side of the double bond [7]. The structures of these ions are represented in Fig. 10.

The mass spectra of the corresponding MSHs show four pair of peaks at *m/z* 201/287, 215/273, 229/259 and 243/245, respectively. These pairs of ions originate from the homolytic cleavage of the C–C bonds next to the –O–TMS group and confirm the position that was previously assigned to the –OH group [7].

To the peaks in the HPLC chromatogram of *trans* MOHs (Fig. 1C) of the following positional isomers were assigned: 11-OH Δ^9 (peak 1); 10-OH Δ^8 (peak 2); 9-OH Δ^{10} (peak 3); 8-OH Δ^9 (peak 4).

A homologous sequence of positional isomers was obtained for the peaks in the HPLC chromatogram of *cis*-MOHs (Fig. 1D): 11-OH Δ^9 (peak 1); 10-OH Δ^8 (peak 2); 9-OH Δ^{10} (peak 3); 8-OH Δ^9 (peak 4).

The order of MOH elution obtained with this type of HPLC column is similar to that achieved in the separation of the corresponding MSH isomers

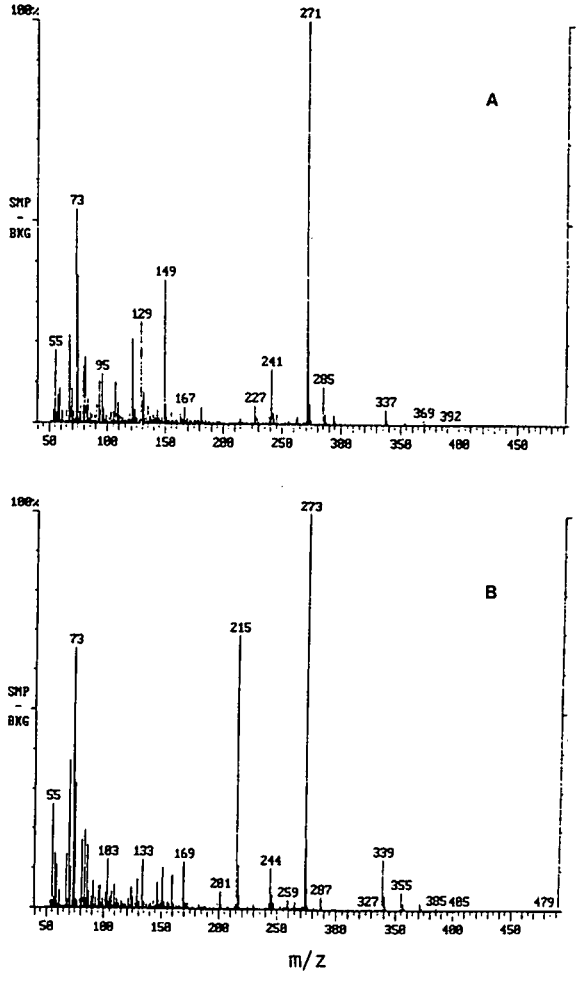

Fig. 7. ITD mass spectra of (A) peak 2 of Fig. 1D and (B) the same compound after hydrogenation.

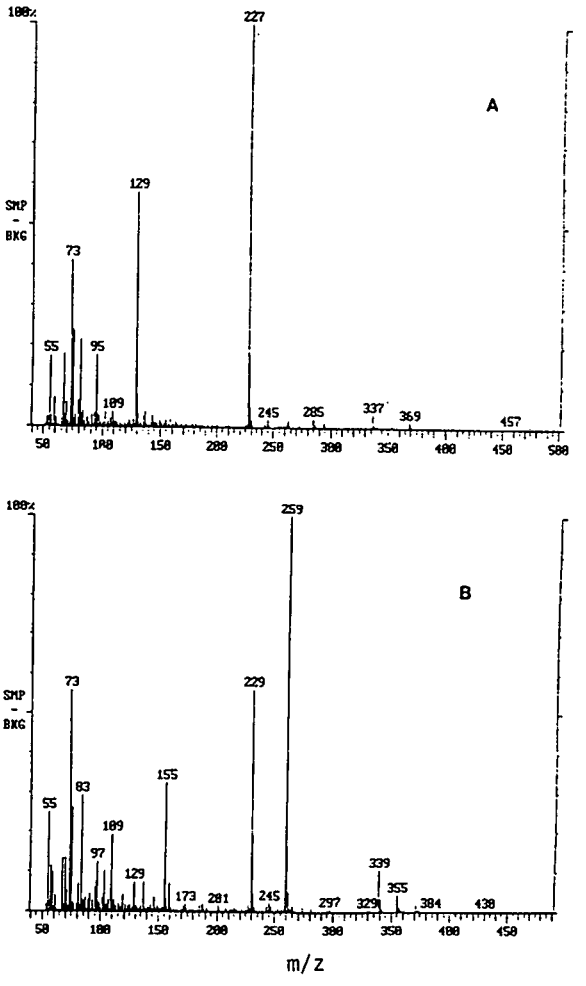

Fig. 8. ITD mass spectra of (A) peak 3 of Fig. 1D and (B) the same compound after hydrogenation.

using a silica column [6]. Thus we suggest that the position of the –OH group determines the order of elution, with 11-OH being the less retained isomer. With respect to the geometric isomerism, the *trans* isomers are slightly less retained than the corresponding *cis* isomers.

HPLC peak areas were used to calculate ratio compositions of each fraction of *trans* and *cis* positional isomers of MOHPs. The corresponding ratio compositions of each fraction of the *trans* and *cis* positional isomers of MSHs were also calculated using the relative intensities of the pairs of GC–MS ions, 201/287, 215/273, 229/259 and 243/245 for the 11-OH, 10-OH, 9-OH and 8-OH isomers, respectively. The mass spectra were obtained by computer processing, by averaging all scans containing the singlet ion monitoring (SIM) peaks. In fact, the SIM analysis showed that with our conditions only a partial separation of the MSH isomers can be achieved, as already noticed by other workers [3,8]. Compositions of *trans* and *cis* positional isomers, as calculated with the HPLC and GC–ITD-MS methods, are listed in Table I. The results obtained by comparing these two independent methods are in good agreement.

Isomers 9 and 10 were present in *trans* fractions

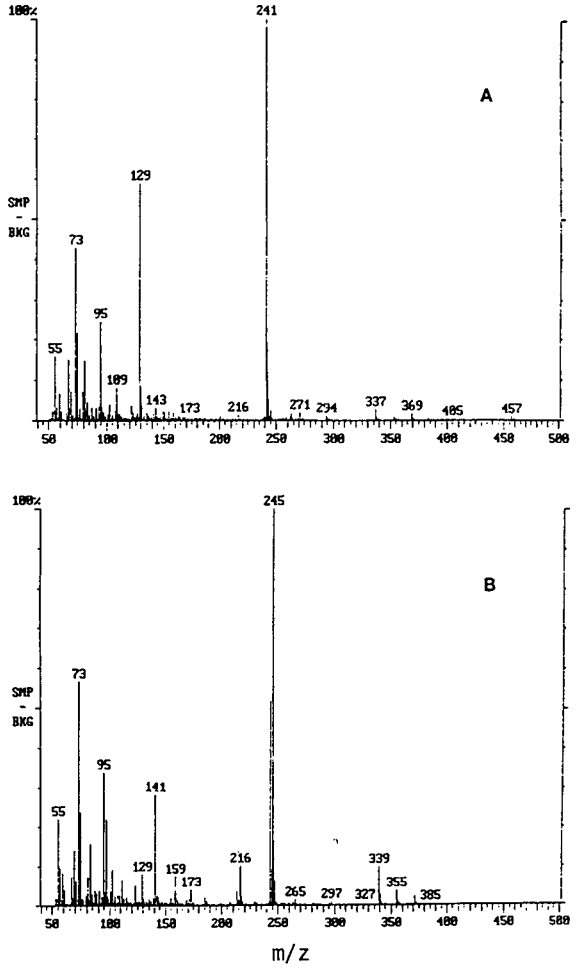

Fig. 9. ITD mass spectra of (A) peak 4 of Fig. 1D and (B) the same compound after hydrogenation.

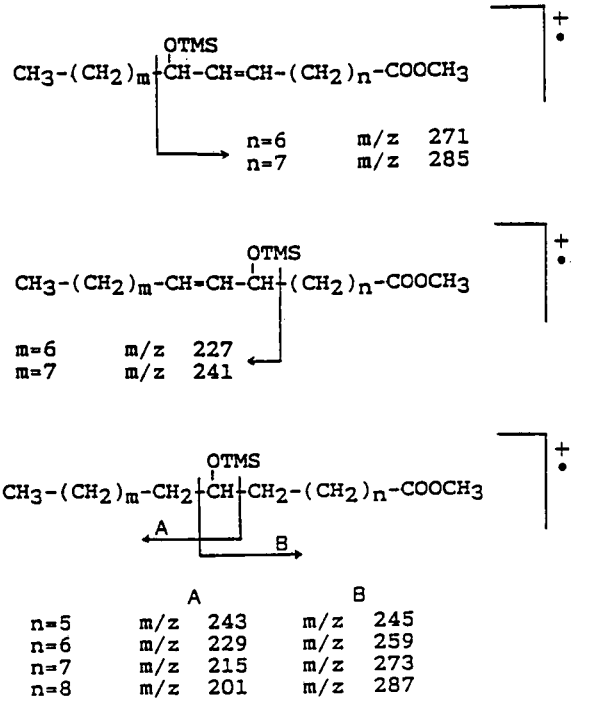

Fig. 10. Structures of ions present in the mass spectra of the four *trans*-MOH (or *cis*-MOH) isomers.

in larger amounts than isomers 8 and 11. In contrast isomers 8 and 11 predominated in the *cis* fractions; in particular, the isomer 8 alone accounted for about 50% of this fraction.

Table I also indicates the ratio compositions of the total *trans*- and *cis*-MOH isomers, as calculated using chromatographic areas obtained with the capillary column SP 2340, which resolved the *cis* from the *trans* isomers as TMS derivatives.

CONCLUSIONS

The use of an SPE column in the purification step of MOHPs allowed the elimination of the largest portion of non-reacted methyl oleate. This step made possible the isolation of MOHPs on a single TLC plate. With this procedure it is possible to collect very small amounts of MOHPs and this is a key factor in the study of the first steps of the reaction mechanisms in the oxidation of lipids. The composition of positional and *cis/trans* MOH isomers obtained by reducing the corresponding MOHPs and separating them by argentation TLC can be determined by a simple HPLC method. The results are in good agreement with those obtained by GC–ITD-MS. The use of a polar capillary column allows the rapid and direct determination of the *cis* and *trans* isomers ratio. This shortened procedure facilitates the complex analysis needed for the study of oxidation of model systems.

TABLE I

COMPARISON BETWEEN THE PERCENTAGE COMPOSITIONS OF THE POSITIONAL AND *trans/cis* ISOMERS OF THE METHYL HYDROXYOCTADECENOATES AS DETERMINED BY HPLC AND GC–ITD-MS

Conditions	Position isomers	*Trans* (84.8%)		*Cis* (15.2%)	
		HPLC	GC–ITD-MS[a]	HPLC	GC–ITD-MS[a]
80°C; 140 h	11-OH Δ^9	22.3	21.1	23.0	20.9
	10-OH Δ^8	27.1	28.0	17.3	20.1
	9-OH Δ^{10}	26.8	26.6	15.7	16.2
	8-OH Δ^9	23.8	24.3	44.0	42.8
		Trans (84.7%)[c]		*Cis* (15.3%)[c]	
		HPLC	GC–ITD-MS[a]	HPLC	GC–ITD-MS[a]
80°C; 120 h[b]	11-OH Δ^9	22.4	22.3	17.4	19.8
	10-OH Δ^8	29.0	28.2	16.3	17.8
	9-OH Δ^{10}	28.3	27.5	14.1	12.2
	8-OH Δ^9	20.3	22.0	52.2	50.2
80°C; 120 h[b]	11-OH Δ^9	20.1	24.1	19.6	21.2
	10-OH Δ^8	27.1	27.4	15.8	17.0
	9-OH Δ^{10}	28.4	25.3	12.6	11.4
	8-OH Δ^9	24.4	23.2	52.0	50.4

[a] Determined as methyl hydroxystearates TMS.
[b] Two sets of analyses shown for comparison.
[c] Mean of two determinations.

ACKNOWLEDGEMENTS

This research was supported by the National Research Council of Italy, Special Project RAISA, Sub-project No. 4, Paper No. 319.

REFERENCES

1 W. Grosch, *Lebensmittelchem. Gerichtl. Chem.*, 38 (1984) 81.
2 M. Piretti, B. Capella and U. Pallotta, *Riv. Ital. Sost. Grasse*, 46 (1969) 652.
3 E. N. Frankel, W. E. Neff, W. K. Rohwedder, B. P. S. Khambay, R. F. Garwood and B. C. L. Weedon, *Lipids*, 12 (1977) 901.
4 G. Lercker, P. Capella, L. S. Conte and U. Pallotta, *Rev. Fr. Corps Gras*, 5 (1978) 227.
5 M. S. J. Dallas and F. B. Padley, *Lebensm.-Wiss. Technol.*, 10 (1977) 328.
6 H. W. S. Chan and G. Levett, *Chem. Ind.*, (1977) 692.
7 U. Pallotta, M. V. Piretti and P. Capella, *Riv. Ital. Sost. Grasse*, 47 (1970) 472.
8 R. F. Garwood, B. P. S. Khambay, B. C. L. Weedon and E. N. Frankel, *J. Chem. Soc. Chem. Commun.*, (1977) 364.

Journal of Chromatography, 626 (1992) 117–126
Elsevier Science Publishers B.V., Amsterdam

CHROM. 24 321

Applicability of a postcolumn photochemical reactor in the high-performance liquid chromatography of 34 polyphenolic compounds with UV detection

R. Cela, M. Lores and C. M. Garcia

Department of Analytical Chemistry, Nutrition and Bromatology, Faculty of Chemistry, University of Santiago de Compostela, 15706 Santiago (Spain)

ABSTRACT

The utility of postcolumn photoderivatization for a better and more reliable identification and discrimination of 34 polyphenolic compounds of interest in oenology was studied. The procedure, which is functionally very simple, allows spectral relationships to be obtained between the compounds and their photoproducts which make them easier to identify. These relationships are presented for cases in which a diode-array detector is not available. The variables affecting the experimental device (open-tubular reactor length, pH, nature of the modifier and acids used in the mobile phase) were optimized and their relative importance is discussed.

INTRODUCTION

The importance of polyphenolic compounds in the vegetable world, and particularly in oenology, has been widely demonstrated [1,2]. These compounds play an active role in organoleptic characteristics and also in various reactions that affect the quality of such products, both positively and negatively. In addition for wines they could actually become a highly valuable 'fingerprint' for classification and characterization.

The analysis of such compounds is usually carried out by means of their separation by gradient high-performance liquid chromatography (HPLC) with UV detection [3]. However, the large number of these compounds present in samples at very different concentration levels (which are nonetheless always low) makes it extremely difficult to resolve them and numerous overlaps involving two or more species are observed. Even when diode-array detectors are used and working with first or second derivative spectra [4], the identification of such species is very difficult in the case of overlaps, owing to the similarity of the spectra of many of these compounds.

On the other hand, the use of postcolumn photochemical reactors has, in recent years, led to improvements in selectivity and sensitivity in the detection of highly diverse types of compounds. The advantages of using this type of postcolumn reactor has now been clearly demonstrated [5–7]: selectivity of the reactions; absence of derivatization reagents, and consequently of interfering residues or decomposition products from the reagent; the fact that light can be introduced without additional pumps or mixing devices, and without using an additional solvent (thus, avoiding analyte dilution); rapidity of the photochemical reactions, allowing the use of shorter reactors (which limits analyte dispersion and band broadening); stability of the light sources as compared with chemical derivatization reagents in solution; no limitations between eluent selection and reagent solubility, etc. Also, several workers [8–

Correspondence to: Dr. R. Cela, Department of Analytical Chemistry, Nutrition and Bromatology, Faculty of Chemistry, University of Santiago de Compostela, 15706 Santiago, Spain.

0021-9673/92/$05.00 © 1992 Elsevier Science Publishers B.V. All rights reserved

10] have described simple techniques for the construction of the reactors, which are also available commercially.

This paper presents the results of a study on the applicability of such photoreactors in order to improve UV detection and identification possibilities for 34 polyphenolic species (22 phenolic acids and 12 aldehydes) having oenological interest and separated by HPLC.

EXPERIMENTAL

The experimental device is outlined in Fig. 1. It consists of a pump (Waters Model 600), a universal injector (Waters Model UK6), a reversed-phase chromatographic column (Waters Novapak C_{18}) and a second injection valve (Rheodyne Model 7010) fitted with a 10-μl loop which was used for injections in the flow-injection analysis (FIA) mode, a photoreactor made in the laboratory and a diode-array detector (Waters Model 990+) with a system for control and data acquisition.

The photoreactor was constructed according the method described by Poulsen *et al.* [10], by preparing a 1.5-m open-tubular reactor (OTR) with a 0.3 mm I.D. PTFE tube (Supelco). This coil was placed around a 10-W germicide lamp (Osram, HNS10/Uofr), operated by manual switch. The lamp and coil assembly was located inside a shiny aluminium cylinder with a diameter that is large enough for the efficient ventilation of the reactor, which is powered by a fan.

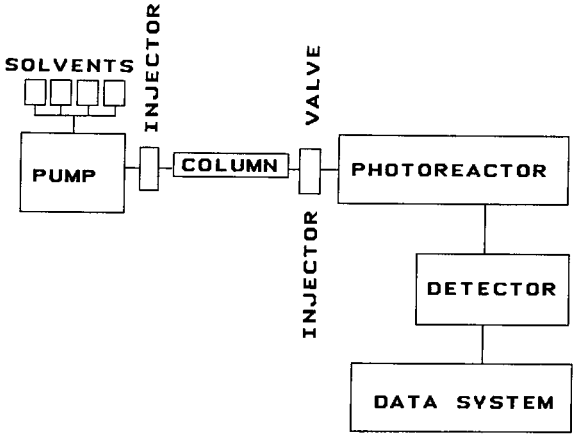

Fig. 1. Schematic view of the experimental system.

Most of the experiments described here (optimization studies) were carried out in the FIA mode, injecting fixed volumes of standard solutions (in the 10–100 ppm range) of the different compounds studied: gallic, 2,4,6-trihydroxybenzoic, 3,4-dihydroxybenzoic, α-, β- and γ-resorcylic, gentistic, *m*- and *p*-hydroxybenzoic, vanillic, 2,6-dimethoxybenzoic, caffeic, veratric, ferulic, *o*- and *m*-coumaric, sinapic, 2,4-dimethoxybenzoic, 3,5-dimethoxybenzoic and 3,4,5-trimethoxybenzoic acids (Fluka), syringic acid (Eastman) and *p*-coumaric acid (Merck) and 2,5-dihydroxybenzaldehyde, 3,5-dimethoxy-4-hydroxybenzaldehyde, 3,5-dimethoxybenzaldehyde, 2,4-dimethoxybenzaldehyde, 3,4,5-trimethoxybenzaldehyde, 3-hydroxybenzaldehyde, 4-hydroxybenzaldehyde, 3,4-dihydroxybenzaldehyde, vanillin, isovanillin, orthovanillin and veratraldehyde (Fluka).

When mixtures of the species under study were injected, isocratic mobile phases consisting of methanol or acetonitrile and water modified with acetic acid (1%), formic acid (0.5%) or sulphuric acid (0.3%) were used in different proportions depending on the retention of compounds in the column. The complex mixtures of the species studied were eluted using a multi-segmented gradient described elsewhere [3]. In all instances, chromatograms were recorded over a range of 200–450 nm with 2.0-nm resolution.

RESULTS AND DISCUSSION

Initial experiments

A study was first done to evaluate the effect of the photoreactor on the compounds under study. For this purpose a mixture of these compounds was injected and eluted under methanol–water gradient conditions [3], with the photoreactor turned off. A second injection under the same conditions, but with the photoreactor turned on, showed that many of the chromatographic peaks were greatly modified by photoreaction. Using a 280-nm chromatogram as a reference, some of the peaks were seen to increase in size, whereas others decreased. Fig. 2 shows a comparison of the chromatograms for the different compound mixtures. All this led us to believe that photoderivatization does not affect all compounds in the same way, and therefore not only would it be possible to improve the detection sensi-

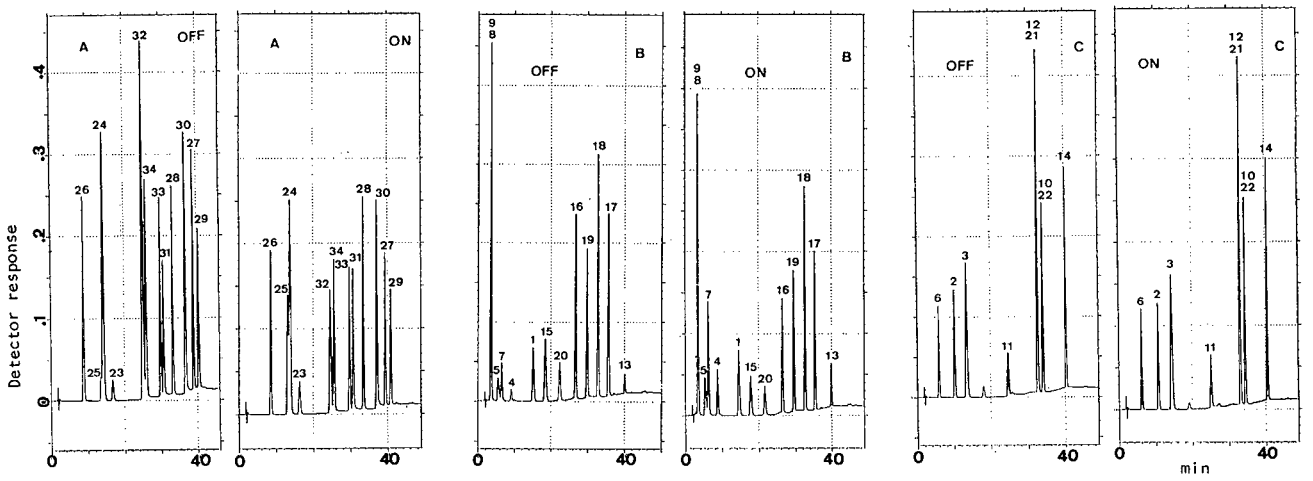

Fig. 2. Comparative chromatograms for three different mixtures of the species under study. (A) Phenolic aldehydes mixture; (B) and (C) phenolic acids mixtures. OFF = chromatograms obtained with photoreactor turned off; ON = chromatograms with photoreactor turned on. For peak identification, see Table I.

tivity in some instances but also it would be feasible to develop work plans for the selective detection or easier identification of some or most of these compounds. However, given that the 34 species could not be resolved in only one elution, an individual study of the photoderivatization of each was deemed necessary.

Optimization of the photoreactor

Before starting the individual study of each species, the operational variables of the photoreactor were optimized. The following variables were studied: coil length, pH of the mobile phase, percentage and nature of the organic modifier and nature of the acid used. All these studies were carried out in the FIA mode, injecting the compounds through the secondary fixed loop injection valve, inserted into the circuit (see Fig. 1). In these instance the chromatographic column was replaced with a damper to avoid deterioration.

Tube length used in the construction of the OTR

The optimization of this parameter was carried out by varying the mobile phase flow-rate in such a way as to make it possible to control the residence time of the compounds in the OTR effectively, simulating variations in length. All the compounds studied were injected several times with a mobile phase [methanol–water–acetic acid (50:49:1)] flow-rate of 1.5 ml/min with the photoreactor turned off. The average spectrum obtained from these injections was used in each instance as a reference point. Next, species were injected (minimum in duplicate for each established flow value) with the photoreactor turned on and for flow-rates of 1.5, 1.0, 0.8, 0.6, 0.4 and 0.2 ml/min. The graphs in Fig. 3 give the results obtained for vanillic acid. The left part refers to the reference chromatogram (in the FIA mode) at 280 nm, alongside which are superimposed the spectra corresponding to each pair of injections carried out for each value of the mobile phase flow-rate. These spectra reveal the advance of the photochemical reaction as the residence time of the compound in the OTR increases. In this particular case, the photoreaction results in the disappearance of the absorption bands at 260 and 295 nm. Similarly, it can be seen that, below 0.4 ml/min, the photoreaction is complete, but owing to the dead volumes in the system, for 0.2 ml/min the peak is noticeably split. With most of the compounds studied, the photoreaction was complete with a 0.6 ml/min flow-rate. It was appreciable at high flow-rate (1.5 and 1.0 ml/min) for some species (3,5-dimethoxybenzaldehyde, 4-hydroxybenzaldehyde and α-resorcylic acid). Only with a few of the species was it necessary to reduce the flow-rate to as low as 0.4

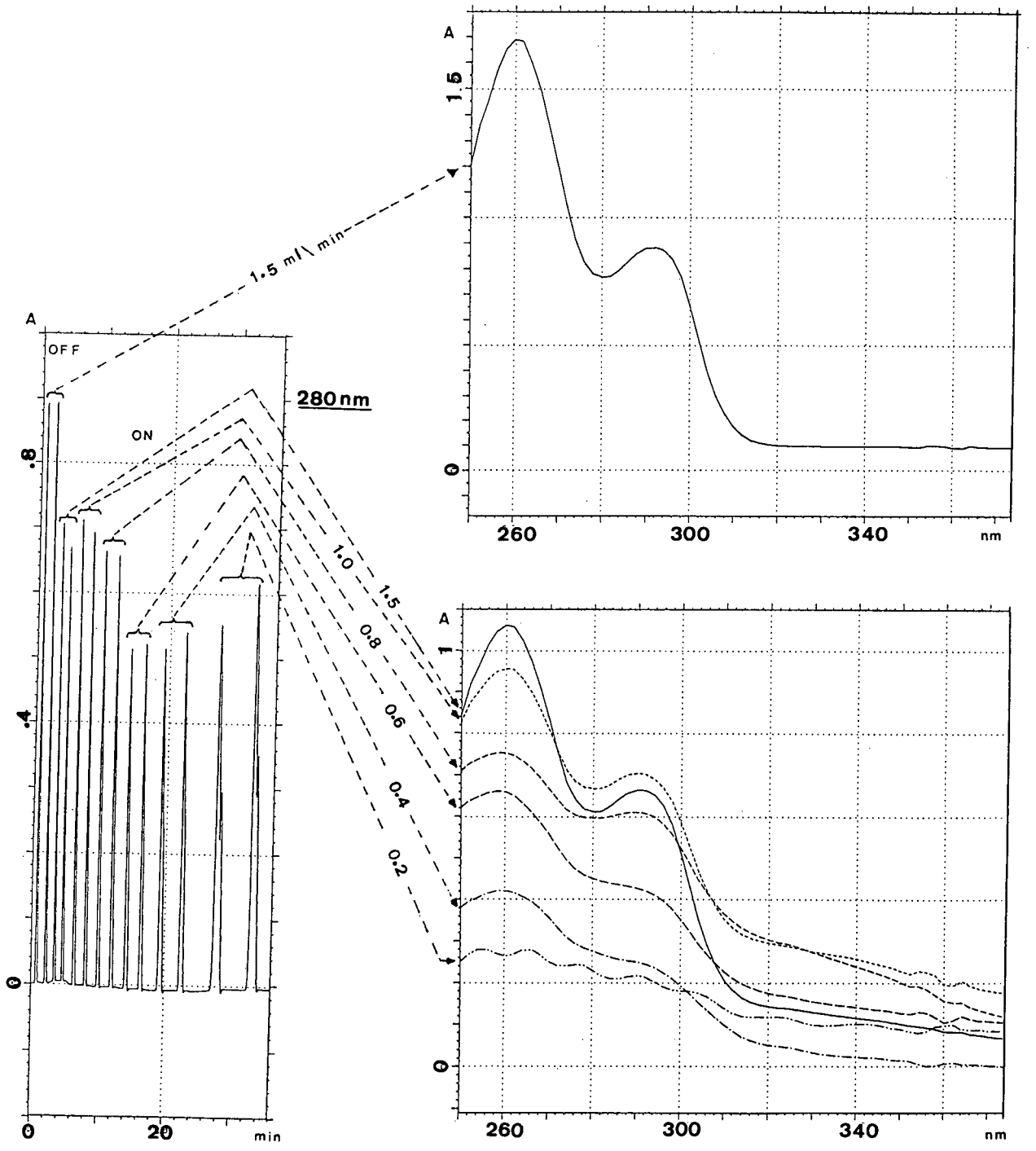

Fig. 3. Influence of the OTR tube length on the completeness of vanillic acid photodegradation (mobile phase acidified with acetic acid).

ml/min (vanillic acid, orthovanillin and vanillin) in order to obtain a complete reaction and so that gentistic and syringic acid would not undergo any appreciable changes in their spectra for any of the flow-rates tested.

It was determined that a flow-rate of 0.5 ml/min was optimum for the whole group of compounds, which is equivalent to a tube length of 4.5–5 m.

Percentage and nature of the organic modifier used

The spectral differences observed in the products from photoreaction with respect to the original species suggest that diverse photoreaction mechanisms are involved. With the aldehydes, a possible hypothesis could be the photoreduction towards the corresponding alcohol, and consequently the nature and proportion of the organic modifier used in the mobile phase could be an influencing factor. In order to verify this influence, two series of injections were made for the species under study. In the first series the proportion of methanol and the mobile phase flow-rate were modified so that for each species the spectra both with the reactor turned on and off for flow-rates of 1.0 and 0.6 ml/min and methanol contents of 20, 40, 60 and 80% were obtained. In no instance were significant modifications observed.

In the second series of injections, methanol was replaced with acetonitrile (in both instances in the presence of 1% acetic acid). The experiment was planned to be identical with the previous one. No significant modifications were observed in the spectra here either, which led to the conclusion that neither the nature of the modifier (at least for the usual solvents in RP-HPLC for these species) nor its percentage has a notable effect on the photoreactions undergone by the species under study. These findings are important from a practical point of view, in that the results of the postcolumn photoderivatization of these species can be compared with each other, regardless of the composition of the mobile phase used and also for gradient elutions.

pH of the mobile phase

Up to this point, all the experiments and injections had been carried out with acidified mobile phases (1% acetic acid, pH 2.7), as this is necessary for the separation of the species under study by RP-HPLC. However, in order to study the influence of the pH of the mobile phase on the photoreactions, two series of injections respective mobile phases of pH 4.6 and 9.1 were carried out.

No noteworthy modifications were observed in the spectra of these species or their photoproducts. Based on these results, acidified mobile phases continued to be used.

Nature of the acid used

Acetic acid is commonly used in the preparation of the mobile phases for the separation of phenolic compounds. In order to find out if the nature of the acid used has any influence on photoreactions, two series of injections were made in which the mobile phase was acidified using formic or sulphuric acid instead of acetic acid in sufficient proportions to obtain a pH that would be low enough to guarantee that all the species to be separated would be in the protonated form. All injections were made with a 0.6 ml/min flow-rate in order to ensure complete reactions. As in previous experiments, the results were deduced from the comparison of the spectra obtained with injections where the photoreactor was turned off and on. The graphs in Fig. 4 serve as typical examples of the series of results obtained in this study. The spectra in Fig. 4a, allow for the comparison of the extension of the photoreaction for 2,5-dihydroxybenzaldehyde, depending on the acid used. It can be seen that the spectra for the products without photodecomposition (solid lines) are similar in mobile phases acidified with acetic and formic acid and slightly different when sulphuric acid is used. In contrast, when the photoreactor is turned on (spectra of the photoproducts in broken lines), the extension of the photoreaction is clearly greater in mobile phases acidified with formic acid, in which event the spectrum of the photoproducts only shows a band having a maximum of 295 nm. When acetic acid is used, this maximum is also visible, but also those related to the original product. Since they are postcolumn reactions, there is no separation between the photoproducts and the non-photodegraded original species, which justifies the spectrum obtained when the photoreaction is not complete. Finally, when sulphuric acid is used, photoreaction does not appear to take place.

The graphs in Fig. 4b show another typical situation. In this instance the photoreaction takes place independent of the nature of the acid, and its

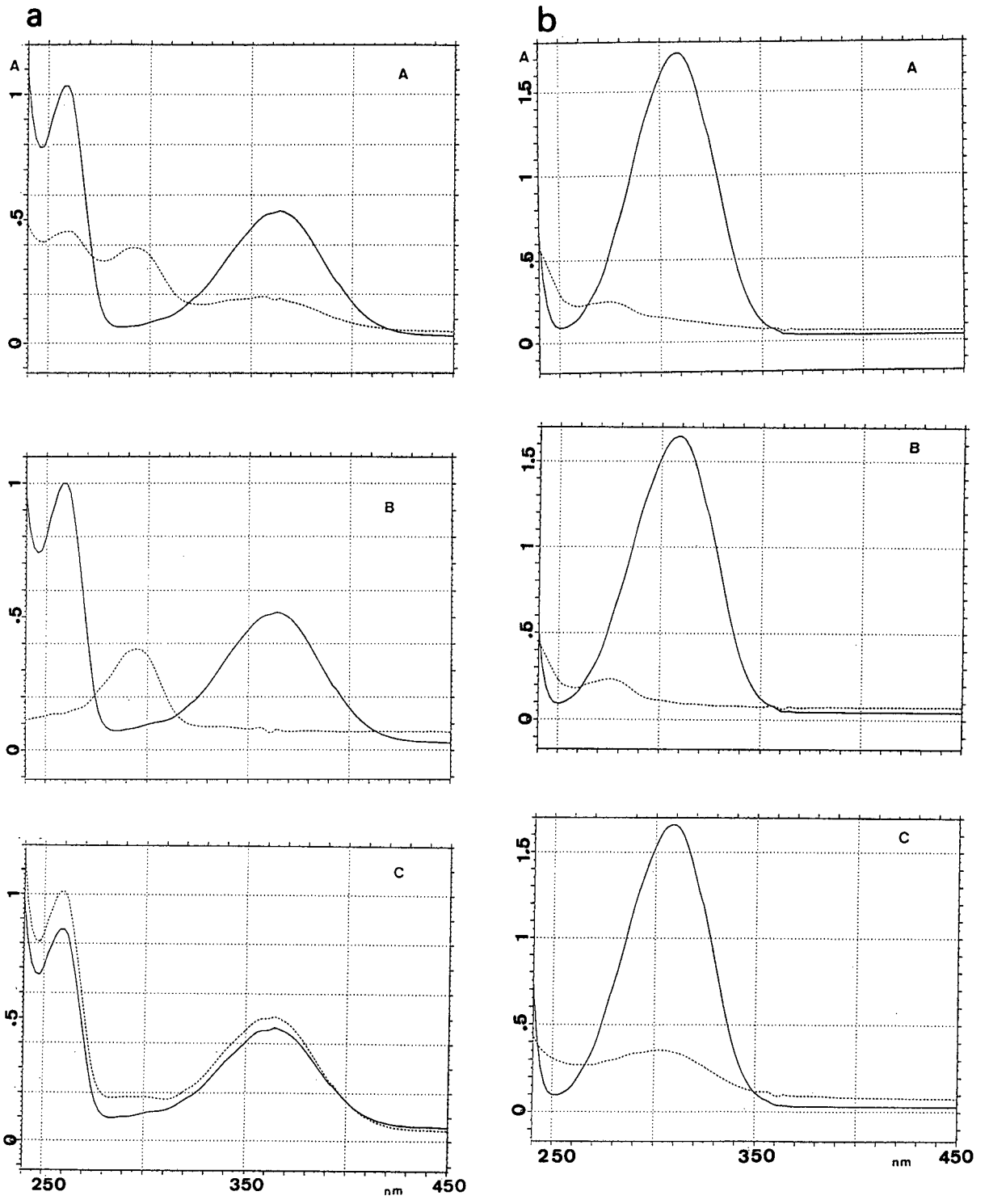

Fig. 4. Influence of the nature of the acid used in mobile phase preparation on photodegradation for (a) 2,5-dihydroxybenzaldehyde and (b), 3,5-dimethoxy-4-hydroxybenzaldehyde. Spectra with solid lines correspond to photoreactor turned off and those with dashed lines to photoreactor turned on. Mobile phases prepared with (A) 1% acetic acid, (B) 0.5% formic acid and (C) 0.3% sulphuric acid.

TABLE I

INFLUENCE OF THE NATURE OF THE ACID USED IN MOBILE PHASE PREPARATION ON THE PHOTODEGRADATION OF POLYPHENOLIC SPECIES

Key: − = no photoreaction; ± = slight or very slow photoreaction; + = partial or slow photoreaction; + + = rapid and complete photoreaction.

No.[a]	Compound	Acetic acid	Formic acid
	Acids		
1	3-Hydroxybenzoic	−	−
2	4-Hydroxybenzoic	+	+ +
3	2,4-Dihydroxybenzoic (β-resorcylic)	−	−
4	2,5-Dihydroxybenzoic (gentisic)	+ +	+
5	2,6-Dihydroxybenzoic (γ-resorcylic)	−	−
6	3,4-Dihydroxybenzoic	−	+
7	3,5-Dihydroxybenzoic (α-resorcylic)	+	+ +
8	2,4,6-Trihydroxybenzoic (protocatechuic)	−	±
9	3,4,5-Trihydroxybenzoic (gallic)	−	−
10	2,4-Dimethoxybenzoic	−	+
11	2,6-Dimethoxybenzoic	−	+ +
12	3,4-Dimethoxybenzoic (veratric)	−	+ +
13	3,5-Dimethoxybenzoic	+	+ +
14	3,4,5-Trimethoxycinnamic	−	+ +
15	4-Hydroxy-3-methoxybenzoic (vanillic)	+	+ +
16	4-Hydroxy-3,5-dimethoxybenzoic (syringic)	+	+ +
17	2-Hydroxycinnamic (*o*-coumaric)	−	+ +
18	3-Hydroxycinnamic (*m*-coumaric)	−	+ +
19	4-Hydroxycinnamic (*p*-coumaric)	−	+ +
20	3,4-Dihydroxycinnamic (caffeic)	−	+ +
21	4-Hydroxy-3-methoxycinnamic (ferulic)	−	+ +
22	3,5-Dimethoxy-4-hydroxycinnamic (sinapic)	+	+ +
	Aldehydes		
23	3-Hydroxybenzaldehyde	−	+
24	4-Hydroxybenzaldehyde	+	+ +
25	2,5-Dihydroxybenzaldehyde	+	+ +
26	3,4-Dihydroxybenzaldehyde (protocatechualdehyde)	−	+
27	2,4-Dimethoxybenzaldehyde	−	+
28	3,4-Dimethoxybenzaldehyde (veratraldehyde)	−	+
29	3,5-Dimethoxybenzaldehyde	+	+ +
30	3,4,5-Trimethoxybenzaldehyde	+	+
31	2-Hydroxy-3-methoxybenzaldehyde (*o*-vanillin)	+	+ +
32	4-Hydroxy-3-methoxybenzaldehyde (vanillin)	+	+
33	3,5-Dimethoxy-4-hydroxybenzaldehyde	+	+
34	3-Hydroxy-4-methoxybenzaldehyde (isovanillin)	−	+

[a] Peak assignments in figures.

extension is similar in mobile phases acidified with acetic and formic acid. It takes place with a smaller extension for phases acidified with sulphuric acid. Table I summarizes the results of this series of experiments with the use of acetic and formic acid, as it was found that in the presence of sulphuric acid, photoreactions always take place with a smaller extension or not at all. It is clear from Table I that the nature of the acid used is a highly important parameter, especially as regards the extension of the photoreactions. A typical example can be seen in the spectra in Fig. 5, which gives a simultaneous view of the influence of the acid used and flow-rate for the photoreactions of α-resorcylic acid. It formic acid is used, the spectra of the photoproducts barely change when the mobile phase flow-rate is varied,

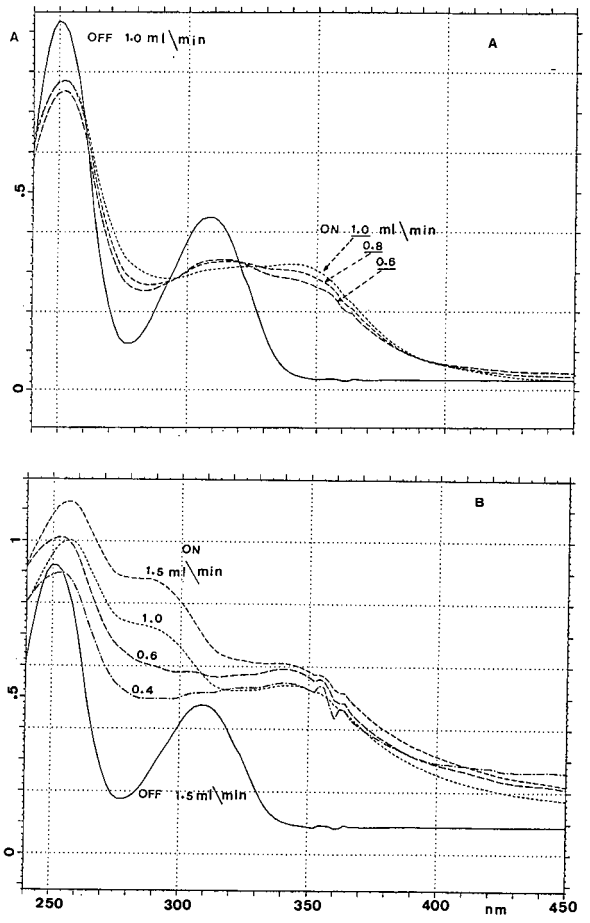

Fig. 5. Influence of the nature of the acid and flow-rate on the photodegradation of α-resorcylic acid. Mobile phases prepared with (A) 0.3% formic acid and (B) 1% acetic acid. Flow-rates as indicated on curves. Spectra with solid lines correspond to photoreactor turned off and are included for comparative purposes.

which points to a rapid and complete photoreaction. However, for mobile phases acidified with acetic acid, the spectra obtained for 0.6 and 0.4 ml/min flow-rates are very similar to those obtained using formic acid. This is not true for higher flow-rates, where a 290-nm absorption band was seen, which is probably due to an intermediate photoproduct that can only be appreciated if the exposure time to luminous radiation is relatively short.

Of the three acids considered, formic acid is the most and sulphuric acid is the least conducive to photoreactions, with acetic acid in an intermediate position. As many of the species considered do not

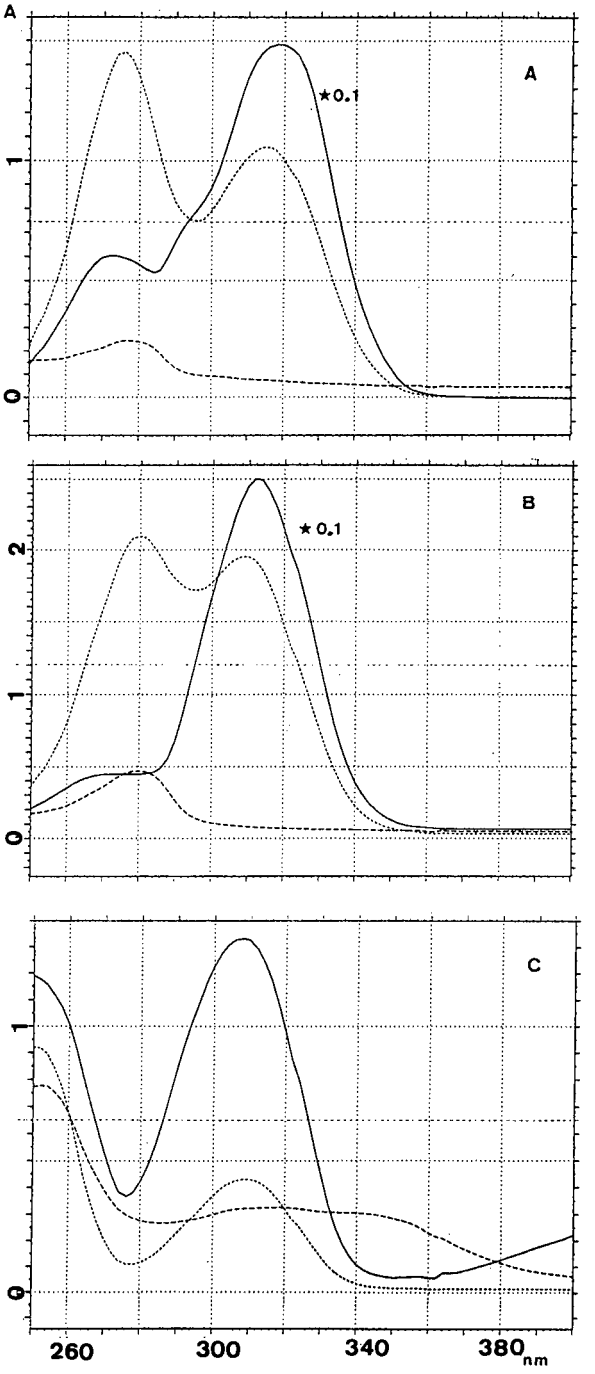

Fig. 6. Ratio spectra (solid lines) for some polyphenolic compounds (dotted lines) and their respective photoproducts (dashed lines). (A) 2,4-Dimethoxybenzaldehyde, (B) vanillin and (C) α-resorcylic acid. Ratio spectra have been multiplied by the indicated factor in order to fit on the absorbance scale for their respective species and photoproduct spectra.

TABLE II

SPECTRAL RATIOS (ABSORBANCE RATIOS FOR SELECTED WAVELENGTHS) FOR POLYPHENOLIC COMPOUNDS SUBJECTED OR NOT TO PHOTOREACTION

Compound	Absorbance ratio[a]		
	260 nm	280 nm	320 nm
Acids			
3-Hydroxybenzoic[b]	0.6	0.9	0.7
4-Hydroxybenzoic	1.5	1.0	0.2
2,4-Dihydroxybenzoic (β-resorcylic)[b]	1.0	0.9	0.9
3,5-Dihydroxybenzoic (α-resorcylic)	1.0	0.4	1.0
2,5-Dihydroxybenzoic (gentisic)	0.5	0.6	0.9
2,6-Dihydroxybenzoic (γ-resorcylic)[b]	0.9	0.8	1.0
3,4-Dihydroxybenzoic	1.4	1.3	0.7
2,4,6-Trihydroxybenzoic (protocatechuic)[b]	0.9	0.9	0.9
3,4,5-Trihydroxybenzoic (gallic)[b]	1.1	1.1	1.5
2,4-Dimethoxybenzoic	2.0	1.5	0.2
2,6-Dimethoxybenzoic	1.9	3.9	0.6
3,4-Dimethoxybenzoic (veratric)	2.8	1.9	0.3
3,5-Dimethoxybenzoic	1.2	0.6	0.8
3,4,5-Trimethoxycinnamic	3.9	12.2	147.8
4-Hydroxy-3-methoxybenzoic (vanillic)	2.7	2.0	0.2
4-Hydroxy-3,5-dimethoxybenzoic (syringic)	1.3	1.5	0.3
3-Hydroxycinnamic (*m*-coumaric)	8.8	10.5	42.1
2-Hydroxycinnamic (*o*-coumaric)	10.3	9.3	61.8
4-Hydroxycinnamic (*p*-coumaric)	2.9	7.2	116.5
3,4-Dihydroxycinnamic (caffeic)	4.7	2.9	147.7
4-Hydroxy-3-methoxycinnamic (ferulic)	3.4	2.9	53.7
3,5-Dimethoxy-4-hydroxycinnamic (sinapic)	2.2	3.7	131.2
Aldehydes			
3-Hydroxybenzaldehyde	6.7	0.4	7.2
4-Hydroxybenzaldehyde	7.4	10.0	2.3
2,5-Dihydroxybenzaldehyde	8.0	0.4	2.7
3,4-Dihydroxybenzaldehyde (protocatechualdehyde)	2.1	4.0	10.9
2,4-Dimethoxybenzaldehyde	3.3	5.1	10.8
3,4-Dimethoxybenzaldehyde (veratraldehyde)	4.8	4.8	42.8
3,5-Dimethoxybenzaldehyde	3.9	2.9	6.2
3,4,5-Trimethoxybenzaldehyde	1.9	6.0	5.3
2-Hydroxy-3-methoxybenzaldehyde (*o*-vanillin)	7.2	1.6	3.0
4-Hydroxy-3-methoxybenzaldehyde (vanillin)	3.8	5.7	51.7
3-Hydroxy-4-methoxybenzaldehyde (isovanillin)	3.1	3.6	13.8
3,5-Dimethoxy-4-hydroxybenzaldehyde	0.7	7.8	22.5

[a] Absorbance at the peak apex for the indicated wavelength with photoreactor turned off divided by absorbance at the peak apex at the same wavelength with photoreactor turned on.

[b] Compounds not affected by photoreactions (see Table I and text).

completely photodegrade in mobile phases acidified with acetic acid, and as the photoreactions take place in the postcolumn mode, its usefulnesss for identification purposes is relatively small. Owing to the lack of research on the influence of other acids, formic acid is recommended for these purposes.

Spectral relationships

The phenomena described above will make it possible for a new qualitative dimension to be available for the analysis of these types of compounds. The inspection of spectra associated with peaks obtained with a photoreactor turned off or on in two

identical, consecutive injections will allow a more reliable identification of species in complex samples. If such a possibility is available, by creating a library of spectra of photoreaction products, the task of identification and discrimination will be greatly simplified. A library could be created where ratio spectra (with the photoreactor turned off and on) could be stored in order to make identification even easier. In fact, these ratio spectra are characteristic for the different species studied. An example of this possibility can be seen in Fig. 6, which shows spectra corresponding to 2,4-dimethoxybenzaldehyde, vanillin and α-resorcylic acid.

If a diode-array detector is not available but a wavelength-programmable detector is, it is possible to determine some spectral relationships for the same purposes. In our study we found that absorbance ratios at 260, 280 and 320 nm allow typical relationships to be determined for each species, and are able to discriminate the species studied here. These relationships are summarized in Table II, where several compounds (see footnote) are considered to be unaffected by photoreactions. In fact, this is not exactly true because, as can be seen from the absorbance ratios, slight modifications have been produced. Hence the criterion was to consider a photoreaction to be significant when one or more characteristic absorption bands in the spectrum were clearly modified and not when the whole spectrum was slightly decreased but conserved all of its typical features. Obviously this fact cannot be seen properly if only the absorbance ratios at the three selected wavelengths are considered.

ACKNOWLEDGEMENT

This research was supported by the Spanish Interministerial Commission for Science and Technology (National Plan for Food Technology, project ALI89/0827).

REFERENCES

1 J. Ribereau-Gayon, E. Peynaud and P. Sudraud, *Sciences et Techniques du Vin*, Vol. 1, Dunod, Paris, 1976.
2 V. L. Singleton and P. Esau, *Phenolics Substances in Grapes and Wines and Their Significance*, Academic Press, New York, 1969.
3 C. Barroso, R. Cela and J. A. Pérez-Bustamante, *Chromatographia*, 17 (1983) 249–252.
4 M. D. Meiriño, *Thesis*, University of Santiago de Compostela, Santiago de Compostela, 1990.
5 H. Jansen and R. W. Frei, in K. Zech and R. W. Frei (Editors), *Selective Sample Handling and Detection in HPLC*, Part B, Elsevier, Amsterdam, 1989, Ch. V.
6 J. R. Poulsen and J. W. Birks, in J. W. Birks (Editor), *Chemiluminiscence and Photochemical Reaction Detection in Chromatography*, VCH, New York, 1989, Ch. VI.
7 I. S. Krull, C. M. Selavska, M. Lockabaugh and W. R. Childresss, *LC · GC Int.*, 2 (1989) 28–39.
8 H. Engelhardt and H. D. Neue, *Chromatographia*, 15 (1982) 403–408.
9 C. M. Selavka, K. S. Jino and I. S. Krull, *Anal. Chem.*, 59 (1987) 2221–2224.
10 J. R. Poulsen, K. S. Birks, M. S. Gandelman and J. W. Birks, *Chromatographia*, 12 (1986) 231–234.

Journal of Chromatography, 626 (1992) 127–134
Elsevier Science Publishers B.V., Amsterdam

CHROM. 24 543

Enhanced chromatographic peak-purity evaluation of phenolic solutes using pH-induced spectral transformations

J. B. Castledine and A. F. Fell

Pharmaceutical Chemistry, University of Bradford, Bradford, BD7 1DP (UK)

R. Modin and B. Sellberg

Analytical Chemistry, Kabi Pharmacia Therapeutics AB, Uppsala (Sweden)

ABSTRACT

The utility of pH-induced spectral shifts for enhanced peak-purity detection in its current form is limited. The practical option of using post-column technology to alter detection pH, rather than liquid chromatography (LC) with alkaline mobile phases, generates extra signal noise. In spite of parameter optimisation, and the use of LC-pump technology to add the post-column reagent, the increased noise is such that practical application of the post-column methodology for enhanced peak-purity determination is not realisable at levels of impurity less than 2% (w/w).

INTRODUCTION

A plethora of peak-purity/homogeneity assessment techniques exists to aid in the detection of simultaneously eluting liquid chromatography (LC) solutes. All such algorithms are limited, in part, by the spectral differences between the two or more compounds involved. This particularly applies in the analysis of pharmaceuticals. The spectral similarity of many drug molecules and their potentially related compounds, namely process impurities, degradation products and metabolites, highlights the need to maximise differences between the spectra, if low levels of related compounds are to be detected spectroscopically while eluting concurrently with the parent drug.

In compounds which contain an auxochrome, such as a phenolic group, reversible ionisation results in characteristic changes of the solute's spectroscopic properties. Several authors, including ourselves, have exploited this attribute to enhance LC solute identification using post-column reaction systems [1–3]. A variety of techniques have been used to characterise the spectral differences which arise. Hostettmann *et al.* [1] used an array of pH-shift inducing reagents, comparing the set of absorption maxima obtained for each unknown solute with data obtained from standards. Fell and co-workers [2,3] combined the spectral information obtained under both acid and alkali conditions through the use of difference spectroscopy, displaying the results graphically by employing a second-derivative transformation to highlight differences between the similar phloroglucinol derivatives examined [2]. Numerical characterisation of the pH-shifted difference spectra was also reported, based on absorbance ratios, for the characterisation of dipeptides containing a tyrosyl residue [3].

While the above techniques may be suitable for

Correspondence to: Professor A. F. Fell, Pharmaceutical Chemistry, University of Bradford, Bradford, BD7 1DP, UK.

0021-9673/92/$05.00 © 1992 Elsevier Science Publishers B.V. All rights reserved

LC solute identification as proposed, they are not appropriate for peak-purity evaluation. The limitations of both graphical techniques and of using absorbance ratios have been previously described [4]. Recently the use of multiple-wavelength peak-area correlation has been proposed for the reliable assessment of peak-purity [5] which through the use of correlation coefficients allows multiple wavelengths to be incorporated into the calculation. The use of peak-area data gives a single figure assessment of purity which is, in principle, independent of the resolution between the overlapping components. In addition, the technique is equally applicable to isocratic and gradient elution [6].

This paper examines the use of pH-induced spectral transformations for enhancing the evaluation of peak-purity for phenolic LC solutes. The multiple peak-area correlation technique (MPACT) is used to characterise the spectral discrimination after post-column addition of alkali. The phenolic drug Olsalazine (OLZ) and several potentially related compounds are used as model pharmaceutical LC systems.

EXPERIMENTAL

Reagents

Methanol (HPLC grade, Rathburn Chemicals, UK), sodium dihydrogen phosphate monohydrate (Merck, Darmstadt, Germany) and sodium hydroxide pellets (GPR grade, BDH, Poole, Dorset, UK) were used as received. Both buffer salts were dissolved in distilled water and filtered using HVLP 0.45-μm filters (Waters, Millipore, Milford, MA, USA). All solutions were degassed prior to use. OLZ (reference material, batch 317 840) and the potentially related compounds (structures given in Fig. 1) were from Kabi Pharmacia Therapeutics AB, Uppsala, Sweden.

Apparatus

For both the LC method and the post-column reaction system the apparatus used consisted of two LKB 2150 HPLC pumps, connected using a high pressure mixer (Model No. 2152-400) and controlled using a LKB 2152 controller (all: LKB, Uppsala, Sweden). Injections were made using a Valco injection valve fitted with a 20-μl loop. The column used was stainless-steel (125 mm × 4.0 mm I.D.) packed with 5-μm Nucleosil C_{18} (Macherey-Nagel, Düren, Germany). The post-column addition of alkali was effected using a M-45 HPLC pump (Waters, Milford, MA, USA). An alkali-resistant PLRP-S 100 Å 8-μm (150 mm × 4.6 mm I.D.) column (Polymer Laboratories, Church Stretton,

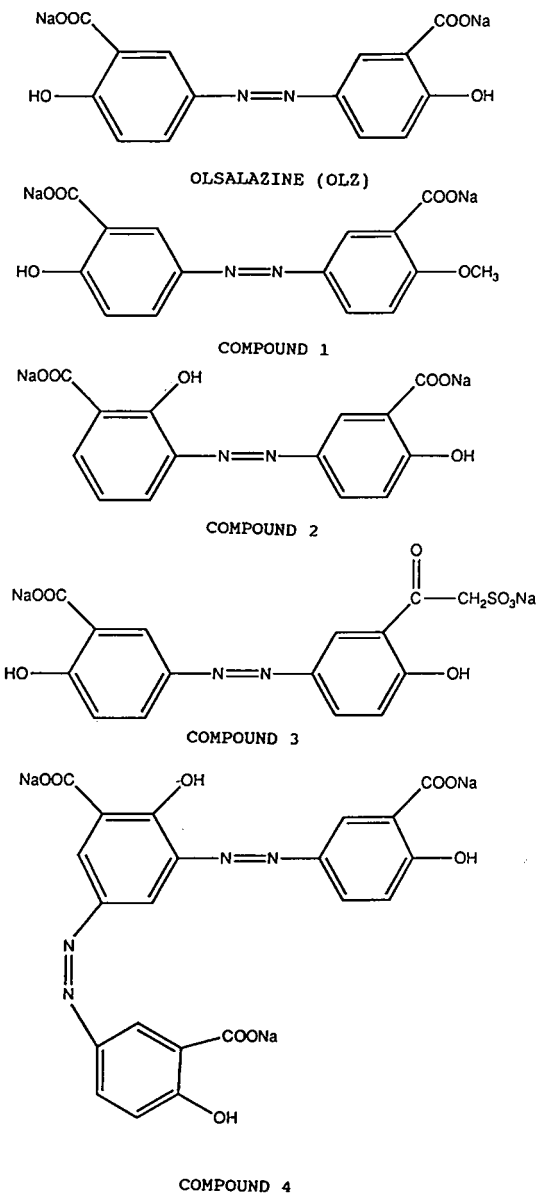

Fig. 1. Structure of Olsalazine (OLZ) and potentially related compounds.

Shropshire, UK) was placed between the pump and a zero volume tee-piece (Supelco, Saffron Walden, Essex, UK) to improve the signal-to-noise performance of the pump. Mixing of the eluent and alkali was generated by using a single-bead string-reactor (250 μm × 300 mm × 0.5 mm I.D.) (Supelco, Saffron Walden, Essex, UK) between the tee-piece and the detector. The post-column apparatus was configured as shown in Fig. 2.

Detection was effected using a HP-1040 diode-array detector (Hewlett-Packard, Waldbron, Germany). Data collection and evaluation were performed using the HP-85 computer, the HP-9000 series Workstation (with HPLC Chemstation software), the HP-7470 plotter and a 9121 dual-disc drive (all: Hewlett-Packard).

Under acidic conditions data were collected at the following wavelengths: 240, 270, 300, 330, 360, 390 and 420 nm. All signals had a bandwidth of 20 nm, and signal noise was reduced further through the use of a reference signal collected at 550 nm with a 100-nm bandwidth.

Detection of the solutes at alkali pH was performed at: 340, 370, 400, 430, 460, 490 and 520 nm. All signals had a bandwidth of 20 nm, and signal noise was reduced further through the use of a reference signal collected at 595 nm with a 10-nm bandwidth. The latter was limited by the spectral range of the detector used.

Acidic LC conditions

The mobile phase, pumped at 1.0 ml/min, consisted of methanol–10 m*M* NaH_2PO_4 buffer, adjusted to pH 5.0. Gradient elution was required to simultaneously elute OLZ and the potentially related compounds (all of which can be readily separated from OLZ using LC [7]). Using mobile phase A [comprising of methanol–buffer (10:90, v/v)] and mobile phase B [comprising of methanol–buffer (90:10, v/v)] the following gradient program was used; 100% A for 1 min, then a linear increase in mobile phase B to 100% over the next two minutes.

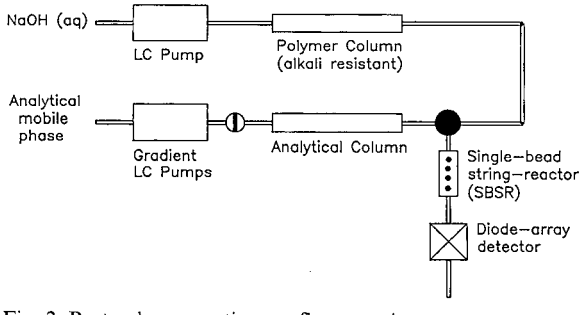

Fig. 2. Post-column continuous-flow reaction system.

Post-column noise reduction

The conditions for optimum signal-to-noise ratio, within the limits set for a suitable change in post-column pH (apparent pH of the methanolic mobile phase, pH* 12.6–12.7), were found to be: flow-rate, 0.5 ml/min; concentration of alkali added 0.7 *M* NaOH.

Computation

Correlation coefficients, r, were calculated using:

$$r = \frac{\Sigma A_{1i} \cdot A_{2i}}{\sqrt{(\Sigma A_{1i}^2 \cdot \Sigma A_{2i}^2)}}$$

where A_{1i} and A_{2i} are the peak-areas at i nm for chromatograms 1 and 2, respectively [8].

It should be noted that this is the appropriate version of the correlation coefficient for use in spectral comparisons since if chromatograms 1 and 2 are of identical samples, differing only in concentration, at i nm: $A_{1i} = m \cdot A_{2i}$, where m = constant. Because the product-moment correlation coefficient determines deviations from the relationship, $y = mx + c$ (where c may be a non-zero value), it is not suitable for this application.

Since correlation coefficients are not normally distributed, Student's t-test was performed after transformation of the data to give the normalised correlation coefficient (NCC) using:

$$\text{NCC} = 0.5 \ln [(1 + r)/(1 - r)]$$

The values of the NCC are approximately normally distributed [9].

Since it was found that the sample standard deviations varied significantly and were dependent, in part, on the absolute value of the NCC, it was considered that the population standard deviations could not be assumed to be equal. Thus the appropriate equation used to calculate the t values was [10]:

$$t = (x_1 - x_2)/\sqrt{(s_1^2/n_1 + s_2^2/n_2)}$$

where x_1 = mean, s_1 = standard deviation, and n_1 = number of normalised correlation coefficients calculated between sample and reference data; and x_2 = mean, s_2 = standard deviation, and n_2 = number of normalised correlation coefficients calculated between two sets of reference data.

Triplicate injections of each sample were made, these injections being bracketed between two sets of reference chromatograms (also in triplicate). This gave rise to nine possible correlations between each sample and each of the two reference sets, albeit with reduced degrees of freedom (DF). These sets of nine correlation coefficients were normalised and compared with the set of nine NCCs generated by correlating the two sets of reference injections using Student's *t*-test. A 95% one-way confidence limit ($t_{TAB} = 1.94$, $DF = 6$) was found to be a suitable discriminator between the reference data and significantly dissimilar sample data (*i.e.*, impure chromatographic peaks).

RESULTS AND DISCUSSION

Comparison of spectral data

It can be shown, using a spectrophotometer, that differences between the spectra of a phenolic drug, in this case OLZ, and certain potentially related compounds may be enhanced by the presence of an alkaline environment. This is shown in Fig. 3, using data collected from the chromatographic injections. Moreover, given the structure of a possible impurity which may be eluting simultaneously with the parent molecule, it is apparent that the benefit, or otherwise, of detection in alkaline conditions may be anticipated.

For the model systems presented it can be observed that the spectral characteristics of the potentially related compounds, compound 1 and compound 4 differ most from OLZ at elevated pH. It is not surprising that in both cases there is a different number of phenolic groups present in these molecules compared with OLZ.

Note that the pK_a values for the two phenolic auxochromes of OLZ are 11.0 and 11.9 [11], thus an environment of pH 13.9 is required to ensure total ionisation. Clearly this is not practicable for this type of experimentation. Thus, results are based upon the maximum achievable ionisation at a defined pH* *ca.* 12.6.

Compound 2 is spectrally more similar to OLZ at the alkaline pH. This may be explained by the loss of weak bonding between the hydrogen of the (ortho) phenolic group and the azo-bond nitrogen when ionised. The spectral differences between OLZ and compound 3 are not greatly affected by pH. This can be explained by considering the two factors involved when there are no differences involving the auxochrome. Firstly, the bathochromic shift induced by the alkali results in a loss of spectral discrimination through band broadening. Counterbalancing this is the hyperchromic shift which is also induced. This improves the signal/noise quality of the data. The application of these observations to aid in the determination of chromatographic peak-purity, and the limitations arising, are examined below.

Chromatographic peak-purity assessment

The results of applying MPACT to the LC systems containing overlapping peaks of OLZ and one of the potentially related compounds, are given in Tables I to IV and summarised in Table V as discussed below.

Acidic LC. From the results it may be observed that, in all cases, the limit of detection for the simultaneously eluting impurity is greater than 1% w/w. This highlights the limits of LC–diode-array detection often found for method development and validation.

In general, the results obtained from the present series of experiments typify those reported for most pharmaceuticals and their potentially related molecules, and arise primarily as a consequence of the strong spectral similarity between these compounds [12–16].

Comparison of the mean correlations between the sets of reference data, bracketing the samples, show both day-to-day and within-day variations. This illustrates the importance of bracketing the samples between standards when estimating the extent of signal variation due to noise.

It is possible to exploit the enhanced spectral differences between OLZ and compound 1 or compound 4 using alkali LC conditions [17]. However, a significant limitation in raising the pH, using for example polymer-based columns, is that this imposes a severe constraint on the range of pH available for optimising the separation of the known impurities. Moreover, not all impurities will be

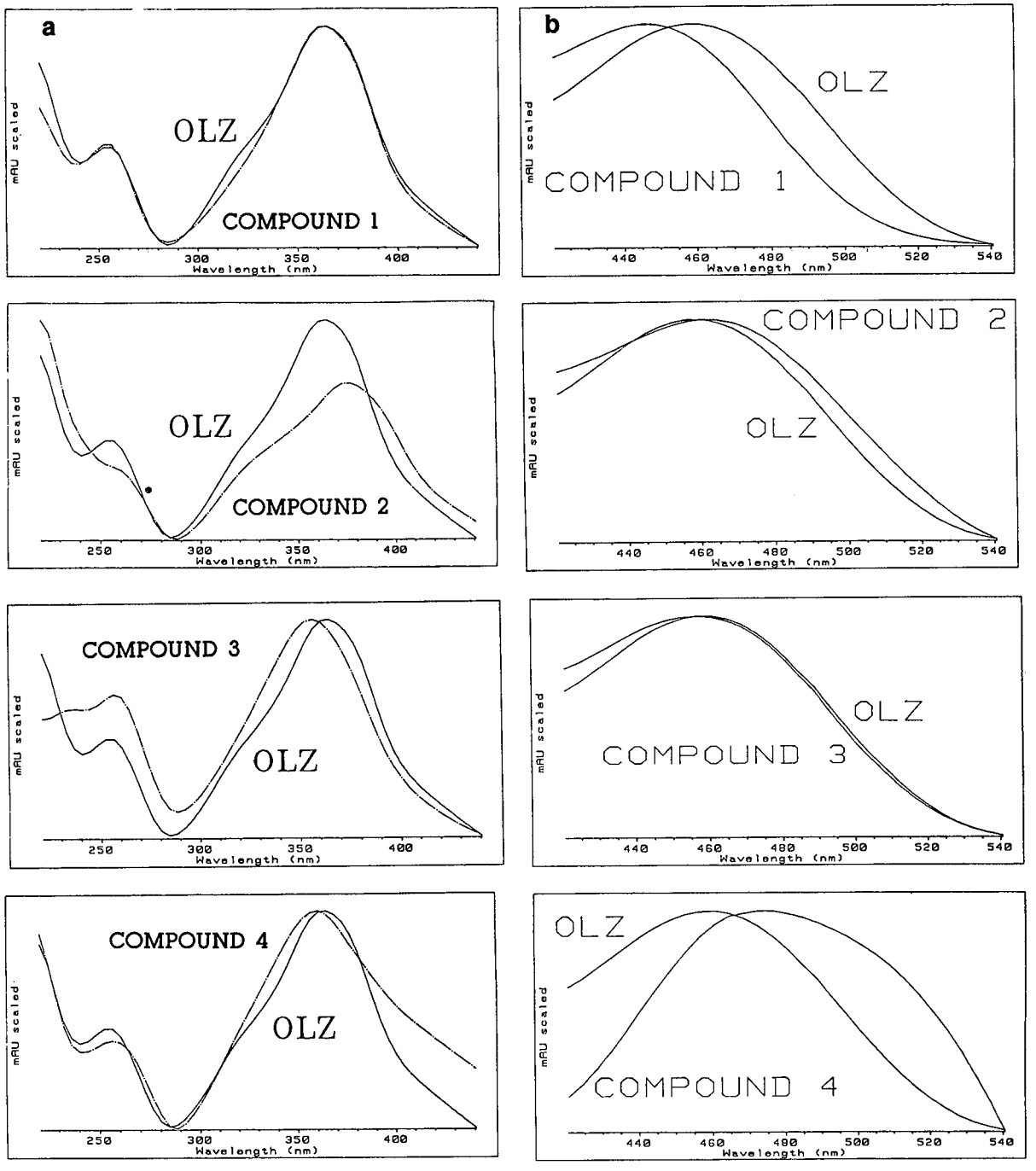

Fig. 3. (a) Spectra of OLZ and the potentially related compounds under acidic conditions (pH 5.5). Compound 1: $r = 0.999$, NCC = 3.81; compound 2: $r = 0.979$, NCC = 2.28; compound 3: $r = 0.987$, NCC = 2.51; compound 4: $r = 0.987$, NCC = 2.53. (b) Spectra of OLZ and the potentially related compounds under alkali conditions (pH* 12.6). Compound 1: $r = 0.966$, NCC = 2.03; compound 2: $r = 0.994$, NCC = 2.88; compound 3: $r = 0.992$, NCC = 2.78; compound 4: $r = 0.935$, NCC = 1.70.

TABLE I

THE LIMIT OF DETECTION FOR THE SIMULTANEOUSLY ELUTING POTENTIALLY RELATED PRODUCT (COMPOUND 1) ADDED TO OLZ

Added compound 1 (% w/w)	Reference			
	A^a		B^b	
	Mean NCC	t^d	Mean NCC	t^d
Acidic LC				
Ref.[c]	7.19	–	–	–
0.5	7.61	−4.60	7.64	−3.32
1.0	7.31	−1.53	7.44	−1.72
2.0	7.06	1.88	7.24	−0.32
4.0	6.93	4.17*[e]	7.34	−1.33
Ref.[c]	7.61	–	–	–
6.0	6.46	5.23*	6.49	5.03*
8.0	6.45	9.20*	6.53	8.52*
10	6.29	11.3*	6.40	9.87*
20	5.74	16.0*	5.81	15.2*
Compound 1 only	3.81	33.2*	3.82	33.1*
Post-column addition of alkali				
Ref.[c]	5.71	–	–	–
0.5	5.66	0.26	5.71	0.02
1.0	5.63	0.51	5.69	0.15
2.0	5.42	1.65	5.52	1.28
4.0	5.49	1.40	5.56	0.84
Ref.[c]	5.50	–	–	–
6.0	5.38	1.14	5.50	0.00
8.0	5.06	3.50*	5.07	3.32*
10	4.71	7.72*	4.80	6.30*
20	4.13	13.4*	4.13	12.9*
Compound 1 only	2.03	35.6*	2.03	35.6*

[a] Correlation between samples and the preceeding reference injections.
[b] Correlation between samples and the successive reference injections.
[c] Correlation between the two pairs of bracketing reference injections.
[d] $t_{TAB} = 1.94$, $p = 0.05$.
[e] * Denotes a significant difference using the t-test (*i.e.*, detection of the co-eluting species).

TABLE II

THE LIMIT OF DETECTION FOR THE SIMULTANEOUSLY ELUTING POTENTIALLY RELATED PRODUCT (COMPOUND 2) ADDED TO OLZ

For key to superscripts see Table I.

Added compound 2 (% w/w)	Reference			
	A^a		B^b	
	Mean NCC	t^d	Mean NCC	t^d
Acidic LC				
Ref.[c]	6.74	–	–	–
0.5	7.29	−2.04	7.12	−1.37
1.0	6.67	0.31	6.75	−6.20
2.0	6.13	3.10*[e]	6.24	2.56*
4.0	5.64	5.84*	5.71	5.51*
Ref.[c]	6.96	–	–	–
6.0	5.33	13.9*	5.46	12.8*
8.0	5.10	15.8*	5.21	15.0*
10	4.83	18.3*	4.90	17.7*
20	4.21	23.6*	4.24	23.3*
Compound 2 only	2.28	40.3*	2.28	40.2*
Post-column addition of alkali				
Ref.[c]	5.27	–	–	–
0.5	4.84	4.38*	5.38	−0.92
1.0	5.48	−1.35	5.39	−0.69
2.0	5.35	−1.12	5.81	−4.79
4.0	5.14	0.90	5.55	−2.59
Ref.[c]	5.21	–	–	–
6.0	6.01	−5.62	5.04	1.91
8.0	5.62	−4.28	5.16	0.52
10	5.04	2.13*	5.27	−0.61
20	4.57	8.83*	4.80	4.70*
Compound 2 only	2.88	33.2*	2.91	32.7*

preferentially discriminated in alkali conditions.

The better strategy should be post-column addition of the pH-shifting reagent. This allows the optimum separation of all known compounds by regular means through the selection of an appropriate column and mobile phase. Furthermore, detection can be effected at any pH (whether acid or alkaline) to ensure optimum peak-purity detection.

Post-column addition of alkali. Post-column continuous-flow analysis has previously been applied to shifting eluent pH [1–3], and the problem of increased signal-to-noise ratio has been described [18]. Differences in the spectral characteristics of the mobile phase and the alkali, together with the slight fluctuations in pressure from both pumps which will affect the post-column eluent constitution, are the

TABLE III

THE LIMIT OF DETECTION FOR THE SIMULTANEOUSLY ELUTING POTENTIALLY RELATED PRODUCT (COMPOUND 3) ADDED TO OLZ

For key to superscripts see Table I.

Added compound 3 (% w/w)	Reference			
	A[a]		*B*[b]	
	Mean NCC	*t*[d]	Mean NCC	*t*[d]
Acidic LC				
Ref.[c]	6.85	–	–	–
0.5	6.84	0.02	7.18	−1.04
1.0	6.60	0.97	7.01	−0.60
2.0	6.15	3.10*[e]	6.39	2.06*
4.0	5.74	5.21*	5.93	4.41*
Ref.[c]	7.46	–	–	–
6.0	5.56	7.60*	5.63	7.34*
8.0	5.29	8.70*	5.34	8.50*
10	5.03	9.76*	5.07	9.60*
20	4.41	12.3*	4.43	12.2*
Compound 3 only	2.51	20.0*	2.51	20.0*
Post-column addition of alkali				
Ref.[c]	5.55	–	–	–
0.5	6.17	−3.99	5.50	0.27
1.0	5.84	−1.73	5.32	1.21
2.0	5.49	0.24	5.49	0.33
4.0	5.26	1.86	5.84	−1.24
Ref.[c]	5.49	–	–	–
6.0	5.83	−1.49	5.27	1.86
8.0	5.80	−1.21	5.21	2.13*
10	5.30	1.30	5.04	4.06*
20	5.01	2.61*	4.72	6.21*
Compound 3 only	2.78	29.2*	2.74	29.7*

TABLE IV

THE LIMIT OF DETECTION FOR THE SIMULTANEOUSLY ELUTING POTENTIALLY RELATED PRODUCT (COMPOUND 4) ADDED TO OLZ

For key to superscripts see Table I.

Added compound 4 (% w/w)	Reference			
	A[a]		*B*[b]	
	Mean NCC	*t*[d]	Mean NCC	*t*[d]
Acidic LC				
Ref.[c]	6.74	–	–	–
0.5	7.20	−2.72	6.81	−0.34
1.0	6.99	−1.92	6.58	0.90
2.0	6.48	2.04*[e]	6.22	3.58*
4.0	5.90	6.59*	5.78	7.36*
Ref.[c]	6.60	–	–	–
6.0	5.48	10.1*	5.59	9.28*
8.0	5.22	12.6*	5.29	12.1*
10	5.05	14.2*	5.09	13.9*
20	4.46	19.7*	4.48	19.6*
Compound 4 only	2.53	37.6*	2.53	37.6*
Post-column addition of alkali				
Ref.[c]	5.66	–	–	–
0.5	5.94	−1.24	5.74	−0.33
1.0	5.66	−0.01	5.82	−0.80
2.0	5.49	0.83	5.67	−0.06
4.0	5.58	0.41	5.35	1.56
Ref.[c]	5.53	–	–	–
6.0	5.37	0.95	5.27	1.53
8.0	5.03	3.29*	5.04	2.96*
10	4.84	4.51*	4.88	4.21*
20	4.35	7.90*	4.38	7.66*
Compound 4 only	1.70	25.9*	1.71	25.8*

main factors involved in reducing the signal/noise quality of the analytical data.

An LC pump was found to be more suited to the application of adding post-column eluent than the previously used peristaltic pump. Noise was further reduced by raising back-pressure of the post-column eluent. This was achieved by placing an alkali-resistant LC polymer column before the mixing tee, allowing the post-column pump to work at its designated back-pressure specification. Alternatively a back-pressure regulator and/or pulse dampener could have been used. The signal-to-noise (S/N) ratio was optimised using a simplex method [19],

TABLE V

SUMMARY TABLE: LIMIT OF DETECTION FOR THE SIMULTANEOUSLY ELUTING POTENTIALLY RELATED COMPOUNDS

Compound added	Conditions	
	Acidic LC	Post-column addition of alkali
1	4–6%	8%
2	2%	10–20%
3	2%	8–20%
4	2%	8%

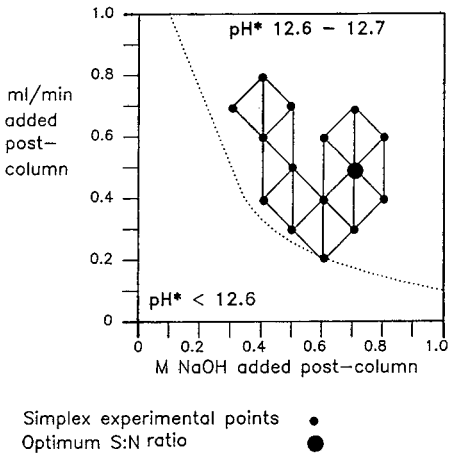

Fig. 4. Simplex optimisation of the post-column signal-to-noise ratio.

with the alkali concentration and post-column reagent flow-rate being varied within the constraint that permitted the highest achievable pH to be obtained (pH* 12.6–12.7) (Fig. 4).

Despite this, Tables I–V show that increased noise (*i.e.*, lower correlation between reference standards) results from the incorporation of the post-column system. The consequence of this is that, in all the model systems presented, a higher limit of detection for the simultaneously eluting impurity was recorded.

Further work is continuing in the Authors' laboratory to develop simpler and more effective methods of post-column pH modification. The use of alternate auxochromes with lower pK_a values, facilitating total ionisation and thus reducing noise, is also being investigated.

ACKNOWLEDGEMENTS

One of the authors (JBC) would like to thank Kabi Pharmacia Therapeutics AB for kindly providing the studentship for this research.

REFERENCES

1 K. Hostettmann, B. Domon, D. Schaufelberger and M. Hostettmann, *J. Chromatogr.*, 297 (1984) 137–147.
2 A. F. Fell, T. Z. Woldemariam, P. A. Linley, Ge Jian, M. D. Luque De Castro and M. Valcarcel, *Anal. Chim. Acta*, 234 (1990) 89–95.
3 A. F. Fell, J. B. Castledine, B. Sellberg, R. Modin and R. Weinberger, *J. Chromatogr.*, 535 (1990) 33–39.
4 J. B. Castledine, A. F. Fell, R. Modin and B. Sellberg, *J. Pharm. Biomed. Anal.*, 9 (1991) 619–624.
5 J. B. Castledine, A. F. Fell, R. Modin and B. Sellberg, *J. Chromatogr.*, 592 (1992) 27–36.
6 J. B. Castledine, A. F. Fell, R. Modin and B. Sellberg, *J. Pharm. Pharmacol.*, (1992) in press.
7 Data on file, *Kabi Pharmacia Therapeutics*, Uppsala, Sweden.
8 J. C. Reid and E. C. Wong, *Applied Spectroscopy*, 20 (1966) 320–325.
9 G. M. Clark and D. Cooke, *A Basic Course in Statistics*, Arnold, London, 2nd ed., 1983, pp. 333–337.
10 J. C. Miller and J. N. Miller, *Statistics for Analytical Chemistry*, Ellis Horwood, Chichester, 2nd ed., 1988, p. 57.
11 Data on file, *Kabi Pharmacia Therapeutics*, Uppsala, Sweden.
12 A. F. Fell, H. P. Scott, R. Gill and A. C. Moffat, *J. Chromatogr.*, 282 (1983) 123–140.
13 P. C. White, *Analyst*, 113 (1988) 1625–1629.
14 T. D. Wilson, W. F. Trompeter and H. F. Gartelman, *J. Liq. Chromatogr.*, 12(7) (1989) 1231–1251.
15 J. G. D. Marr, G. G. R. Seaton, B J. Clark and A. F. Fell, *J. Chromatogr.*, 506 (1990) 289–301.
16 H. K. Chan and G. P. Carr, *J. Pharm. Biomed. Anal.*, 8 (1990) 271–277.
17 J. B. Castledine, *PH.D. Thesis*, University of Bradford, Bradford, 1992.
18 J. B. Castledine, A. F. Fell, B. Sellberg, R. Modin, M. D. Luque De Castro and M. Valcarcel, *J. Pharm. Biomed. Anal.*, 8 (1990) 1079–1082.
19 J. C. Berridge, *Techniques for the Automated Optimisation of HPLC Separations*, Wiley, London, 1985, p. 126.

Journal of Chromatography, 626 (1992) 135–143
Elsevier Science Publishers B.V., Amsterdam

CHROM. 24 338

Supercritical fluid extraction of polychlorinated biphenyls and pesticides from soil

Comparison with other extraction methods

E. G. van der Velde, W. de Haan and A. K. D. Liem

Laboratory of Organic-Analytical Chemistry, National Institute of Public Health and Environmental Protection (RIVM), P.O. Box 1, 3720 BA Bilthoven (Netherlands)

ABSTRACT

A comparison is made of supercritical fluid extraction (SFE) with two other techniques widely used for the extraction of polychlorinated biphenyls (PCBs) and organochlorine pesticides in soil. Extraction conditions for the SFE of PCBs and pesticides were first determined. An experimental approach was set up to determine the influence of different extraction parameters such as pressure, extraction time, static and dynamic extraction, restrictor type and collection solvent for off-line SFE. The use of carbon dioxide at 50°C and 20 MPa, 10 min static followed by 20 min dynamic extraction with collection in iso-octane were been found to be the optimum conditions. Two types of soil, with a low and high content of organic carbon, respectively, spiked with 16 PCBs and organochlorine pesticides with a wide range of volatility and polarity at a level of 5 ng/g dry matter, were used as test materials. Conventional solvent extraction gives a good extraction yield for soil with a low content of organic carbon, but for peat soil the recoveries decrease dramatically to 30% for DDE, DDT and PCB 138 and 153. The recoveries with Soxhlet extraction are good, but an extra clean-up step before analysis is necessary. SFE gives good extraction yields for PCBs and organochlorine pesticides, varying between 85 and 105% with a reproducibility of 5% for each component for both types of soil. SFE is a fast, clean and reproducible method for the extraction of PCBs and organochlorine pesticides from these two soil matrices.

INTRODUCTION

Every five years a monitoring programme for organochlorine pesticides and polychlorinated biphenyls (PCBs) is carried out to observe trends in the levels of these components in soils in the Netherlands [1]. Several studies have shown that supercritical fluid extraction (SFE) results in good extraction yields for chlorinated contaminants in soils [2–12]. Therefore the application of SFE as an alternative extraction technique to conventional methods for the extraction of soil samples was evaluated in this laboratory. The latter techniques are laborious, time consuming and require large amounts of high purity solvents which produce problems of hazardous waste. In addition especially for the more non-polar components [hexachlorobenzene (HCB), 2,2-bis(*p*-chlorophenyl)-1,1,1-trichloroethane (DDT) complexes and PCBs] solvent extraction often gives low extraction yields when applied to soils with high contents of organic carbon.

Several studies have described the use of SFE for the extraction of organic contaminants from different matrices. Lopez-Avila *et al.* [2] extracted several groups of organochlorine and organophosphorus pesticides spiked on sand with good recoveries (from 80 to 125%) using either CO_2 or, more advantageously, CO_2 modified with 10% methanol. Hawthorne and Miller [3–5] studied the extraction of polycyclic aromatic hydrocarbons from reference

Correspondence to: Dr. E. G. van der Velde, Laboratory of Organic-Analytical Chemistry, National Institute of Public Health and Environmental Protection (RIVM), P.O. Box 1, 3720 BA Bilthoven, Netherlands.

0021-9673/92/$05.00 © 1992 Elsevier Science Publishers B.V. All rights reserved

materials and other matrices and obtained results in good agreement with certified values, in contrast to the results reported by Lopez-Avila *et al.* [2]. The extraction of total PCBs from a certified sediment sample was demonstrated by Onuska and Terry at 20 mPa, 40°C in 8 min using CO_2 with 2% methanol [6]. SFE of pesticides from soils and sediments has been studied using CO_2 saturated with water or with the direct addition of methanol to the extraction cell to increase recoveries [7–9]. Several studies have reported the optimization in terms of the modifier, pressure, temperature and flow-rate of the extraction of diuron and linuron from sand [10] and several chlorinated components [11] and 2,3,7,8-tetrachlorodibenzo-*p*-dioxin from sediments [12].

SFE has many potential advantages compared with conventional solvent extraction methods, including reduced extraction times and amounts of extraction solvents. It also gives more efficient extractions, increased selectivity and the possibility of coupling with other chromatographic techniques. Based on their variable solvating power as a function of density, supercritical fluids have several characteristics that make them ideal extraction solvents to selectively extract and isolate discrete fractions from sample matrices. Rapid mass transfer during extraction is facilitated by the low viscosity and high solute diffusivities due to the liquid- and gas-like behaviour of supercritical fluids. In SFE CO_2 is most often chosen as the extraction solvent because of its moderate critical temperature (31°C) and pressure (73 atm), its non-flammable and non-toxic properties, low cost and minimized problems of waste.

In this paper results are presented for the optimization of SFE conditions for the determinations of organochlorine pesticides and PCBs in soils containing different amounts of organic carbon. Results are compared with those obtained by the application of conventional extraction techniques.

EXPERIMENTAL

Samples

Two types of soil characterized by the percentage of moisture, dry matter, pH and organic carbon were used as test materials: a peat soil with a relatively high organic carbon content (3.3%) and a sand with a low organic content (0.3%). Soils were air-dried, allowed to pass through a 2.8 mm sieve and subsequently homogenized in a ball mill. Individual soil samples were spiked just before analysis, waiting for 15 min to 1 h to allow evaporation of the solvents (the evaporation time depended on the amount of solvent used). Based on their occurrence in Dutch soils, the following compounds were selected for this study: α-hexachlorocyclohexane (α-HCH), HCB, β-HCH, γ-HCH, β-heptachlorepoxide (β-HEPO), 2,2-bis(*p*-chlorophenyl)-1,1-dichloroethene (*p,p'*-DDE), dieldrin, 2,2-bis(*p*-chlorophenyl)-1,1-dichloroethane (TDE), *o,p'*-DDT, *p,p'*-DDT and PCB 28, PCB 52, PCB 101, PCB 118, PCB 138 and PCB 153. PCBs were from CIL (Cambridge Isotope Laboratories, Woburn, MA, USA), pesticides from Promochem (Wesel, Germany). Spiking levels were chosen based on levels previously observed and were typically between 1 and 10 ng/g of dry soil.

Extraction procedures

Solvent extraction. Aliquots of 25 g of soil were extracted twice with 40 ml of acetone for 30 min using a shaking machine. The liquid fractions were mixed with 800 ml of water and a few millilitres of saturated sodium chloride, and were then extracted twice with 50 ml of hexane. The combined hexane fractions were dried and, after the addition of internal standards (PCBs 44 and 141), were concentrated in a Kuderna-Danish apparatus until 10 ml remained. All solvents used were pesticide-grade (hexane) or distilled (acetone, light petroleum).

Soxhlet extraction. Aliquots of 5 g of soil mixed (1:3, w/w) with quartz sand (Boom, Meppel, Netherlands) were placed in a modified Soxhlet extraction unit consisting of a fritted porosity glass extraction tube and were extracted for 14 hours with 150 ml of acetone–light petroleum (b.p. 30–60°C) (1:1, v/v). After cooling, 600 ml of water and a few millilitres of saturated sodium chloride were added for solvent extraction; light petroleum was separated and a second extraction with 50 ml of light petroleum was performed. The combined light petroleum fractions were dried and, after the addition of internal standards, were concentrated in a Kuderna-Danish apparatus until 5 ml remained.

Supercritical fluid extraction. The SFEs were performed on a Carlo Erba SFC 3000 instrument using a double 70-ml syringe pump (SFC 300) and an

SFE-30 extraction unit (Carlo Erba Instruments, Milan, Italy). The apparatus can be used in on-line and off-line modes; in the latter the restrictor is disconnected from the transfer tube and solvent sample collection can be performed. Extractions can be performed using constant pressure (varying from 15 to 50 MPa) or at constant flow and the temperature of the extraction unit can be varied between 40 and 150°C. The extraction process was pre-programmed using integrated software to perform valve switching and time programmed extractions with combinations of static and dynamic extraction conditions at various pressure settings. Supercritical pressure was maintained inside the extraction vessel using a deactivated fused-silica 1.5 m × 25 or 50 μm I.D. restrictor (SGE, Austin, TX, USA). Optimization experiments were carried out using glass beads (250 μm, acid washed and silanized; Supelco, Bellefonte, PA, USA) as the sample matrix, an 0.5-ml extraction vessel and sample collection into a 2-ml vial containing approximately 1 ml of organic solvent spiked with a known concentration of internal standard mixture (PCB 44 and 141). CO_2 was of SFC grade from Ucar (Union Carbide, Westerlo, Belgium).

Analysis

An HP 5890 gas chromatograph equipped with an HP 7673A autosampler, an electron-capture detector and a 50 m × 0.2 mm I.D. fused-silica capillary column (Ultra-2, HP, 0.33 μm film) was used for the chromatographic separation and was interfaced with an HP-Chem data system (Hewlett-Packard, Palo Alto, CA, USA). Helium was used as the carrier gas (2 ml/min) and argon–methane as the purge gas (60 ml/min). After the injection of 4 μl the temperature programme consisted of an initial temperature of 80°C, 2 min hold, then an increase to 170°C at 30°C/min, then 3°C/min to the final temperature of 290°C and held for 5 min. The injector temperature was 200°C and the detector temperature was 325°C. Quantification was performed by comparison with a reference standard mixture using PCB 44 and 141 as internal standards.

RESULTS AND DISCUSSION

Optimization of extraction conditions

Optimization experiments were carried out using glass beads spiked with a standard mixture of sixteen pesticides and PCBs in hexane followed by off-line SFE with sample collection in hexane. After each experiment a second extraction was performed to check if all the components had been extracted under the conditions used and to confirm that a clean system was used for the next experiment. Preliminary experiments were performed using different tapered and linear restrictors. Tapered restrictors caused clogging problems, so linear restrictors of 25 and 50 μm I.D. were used in spite of the disadvantages of a decrease in pressure over the whole linear range of the restrictor. The internal diameter of the restrictor in combination with its length (at fixed pressure) determines the flow-rate and the volume of CO_2 passing through the extraction cell during a certain time period. Table I gives the results for 25 and 50 μm restrictors for 20 and 50 min dynamic extractions, respectively. The same extraction yields (89 and 88%, respectively) can be obtained for a restrictor with a larger internal diameter in a shorter time (50 μm and 20 min) than for restrictors with a smaller I.D. (25 μm and 50 min). Finally 50-μm restrictors were chosen because of

TABLE I

COMPARISON OF EXTRACTION RECOVERIES (%) FOR 25 AND 50 μm LINEAR RESTRICTORS WITH DIFFERENT EXTRACTION TIMES (min)

Component	Restrictor (static/dynamic extra time) diameter		
	25 μm (10/20)	25 μm (10/50)	50 μm (10/20)
α-HCH	26	34	55
HCB	–	–	37
β-HCH	63	90	91
γ-HCH	44	–	64
β-HEPO	63	82	91
p,p'-DDE	69	96	106
Dieldrin	67	87	96
TDE	69	91	96
o,p'-DDT	73	116	107
p,p'-DDT	80	109	106
PCB 28	53	74	78
PCB 52	61	83	88
PCB 101	71	100	97
PCB 118	70	90	99
PCB 153	70	94	105
PCB 138	70	91	101
Mean	63	88	89

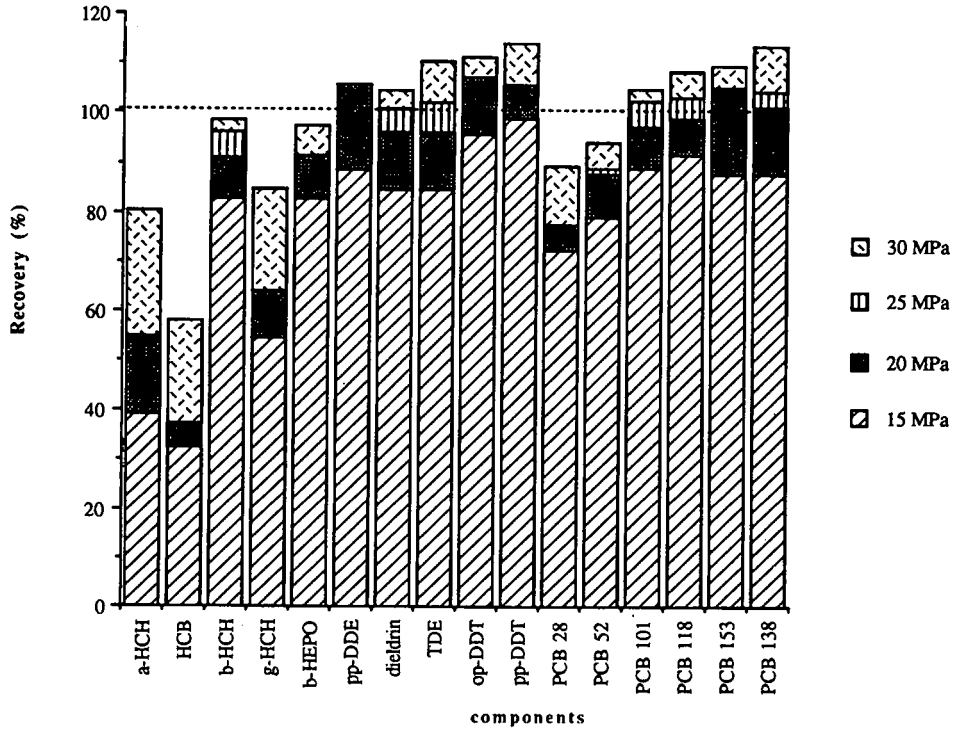

Fig. 1. Influence of variations in pressure on extraction recoveries. The largest improvement in recovery can be observed when increasing the pressure from 15 to 20 MPa. a = α; b = β; g = γ; pp = p,p'; op = o,p'.

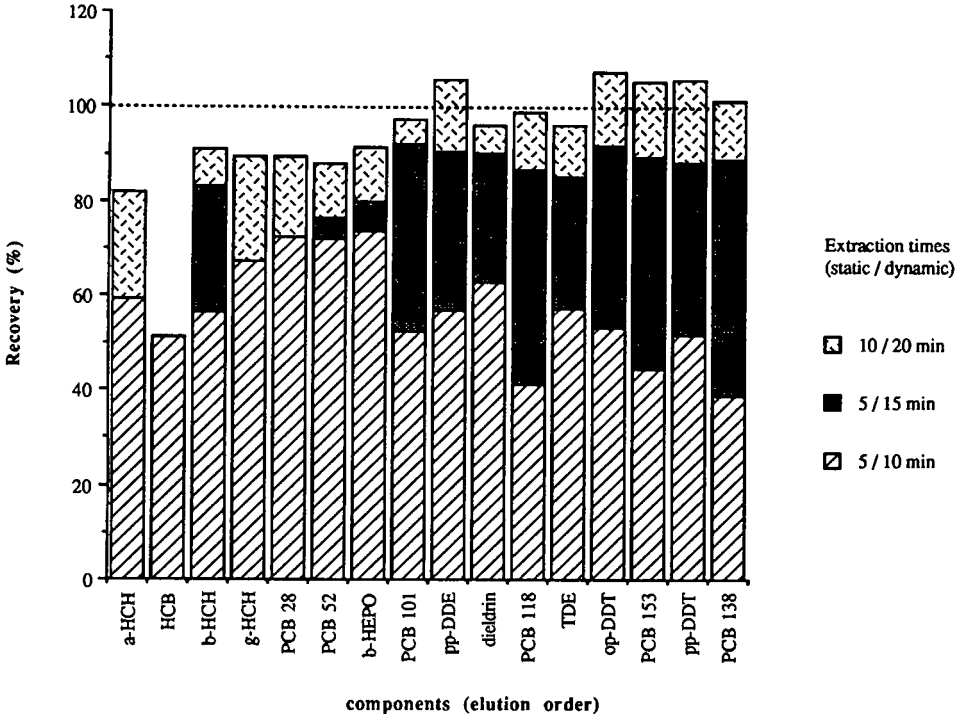

Fig. 2. Influence of extraction times (static/dynamic in min) on extraction yields. Better extraction yields are obtained, especially for the less volatile components, when using longer extraction times (note: components given in order of elution).

TABLE II

REPRODUCIBILITY OF EXTRACTION RECOVERIES (%) OF SFE PROCEDURE

Conditions: 20 MPa; 50°C; 10 min static and 20 min dynamic extraction.

Component	Reproducibility (%)			
	Experiment			Mean ± S.D.
	1	2	3	
α-HCH	55	56	54	55 ± 0.5
HCB	37	37	40	38 ± 1.0
β-HCH	91	98	90	93 ± 1.6
γ-HCH	64	63	64	64 ± 0.1
β-HEPO	91	93	87	90 ± 2.0
p,p'-DDE	106	103	96	101 ± 2.8
Dieldrin	96	97	92	95 ± 1.5
TDE	96	98	89	94 ± 2.6
o,p'-DDT	107	122	102	110 ± 4.2
p,p'-DDT	106	137	104	116 ± 5.7
PCB 28	78	88	80	82 ± 0.9
PCB 52	88	91	87	89 ± 0.8
PCB 101	97	101	93	97 ± 2.0
PCB 118	99	106	96	100 ± 2.3
PCB 153	105	100	94	100 ± 2.8
PCB 138	101	102	94	99 ± 2.5
Mean	89	93	85	89 ± 1.9

TABLE III

INFLUENCE OF COLLECTION SOLVENT ON EXTRACTION RECOVERIES (%)

Conditions: 20 MPa; 50°C; 10 min static and 20 min dynamic extraction.

Component	Hexane	Isooctane
α-HCH	55	95
HCB	38	78
β-HCH	93	105
γ-HCH	64	91
β-HEPO	90	103
p,p'-DDE	101	107
Dieldrin	95	105
TDE	94	102
o,p'-DDT	110	105
p,p'-DDT	116	101
PCB 28	82	105
PCB 52	89	102
PCB 101	97	108
PCB 118	100	110
PCB 153	100	104
PCB 138	100	101
Mean	89	101

the shorter time of analysis. Extraction pressure, combinations of static and dynamic extractions, extraction times and collection solvents were varied and the reproducibility of the system was tested. The extraction pressure was varied from 15 to 30 MPa at constant temperature of 50°C and 30 min extraction. Fig. 1 shows the recoveries for the different extraction conditions. A second extraction of the same sample did not give any increase in yield. A few components, α-HCH, HCB and γ-HCH, show relatively low recoveries compared with the other components, probably as a result of their volatility, which resulted in a less efficient trapping in the solvent used. Excluding the latter components, the largest improvement in recovery can be observed when increasing the pressure from 15 to 20 MPa, whereas only a slight increase in recovery is obtained from 25 to 30 MPa. As higher pressures increase the risk of co-extractants from the matrix, 20 MPa was chosen as the optimum pressure.

Several experiments were performed to establish the ideal extraction times at various combinations of static and dynamic extraction times. Earlier experiments with long static extractions and shorter dynamic extractions showed that the recoveries were low and that second extractions of these samples gave higher yields. Therefore experiments were carried out with 15, 20 and 30 min of extraction (Fig. 2). From Fig. 2 it can be seen that better extraction yields are reached, especially for the less volatile components, when using longer dynamic extraction times. Using the longest extraction time of 10 min static and 20 min dynamic extraction yields between 78 and 107% were found for all except the more volatile components.

The reproducibility of the extraction procedure was studied by triplicate extractions using the proposed conditions (50°C, 20 MPa, 10 min static and 20 min dynamic extractions). Table II shows that SFE gives reproducible extractions with good mean recoveries (89%) and low mean standard deviations (4.2%), with a range of 90.4 ± 3.2% to 115.5 ± 12.9% for all PCBs and chlorinated pesticides, excluding the more volatile pesticides.

To improve the recovery for the volatile pesti-

TABLE IV

COMPARISON OF EXTRACTION RECOVERIES (%) FOR PCBs AND PESTICIDES FROM SAND FOR DIFFERENT EXTRACTION TECHNIQUES

Conditions: 20 MPa; 50°C; 10 min static and 20 min dynamic; collection in iso-octane.

Components	Addition (ng/g)	Solvent extraction (n = 5)		Soxhlet extraction (n = 5)		SFE (n = 3)	
		Recovery (%)	S.D. (%)	Recovery (%)	S.D. (%)	Recovery (%)	S.D. (%)
α-HCH	2.3	86.9	4.3	100.7	1.3	98.8	2.1
HCB	0.9	94.0	5.2	113.0	1.9	88.7	7.2
β-HCH	3.3	93.3	4.0	120.0	4.7	100.5	5.1
γ-HCH	2.2	89.6	4.2	120.9	6.6	100.2	5.2
β-HEPO	3.2	88.3	4.2	106.0	2.7	94.2	1.9
p,p'-DDE	5.1	89.0	3.8	116.1	3.6	92.9	9.6
Dieldrin	4.8	88.1	3.2	101.3	2.8	92.9	3.5
TDE	8.2	87.8	8.2	95.6	2.8	96.2	5.0
o,p'-DDT	8.9	91.5	3.5	164.0	8.0	89.2	2.0
p,p'-DDT	10.1	96.9	3.8	–	–	91.2	5.4
PCB 28	4.9	96.3	4.8	139.6	3.1	98.0	1.5
PCB 52	4.6	92.0	5.3	121.3	4.4	–	–
PCB 101	2.9	94.9	5.0	125.5	4.8	88.2	1.9
PCB 118	2.3	93.2	4.4	136.8	5.3	90.2	6.9
PCB 138	2.4	94.1	3.8	126.0	4.4	86.5	4.7
PCB 153	2.1	94.6	4.4	120.3	3.5	96.2	3.9
Mean	4.3	91.9	4.5	120.5	3.7	93.6	4.1

cides iso-octane was investigated as a collection solvent. Table III shows that a considerable increase in recovery is obtained by chosing the most appropriate collection solvent. By changing to iso-octane acceptable recoveries are also found for α-HCH, HCH and γ-HCH. The mean recovery for all components was 101%, at a level of 5 ng absolute.

Comparison of SFE with other techniques

The optimized conditions (20 MPa, 50°C, 10 min static and 20 min dynamic extraction and solvent collection is isooctane) have been used for the SFE of compounds from two soil samples spiked with a standard mixture of sixteen pesticides and PCBs at a level of 5 ng/g of dry matter. Separate aliquots of the samples were also extracted with two conventional techniques: solvent extraction with acetone–hexane and Soxhlet extraction with acetone–light petroleum. All samples were extracted directly after a fixed time to evaporate the solvent after spiking, thus minimizing the influence of the spiking solvent acting as a modifier during extraction. In this way the analytical recovery was determined.

Tables IV and V give the recoveries and standard deviations for the various techniques applied to sand and peat soils. Solvent extraction of sand gives good recoveries with low standard deviations for all components, varying from 79 ± 3.8% for *p,p'*-DDT to 87 ± 4.3% for α-HCH. For peat soil the recoveries show more variation, with fairly low recoveries for *p,p'*-DDE (32 ± 6.5%), *o,p'*-DDT (41.6 ± 7.0%), *p,p'*-DDT (41 ± 9.6%), PCB 138 (18 ± 8.1%) and PCB 153 (12 ± 6.9%). These results are in agreement with values found for these components in the Dutch soil monitoring programme [1]. Rapid, almost irreversible, adsorption of these components takes place in soils with high organic carbon contents.

Using Soxhlet extraction, very high recoveries are found for sand (mean 121 ± 3.7%) and peat soils (125 ± 7.1%), probably caused by impurities co-extracted during the more intensive Soxhlet extrac-

TABLE V

COMPARISON OF EXTRACTION RECOVERIES (%) FOR PCBs AND PESTICIDES FROM PEAT SOIL FOR DIFFERENT EXTRACTION TECHNIQUES

Conditions: 20 MPa; 50°C; 10 min static and 20 min dynamic; collection in iso-octane.

Components	Addition (ng/g)	Solvent extraction (n = 5)		Soxhlet extraction (n = 5)		SFE (n = 3)	
		Recovery (%)	S.D. (%)	Recovery (%)	S.D. (%)	Recovery (%)	S.D. (%)
α-HCH	2.3	98.2	7.5	103.6	5.2	83.9	1.8
HCB	0.9	78.2	7.7	127.4	7.6	88.3	2.2
β-HCH	3.3	115.6	9.2	137.7	8.4	108.0	1.6
γ-HCH	2.2	101.7	8.2	117.0	6.4	94.7	6.4
β-HEPO	3.2	110.3	9.0	124.2	5.8	107.0	3.9
p,p'-DDE	5.1	32.6	6.5	127.6	7.8	86.9	1.1
Dieldrin	4.8	90.8	8.3	108.9	5.6	89.2	2.5
TDE	8.2	71.9	8.3	88.9	14.2	86.7	3.1
o,p'-DDT	8.9	41.6	7.0	134.5	0.4	94.6	2.6
p,p'-DDT	10.1	40.9	9.6	–	–	98.0	1.9
PCB 28	4.9	79.1	7.9	148.1	8.3	101.0	6.5
PCB 52	4.6	63.9	6.6	114.1	1.8	–	–
PCB 101	2.9	53.3	6.9	133.2	18.8	101.3	1.9
PCB 118	2.3	53.9	7.3	154.1	6.3	96.0	2.7
PCB 138	2.4	18.4	8.1	116.4	6.5	90.8	1.7
PCB 153	2.1	11.9	6.9	134.6	11.2	86.4	2.3
Mean	4.3	66.4	7.8	124.7	7.1	94.2	2.6

tion procedure. In Fig. 3a and b, the chromatograms are shown for peat soil extracted with solvent and Soxhlet extraction, respectively. The chromatograms show several impurities giving increased baselines. An extra clean-up step before analysis, which was not applied here, is necessary to obtain reliable analytical data. SFE of sand and peat soils gives good recoveries for all components, varying from 87 ± 4.7% for PCB 138 to 101 ± 5.1% for β-HCH in sand, and from 84 ± 1.8% for α-HCH to 107 ± 3.9% for β-HEPO in peat soils. In Fig. 3c the chromatogram of a peat-soil extracted with SFE shows a clean extract giving a straight baseline, better than the results obtained for the other techniques. The reproducibility is fairly good (1.9–6.9%), and is comparable with that found in the optimization experiments on glass beads. SFE is comparable with the other techniques for sand with respect to reproducibility and gives better results for peat soils, especially for the more apolar components.

SFE is more efficient than conventional techniques, giving higher recoveries than solvent extraction and with no need for the clean-up steps required in Soxhlet extraction. Furthermore SFE is faster and requires less sample handling; an extraction with SFE takes only 30 min compared with solvent and Soxhlet extractions, which take one or two days for a series of samples. Automation of the SFE procedure will further increase the speed of analysis. The amount of extraction solvent is significantly reduced to only 1 ml.

CONCLUSIONS

SFE using CO_2 at 50°C and 20 MPa, 10 min static followed by 20 min dynamic extraction with collection in iso-octane, has been found to give the optimum extraction of organochlorine pesticides and PCBs from soils. After establishing the optimum conditions, SFE can be used for the extraction of organochlorine pesticides and PCBs from soils with high recoveries (85–105%) and good reproducibility. SFE is more efficient than solvent extrac-

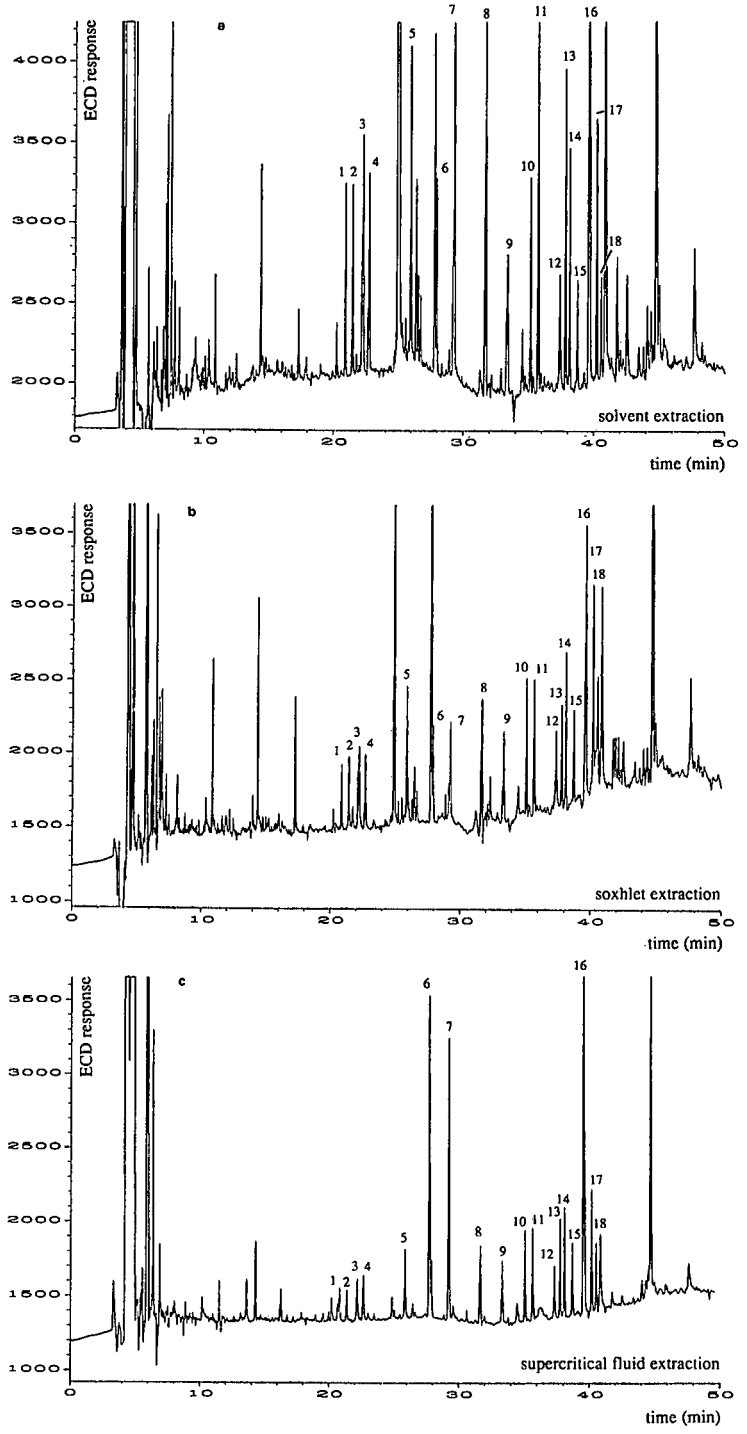

Fig. 3. Chromatograms of pesticides and PCBs extracted from peat soil. (a) Solvent extraction; (b) Sohxlet extraction; and (c) SFE. ECD = Electron-capture detection. 1 = α-HCH; 2 = HCB; 3 = β-HCH; 4 = γ-HCH; 5 = PCB 28; 6 = PCB 52; 7 = PCB 44 (I.S.); 8 = β-HEPO; 9 = PCB 101; 10 = *p,p'*-DDE; 11 = dieldrin; 12 = PCB 118; 13 = TDE; 14 = *o,p'*-DDT; 15 = PCB 153; 16 = PCB 141 (I.S.); 17 = *p,p'*-DDT; and 18 = PCB 138 (see under Experimental for gas chromatographic conditions).

tion for the extraction of more apolar components from soils with high organic carbon contents. No additional clean-up step is needed after the SFE of these components from soil, unlike Soxhlet extraction.

This work shows the potential of SFE for the determination of environmental contaminants in soil. The next step will be the SFE of real samples and the evaluation of extraction conditions for unknown matrices. Special attention should be devoted to the pretreatment and homogenization of small soil samples for analysis using SFE.

ACKNOWLEDGEMENT

R. Leenderts from Interscience Breda is gratefully acknowledged for his good advice and assistance by beginning the work with SFE.

REFERENCES

1 P. A. Greve, H. A. G. Heusinkveld, R. Hoogerbrugge, A. P. J. M. de Jong, G. A. L. de Korte, A. K. D. Liem and P. van Zoonen, *Organochloorbestrijdingsmiddelen en PCB's in bodemmonsters (Organochlorine pesticides and PCBs in soil)*, RIVM Report No. 728709001 (in Dutch), National Institute of Public Health and Environmental Protection (RIVM), Bilthoven, 1989.
2 V. Lopez-Avila, N. S. Dodhiwala and W. F. Beckert, *J. Chromatogr. Sci.*, 28 (1990) 468.
3 S. B. Hawthorne and D. J. Miller, *J. Chromatogr.*, 403 (1987) 63.
4 S. B. Hawthorne and D. J. Miller, *Anal. Chem.*, 59 (1987) 1705.
5 S. B. Hawthorne and D. J. Miller, *J. Chromatogr. Sci.*, 24 (1986) 258.
6 F. I. Onuska and K. A. Terry, *J. High Resolut. Chromatogr.*, 12 (1989) 357.
7 K. Schäfer and W. Baumann, *Fresenius' Z. Anal. Chem.*, 332 (1989) 884.
8 V. Janda, G. Steenbeke and P. Sandra, *J. Chromatogr.*, 479 (1989) 200.
9 M. E. McNally and J. R. Wheeler, *J. Chromatogr.*, 435 (1988) 63.
10 M. E. McNally and J. R. Wheeler, *J. Chromatogr.*, 447 (1988) 53.
11 M. Richards and R. M. Campbell, *LC · GC Int.*, 4 (1991) 33.
12 F. I. Onuska and K. A. Terry, *J. High Resolut. Chromatogr.*, 12 (1989) 527.

Journal of Chromatography, 626 (1992) 145–150
Elsevier Science Publishers B.V., Amsterdam

CHROM. 24 405

Determination of organophosphorus pesticides in fruits by on-line size-exclusion chromatography–liquid chromatography–gas chromatography–flame photometric detection

Mauro De Paoli, Maria Taccheo Barbina, Rita Mondini, Alessandra Pezzoni and Alan Valentino

Centro Regionale per la Sperimentazione Agraria, Via Sabbatini 5, I-33050 Pozzuolo del Friuli (UD) (Italy)

Konrad Grob

Kantonales Labor, P.O. Box, CH-8030 Zurich (Switzerland)

ABSTRACT

The determination of organophosphorus pesticides in fruits by size-exclusion chromatography (SEC) on a polystyrene column coupled on-line to a gas chromatography (GC) system was unsatisfactory as a result of interfering peaks in GC. A liquid chromatography step on silica gel was therefore inserted between the SEC and GC steps to filter out polar by-products. Samples of fruit (apples, grapes and kiwi fruits) were extracted, then the extract filtered or centrifuged and injected into an automated on-line SEC–liquid chromatography–GC–flame photometric detection. Recoveries were about 95% and the detection limits about 1 ng/g.

INTRODUCTION

The large number of analyses carried out in laboratories to determine pesticide residues justifies the construction of an automated analyser. However, although considerable time has been devoted to improving analysis speed, resolution and automation in additon to developing and improving instrumentation and detectors for pesticide analysis, sample processing, particulary its automation, has largely been neglected. This is in spite of the fact that an analytical procedure may require only a few minutes, but sample preparation steps, including extraction, clean-up and concentration, are often more time consuming.

One of the methods widely used for the clean-up of pesticides is gel permeation chromatography (GPC). Pflugmacher and Ebing [1] described a combination of partitioning and GPC for the clean-up of 22 organophosphorus pesticides using the dextran gel Sephadex LH-20 (Pharmacia). GPC clean-up using polystyrene-type gels, such as Bio-Beads SX-2, and SX-6, was introduced by Stalling *et al.* [2] and automated by Tindle and Stalling [3]. Bio-Beads SX-3 has been used with solvents such as ethyl acetate, cyclohexane, toluene, or mixtures of these [4–10]. Lunardini and Passini [11] described a clean-up procedure using a Waters Ultrastyrogel 500 Å column with toluene.

All these GPC techniques, using large columns and low flow-rates, need long analysis times and large amounts of solvents. For these reasons and because the large capacity of such columns is not required for the on-line transfer of complete frac-

Correspondence to: Dr. M. De Paoli, Centro Regionale per la Sperimentazione Agraria, Via Sabbatini 5, I-33050 Pozzuolo del Friuli (UD), Italy.

0021-9673/92/$05.00 © 1992 Elsevier Science Publishers B.V. All rights reserved

tions, traditional GPC columns are not suitable for on-line coupling to gas chromatography (GC); small columns preferred to reduce the volumes transferred. Ghijs *et al.* [12], Tuinstra *et al.* [13] and Van Rhijn and Tuinstra [14,15] described the packing of small size-exclusion chromatography (SEC) columns. It was noticed that the retention times of the analytes from columns packed with materials such as Bio Beads were unstable due to the compressibility of the packings. This difficulty was overcome by using a harder, cross-linked polystyrol suitable for high-performance liquid chromatography.

Grob and Kälin [16] described on-line SEC–GC for the determination of chlorinated pesticides in fat-containing foods. They used a 250 × 3 mm I.D. column packed with PSS SDV and were able to inject up to 0.3 mg of fat. Reasonable chromatograms were obtained for olive oil and extracts of fish, chicken and lettuce. Detection limits for pesticide in the fat were less than 10 ng/g.

In classical methods, clean-up for GPC is followed by further clean-up with a variety of systems such as solvent partitioning, Florisil, silica, or aluminum oxide liquid chromatography (LC) columns, which separate the extracts by polarity. The combination of two techniques gives a powerful two-dimensional clean-up by molecular size and polarity.

On-line SEC–GC–flame photometric detection applied to the determination of organophosphorus pesticides in fruits gave gas chromatograms with many interfering peaks. Tailing peaks suggested that the interfering components were primarily of high polarity. These were removed by inserting a silica gel column between the SEC and GC steps, which acted as a filter, removing all components more polar than the pesticides of interest.

The proposed method starts with clean-up of the crude dichloromethane extract by SEC on a polystyrene column and is followed by a second clean-up step on a silica column; the fraction containing the pesticides is transferred to a GC system by concurrent solvent evaporation using a loop-type interface. This on-line SEC–LC–GC method was used for the dermination of 22 organophosphorates. One analysis, including the extraction step, took about 50 min.

EXPERIMENTAL

Chemicals

The analytical standards for the pesticides were obtained from Riedel-de Haën (Selze, Germany) and included phorate, fonofos, diazinon, parathion-methyl, fenchlorphos, fenitrothion, pirimiphos-methyl, malathion, parathion, bromophos-ethyl, tetrachlorvinphos, ditalmifos, isoxathion, ethion, carbophention, pyridaphention, azinphos-methyl, azinphos-ethyl and pyrazophos. Triphenyl phosphate was obtained from Janssen (Geel, Belgium). Dichloromethane and methyl *tert.*-butyl ether (MTBE) were of HPLC grade from Fluka (Buchs, Switzerland).

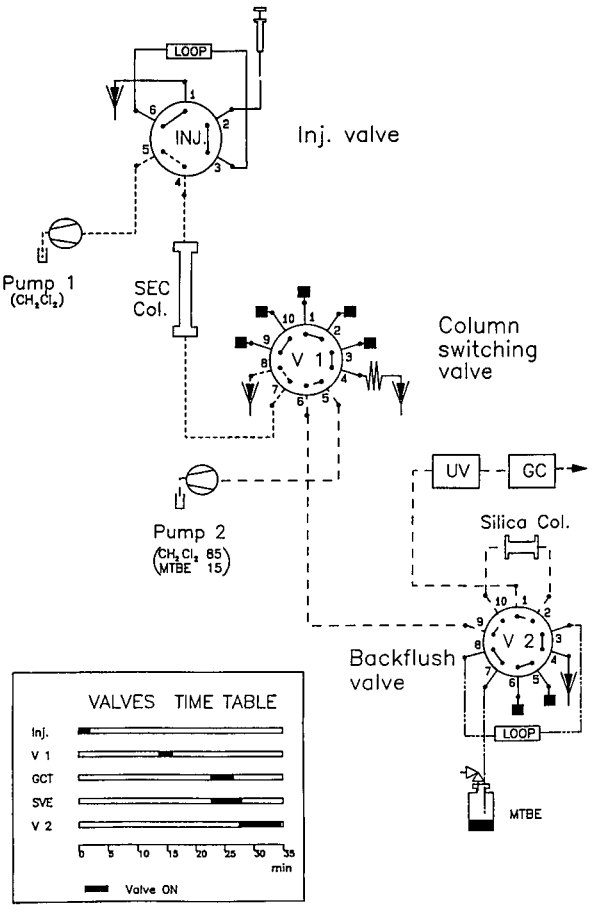

Fig. 1. Schematic diagram of experiment set-up.

Extraction

Chopped fruit (15 g) was extracted with 30 ml of dichloromethane in a 100-ml blender for 30 s. The liquid phase was then centrifuged at 1500 *g* for 30 s to separate solids. The supernatant was filtered through a 0.45-μm disposable syringe filter; a 20-μl volume was injected into the SEC–LC–GC system.

Instrumentation

Analyses were carried out using a Carlo Erba (Milan, Italy) LC-GC Dualchrom 3000 system equipped with two syringe pumps, three multi-port switching valves, a UV detector, an on-column and a loop-type interface, and an automated solvent vapour exit, all under the control of a personal computer. Fig. 1 is a schematic diagram of the experimental layout. The flame photometric detector was a Carlo Erba FPD 500 instrument equipped with a 526 nm interference filter.

Size-exclusion chromatography

SEC was carried out on a 250 × 3 mm I.D. column packed with PSS SDV 100Å, a polystyrene-type material (Polymer Standards Service, Mainz, Germany), with dichloromethane as the mobile phase at a flow-rate of 80 μl/min.

SEC–LC transfer was via the column switching valve (V1) which was actuated 13.5 min after injection and returned 2.5 min later.

Liquid chromatography conditions

LC was performed on a 100 × 2 mm I.D. column packed with Spherisorb Si 5 μm (Stragoma, Wallisellen, Switzerland) with dichloromethane–MTBE (85:15, v/v) as the eluent at a flow-rate of 80 μl/min. The column was cleaned by back-flush with 1 ml of MTBE immediately after the transfer of the fraction of interest to the gas chromatograph.

Liquid chromatograph–gas chromatograph transfer

LC–GC transfer was performed by concurrent eluent evaporation using a loop-type interface [17]. The transfer valve was switched on 22 min 40 s after injection into the SEC system. The volume of the transferred fraction was 450 μl. The carrier gas inlet pressure imposed by the pressure regulator was 1.0 bar (hydrogen); the flow regulator delivered a flow-rate of 2 ml/min. The column temperature during transfer was 80°C. The early vapour exit was closed 1 min after the inlet pressure started to decrease (pressure threshold 20 kPa).

Gas chromatography

Gas chromatographic analysis used a column made up of a 3 m × 0.53 mm I.D. uncoated pre-column deactiviated by phenyldimethyl silation (MEGA, Legnano, Italy), a 3 m × 0.32 mm I.D. retaining pre-column taken from the separation column, a vapour exit with a press-fit T-piece, and a 20 m × 0.32 mm I.D. separation column coated with SE-54 of 0.15-μm film thickness (MEGA). After an isothermal period of 5 min at 80°C (transfer), the temperature was increased at 15°C/min to 130°C/min, at 5°C/min to 260°C and then at 15°C/min to 300°C.

Quantitative data were obtained by the internal standard (I.S.) method, adding 10 μl of triphenyl phosphate at 1 ppm as an I.S. to 1 ml of the sample solution before injection.

Determination of SEC–LC and LC–GC transfer times

The pesticide fraction in the SEC column was determined as follows. Ethion and diazinon were the pesticides least retained in the SEC column. The beginning of the fraction was first determined by injection of ethion (1 ppm) and UV detection at 225 nm. It was then confirmed by transferring fractions before the assumed pesticide fraction to the GC system, shifting the fraction window until the first pesticide peaks appeared on the gas chromatogram. The analogous procedure was applied to determine the end of the fraction using azinphos-methyl. The pesticide fraction in the SEC system had a volume of 200 μl. A similar procedure was adopted to determine the beginning and end of the fraction from LC, *i.e.* the LC–GC transfer time and the volume of the transferred fraction.

RESULTS AND DISCUSSION

The method described here can be used for the automated on-line clean-up and determination of at least 22 organophosphorus pesticides in various fruits such as apples, grapes and kiwi fruit. The method simply requires the extraction of the sample in a blender and, after filtration, injection into the SEC–LC–GC system. Table I gives the recoveries

TABLE I

RECOVERIES FROM UNTREATED FRUITS SPIKED WITH 10 ng/g OF PESTICIDES

Results are means of five determinations. R.S.D. = Relative standard deviation.

Compound (abbreviation)	Grapes		Apples		Kiwi fruits	
	Recovery (%)	R.S.D. (%)	Recovery (%)	R.S.D. (%)	Recovery (%)	R.S.D. (%)
Phorate (Pho)	88.5	4.40	86.3	4.78	82.3	5.54
Fonofos (Fon)	89.4	4.76	80.3	4.35	80.3	5.54
Diazinon (Dia)	94.6	2.11	94.2	2.69	96.3	3.03
Parathion methyl (Par-m)	92.4	0.81	88.8	2.03	93.5	2.20
Fenchlorphos (Fcp)	94.8	1.23	94.7	3.43	92.4	3.12
Fenitrothion (Ftt)	90.7	0.34	94.6	2.33	98.6	1.89
Pirimiphos methyl (Pir-m)	94.5	3.30	91.2	3.33	91.4	2.03
Malathion (Mal)	97.1	3.60	92.5	3.67	88.7	3.23
Parathion (Par)	97.2	2.60	89.5	3.95	96.9	3.48
Bromophos methyl (Brp-m)	97.7	2.22	90.6	3.87	90.5	4.27
Quinalphos (Qui)	98.6	2.59	92.6	2.68	88.8	4.04
Methidathion (Met)	94.4	2.21	93.7	4.50	97.4	2.34
Bromophos ethyl (Brp-e)	98.8	3.34	92.6	4.33	92.3	3.25
Tetrachlorvinphos Tcv)	93.3	4.43	90.8	3.56	86.8	2.75
Ditalmifos (Dit)	94.4	3.23	97.5	3.54	95.6	3.53
Isoxathion (Iso)	97.9	3.76	98.2	4.34	97.6	4.01
Ethion (Eth)	98.4	4.22	96.8	5.22	89.3	4.00
Carbophenthion (Car)	96.4	4.47	92.3	4.64	83.5	3.58
Pyridaphenthion (Pyr)	99.3	3.39	95.4	3.43	97.3	2.22
Azinphos methyl (Azp-m)	99.5	4.23	94.7	5.12	96.8	4.60
Azinphos ethyl (Azp-e)	96.6	3.09	88.9	4.04	94.4	3.23
Pyrazophos (Pzp)	97.2	4.12	95.2	4.32	90.3	4.30

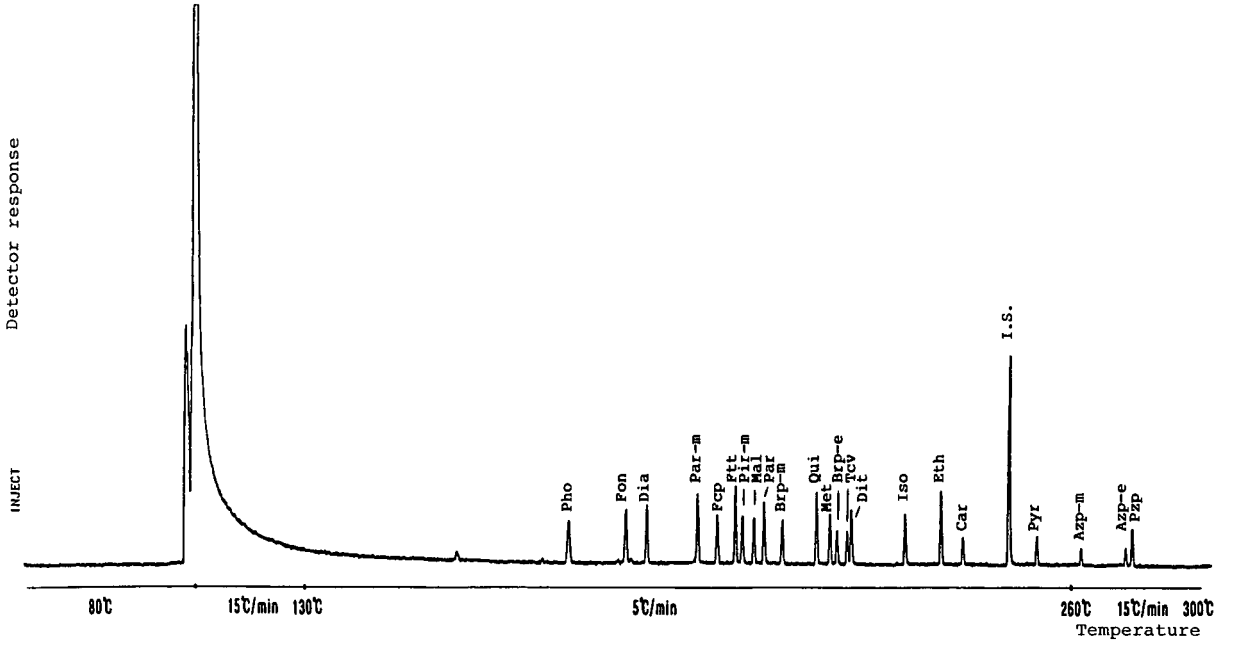

Fig. 2. Chromatogram of pesticides spiked at 5 ng/g in apple samples determined by SEC–LC–GC–flame photometric detection. I.S. = Internal standard (10 ng/ml). For peak identification, see Table I.

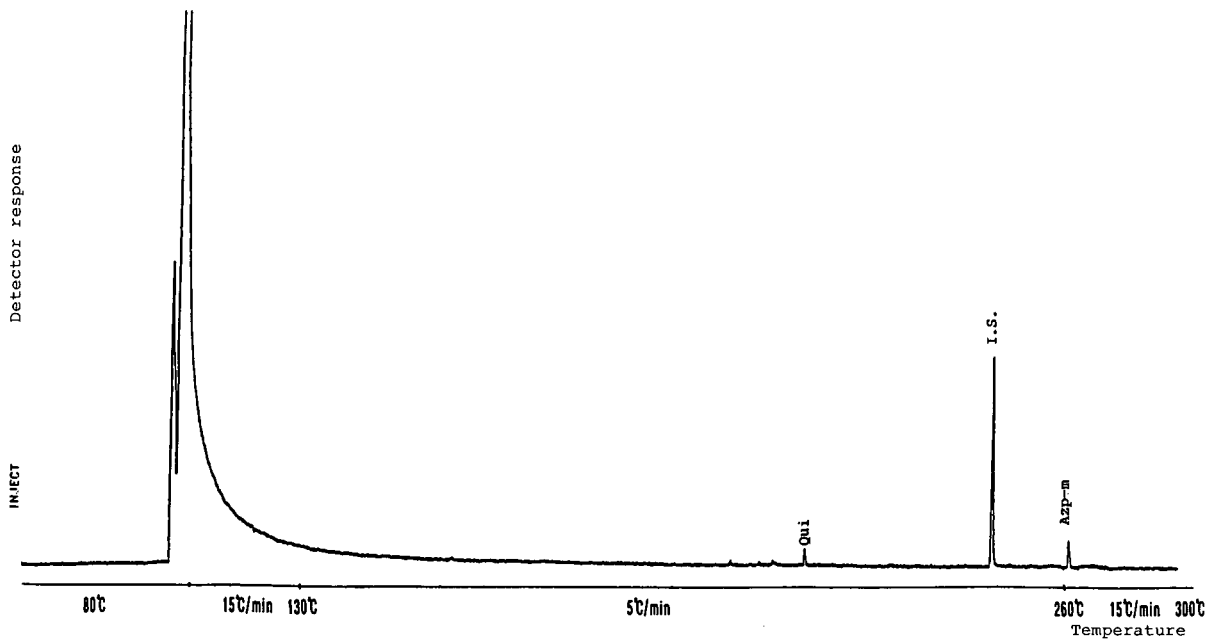

Fig. 3. Chromatogram of pesticides in a real sample containing 1 ppb of quinalphos and 10 ppb of azinophos methyl determined by SEC–LC–GC–flame photometric detection. Note the complete absence of peaks other than the insecticides.

obtained by adding known amounts (10 ng/g) of pesticides to an apple sample; they averaged more than 95%, with a coefficient of variation of about 3%. High recoveries are obtained as losses in on-line systems are largely non-existent. The low coefficients of variation are a consequence of increased accuracy.

Fig. 2 shows a gas chromatogram of an apple spiked with 5 ng/g of the pesticides tested. It shows that the detection limit is about 1 ng/g. Fig. 3 shows the presence of small amounts of quinalphos and azinphos-methyl in apple, approximately 1 and 10 ng/g, respectively, but also the complete absence of interfering peaks. The concentrations of the two insecticides are 100 and 50 times lower than the maximum permitted under Italian law and show the low detection limit obtained. As a result of these low detection limits, maximum residue levels for autorized pesticides can easily be determined. For some pesticides these limits can be determined even with normal analytical methods, although with the method described here it is also possible to monitor some organic products where the illicit use of pesticides is suspected, and the theoretical zero residue can be approached even more closely.

As a result of the efficient clean-up step in this method, a more accurate determination of residues in fatty animal or vegetable samples, such as avocado pears, olives and flours, can be obtained.
No desactivation or loss of efficiency of the analytical column used for GC was noted, even after the analysis of 50 samples.

ACKNOWLEDGEMENTS

We thank Carlo Erba Instruments, in particular Dr. Munari and Dr. Saravalle, for technical support.

REFERENCES

1 J. Pflugmacher and W. Ebing, *J. Chromatogr.*, 93 (1974) 457–463.
2 D. L. Stalling, R. C. Tindle and J. L. Johnson, *J. Assoc. Off. Anal. Chem.*, 55 (1972) 32–38.
3 R. C. Tindle and D. L. Stalling, *Anal. Chem.*, 44 (1972) 1768–1773.
4 L. D. Johnson, R. H. Waltz, J. P. Ussary and F. E. Kaiser, *J. Assoc. Off. Anal. Chem.*, 59 (1976) 174–187.
5 J. A. Ault, C. M. Schofield, L. D. Johnson and R. H. Waltz, *J. Assoc. Off. Anal. Chem.*, 27 (1979) 825–828.
6 W. Specht and M. Tillkes, *Fresenius' Z. Anal. Chem.*, 301 (1980) 300–307.

7 W. Specht and M. Tillkes, *Fresenius' Z. Anal. Chem.*, 322 (1985) 443–455.
8 J. J. Blaha and P. J. Jackson, *J. Assoc. Off. Anal. Chem.*, 68 (1985) 1095–1099.
9 A. H. Roos, A. J. Van Munsteren, F. M. Nab and L. G. M. Th. Tuinstra, *Anal. Chim. Acta*, 196 (1987) 95–102.
10 S. J. Chamberlain, *Analyst (London)*, 115 (1990) 1161–1165.
11 C. Lunardini and V. Passini, *Boll. Chim. Ig., Parte Sci.*, 40 (1989) 65–70.
12 M. Ghijs, J. Van Dijck, C. Dewaele, M. Verzele and P. Sandra, in P. Sandra and G. Redant (Editors), *Proceedings of the 10th International Symposium on Capillary Chromatography, Riva del Garda, 1989*, Hüthig, Heidelberg, p. 726.
13 L. G. M. Th. Tuinstra, J. A. Van Rhijn and A. Ruiter, *Poster presented at the 18th International Symposium on Chromatography, Amsterdam, September 1990.*
14 J. A. Van Rhijn and L. G. M. Th. Tuinstra, in P. Sandra (Editor), *Proceedings of the 13th International Symposium on Capillary Chromatography, Riva del Garda, 1991*, Hüthig, Heidelberg, p. 691.
15 J. A. Van Rhijn and L. G. M. Th. Tuinstra, *J. Chromatogr.*, 552 (1991) 517–526.
16 K. Grob and I. Kälin, *J. Agric. Food Chem.*, 39 (1991) 1950–1953.
17 K. Grob, *On-line Coupled LC-GC*, Hüthig, Heidelberg, 1991.

Journal of Chromatography, 626 (1992) 151–157
Elsevier Science Publishers B.V., Amsterdam

CHROM. 24 447

Simultaneous determination of methyl-, ethyl-, phenyl- and inorganic mercury by cold vapour atomic absorption spectrometry with on-line chromatographic separation

Corrado Sarzanini, Giovanni Sacchero, Maurizio Aceto, Ornella Abollino and Edoardo Mentasti

Department of Analytical Chemistry, Via P. Giuria 5, 10125 Turin (Italy)

ABSTRACT

A fully automated system for on-line high-performance liquid chromatographic separation, reduction and determination by cold vapour atomic absorption spectrometry (CVAAS) of methyl-, ethyl-, phenyl- and inorganic mercury is described. Reversed-phase chromatography on an ODS column and elution with an acetonitrile–water–ammonium tetramethylenedithiocarbamate buffered mixture was investigated with or without ammonium tetramethylenedithiocarbamate precomplexation. A simple glass flow cell, properly designed as an interface between the chromatographic system and CVAAS, is proposed. The influence of the composition of the eluent, reducing solution and stripping gas flow-rate was investigated and optimized in order to obtain better detection limits. The method, applied to synthetic mixtures and natural samples of tap water furnished satisfactory results. It is shown that, with the on-line preconcentration procedure, sub-ng/ml concentration levels can be determined for all the species considered.

INTRODUCTION

Mercury determinations have been achieved by several methods in recent years, all using basically the same approach [1,2]. A closed reduction purging system converts the mercury compound into a volatile form by reduction to elemental mercury, which is swept from the solution by a gas stream into a detector, sometimes after a preconcentration step (usually a gold trap). The most frequently used detectors are atomic absorption spectrometers, *e.g.*, in cold vapour atomic absorption spectrometric (CVAAS) measurements [3–7].

In view of the high toxicity of organomercury(II) compounds, speciation of the chemical forms is required. Inorganic and organic mercury compounds have been separated by high-performance liquid chromatography (HPLC) as alkyl- or tetramethylenedithiocarbamates [8] and dithizonates [9] after extraction of the complexes, but UV spectrophotometric detection gave too high detection limits. Speciation of inorganic and organomercury compounds was also determined by liquid chromatography, coupling cold vapor generation with inductively coupled plasma emission spectrometry [10] or inductively coupled plasma mass spectrometry [11]. The high instrumental costs in relation to the detection limits obtained (32–62 and 0.6–12 μg/l, respectively) make it difficult to justify. More recently, a speciation of mercury compounds by microcolumn liquid chromatography using a preconcentration column with CVAAS detection furnished 1 μg/l detection limits for all species considered [12].

The purpose of this work was to evaluate the efficiency of ammonium tetramethylenedithiocarbamate [ammonium pyrrolidine dithiocarbamate (APDC)] reagent for the reversed-phase separation of methyl-, ethyl, phenyl- and inorganic mercury, accomplished with on-line reduction and CVAAS

Correspondence to: Professor C. Sarzanini, Department of Analytical Chemistry, Via P. Giuria 5, 10125 Turin, Italy.

0021-9673/92/$05.00 © 1992 Elsevier Science Publishers B.V. All rights reserved

determination. Experiments were also carried out with a preconcentration procedure in order to achieve lower detection limits.

EXPERIMENTAL

Apparatus and materials

A schematic diagram of the system is shown in Fig. 1. All experiments were carried out on a Varian Model LC 5000 instrument equipped with a Rheodyne injection valve (100-μl sample loop), a Vista 401 Data Station and a Varian UV-100 detector (Varian, Walnut Creek, CA, USA) or a CVAAS detector (Milton Roy, Stone UK). The analytical column was LiChrospher 100 RP-18 (5 μm) (250 × 4 mm I.D.), coupled with a LiChroCART 100 RP-18 (5 μm) guard column (25 × 4 mm I.D.), obtained from Merck (Darmstadt, Germany). The CVAAS signal due to mercury was recorded on a Model 56 strip-chart recorder (Perkin-Elmer, Norwalk, CT, USA). A Model 302 pump and Model 802 manometric module, Gilson, Middleton, WI, USA) ensured, through a T-mixer, the addition of reductive solution to the eluted chromatographic fractions. The mixed solutions containing the dissolved elemental mercury were introduced into a Pyrex flow cell (FC), which also acted as gas–liquid separator. A peristaltic pump (Gilson Minipuls 2) was used for draining the solution from the gas–liquid separator and for ensuring that a constant volume entered the cell. For pH measurements a digital pH meter (Orion, Cambridge, MA, USA) equipped with a combined glass–calomel electrode was used.

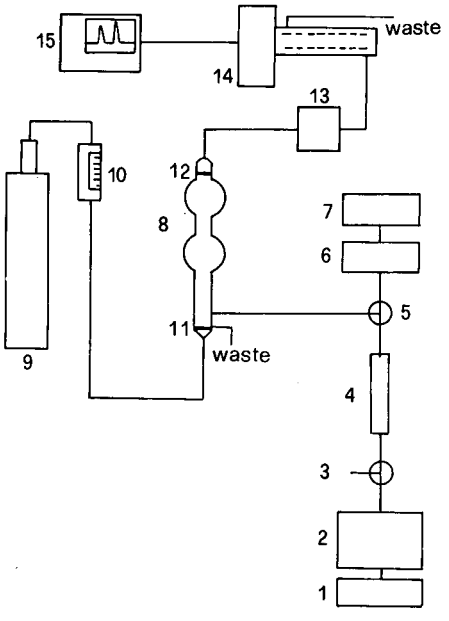

Fig. 1. Schematic representation of the major instrumental components employed: 1 = eluent; 2 = chromatographic system; 3 = injector (100-μl loop or preconcentrator); 4 = chromatographic column; 5 = T-mixer; 6 = manometric pump module; 7 = $NaBH_4$ reservoir; 8 = flow cell; 9 = carrier (N_2); 10 = flow meter; 11, 12 = glass frits; 13 = $Mg(ClO_4)_2$ traps; 14 = CVAAS detector; 15 = recorder.

High-purity water (HPW) obtained from a Milli-Q System (Millipore, Bedford, MA, USA), supplied with deionized water produced with a mixed-bed twin ion-exchange column, was used for preparing all solutions. Acetonitrile used for HPLC, sodium hydroxide, magnesium perchlorate, mercury nitrate and methylmercury chloride were obtained from Merck, ethylmercury chloride from Alfa (Karlsruhe, Germany) and phenylmercury chloride from Aldrich (Steinheim, Germany). Acetic acid (Merck) was purified with a sub-boiling distillation apparatus (Kurner, Rosenheim, Germany). All other reagents employed were of analytical-reagent grade.

APDC (Merck) was used without further purfication. The reducing solution, containing 1.0 g/l of sodium tetrahydroborate (Fluka, Buchs, Switzerland) and adjusted to pH 11.5 with 0.1 *M* NaOH, was prepared and filtered just before use. This solution was purified by bubbling with nitrogen overnight.

Preparation and measurement of solutions

The working methyl-, ethyl-, phenyl- and inorganic mercury solutions were prepared before use by dilution of 100.0, 100.0, 20.0 and 1000 ppm stock standard solutions, respectively. Standards and samples were prepared daily with HPW, stored in the dark and refrigerated.

Chromatographic determinations were performed, unless stated otherwise, with a mobile phase consisting of acetonitrile–water (58:42, v/v), previously buffered to pH 5.5 with ultrapure acetic acid and sodium hydroxide, and added of the appropriate amount of APDC (see below). The eluent composition gave better resolved peaks at a 0.5 m*M* APDC concentration. The flow-rate was 1.5 ml/min.

Sample solutions were introduced into the injection loop (100 μl) or passed through a LiChroCART RP-18 (5 μm) microcolumn (4 × 4 mm I.D.) with the aid of a Model DQP-1 pump (Dionex, Sunnyvalle, CA, USA) for the preconcentration procedure.

Preliminary experiments, using low APDC concentrations, were performed with a UV–VIS detector and the direct injection of aqueous sample solutions was accomplished by incorporating, or not, APDC reagent (1 m*M*) in the samples. For the precomplexation procedure the samples had a composition of acetonitrile-methanol-water (25:25:50, v/v/v) in order to avoid precipitation of complexes. In the optimized procedure metal complexes were formed by on-column derivatization during the separation.

RESULTS AND DISCUSSION

The method is based on the formation, separation and subsequent detection of the metal–APDC complexes (Fig. 2). The on-column in comparison with the precomplexation procedure showed a reduced detection sensitivity only for inorganic mercury species (see below). On the other hand, the on-column complexation procedure avoids tedious manipulations of the sample, due to the low solubility of the APDC complexes, which require a solvent medium for reaction or organic extraction prior to chromatographic separation. Taking into account the high sensitivity of inorganic mercury in comparison with the other species, and that on-line complexation avoids contamination of the sample, the on-line procedure was concluded to be the best approach.

Optimization of procedures

Several factors had to be optimized in order to achieve the maximum selectivity, sensitivity, reproducibility and resolution. These included capacity factor, the width of the peaks at half-height ($W/2$) and ligand concentration (APDC). For detection by CVAAS, the flow-rate of reducing solution and residence times in the reaction coil and in the flow cell must be considered.

It was noted that the peak areas of the separated mercury complexes varied considerably with repeated injections of the sample at low APDC concentration. It is believed that these variations arise from interaction of the charged uncomplexed species, in equilibrium with APDC complexes, with residual silanol groups on the C_{18} column packing. The addition of higher APDC concentrations blocks this effect, in fact the ligand concentration acts on the complexation of mercury species and in addition it avoids adsorption phenomena on the column. In particular, as the concentration of ligand in the mobile phase increased, the retention time of the analytes decreased linearly.

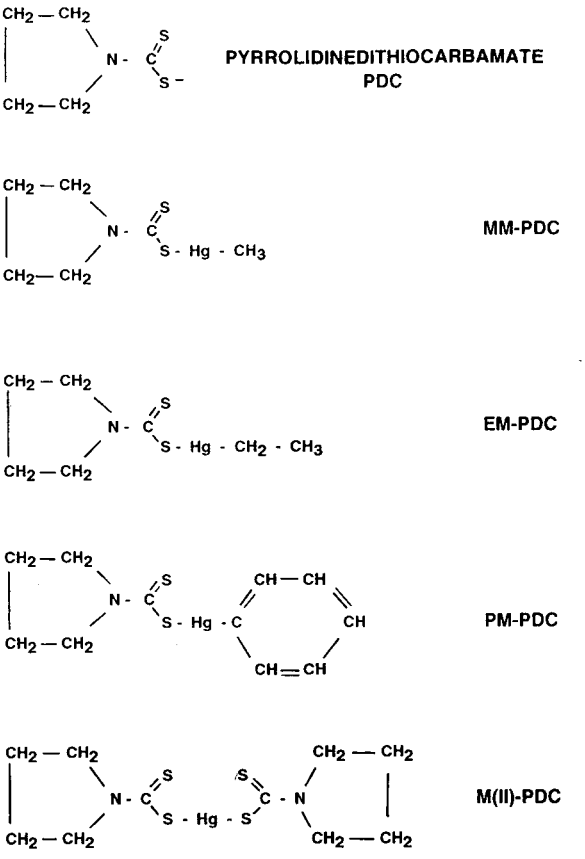

Fig. 2. Structure of APDC complexes: MM = methylmercury; EM = ethylmercury; PM = phenylmercury; M = inorganic mercury.

Fig. 3 shows the behaviour of retention times and $W/2$ as a function of complexing agent (APDC) concentration in the eluent. The UV–VIS detection of mercury complexes was hindered by the increased background absorbance when higher concentrations of reagent were used in the mobile

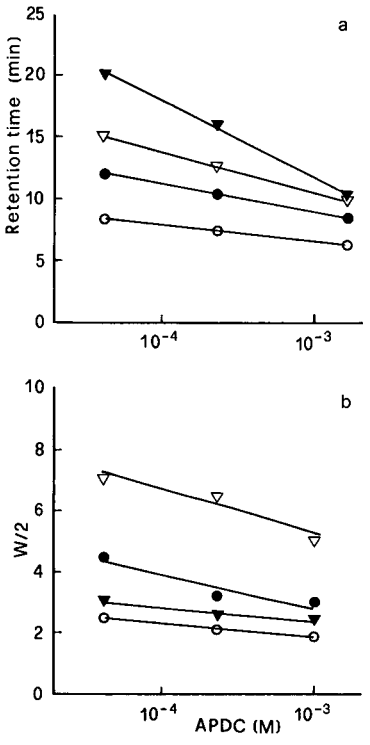

Fig. 3. Effect of APDC concentration on (a) retention times and (b) $W/2$ for a 100-μl sample. Chromatographic conditions: mobile phase, acetonitrile–water (58:42, v/v) containing 20.0 mM acetic acid, APDC as shown and sodium hydroxide up to pH 5.5; flow-rate, 1.5 ml/min. ○ = CH_3Hg^+ (100 ng as Hg); ● = $C_2H_5Hg^+$ (100 ng as Hg); ▽ = $C_6H_5Hg^+$ (100 ng as Hg); ▼ = Hg^{2+} (20 ng).

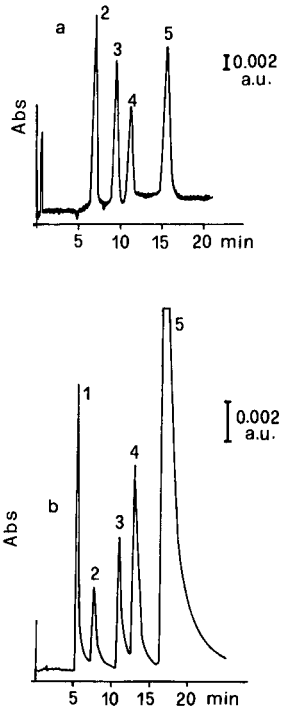

Fig. 4. Comparison between UV absorption and CVAAS detection of mercury–APDC complexes separated by HPLC. (a) UV detection, 254 nm; (b) CVAAS detection, 254 nm. Chromatographic conditions: mobile phase, acetonitrile–water (60:40, v/v) containing 20.0 mM acetic acid, 0.1 mM acetic acid, 0.1 mM APDC and sodium hydroxide up to pH 5.5; flow-rate, 1.5 ml/min; 100-μl sample. Peaks: 1 = ghost peak (CH_3OH); 2 = CH_3Hg^+ (200 ng as Hg); 3 = $C_2H_5Hg^+$ (200 ng as Hg); 4 = $C_6H_5Hg^+$ (200 ng as Hg); 5 = Hg^{2+} (200 ng).

phase. CVAAS was employed for APDC concentrations >0.1 mM to optimize the method. The removal of adsorption phenomena during the chromatographic separation, due to increased APDC concentration, gave better reproducibility and enhanced the detection signal, and on the basis of the results obtained, a 0.5 mM APDC concentration was selected. In fact, shorter retention times are obtained with a decrease in broadening of the ethylmercury peak and a good separation of components in a shorter analysis time and with total recovery of the investigated species.

Comparison of the spectrophotometric detection of metal complexes based on their UV–VIS adsorption around the maximum allowed APDC concentration in the eluent (0.1 mM) and the CVAAS determination is shown in Fig. 4. The precomplexation procedure was adopted. It must be noted that if the samples are not freshly prepared, an anomalous peak, due to inorganic mercury, appears during the analysis of methyl-, ethyl- or phenylmercury samples as a result of decomposition of the latter. In addition, a ghost peak appears when standard solutions of organic species involve the use of methanol.

In order to perform CVAAS determinations, the detector was interfaced with the chromatographic system through a flow cell (FC) which permitted the recovery of Hg(0) after the reduction of the eluted species. The chromatographic eluate, connected by a T-joint with reducing reagent, was passed to the FC through a reaction coil. The lenght of the tube (300 × 0.3 mm I.D.) allows the reduction of mercury species before the sample is introduced into the FC and the design of the cell was such as to ensure a

residence time of chromatographic fractions sufficient to permit complete removal of mercury without overlap of the previously separated species.

Fig. 5 shows the FC optimized to reduce the residence time of the eluate, to minimize the vapour dispersion and to permit the maximum flow-rate of carrier according to the maximum detection sensitivity. A countercurrent nitrogen flow into the FC swept out the reduced mercury from an outlet located on top of the separator and then introduced it into the CVAAS system, after removal of water through a trap filled with $Mg(ClO_4)_2$, which was replaced daily.

The effect of reducing solution flow-rate on detection was also investigated. Fig. 6 shows that the maximum peak height is obtained with a flow-rate of 0.1–0.2 ml/min and an increase in this parameter affects the peak width and symmetry, probably owing to dilution effects, without improving the sensitivity. Different flow-rates of the reductant also affect the pH value, which ranged from 6 to 11, but this did not affect the detection sensitivity. Therefore, a flow-rate of 0.1 ml/min was selected for the reductant.

In order to optimize the sensitivity, the effect of nitrogen flow-rate was investigated. Fig. 7 shows

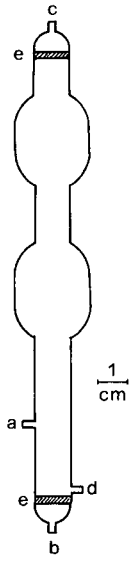

Fig. 5. Flow cell: a = inlet of effluent from HPLC column and reductant mixture; b = inlet of nitrogen flow; c = outlet of mercury vapour; d = outlet of waste; e = glass frits.

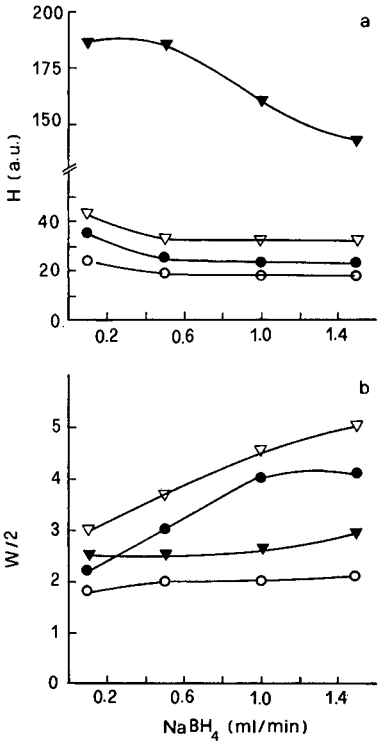

Fig. 6. Dependence of (a) peak height (H) and (b) $W/2$ on flow-rate of $NaBH_4$. Chromatographic conditions: mobile phase, acetonitrile–water (58:42, v/v) containing 20.0 mM acetic acid, 0.5 mM APDC and sodium hydroxide up to pH 5.5; flow-rate, 1.5 ml/min; 100-μl sample. ○ = CH_3Hg^+ (100 ng as Hg); ● = $C_2H_5Hg^+$ (100 ng as Hg); ▽ = $C_6H_5Hg^+$ (100 ng as Hg); ▼ = Hg^{2+} (20 ng).

the behaviour of peak height, $W/2$ and the time delay as function of flow-rate. The time delay is defined as

$$\text{time delay} = \frac{t_{rCV} - t_{rUV}}{t_{rUV}} \cdot 100\%$$

where t_{rCV} = retention time for the CVAAS detector and t_{rUV} = retention time for the UV–VIS detector.

As expected, at too low a flow-rate, the sensitivity is reduced and the peaks become broadened. On the other hand, the flow-rate corresponding to the maximum peak height cannot be selected because in this range the peak broadening is still too large with poor resolution; moreover, a slight variation in the nitrogen flow-rate can dramatically affect the time delay and sensitivity, reducing the reproducibility

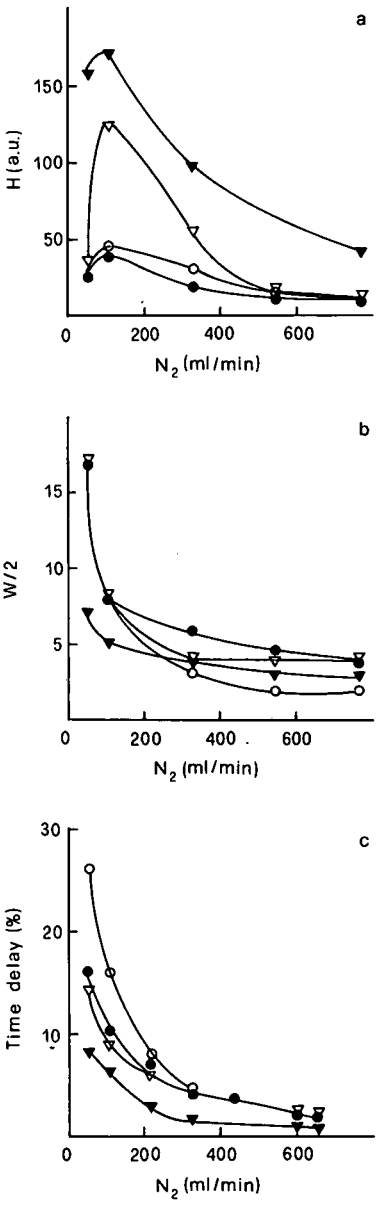

Fig. 7. Effect of flow rate of carrier (N_2) on (a) peak height (H), (b) $W/2$ and (c) time delay. Chromatographic conditions as in Fig. 6.

of the measurements. In order to avoid these phenomena, a flow-rate of 550 ml/min was selected, at which a relatively reduced sensitivity is shown but good symmetry and reproducibility are achieved.

Preconcentration procedure

Preliminary studies were made of the ability of the microcolumn to preconcentrate samples with the on-line complexation procedure. The 100-μl loop on the Reodyne valve was replaced with a LiChroCART RP-18 (5 μm) microcolumn (4 × 4 mm I.D.). Samples of 100 ml were passed at 4.0 ml/min through the microcolumn, in the same direction as the elution step, followed with washing with 10.0 ml of HPW to remove the matrix. Usually a counter-flow is preferred for the preconcentration procedure in order to avoid interferences in the chromatographic behaviour; in this case the limited length of the preconcentrator did not affect the separation. Each sample solution was analysed in triplicate and the amounts ranged from 50 to 500 ng (as Hg) for inorganic and organic species, respectively. The analyte recoveries were evaluated by comparing the height of the peaks obtained for samples analysed by this procedure with those obtained for 100-μl samples, containing the same absolute amounts of mercury species, analysed without preconcentration. Recoveries of 40% were obtained except for methylmercury, which showed an anomalous recovery of only 16%. The expected preconcentration factor of 1000 was so reduced to 400 for ethyl-, phenyl and inorganic mercury and 160 for methylmercury, but good reproducibility was obtained over the range of concentrations studied. The calibration graph (Fig. 8) shows the linear response for the species considered and illustrates the order of sensitivity of CVAAS, which increases in the order phenyl-, methyl- and ethylmercury.

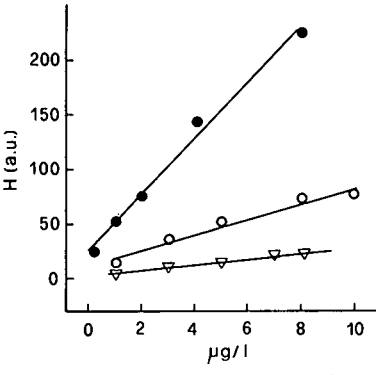

Fig. 8. Calibration graphs for on-line preconcentration procedure. Chromatographic conditions as in Fig. 6; 100-ml sample volume. ○ = CH_3Hg^+; ● = $C_2H_5Hg^+$; ▽ = $C_6H_5Hg^+$

Detection limits

As shown above (optimization of the parameters), there is a large difference between the sensitivity of inorganic mercury and organic species. The detection limits (DL) were determined for each analyte in ultrapure water with a 100-μl loop and for 100 ml in the on-line preconcentrated sample procedure. Table I compares the DLs (three times the blank value) calculated for both procedures and indicates that the DLs for inorganic mercury with or without precomplexation and DLs of organic species were the same for both procedures.

Real samples

The performance of the proposed system was also evaluated on a real sample of tap water. The sample was filtered (0.45 μm) and analysed as such as or spiked with 0.1–0.3 ng/ml concentrations for inorganic mercury. Fig. 9 compares the chromatogram of tap water with that for samples spiked with organic species at ng/ml and sub-ng/ml concentration levels. The chromatograms show that the method is unaffected by the matrix composition, and moreover a good reproducibility is obtained for this kind of sample. The sample concentration, evaluated by the standard addition procedure, was of 170 ng/l of inorganic mercury with a linear regression coefficient $R = 0.995$. In the light of these results, it is concluded that the developed method is well suited to speciation studies on natural and polluted waters.

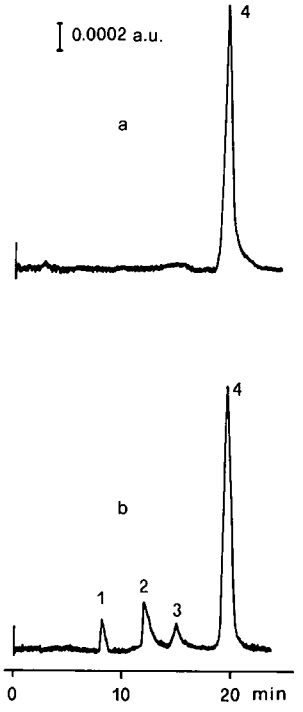

Fig. 9. Analysis of tap water by on-line preconcentration procedure: (a) as such; (b) spiked sample. Peaks: = 1 CH_3Hg^+; 2 = $C_2H_5Hg^+$; 3 = $C_6H_5Hg^+$; 4 = Hg^{2+}. Chromatographic conditions as in Fig. 6.

TABLE I

DETECTION LIMITS FOR DIRECT INJECTION AND ON-LINE PRECONCENTRATION PROCEDURE

Signal-to-noise ratio = 3. Chromatographic conditions: mobile phase, acetonitrile–water (58:42, v/v) containing 20.0 m*M* acetic acid, 0.5 m*M* APDC and sodium hydroxide up to pH 5.5; flow-rate 1.5 ml/min; sample loading flow-rate 4.0 ml/min; CVAAS detection, 253.7 nm.

Species	Detection limit (ng/ml)	
	100 μl[a]	100 ml[b]
CH_3Hg^+	100	0.50
$C_2H_5Hg^+$	50	0.09
$C_6H_5Hg^+$	300	0.50
Hg^{2+}	8; 1[c]	0.015

[a] Direct injection.
[b] On-line preconcentration procedure.
[c] Without and with precomplexation, respectively.

REFERENCES

1 W. R. Hatch and W. L. Ott, *Anal. Chem.*, 40 (1968) 2085.
2 N. S. Poluektov, R. A. Vikun and Y. V. Zelyukova, *Zh. Anal. Khim.*, 18 (1963) 33.
3 B. Welz and M. Schubert-Jacobs, *Fresenius' Z. Anal. Chem.*, 331 (1988) 324.
4 W. Baeyens and M. Leermakers, *J. Anal. At. Spectrom.*, 4 (1989) 635.
5 E. Temmerman, C. Vandecasteele, G. Vermeir, R. Leyman and R. Dams, *Anal. Chim. Acta*, 236 (1990) 371.
6 G. A. Zachariadis and J. A. Stratis, *J. Anal. At. Spectrom.*, 6 (1991) 239.
7 M. Horvat, V. Lupsina and B. Pihlar, *Anal. Chim. Acta*, 243 (1991) 71.
8 W. Langseth, *Fresenius' Z. Anal. Chem.*, 325 (1986) 267.
9 W. Langseth, *Anal. Chim. Acta*, 185 (1986) 249.
10 I. S. Krull, D. S. Bushee, R. G. Schleicher and S. B. Smith, *Analyst (London)*, 111 (1986) 345.
11 D. S. Bushee, *Analyst (London)*, 113 (1988) 1167.
12 E. Munaf, H. Haraguchi, D. Ishii, T. Takeuchi and M. Goto *Anal. Chim. Acta*, 235 (1990) 399.

END OF SYMPOSIUM PAPERS

PUBLICATION SCHEDULE FOR THE 1993 SUBSCRIPTION

Journal of Chromatography and *Journal of Chromatography, Biomedical Applications*

MONTH	O 1992	N 1992	D 1992	
Journal of Chromatography	623/1 623/2 624	625/1 625/2	626/1 626/2 627/1+2	The publication schedule for further issues will be published later
Cumulative Indexes, Vols. 601–650				
Bibliography Section				
Biomedical Applications				

INFORMATION FOR AUTHORS

(Detailed *Instructions to Authors* were published in Vol. 609, pp. 439–445. A free reprint can be obtained by application to the publisher, Elsevier Science Publishers B.V., P.O. Box 330, 1000 AH Amsterdam, The Netherlands.)

Types of Contributions. The following types of papers are published in the *Journal of Chromatography* and the section on *Biomedical Applications:* Regular research papers (Full-length papers), Review articles, Short Communications and Discussions. Short Communications are usually descriptions of short investigations, or they can report minor technical improvements of previously published procedures; they reflect the same quality of research as Full-length papers, but should preferably not exceed five printed pages. Discussions (one or two pages) should explain, amplify, correct or otherwise comment substantively upon an article recently published in the journal. For Review articles, see inside front cover under Submission of Papers.

Submission. Every paper must be accompanied by a letter from the senior author, stating that he/she is submitting the paper for publication in the *Journal of Chromatography*.

Manuscripts. Manuscripts should be typed in **double spacing** on consecutively numbered pages of uniform size. The manuscript should be preceded by a sheet of manuscript paper carrying the title of the paper and the name and full postal address of the person to whom the proofs are to be sent. As a rule, papers should be divided into sections, headed by a caption (*e.g.*, Abstract, Introduction, Experimental, Results, Discussion, etc.). All illustrations, photographs, tables, etc., should be on separate sheets.

Abstract. All articles should have an abstract of 50–100 words which clearly and briefly indicates what is new, different and significant. No references should be given.

Introduction. Every paper must have a concise introduction mentioning what has been done before on the topic described, and stating clearly what is new in the paper now submitted.

Illustrations. The figures should be submitted in a form suitable for reproduction, drawn in Indian ink on drawing or tracing paper. Each illustration should have a legend, all the *legends* being typed (with double spacing) together on a *separate sheet.* If structures are given in the text, the original drawings should be supplied. Coloured illustrations are reproduced at the author's expense, the cost being determined by the number of pages and by the number of colours needed. The written permission of the author and publisher must be obtained for the use of any figure already published. Its source must be indicated in the legend.

References. References should be numbered in the order in which they are cited in the text, and listed in numerical sequence on a separate sheet at the end of the article. Please check a recent issue for the layout of the reference list. Abbreviations for the titles of journals should follow the system used by *Chemical Abstracts.* Articles not yet published should be given as "in press" (journal should be specified), "submitted for publication" (journal should be specified), "in preparation" or "personal communication".

Dispatch. Before sending the manuscript to the Editor please check that the envelope contains four copies of the paper complete with references, legends and figures. One of the sets of figures must be the originals suitable for direct reproduction. Please also ensure that permission to publish has been obtained from your institute.

Proofs. One set of proofs will be sent to the author to be carefully checked for printer's errors. Corrections must be restricted to instances in which the proof is at variance with the manuscript. "Extra corrections" will be inserted at the author's expense.

Reprints. Fifty reprints will be supplied free of charge. Additional reprints can be ordered by the authors. An order form containing price quotations will be sent to the authors together with the proofs of their article.

Advertisements. The Editors of the journal accept no responsibility for the contents of the advertisements. Advertisement rates are available on request. Advertising orders and enquiries can be sent to the Advertising Manager, Elsevier Science Publishers B.V., Advertising Department, P.O. Box 211, 1000 AE Amsterdam, Netherlands; courier shipments to: Van de Sande Bakhuyzenstraat 4, 1061 AG Amsterdam, Netherlands; Tel. (+31-20) 515 3220/515 3222, Telefax (+31-20) 6833 041, Telex 16479 els vi nl. *UK*: T. G. Scott & Son Ltd., Tim Blake, Portland House, 21 Narborough Road, Cosby, Leics. LE9 5TA, UK; Tel. (+44-533) 753 333, Telefax (+44-533) 750 522. *USA and Canada*: Weston Media Associates, Daniel S. Lipner, P.O. Box 1110, Greens Farms, CT 06436-1110, USA; Tel. (+1-203) 261 2500, Telefax (+1-203) 261 0101.

Reversed Phase CHIRAL HPLC Column

NEW CHIRALCEL® OD-R

Indapamide	Verapamil	Hydroxyzine
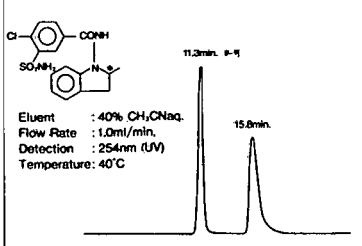 Eluent : 40% CH_3CNaq. Flow Rate : 1.0ml/min. Detection : 254nm (UV) Temperature: 40°C	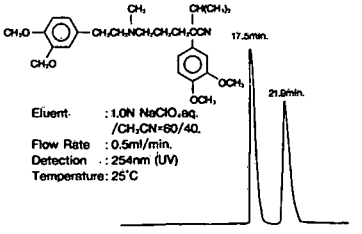 Eluent : 1.0N $NaClO_4$aq. /CH_3CN=60/40. Flow Rate : 0.5ml/min. Detection : 254nm (UV) Temperature: 25°C	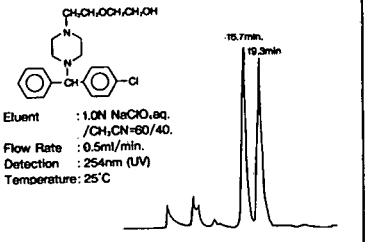 Eluent : 1.0N $NaClO_4$aq. /CH_3CN=60/40. Flow Rate : 0.5ml/min. Detection : 254nm (UV) Temperature: 25°C
Propranolol	**Pindolol**	**1-Phenoxy-2-Propanol**
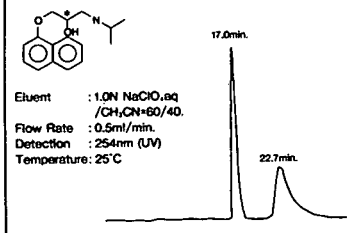 Eluent : 1.0N $NaClO_4$aq /CH_3CN=60/40. Flow Rate : 0.5ml/min. Detection : 254nm (UV) Temperature: 25°C	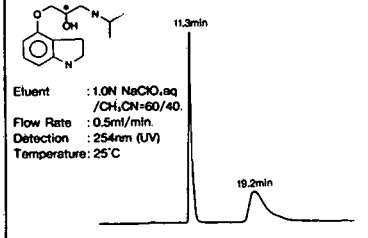 Eluent : 1.0N $NaClO_4$aq /CH_3CN=60/40. Flow Rate : 0.5ml/min. Detection : 254nm (UV) Temperature: 25°C	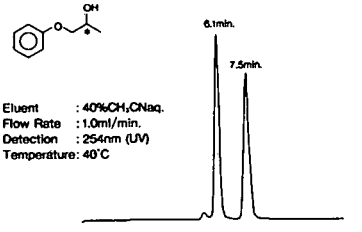 Eluent : 40%CH_3CNaq. Flow Rate : 1.0ml/min. Detection : 254nm (UV) Temperature: 40°C
Alimemazine	**Trimepramine**	**4-Pheny-2-butanol**
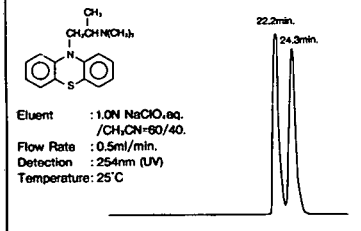 Eluent : 1.0N $NaClO_4$aq. /CH_3CN=60/40. Flow Rate : 0.5ml/min. Detection : 254nm (UV) Temperature: 25°C	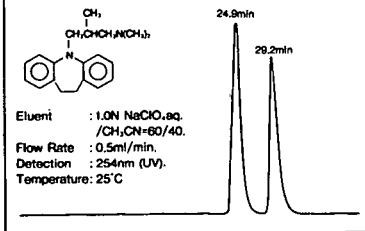 Eluent : 1.0N $NaClO_4$aq. /CH_3CN=60/40. Flow Rate : 0.5ml/min. Detection : 254nm (UV). Temperature: 25°C	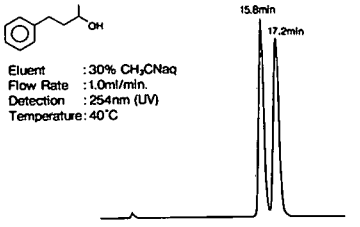 Eluent : 30% CH_3CNaq Flow Rate : 1.0ml/min. Detection : 254nm (UV) Temperature: 40°C
CBZ-Val.	**3-Phenylbutyric acid**	**2-Phenylbutyric acid**
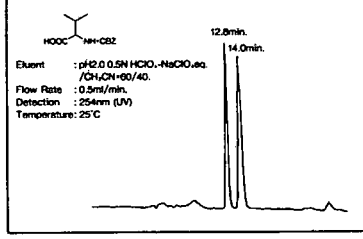 Eluent : pH2.0 0.5N $HClO_4$-$NaClO_4$aq. /CH_3CN=60/40. Flow Rate : 0.5ml/min. Detection : 254nm (UV) Temperature: 25°C	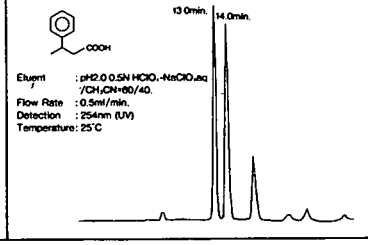 Eluent : pH2.0 0.5N $HClO_4$-$NaClO_4$aq /CH_3CN=60/40. Flow Rate : 0.5ml/min. Detection : 254nm (UV) Temperature: 25°C	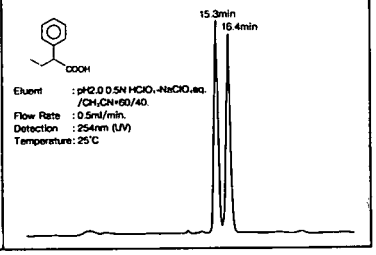 Eluent : pH2.0 0.5N $HClO_4$-$NaClO_4$aq. /CH_3CN=60/40. Flow Rate : 0.5ml/min. Detection : 254nm (UV) Temperature: 25°C

For more information about CHIRALCEL OD-R column, please give us a call.

DAICEL CHEMICAL INDUSTRIES, LTD.
CHIRAL CHEMICALS DIVISION 8-1, Kasumigaseki 3-chome, Chiyoda-ku, Tokyo 100, JAPAN
Phone: +81-3-3507-3151 Facsimile: +81-3-3507-3193

AMERICA
CHIRAL TECHNOLOGIES, INC.
730 SPRINGDALE DRIVE
DRAWER I EXTON, PA 19341
Phone: 215-594-2100
Facsimile: 215-594-2325

EUROPE
DAICEL (EUROPA) GmbH
Ost Street 22
4000 Düsseldorf 1, Germany
Phone: +49-211-369848
Facsimile: +49-211-364429

ASIA/OCEANIA
DAICEL CHEMICAL (ASIA) PTE. LTD.
65 Chulia Street #40-07
OCBC Centre, Singapore 0104.
Phone: +65-5332511
Facsimile: +65-5326454

10 มิ.ย. 41 10 มิ.ย. 2526